Low-cost sensors for monitoring stormwater source control measures

Qingchuan Zhu

N° d'ordre NNT : 2023ISAL0035

THESE de DOCTORAT DE L'INSA LYON, membre de l'Université de Lyon

Ecole Doctorale N° ED162
Mécanique, énergétique, génie civil, acoustique

Spécialité : Génie Civil

Soutenue publiquement le 31/05/2023, par :
Qingchuan ZHU

Low-cost sensors for monitoring stormwater source control measures

---

Devant le jury composé de :

VIKLANDER, Maria	LULEA UNIVERSITY OF TECHNOLOGY	Rapporteure
ZHU, David	UNIVERSITY OF ALBERTA	Rapporteur
BRANGER, Flora	INRAE LYON-GRENOBLE	Examinatrice
VERSINI Pierre-Antoine	ENPC	Examinateur
LIPEME KOUYI Gislain	INSA LYON	Examinateur
BERTRAND-KRAJEWSKI, Jean-Luc	INSA LYON	Directeur de thèse
CHERQUI, Frédéric	UNIVERSITE LYON 1	Co-directeur de thèse

Département FEDORA – INSA Lyon - Ecoles Doctorales

SIGLE	ECOLE DOCTORALE	NOM ET COORDONNEES DU RESPONSABLE
CHIMIE	**CHIMIE DE LYON** https://www.edchimie-lyon.fr Sec. : Renée EL MELHEM Bât. Blaise PASCAL, 3e étage secretariat@edchimie-lyon.fr	**M. Stéphane DANIELE** C2P2-CPE LYON-UMR 5265 Bâtiment F308, BP 2077 43 Boulevard du 11 novembre 1918 69616 Villeurbanne directeur@edchimie-lyon.fr
E.E.A.	**ÉLECTRONIQUE, ÉLECTROTECHNIQUE, AUTOMATIQUE** https://edeea.universite-lyon.fr Sec. : Stéphanie CAUVIN Bâtiment Direction INSA Lyon Tél : 04.72.43.71.70 secretariat.edeea@insa-lyon.fr	**M. Philippe DELACHARTRE** INSA LYON Laboratoire CREATIS Bâtiment Blaise Pascal, 7 avenue Jean Capelle 69621 Villeurbanne CEDEX Tél : 04.72.43.88.63 philippe.delachartre@insa-lyon.fr
E2M2	**ÉVOLUTION, ÉCOSYSTÈME, MICROBIOLOGIE, MODÉLISATION** http://e2m2.universite-lyon.fr Sec. : Bénédicte LANZA Bât. Atrium, UCB Lyon 1 Tél : 04.72.44.83.62 secretariat.e2m2@univ-lyon1.fr	**Mme Sandrine CHARLES** Université Claude Bernard Lyon 1 UFR Biosciences Bâtiment Mendel 43, boulevard du 11 Novembre 1918 69622 Villeurbanne CEDEX sandrine.charles@univ-lyon1.fr
EDISS	**INTERDISCIPLINAIRE SCIENCES-SANTÉ** http://ediss.universite-lyon.fr Sec. : Bénédicte LANZA Bât. Atrium, UCB Lyon 1 Tél : 04.72.44.83.62 secretariat.ediss@univ-lyon1.fr	**Mme Sylvie RICARD-BLUM** Institut de Chimie et Biochimie Moléculaires et Supramoléculaires (ICBMS) - UMR 5246 CNRS - Université Lyon 1 Bâtiment Raulin - 2ème étage Nord 43 Boulevard du 11 novembre 1918 69622 Villeurbanne Cedex Tél : +33(0)4 72 44 82 32 sylvie.ricard-blum@univ-lyon1.fr
INFOMATHS	**INFORMATIQUE ET MATHÉMATIQUES** http://edinfomaths.universite-lyon.fr Sec. : Renée EL MELHEM Bât. Blaise PASCAL, 3e étage Tél : 04.72.43.80.46 infomaths@univ-lyon1.fr	**M. Hamamache KHEDDOUCI** Université Claude Bernard Lyon 1 Bât. Nautibus 43, Boulevard du 11 novembre 1918 69 622 Villeurbanne Cedex France Tél : 04.72.44.83.69 hamamache.kheddouci@univ-lyon1.fr
Matériaux	**MATÉRIAUX DE LYON** http://ed34.universite-lyon.fr Sec. : Yann DE ORDENANA Tél : 04.72.18.62.44 yann.de-ordenana@ec-lyon.fr	**M. Stéphane BENAYOUN** Ecole Centrale de Lyon Laboratoire LTDS 36 avenue Guy de Collongue 69134 Ecully CEDEX Tél : 04.72.18.64.37 stephane.benayoun@ec-lyon.fr
MEGA	**MÉCANIQUE, ÉNERGÉTIQUE, GÉNIE CIVIL, ACOUSTIQUE** http://edmega.universite-lyon.fr Sec. : Stéphanie CAUVIN Tél : 04.72.43.71.70 Bâtiment Direction INSA Lyon mega@insa-lyon.fr	**M. Jocelyn BONJOUR** INSA Lyon Laboratoire CETHIL Bâtiment Sadi-Carnot 9, rue de la Physique 69621 Villeurbanne CEDEX jocelyn.bonjour@insa-lyon.fr
ScSo	**ScSo*** https://edsciencessociales.universite-lyon.fr Sec. : Mélina FAVETON INSA : J.Y. TOUSSAINT Tél : 04.78.69.77.79 melina.faveton@univ-lyon2.fr	**M. Bruno MILLY** Université Lumière Lyon 2 86 Rue Pasteur 69365 Lyon CEDEX 07 bruno.milly@univ-lyon2.fr

*ScSo : Histoire, Géographie, Aménagement, Urbanisme, Archéologie, Science politique, Sociologie, Anthropologie

Acknowledgements

I wish to express my gratitude and appreciation to all who have contributed to this thesis.

I would like to thank most specially my supervisors, Jean-Luc Bertrand-Krajewski and Frédéric Cherqui. Without their continuous guidance, fruitful discussions and invaluable support, this work would not have been possible. They both gave me very constructive comments and were always there when I needed help. Working with them over the past three and a half years helped me greatly to improve my research skills and to learn meaningful things beyond the academic world.

I am grateful to the thesis committee members for accepting to read this manuscript and to take part in the defense of this thesis. Their kind support is truly appreciated.

I wish to thank Nicolas Walcker, Hervé Perier-Camby, Richard Poncet, Stéphane Vacherie and other team members for their contributions to the experimental work, which were important for the progress of this thesis.

Finally, I must say thanks to the most important people of my life: my parents in China and my dear wife. They gave me endless care and permanent encouragement during the past years. They are simply my main source of motivation to overcome all challenges in life.

Abstract

The large-scale deployment of low-cost sensors has the potential to revolutionize the field of urban hydrology monitoring, especially for decentralized stormwater management systems, bringing expanded research scope and improved urban water management. In this thesis, a sensor is identified to be low-cost according to two possible criteria: (i) its price is at least 10 times lower than equivalent traditional sensors, or (ii) it has been reported in the literature to be working with open-source hardware to build a low-cost monitoring unit. However, this area is still in its infancy stage and needs a more systematic assessment framework to ensure data reliability and facilitate its implementation by researchers and practitioners.

To contribute to fill this gap, this thesis explores low-cost monitoring systems dedicated to stormwater source control measures (SCM). Several open-source low-cost sensors and systems have been calibrated and validated in a DIY (Do It Yourself) approach, aiming to assess the medium and long-term performance and identify maintenance problems. After successive versions of hardware and software improvements, a reliable design for a low-cost monitoring node is proposed and shared.

This thesis provides:

(i) A review of low-cost meteorological, water quantity and quality sensors that are used in the literature published in recent years, in a unified metrological framework considering numerous indicators.(ii) A low-cost meteorological sensors testbench on the INSA GROOF platform, with a comparison between low-cost and conventional sensors. Low-cost anemometer WH-SP-WS01 (enlarged uncertainty 0.24 m/s) and air temperature and humidity sensor DHT22 (enlarged uncertainty 2.3 ℃, 5.7 %RH) are found to have performance comparable to those of conventional sensors.

(iii) The development of a low-cost stand-alone rain gauge station, with a method to calibrate low-cost tipping bucket rain gauges, and a comparison between low-cost and conventional rain gauges in winter period. The rainfall catchment funnel of low-cost tipping bucket rain gauge WH-SP-RG needs to be enlarged to improve the poor initial resolution (0.60 mm/tip). The optical rain gauge RG-15 has significant sensor-to-sensor variability.

(iv) The development of a low-cost stand-alone water level monitoring station based on pressure water level transmitter YB-2J-F, with a method to calibrate the water level transmitters, and a one-and-a-half-year long operation assessment. YB-2J-F performs stable (enlarged uncertainty 0.11 mm) in calibration. The system developed works continuously without any outlier, but the time step of its data transmission is not regular and therefore *in situ* data storage is necessary. In this thesis, sensor accuracy given by manufacturers is assumed to correspond to the enlarged uncertainty in sensor evaluation, and inter-sensor comparison is carried out to by comparing sensor output coverage intervals. Innovatively, the correctness rate of the sensor output is proposed to characterize the fraction of overlap between output coverage intervals in time series of both the tested sensor and the reference sensor.

Résumé

Le déploiement à grande échelle de capteurs à faible coût a le potentiel pour révolutionner le domaine de la métrologie en hydrologie urbaine, en particulier pour les systèmes décentralisés de gestion des eaux pluviales, en élargissant le champ de la recherche et en améliorant la gestion de l'eau en milieu urbain. Dans cette thèse, un capteur est identifié comme étant à bas coût selon deux critères possibles : (i) son prix est au moins 10 fois inférieur à celui des capteurs traditionnels équivalents, ou (ii) il a été mentionné dans la littérature qu'il fonctionne avec du matériel open-source pour construire une unité de mesure à faible coût. Toutefois, ce domaine en est encore à ses débuts et nécessite un cadre d'évaluation plus systématique pour garantir la fiabilité des données et faciliter sa mise en œuvre par les chercheurs et les praticiens.

Pour contribuer à combler cette lacune, cette thèse s'intéresse aux systèmes de mesure à faible coût dédiés aux dispositifs de contrôle à la source des eaux pluviales (SCM). Plusieurs capteurs et systèmes open-source à bas prix ont été étalonnés et validés dans une approche DIY (Do It Yourself), visant à évaluer leurs performances à moyen et long termes, et à identifier les problèmes de maintenance. Après des versions successives d'améliorations matérielles et logicielles, une conception fiable pour une station de mesure à faible coût est proposée et partagée.

Cette thèse contient :

(i) Une revue bibliographique des capteurs météorologiques pour le suivi de la quantité et de la qualité de l'eau à faible coût, qui ont été cités dans des publications parues ces dernières années, dans un cadre métrologique unifié prenant en compte de nombreux indicateurs.

(ii) Un banc d'essai de capteurs météorologiques à faible coût installé sur la plateforme GROOF de l'INSA Lyon, avec une comparaison entre capteurs à faible coût et capteurs conventionnels. L'anémomètre à faible coût WH-SP-WS01 (incertitude élargie de 0,24 m/s) et le capteur de température et d'humidité de l'air DHT22 (incertitude élargie de 2,3 ℃, 5,7 %HR) ont des performances comparables à celles des capteurs conventionnels.

(iii) Le développement d'une station pluviométrique autonome à faible coût, avec une méthode d'étalonnage des pluviomètres à auget basculant à faible coût, et une comparaison entre les pluviomètres à faible coût et les pluviomètres conventionnels en période hivernale. L'entonnoir de collecte des précipitations du pluviomètre à augets basculants WH-SP-RG doit être agrandi pour améliorer la médiocre résolution initiale (0,60 mm/basculement). Le pluviomètre optique RG-15 présente une variabilité importante d'un capteur à l'autre.

(iv) Le développement d'une station de mesure de niveau d'eau autonome et peu coûteuse basée sur le transmetteur piézorésistif YB-2J-F, avec une méthode d'étalonnage du capteur et une évaluation de l'exploitation sur une période d'un an et demi. L'étalonnage du capteur YB-2J-F est stable (incertitude élargie de 0,11 mm). Le système développé fonctionne en continu sans aucune valeur aberrante, mais le pas de temps de sa transmission de données n'est pas régulier et il est donc nécessaire de stocker les données *in situ*.

Dans cette thèse, la précision du capteur indiquée par les constructeurs est considérée comme équivalente à l'incertitude élargie déterminée lors de l'évaluation du capteur, et la comparaison entre capteurs est effectuée en comparant les intervalles de couverture des données des sortie des capteurs. De manière innovante, le taux d'exactitude des données d'un capteur est proposé pour caractériser la fraction de recouvrement des intervalles de couverture des séries chronologiques entre le capteur à faible coût testé et le capteur de référence.

Table of Contents

CHAPTER 1: INTRODUCTION

This chapter presents the context of the work, the connection with the Cheap'eau project, the objective, and the structure of the thesis.

1.1 GENERAL OVERVIEW

(This section is adapted from Zhu *et al*. 2023.)

Urban stormwater refers to water transferred in built environments from rainfall or snowmelt (Müller *et al.*, 2020). In the past centuries, with the development of economy and society, there were more and more built areas all over the world. In these built environments, biodiversity and ecosystems services related to stormwater are reduced due to impervious surfaces such as streets, parking lots, and rooftops (Berland *et al.*, 2017), and as a result, many environmental issues have arisen (Prudencio and Null, 2018). These environmental issues include but are not limited to (i) urban flooding due to reduced water infiltration that is also linked to climate change (Cousins, 2017), such as floods in Zhengzhou City, China on July 20, 2021 (Wang *et al.*, 2021); or (ii) water contamination due to stormwater runoff over polluted impervious surfaces (Becouze-Lareure *et al.*, 2016; Gasperi *et al.*, 2014; Liu *et al.*, 2019; Müller *et al.*, 2020).

Since the middle of the 19th century, modern storm drains, gutters, and underground systems which are also known as gray infrastructures are constructed in cities worldwide (Fu *et al.*, 2019; Qiao *et al.*, 2018). The last decades have also seen the emergence of green infrastructures including wet ponds, constructed stormwater wetlands, bioretention, infiltration facilities, permeable pavement, swales, green roofs, and rainwater harvesting systems, etc., also named source control measures (SCM), nature-based solutions (NBS), best management practices (BMP), with issues related to their design, operation, and long-term performance (Cherqui *et al.*, 2019; Fletcher *et al.*, 2015). Traditionally, stormwater quantity and quality in the above-mentioned decentralized infrastructures are monitored by both researchers and practitioners (Nickel *et al.*, 2021; Salehi *et al.*, 2020; Thebault *et al.*, 2020). Because of resource limitation, it is difficult in theory, and impossible in practice, to monitor stormwater in these infrastructures with high temporal and spatial resolution. The drawbacks of this condition are numerous and

include (i) lag in urban flood warning and relief decision making due to inaccurate rainfall estimates (Wang *et al.*, 2021); (ii) lack of proactive response to water contamination due to inadequacy of data (Pule *et al.*, 2017); (iii) lack of maintenance due to lack of monitoring leading to failure of the stormwater infrastructures themselves (Al-Rubaei *et al.*, 2017; Thomas *et al.*, 2016; Wong and Kerkez, 2016).

Facing the above-mentioned drawbacks of insufficient monitoring, thanks to the development of open-source hardware, wireless communication technology and sensors in the last few years, a promising paradigm for soil, air and water monitoring appeared and a large number of papers have emerged in this area (Montserrat *et al.*, 2013; Morawska *et al.*, 2018; Rai *et al.*, 2017; Valente *et al.*, 2020). In this paradigm, high-resolution spatiotemporal and relatively reliable data are collected by means of a ubiquitous network of low-cost sensors. The potential benefits of applying such a paradigm for stormwater monitoring are (i) supplementing conventional stormwater monitoring; (ii) enhancing the capacity of urban flood warning; (iii) improving the ability of water contamination detection; (iv) accumulating a wealth of new knowledge on stormwater and stormwater infrastructure management and maintenance; (v) provide the means for real-time control of infrastructure; (vi) making the most of the Big Data approach to discover new beneficial information. Therefore, this paradigm attracts urban hydrologists like the author of this thesis to devote themselves to this area to build their own monitoring network to support research and operation.

Indeed, as urban stormwater management rapidly evolves worldwide toward numerous decentralized source control facilities, widely disseminated across catchments and cities, there is a growing need for monitoring these facilities, to obtain spatially distributed information and data about their functioning. With traditional reliable and well-known but expensive sensors and monitoring systems, only a few of these facilities can be monitored. This is why it is worth evaluating the potential of using low-cost sensors to monitor these numerous decentralized stormwater facilities, with particular attention to their levels of reliability, accuracy, and uncertainty, along with adapted specifications. An example of applicability of crowd-sourcing approach to urban rainfall monitoring with low-cost sensors used by citizens has shown that it could, under some conditions, overperform for rainfall runoff modelling compared to a sparse traditional rain gauge network (Yang and Ng, 2017).

Three technical parts can be distinguished in this emerging paradigm: (i) open-source hardware, (ii) communication protocols, and (iii) low-cost sensors. Open-source hardware and communication protocols are

relatively reliable and there are a few commonly used solutions. These solutions have been in development for several years and are designed, developed, promoted, and guaranteed by professional companies such as e.g., Arduino or Raspberry Pi. On the contrary, low-cost sensors are a more complex part. Most of them were originally designed either for teaching purposes, or small parts for other goods, or also for DIY (Do It Yourself) use by electronics enthusiasts. Their reliability for research and operation applications is however questionable (Kumar *et al.*, 2015). As a trade-off of price, some of them do not have a clear manufacturing company and brand, and do not provide end-users with (detailed) datasheets. There is also no universally agreed definition of "low-cost" sensors.

1.2 THESIS OBJECTIVES AND OUTLINE

1.2.1 The Cheap'eau project

This thesis is linked to the collaborative project Cheap'eau, funded by the French Rhône-Méditerranée-Corse water agency (http://graie.org/othu/progr_cheapeau.htm, visited on 28 February 2023.). Cheap'eau aims to evaluate if and how low-cost sensors can be used by researchers and practitioners for stormwater monitoring. In addition to this thesis, various low-costs sensors are presently tested for monitoring stormwater facilities like green roofs, detention tanks, and trenches by Cheap'eau partners (Cherqui *et al.*, 2020). The results and conclusions of the on-going Cheap'eau project will be published separately at the end of 2023.

1.2.2 Objective and outline of the thesis

This thesis aims at (i) testing selected low-cost sensors in the context of stormwater source control measures with appropriate metrology practice, and (ii) answering what type of low-cost sensor can be used and how to evaluate the uncertainty of low-cost sensors. Given the above objectives, the main steps of the work were:

i. Review of the low-cost sensors used by other researchers for monitoring meteorological quantities, water quantity and water quality.
ii. Choice of low-cost sensors with application potential according to literature review and communication in the open-source community for stormwater monitoring applications.

iii. Development, installation, maintenance, and improvement of low-cost monitoring stations in the selected experiment site.

iv. Collection of *in situ* data over weeks to months, and if possible, during a full year.

v. Final assessment of the low-cost sensors' performance.

In the actual work, the last three steps were intertwined, low-cost monitoring stations were always improved due to data logging interruption or abnormality . According to the above objective and steps, the thesis includes seven chapters, as described in Table 1-1.

Table 1-1. Outlines of the thesis.

Chapter 1	• Context of low-cost stormwater monitoring; • Objective and structure of the thesis.
Chapter 2	• Review of low-cost meteorology sensors; • Review of low-cost water quantity sensors; • Review of low-cost water quality sensors.
Chapter 3	• Description of sensor performance assessment methods; • Description of experimental sites.
Chapter 4	• Description of low-cost meteorology sensors test setups; • Presentation of low-cost meteorology sensors test results.
Chapter 5	• Description of low-cost rainfall monitoring station design and test setups; • Presentation of low-cost rain gauges *in situ* performance assessment results, calibration results and low-cost rainfall monitoring station performance assessment results.
Chapter 6	• Description of low-cost water level monitoring station design and test setups; • Presentation of low-cost water level sensor calibration results and the low-cost water level monitoring station performance assessment results.
Chapter 7	• Conclusions and perspectives.

CHAPTER 2: LITERATURE REVIEW

(This chapter is adapted from Zhu *et al*. (2023).)

2.1 INTRODUCTION

This chapter reviews scientific articles about using or assessing commercially available low-cost sensors for monitoring stormwater and related meteorological variables. The author speculates that the main readers of this review are stormwater researchers who are aiming to conduct stormwater monitoring projects with full control but a limited budget. On the one hand, one may to some extent assume they are low-cost sensors hobbyists: the information provided in this review is important to design and build their own systems. On the other hand, they are researchers who must ensure reliable and robust best practice in stormwater monitoring. Performance criteria like trueness, repeatability, uncertainty, etc. are of key importance in their evaluation of low-cost sensors and in their possible use of such sensors for data acquisition to support research conclusions.

The literature review considers meteorological sensors (third section) for monitoring air humidity, wind speed, solar radiation, and rainfall; water quantity sensors (forth section) for monitoring water level, water flow and soil moisture; and water quality sensors (fifth section) for monitoring pH, conductivity, turbidity, nitrogen, and phosphorus. The last section discusses the current status of low-cost water sensors.

2.2 METHODOLOGY

2.2.1 Paper selection

To make this review paper as comprehensive as possible, there are no specific price restrictions when using the term ‘low-cost’. A sensor is identified to be low-cost according to two possible criteria: (i) its price is at least 10 times lower than equivalent traditional sensors, or (ii) it has been reported in the literature to be working with open-source hardware to build a low-cost monitoring unit. Web of Science and Google Scholar (Martín-Martín *et*

al., 2021) are used to search papers in which commercial off-the-shelf (COTS) low-cost sensors are used in sensing networks.

In the advanced search query builder tool of Web of Science, for example, query "ALL= ((Low-cost OR cheap OR frugal) AND (sensor OR instrument) AND (off-the-shelf OR commercial) AND (sensor network OR sensing network) AND (water flow OR discharge OR flow rate))" is used to search the usage of COTS low-cost water flow sensors. Search timespan is from 2012-01-01 to 2022-12-31 (publication date). And then, all results are browsed. A paper which indicates the usage of specific COTS sensors is selected to review. However, most of the literature searched out have no relationship to a specific COTS sensor. This is why, for example, all the water flow papers searched out from Web of Science are not selected.

In the advanced search tool of Google Scholar, similar queries are used. Google Scholar is also forced to return articles dated between 2012 to 2022. Papers are sorted by relevance based on full text matching and information on journal, author, and citation. The results in the first five pages are browsed to select papers to review due to the high number of references (several tens of thousands) returned by Google Scholar.

When a specific sensor model is detected, Google Scholar is used to search for papers that give the performance assessment of this specific type of sensor (e.g., search "SHT20", "HC-SR04", "SEN0161"). Papers are sorted by relevance. The results in the first three pages are browsed to select papers to review.

Numbers of search results and final selected papers are given in Table 2-1.

Table 2-1. Numbers of Web of Science and Google Scholar search results, selected papers, and reviewed papers.

Search category	Web of Science		Google Scholar		Reviewed number
	Total number	Selected number	Total number	Selected number	
Low-cost sensor	49135	40	about 18000	163	202
COTS low-cost sensor	4148	40	about 45100	163	202
Sensor network	776	40	about 17100	163	202
Air humidity sensor	26	17	about 17100	15	32
Anemometer	8	2	about 23000	12	14
Pyranometer	7	3	about 25600	13	16
Rainfall	5	1	about 10900	16	17
Water level sensor	16	4	about 17200	10	13
Water flow sensor	15	0	about 17200	10	10
Soil moisture sensor	14	5	about 17300	13	18
Water pH sensor	8	3	about 17500	28	31
Water conductivity sensor	19	3	about 17000	19	22
Turbidimeter	5	2	about 6810	16	18
Water nitrogen and phosphorus sensor	11	0	about 16100	11	11

202 papers have been reviewed by authors for this review. A general concern is that these low-cost sensors quickly evolve thanks to the rapid development of technologies. There is a lag between the application of sensors in projects and the publication of papers. During the review, we found that most low-cost sensor models are sold, tested, and used for several years which proves they have a stable design and supply. This review also included some abstracts to enhance its timeliness.

2.2.2 Sensor performance evaluation

Even though the evaluation of sensors is dependent on application scenarios, contexts, and purposes, the authors of this review believe that the greatest challenge is to identify sensors which are not only low-cost, but which can generate useful data over an extended period. Like any sensors, the performance information of low-cost sensors is collected and classified by parameters as shown in Table 2-2.

Table 2-2. Major performance criteria for low-cost sensors performance assessment.

Parameters	Description
Trueness	Output closeness with the reading of the reference measurement at the same place and same time.
Repeatability	Output closeness under a set of repeatable conditions of measurement (NF EN 17075, 2018).
Reproducibility	Dispersion between measurements obtained using different sensors of the same model (Rai *et al.*, 2017).
Resolution	Smallest change in a quantity being measured that causes a perceptible change in the corresponding indication (JCGM, 2012).
Response time	Time interval between the instant when a continuous measuring device is subjected to an abrupt change in the measurand value and the instant when the readings cross the limits of (and remain inside) a band defined by the 90 % and the 110 % of the difference between the initial and final value of the abrupt change (NF EN 17075, 2018).
Sensitivity to environment	Effect of environmental factors (temperature, relative humidity and so on) on sensor output (Rai *et al.*, 2017).
Maintenance needs	Frequency and hours dedicated to the maintenance of sensors (including controls and cleaning).
Longevity	Time of operation before replacement (Kumar *et al.*, 2015).

Information from manufacturers and scientific literature of every type of sensor is connected as much as possible. Many low-cost sensor's datasheets use the term "accuracy" to describe their sensor's performance, combining and/or likely confusing trueness and repeatability. In the tables of this review, we put manufacturers' accuracy metric into trueness criteria. As in low-cost air quality field (e.g., Rai *et al.* 2017), due to the lack of a standard calibration protocol specific for low-cost sensors, studies have used dissimilar calibration methods, against a variety of reference instruments, which makes intercomparison between them infeasible. Nevertheless, these studies provide valuable information about the performance of low-cost sensors under a variety of operating conditions (Rai *et al.*, 2017). Some authors used subjective judgment vocabulary such as "good", "acceptable", "reasonable", "satisfactory", "not severe" to describe the performance of low-cost sensors. We use quotation marks to indicate that this is the judgement of the authors of the papers, and not our own opinion. Various performance metrics have been cited in this review and their definitions are given and harmonized in Table 2-3 in the order of their appearance. All notations are unified in this review[1], where n is the number of samples, p_i is the reading of low-cost sensors, P_i is the reading of reference sensors, $\bar{p}$ and $\bar{P}$ are the average values of p_i and P_i, $R(p_i)$ and $R(P_i)$ are the ranks of p_i and P_i. When computing dynamic residuals (DR), $\widehat{p_i}$ is the averaged linear model output of the given sensor (Araújo *et al.*, 2020). When computing pooled relative standard deviation ($s_{r,p}$), k, n_k, m and

[1] These notations are applicable only in Chapter 2.

s^k are the index of the current series, number of measurements in series k, total number of series, and corresponding standard deviation of the series, respectively (Adla *et al.*, 2020).

Table 2-3. Performance metrics used in references of this review.

Symbol	Metric	Equation	References
r_s	Spearman's rank-order correlation	$1-\frac{1-6\sum_{i=1}^{n}(R(P_i)-R(p_i))^2}{n(n^2-1)}$	(Moreno-Rangel *et al.*, 2018)
R^2	Coefficient of determination	$\frac{(n\sum_{i=1}^{n}p_iP_i)-(\sum_{i=1}^{n}p_i)(\sum_{i=1}^{n}P_i)}{\sqrt{n\sum_{i=1}^{n}(p_i)^2-(\sum_{i=1}^{n}(p_i))^2}\sqrt{n\sum_{i=1}^{n}(P_i)^2-(\sum_{i=1}^{n}(P_i))^2}}$	(Akhter *et al.*, 2018; Angraini *et al.*, 2016; Bitella *et al.*, 2014; Coloch Tahuico, 2021; Demetillo *et al.*, 2019a; Faisal *et al.*, 2016)
DR	Dynamic Residual	$\sqrt{\frac{\sum_{i=1}^{n}(\widehat{p_i}-P_i)^2}{P_n-P_1}}$	(Araújo *et al.*, 2020)
MBE	Mean Bias Error	$\frac{1}{n}\sum_{i=1}^{n}(P_i-p_i)$	(Domínguez-Brito *et al.*, 2020, Azouzoute *et al.*, 2019)
RMSE	Root Mean Square Error	$\sqrt{\frac{\sum_{i=1}^{n}(P_i-p_i)^2}{n}}$	(Adla *et al.*, 2020; Bitella *et al.*, 2014; Burgt, 2020; Domínguez-Brito *et al.*, 2020; Nagahage *et al.*, 2019)
MAE	Mean Absolute Error	$\frac{1}{n}\sum_{i=1}^{n}(\lvert P_i-p_i\rvert)$	(Adla *et al.*, 2020)
RAE	Relative Absolute Error	$\frac{\sum_{i=1}^{n}\lvert P_i-p_i\rvert}{\sum_{i=1}^{n}\lvert p_i-\bar{P}\rvert}$	(Adla *et al.*, 2020)
NRMSE	Normalized Root Mean Square Error	$\frac{RMSE}{\bar{P}}$	(Azouzoute *et al.*, 2019; Bitella *et al.*, 2014)
SD	Standard Deviation	$\sqrt{\frac{n(RMSE^2-MBE^2)}{n-1}}$	(Azouzoute *et al.*, 2019)
TS	t-statistic	$\sqrt{\frac{(n-1)MBE^2}{RMSE^2-MBE^2}}$	(Azouzoute *et al.*, 2019)
$s_{r,p}$	Pooled relative standard deviation	$\sqrt{\frac{\sum_{k=1}^{m}(n_k-1)s_k^2(1/\overline{P_k}^2)}{\sum_{k=1}^{m}(n_k-1)}}$	(Adla *et al.*, 2020)

In addition, price ranges are estimated as indicated on commercial websites in October-November 2022. We found only a limited number of papers reporting about sensitivity to environment, maintenance needs and longevity of the tested sensors. Consequently, we provide this information only when it is available.

The review revealed that low-cost sensors are frequently poorly documented and described in the literature, with many of the criteria listed in Table 2 not provided, or, when provided, given without or with insufficient details or references to the protocols and methods used. To reflect this finding, we indicate "NA" when information is missing. In the same way, the review also shows that the available literature on low-cost sensors is not always sufficiently detailed, according to metrology good practice requirements, which leads to some difficulties in interpretation. These difficulties are discussed further in Section 6.

2.3 LOW-COST METEOROLOGICAL SENSORS REVIEW

In this chapter, performance assessments of four low-cost meteorological sensors are reviewed: air humidity, wind speed, solar radiation, and rainfall, which are typical components of weather monitoring stations.

The reason for measuring air humidity, wind speed and solar radiation is that a critical component of the water cycle in urban areas and green infrastructures is evapotranspiration, which can be estimated by the FAO Penman-Monteith equation using air humidity, radiation, and wind speed data (Ndulue and Ranjan, 2021). In addition, the optimization of management and maintenance of some stormwater control measures such as wet ponds, wetlands, swales, and green roofs also depend on these local weather data (Czemiel Berndtsson, 2010).

Accurate rainfall measurements are essential for the effective management of stormwater. Historical rainfall records are used extensively in the design of water infrastructure, while at finer scales, real-time rainfall measurements are a key component of flood forecasting systems. But current methods for measuring precipitation often do not provide the spatial resolution or measurement quality required for real-time applications (Bartos *et al.*, 2019) despite the progress of rainfall radar measurement with high spatial resolution (Vos *et al.*, 2018). Large-scale ubiquitous low-cost rain gauge sensor networks hold promise to fill this gap.

2.3.1 Air humidity sensors

There are three basic types of air humidity sensors: capacitive, resistive, and thermal. Lorek (2014) tests the capacitive sensor Sensirion SHT75 in low vacuum (10 to 1000 hpa) and temperature (-70 to 25 °C) ranges and reports that it works “reliably and with reproducibly measured values”.

Most low-cost humidity sensors mentioned in the scientific literature are DHT11(Adepoju *et al.*, 2020; Hernández *et al.*, 2020; Hussein *et al.*, 2020; Leonowicz *et al.*, 2020; Morales-Morales *et al.*, 2020), DHT22 (also named AM2302) (Arzoumanian *et al.*, 2019; Azma Zakaria *et al.*, 2018; Bankar and Sagat, 2020; Math and Dharwadkar, 2017; Morón *et al.*, 2018; Pereira *et al.*, 2020; Sulzer *et al.*, 2022), BME280 (Cowell *et al.*, 2022; Lee *et al.*, 2020; Radogna *et al.*, 2022; Tagle *et al.*, 2020), 808H5V5 (SM *et al.*, 2019), SHT20 (Moreno-Rangel *et al.*, 2018; Nouman *et al.*, 2019), HTU21D (Farhat *et al.*, 2017) and HIH4000 (Bastos *et al.*, 2020).

According to manufacturer’s manuals, DHT11 cannot read the full range of relative humidity (only 20 to 90% RH), and 808H5V5 and HIH4000 cannot provide satisfactory performance (trueness of 808H5V5 at 25°C, over the range 30 to 80% RH is 4% RH, trueness of HIH4000 at 25°C, over the range 0 to 59% RH is 5% RH and increases to ±8% RH over the sub-range 60 to 100% RH). HTU21D is observed presenting significantly biased data (Araújo *et al.*, 2020). We thus do not discuss them further. The sensors we consider the most promising ones (low cost, full humidity range, best accuracy) are presented in Table 2-4 including their main technical specifications. About the performance assessments of SHT20, DHT22 and BME280, Table 2-5 gives a summary based on manufacturers data and tests in scientific studies.

Table 2-4. Specifications of low-cost air humidity sensor modules.

Model	SHT20	DHT22 / AM2302	BME280
Type	capacitive	capacitive	resistive
Size (mm)	73 × 17	14 × 18 × 5.5	15 × 12
Weight (g)	44	~ 1	~ 1
Operating range	0 to 100 %RH, -10 to 125 °C	0 to 100 %RH, -40 to 80 °C	0 to 100 %RH, -40 to 85 °C
Power supply	3.36 to 5 V DC	3.3 to 6 V DC	3.3 or 5 V DC
Communication	I2C protocol	digital signal via single bus	I^2C or SPI protocol
Performance tested in scientific literature	Yes	Yes	Yes

Table 2-5. A summary of performance characteristics of low-cost humidity sensors. *For each parameter, the source of the information is given in the superscript and when available, criteria are given (associated formulae can be found in Table 2).*

	SHT20	**DHT22 / AM2302**	**BME280**
Trueness	*3 %RH* *	*2 %RH*	*3 %RH* [b]
	Mean deviation = 0.01 %RH, r_s = 0.935 to 0.948, $p < 0.001$ [a]	Error ~ 5 %RH [b]	Mean error < 4 %RH,
		Mean error < 5 %RH, $R^2 = 0.992$, DR = 3.5 %RH [c]	$R^2 = 0.995$, DR = 2.3 %RH [c]
Repeatability	±0.1 %RH	±1 %RH	Average standard deviation
		0.5 to 1%RH [b]	< 0.6 %RH [c]
		Average standard deviation < 0.7 %RH [c]	
Reproducibility	Mean deviation = 0.52 %RH, r_s = 0.985 to 0.991, $p < 0.001$ [a]	~ 5 %RH [b]	$R^2 = 0.92, 0.76, 0.90$ [e]
Resolution	*0.04 %RH*	*0.1 %RH*	*0.008 %RH*
Response time	*8 s*	*2 s*	*1 s*
		~ 30 s [b]	
Sensitivity to environment	NA	Dependent on temperature [b]	"Least" dependent on temperature [b]
Maintenance needs	NA	NA	NA
Longevity	NA	~ 1 year [b]	NA

* According to manufacturers (*Italic type*).

NA stands for not available.

[a] Moreno-Rangel *et al.* (2018) test five SHT20 used in Fooboot FBT0002100 air quality monitor compared to a validated instrument from GrayWolf and show two days data.

[b] Smith (2018, 2017) tests six DHT22 and nine BME280 with reference to saturated solutions and distilled water.

[c] Araújo *et al.* (2020) test three AM2302 and three BME280 inside a controlled climatic chamber (Aralab© Fitoclima®) with reference to Lascar Electronics EL-USB-2.

[e] Tagle *et al.* (2020) compare the output of three BME280 with three regulatory air quality monitoring stations (HMP 35A, Vaisala) in three sites.

Moreno-Rangel et al. 2018 report that for SHT20 deviations are from -0.78 to 1.08 %RH and average deviation is -0.01 %RH, Spearman's rank-order correlation (r_s) are from 0.935 to 0.948, *p-value* < 0.001. About its reproducibility, deviations are from -1.86 to 0.75 %RH and average deviation is 0.52 %RH, r_s are from 0.985 to 0.991, *p-value* < 0.001. They conclude that SHT20 inside air quality monitoring has "very low variability" in trueness and "very strong uniformity" in reproducibility. According to the datasheet, trueness is 3 %RH, repeatability is ±0.1 %RH, resolution is 0.04 %RH and response time is 8 s.

About DHT22 (also named AM2302), (Smith, 2017, 2018) report that its trueness is expected to be around 5%, repeatability in a range 0.5 to 1 %RH and reproducibility is around 5 %RH, response time is about 30 seconds (30 seconds delay in response comparing to other humidity sensors). The authors of this review think this delay may be due to a mistake in the Arduino library. Smith also reports that the sensor output shows a dependence of up to 8 %RH over the temperature range 10 to 40°C. We cannot understand this statement because relative humidity

itself is a quantity related to air temperature. About longevity, in this test, two sensors failed after about one year and five failed after three years, with output which may suddenly increase or even saturate. (Araújo *et al.*, 2020) report that AM2302 showed mean error -4.4 to -4.2 %RH at 30 %RH, -4.2 to -2.5 %RH at 50 %RH and 0.0 to 1.5 at 80 %RH when temperature is 10, 24 and 40 °C respectively, and standard deviation of mean errors is 2.7 %RH. When using linear model to fit AM2302 output p and reference output P, they get $p = 1.118P - 9.626$ with R^2 = 0.992 and dynamic residual is 3.5 %RH. They concluded that AM2302 is "overestimating the relative humidity variations". In all above situations, average standard deviation of repeatability is less than 0.70 %RH. The sensor datasheet claims that trueness is 2 %RH, repeatability is ±1 %RH, resolution is 0.1 %RH and response time is 2 seconds.

About BME280, Smith (2018) reports that it performed within specifications. Its output values had dependence of less than 3 %RH over the range 10 to 40°C. (Araújo *et al.*, 2020) report that BME280 showed mean error -1.4 to -3.9 %RH at 30 %RH, -3.0 to -1.2 %RH at 50 %RH and 0.7 to 2.2 at 80 %RH when temperature is 10, 24 and 40 °C respectively, and standard deviation of mean error is 2.1 %RH. When using linear model to fit BME280 output p and reference output P, they get $p = 1.084P - 6.333$ with R^2 = 0.995 and dynamic residual is 2.3 %RH. In all above situations, average standard deviation of repeatability is less than 0.60 %RH. In the comparison work of (Tagle *et al.*, 2020), some of their BME280 modules show output saturation (at 30 %RH) and underestimate 100 %RH, this indicates its poor reproducibility. The sensor datasheet claims that trueness is 3 %RH, resolution is 0.0008 %RH and response time is 1 s.

The World Meteorological Organization (WMO) recommends the following accuracy performances: 1% at high values of relative humidity (80% or more) and 5% at moderate values of relative humidity (Araújo *et al.*, 2020). According to available literature, trueness, repeatability, and resolution of SHT20, DHT22 and BME280 modules are close to this recommendation. Their resolution and response time can meet every minute monitoring. We do not think they have maintenance needs, because it is more convenient to replace them when using separate modules. The main problems of these low-cost air humidity sensors are their reproducibility (high variability from sensor to sensor) and longevity (output saturation or underestimation). Facing these problems, we recommend end-users to purchase them from reliable sources, take care of data quality and replace them every year. Sensor housing is another key concern. We note that these low-cost sensors are provided with naked circuit boards, plastic housings

or waterproof probes. What housing is more suitable for field use and the effect of the housing on sensor performance are issues that need to be investigated.

2.3.2 Wind speed sensors

Many types of anemometers exist. When examining the low-cost anemometers cited in the literature, we found that three-cup anemometers are used in many applications due to their simplicity and low-cost features. The modules mentioned in the papers are SKU: SEN-08942 (Khattab *et al.*, 2016; Prabhakaran and Ravindran, 2019; Sarkar *et al.*, 2020), SKU: SEN-15901 (Flores, 2020; Fortes *et al.*, 2021; Kaewwongsri and Silanon, 2020), WS-2080 (Domínguez-Brito *et al.*, 2020; Tai *et al.*, 2017), and SKU: SEN0170 (Hussein *et al.*, 2020; Nouman *et al.*, 2019; Semenov *et al.*, 2019).

Based on the information available on the internet, SEN-08942, SEN-15901 and WS-2080 are weather station kits. SEN-15901 is the latest version of SEN-08942 and has the same appearance as WS-2080. It seems that the difference between SEN-15901 and WS-2080 is that SEN-15091 has only mechanical parts and does not contain electronic parts such as controller and monitor. The separate anemometer module used in SEN-15901 is called WH-SP-WS01. SEN0170 is a separate anemometer module. Specifications of WS-2080, WH-SP-01 and SEN0170 are presented in Table 2-6. Table 2-7 gives a summary of the performance of the low-cost anemometer modules by manufacturer and tested by scientific studies.

Table 2-6. Specifications of low-cost anemometer modules.

Model	WS-2080	WH-SP-WS01	SEN0170
Type	Weather station kit	Three cups anemometer	Three cups anemometer
Material	Plastic	Plastic	Aluminum alloy
Size (cm)	76 ×48	~ 7 ×10 ×10	13 ×20×20
Weight (kg)	2.5	0.3	NA
Measurement range (m/s)	0 to 50	NA	0.8 to 30
Power supply	Batteries	No need	9 to 24 V DC
Output signal	Wireless communication	Close of reed switch	0 to 5 V
Price range (€)	~ 150	~ 20	~ 50
Performance tested in scientific literature	Yes	No	Yes

Table 2-7. A summary of performance characteristics of low-cost anemometer modules.

Model	WS-2080	WH-SP-WS01	SEN0170
Trueness	*0.98 m/s or 10 %* [a] R^2 = 0.951, MBE = - 0.167 m/s, RMSE = 0.468 m/s [d]	NA	*3 %* R^2 = 0.3162 [f]
Repeatability	NA	NA	NA
Reproducibility	NA	NA	NA
Resolution	*0.04 m/s*	*0.33* [b] *or 0.67* [c]	*0.1 m/s*
Response time	NA	NA	NA
Sensitivity to environment	NA	NA	*Working humidity: 35 to 85 %RH (no condensation)*
Maintenance needs	*Clean the connectors once every 1 to 2 year*	NA	NA
Longevity	> 1 year [e]	NA	NA

[a] The original remark in user manual is "whichever is greater".

[b] The original text in the datasheet is "wind speed 0.33 m/s causes the switch to close once" in Chinese.

[c] The original text in the datasheet is "a wind speed of 2.4 km/h causes the switch to close once per second" in English.

[d] Domínguez-Brito *et al.* (2020) undertake an experimental comparison in real conditions with scientific-grade Thies Clima anemometer model 4.3159.00.140 for 90 minutes.

[e] Tai *et al.* (2017) use WS-2080 at northern Lake Tahoe.

[f] Nouman *et al.* (2019) test performance of SEN0170 compared to a TESTO Air Flow Probe 06280143 whose accuracy is ±0.03 m/s.

About anemometer part of WS-2080 or named WH-SP-WS01, regarding its trueness, in the test of Domínguez-Brito et al. (2020), data were collected at 1 Hz, and they applied a centered median filter with 30 seconds threshold to cancel noises in the wind speed data. They report that between low-cost sensor and reference, regression analysis coefficient is 0.951, but they do not give the function, mean bias error is -0.167 m/s and mean square error is 0.468 m/s. They consider these results "to be a good fit" because that "sensors not being mechanically identical and not being situated at exactly the same position". Regarding its longevity, Tai *et al.* (2017) use it in field for one year and do not mention any running problems. According to the user manual of WS-2080, the maintenance need is cleaning the connectors once every 1 to 2 years. Unfortunately, user manual of WS-2080 and data sheet of WH-SP-WS01 give three resolutions to convert raw signal (close of reed switch) to wind speeds (0.04, 0.33 and 0.67 m/s) and Domínguez-Brito *et al.* (2020) do not report the value that they use.

About SEN0170, it showed poor trueness (R^2 = 0.3162) as it is not sensitive to wind speed below 0.8 m/s (Nouman *et al.*, 2019). According to the datasheet, accuracy is 3%, resolution is 0.1 m/s, and it is recommended to work in air humidity range 35 to 85 %RH (no condensation). We do not find assessments of other criteria.

In general, it seems that the only low-cost anemometer choice is WH-SP-WS01. The maintenance need is that the connectors should be cleaned every one or two years and users can avoid this if they don't use the original

connectors. Main problems of WH-SP-WS01 are (i) unknown repeatability and reproducibility which is especially critical when use many of them to model a wind field, and (ii) unknown true resolution to convert the close signal of internal reed switch into wind speed: this problem can be solved when comparing it with a reference.

2.3.3 Solar radiation sensors

Broadband solar radiation or global irradiance is an electromagnetic spectrum in the wavelength range of 300 to 3000 nm (WMO) or 350 to 1500 nm (ISO) (Azouzoute *et al.*, 2019). Pyranometers are designed to measure this physical quantity. They are standardized according to the ISO 9060 (International Organization for Standardization, 2018) standard, which is also adopted by the World Meteorological Organization (WMO). This standard discriminates three classes: the best is called Class A (old name: secondary standard), the second-best Class B (old name: first class) and the last one Class C (old name: second class).

There are three kinds of pyranometers: thermopile pyranometers, silicon photodiode pyranometers and photovoltaics (PV) reference cells (Karki *et al.*, 2021). Thermopile pyranometers measure irradiance with a spectral response from 280 to 2800 nm. They usually cost thousands of euros, are often considered as Class A standards and used as reference devices to test other types of pyranometers. Silicon photodiode pyranometers usually cost hundreds of euros. They are a low-cost and lower-maintenance option compared to thermopile pyranometers but can only measure irradiance with a spectral response from 300 to 1100 nm (López Lorente *et al.*, 2020). Recently, an emphasis focused on the use of separate photodiodes which cost tens of euros to measure solar radiation (Espinosa-Gavira *et al.*, 2018; Salgado *et al.*, 2020; Tohsing *et al.*, 2019). As for photovoltaic reference cells, we found that their prices were hundreds of euros in 2010 and decrease due to price decrease of photovoltaic modules.

The authors of this review believe that there are hundreds of commercially available pyranometers on the shelf. There are no need and necessity to list them all out. We present four widely used and representative sensors: Apogee CS300 (Patrignani *et al.*, 2020; Schenk *et al.*, 2015), ISET (Azouzoute *et al.*, 2019), Si1145 (Burgt, 2020; Theisen *et al.*, 2020) and ML8511 (Burgt, 2020). Their specifications are given in Table 2-8. Table 2-9 gives a summary of the performance of the low-cost pyranometers given by manufacturer and tested by scientific studies.

Table 2-8. Specifications of low-cost pyranometers.

Model	CS300	ISET	Si1145	ML8511
Type	photodiode	photovoltaics	light sensor	UV sensor
Size (mm)	24×24×25	NA	20×18×2 [a]	30×22 [b]
Weight (g)	65	NA	1.4 [a]	NA
Light spectrum waveband (nm)	360 to 1120	NA	400 to 1000	280 to 560 [d]
Measurement range	0 to 2000 W/m^2	NA	1 to 128 kilolux	NA
Output	Voltage signal	Voltage signal	Counts through I2C	1 to 2.8 V DC
Power requirements	non, self-powered	NA	3 to 5 V DC	3.3 to 5 V DC
Price range (€)	~ 300	~ 400	~ 10	~ 10
Performance tested in scientific literature	Yes	Yes	Yes	Yes

[a] Specifications of module from Adafruit.

[b] Specifications of module from DFRobot.

[c] Infrared sensor spectrum: wavelength: 550 to 1000 nm (centered on 800 nm), visible light sensor spectrum: wavelength: 400 to 800 nm (centered on 530 nm).

[d] Sensitivity wavelength: UV-A (320 to 400nm), UV-B (280 to 320nm).

Table 2-9. A summary of performance characteristics of low-cost pyranometers.

Model	CS300	ISET	Si1145	ML8511
Trueness	*± 5%* [a] Mean deviation = -10.4 to 9.1 W/m^2, standard deviation = 41.4 to 47.1 W/m^2 [c]	*<± 5%* [b] MBE = -19.57 W/m^2 (June), MBE = -2.398 W/m^2 (December) [d]	RMSE = 34.14 to 81.64 W/m^2, R^2 = 0.96 to 0.99 [e] RMSE = 46.37 W/m^2 [f]	RMSE = 46.37 W/m^2 [f]
Repeatability	*manufacture calibration*	*manufacture calibration*	NA	NA
Reproducibility	*manufacture calibration* "Show good agreement when not shaded" [c]	*manufacture calibration*	NA	NA
Resolution	*0.2 mV per W/m^2*	*0.1 mV per W/m^2*	*100 microlux*	NA
Response time	*< 1 ms*	< 10 s [d]	< 2 s [f]	< 2 s [f]
Sensitivity to environment	NA	"PV cells are highly affected by the high temperature values." [d]	NA	NA
Maintenance needs	*Check and clean once every month*	NA	NA	NA
Longevity	> 1 year [c]	NA	> 8 months [e]	NA

[a] For daily total radiation.

[b] The relative measurement uncertainty is < ±4% (crystalline Material) and /< ±5% (amorphous material). The measurement uncertainty refers to a confidence level of 1-alpha = 95%.

[c] Schenk *et al.* (2015) compare three CS300 with a Kipp & Zonen CMP11 thermopile pyranometer that is installed 250 meters away and then use CS300 in field.

[d] Azouzoute *et al.* (2019) compare ISET sensor 02581 with a Hukseflux thermal sensor SR11 classified as a Class B specification sensor at same site and give the results in June and December respectively.

[e] Theisen *et al.* (2020) compare output counts of Si1145 with LI-COR pyranometer that has an accuracy of ±5 % from August 2018 to March 2019.

[f] Burgt (2020) calibrate and validate output of ML8511 and Si1145 comparing to pyranometer Davis Instruments Vantage Pro 2.

About CS300, regarding its trueness, Schenk *et al.* (2015) reported that, compared to reference, the mean deviations of three CS300 are 6.2, 9.1 and -10.4 W/m^2 respectively and standard deviations are 43.2, 41.4 and 47.1 W/m^2 respectively. They conclude that CS300 is "the most economical solution" compared to two semiconductor pyranometers they tested. After this test, Schenk *et al.* (2015) use 20 CS300 in the field for more than one year and report that CS300 show "good agreement between the sensors" when they are not shaded but do not give any metric details. The manufacturer of CS300 indicates that it is calibrated against a Kipp & Zonen CM21 thermopile pyranometer and have an absolute accuracy of ±5% for daily total radiation, its resolution is 0.2 mV per W/m^2, its response time is less than 1 ms and it needs to be checked and cleaned every month.

About ISET sensor, Azouzoute *et al.* (2019) read its output every 10 seconds and compare to reference in time resolution 1 minute. Regarding to trueness, they report that in June, mean bias error (MBE) is -19.57 W/m^2, root mean square error (RMSE) is 45.946 W/m^2, normalized root mean square error (NRMSE) is 11.292%, *t*-statistic (TS) is 82.381, standard deviation (SD) is 41.569 and coefficient of determination (R^2) is 0.993. In December, MBE is -2.398 W/m^2, RMSE is 13.027 W/m^2, NRMSE is 3.913 %, TS is 30.975, SD is 12.804 and R^2 is 0.999. They conclude that "the reference cells underestimate the plane of array irradiance values. This underestimation is much higher in the summer than the winter, which is completely understandable, since the PV cells are highly affected by the high temperature values", even though the ISET sensor has an integrated Pt100 temperature sensor to compensate its output. According to manufacturer, it is professionally calibrated and came with a certificate. It has a relative measurement uncertainty of < ±5%, and a resolution of 0.1 mV per W/m^2.

About light sensor Si1145 and ML8511, they are not initially designed to be a pyranometer. Theisen *et al.* (2020) find there is a linear correlation between the downwelling global solar radiation measured by LI-COR pyranometer P and the output counts p of Si1145: $P = 0.70p + 170.66$. But Si1145 has three outputs: infrared light counts, visible light counts, and UV index, and Theisen *et al.* (2020) do not describe which Si1145 output they use. Using this calibration function, they report that from August 2018 to March 2019, every month RMSE is from 34.14 to 81.64 W/m^2 and correlation coefficient is from 0.96 to 0.99. Burgt (2020) connects ML8511, Si1145 and reference pyranometer to a Wemos D1 Mini microcontroller and uses an analog to digital converter ADS1115 to read output of ML8511 and reference pyranometer. All his measurements are taken every 2 seconds. He reports that calibration function is $P = -224.739p_{Si\,UV} + 1.410168p_{Si\,VIS} + 0.036012p_{Si\,IR} + 3.626188p_{ML} - 397.597$ where P is the output of the reference pyranometer in W/m^2. The authors of this review guess that $p_{Si\,UV}$ is the UV index

output of Si1145, $p_{Si\,VIS}$ is the visible light counts output of Si1145, $p_{Si\,IR}$ is the infrared light counts output of Si1145 and P_{ML} is the output voltage of ML8511 but we do not know their units. About this calibration function, adjusted R^2 is 0.995, standard deviation is 23.93, significance F is 0 and all p-values are below 0.05. In the 2 hours validation test at a sunny afternoon, RMSE is 46.37 W/m^2, but there is a negative "offset of about 50 W/m^2, when the solar irradiance is at a value of about 200 to 400 W/m^2." (Burgt, 2020). The datasheet of Si1145 indicates that its resolution is 100 microlux.

When designing a solar radiation sensing network, there are two main choices. One choice is to use commercial pyranometers such as CS300 and ISET: they are calibrated by manufacturers and provide reliable trueness, repeatability, reproducibility, resolution, response time and longevity (Azouzoute *et al.*, 2019; Schenk *et al.*, 2015). Another choice is to use cheaper light sensors such as Si1145 and ML8511. In that case, users need to calibrate and house them (Burgt, 2020; Theisen *et al.*, 2020). If funds allow, it is highly recommended to use a Class A thermopile pyranometer as reference. WMO standard specifies a resolution of 5 W/m^2 and an uncertainty of 8% hourly totals (5% daily totals for Class B pyranometers). According to the authors of this review experience, the output of CS300, ISET and ML8511 is voltage signal and the analog to digital conversion module of Arduino is not accurate enough, it is thus necessary to use an additional analog-to-digital converter such as an ADS1115. All pyranometers are recommended to be checked and cleaned every month.

2.3.4 Rainfall sensors

In stormwater management, accurate and timely rainfall monitoring is a prerequisite. Rain gauges are the key standard equipment for monitoring rainfall. A variety of rain gauges exist. To compare rain gauges based on different measuring principles, the World Meteorological Organization (WMO) organized field intercomparison from October 2007 to April 2009 in Vigna di Valle, Rome (Italy) involving 30 different types of rain gauges. Results indicate that synchronized tipping-bucket rain gauges (TBRG), using internal correction algorithms, and weighing gauges (WG) with improved dynamic stability and short step response are the most accurate gauges for one-minute rainfall intensity measurements, providing the lowest measurement uncertainty with respect to the assumed working reference (Lanza and Vuerich, 2009). But this report does not mention any gauge model or any manufacturer.

We identified four low-cost rainfall sensors mentioned in the scientific literature: droplet detector YL-83 (Islam *et al.*, 2021; Rivas-Sánchez *et al.*, 2019), tipping bucket rain gauge WH-SP-RG (Abeledo *et al.*, 2016; Chan *et al.*, 2021), optical rainfall detector RG-11 (Bartos *et al.*, 2018) with no guaranteed accuracy to measure rainfall intensity, and Pluvimate drop-counting rain gauge (Michelon *et al.*, 2020). According to information available on the internet, WH-SP-RG is part of the weather station kit SEN-15901 or WS-2080. RG-11's manufacturer also provides a latest version named RG-15 with guaranteed accuracy. Their specifications are given in Table 2-10.

Table 2-10. Specifications of low-cost rain sensors.

Model	YL-83	WH-SP-RG	RG-15	Pluvimate
Type	droplet detection [a]	tipping bucket	optical monitoring	drop counting
Size (mm)	90×46×157	110×55×95	120×70×55	NA
Wight (g)	500	160	155	NA
Range (mm)	NA	0 to 155[b]	NA	NA
Supply voltage	12 V DC ±10%	NA	5 to 15 V or 3.3 V [c]	3.6 V battery
Supply current	<= 260 mA	NA	<= 4 mA	NA
Output	1 to 3 V	tips	RS232 at 3.3 V	NA
Price range (€)	~ 3	~ 20	~ 80	~ 600
Performance tested in scientific literature	No	Yes	No	Yes

[a] Minimum wet area 0.05 cm^2 and sensing area is 7.2 cm^2.

[b] According to user manual of WS-2080 page 35.

[c] 5-15 V DC on J1 (reverse polarity protected to 50V), or 3.3V DC through pin 8 on J2.

According to the datasheet from VASALA, YL-83 capacitive sensor has a housing which makes it waterproof. But only its bare circuit boards can be retrieved and purchased online. Although some applications have been reported (Islam *et al.*, 2021; Rivas-Sánchez *et al.*, 2019; Wisudawan, 2021), papers do not mention any evaluation. Rivas-Sánchez *et al.* (2019) calibrate YL-83 with the value (ON/OFF) to detect if there is a rainfall or not and they show the output voltage change of YL-83 during a rainfall event. But they do not describe the method of calibration and the correspondence of the output of YL-83 to the rainfall intensity. Dias (2019) reports that YL-83 is oxidated after the first occurrence of rain.

Probably because RG-15 appeared more recently on the market, there is no scientific literature reporting the application of RG-15. RG-15 and RG-11 appear similar and there are some scientific papers about RG-11.

Table 2-11 gives a summary of the performance of the low-cost rain gauges given by manufacturer and tested by scientific studies.

Table 2-11. A summary of performance characteristics of low-cost rain gauges.

Model	WH-SP-RG	RG-15/ RG-11	Pluvimate
Trueness	*10%* [a]	*10%* [b] Average absolute percent deviation = 86.9 %, R^2 = 0.75 [h]	<15% (before calibration, 0to150 mm/h) [k] ~ 5 % (after calibration, 5 to 20 mm/h) [j]
Repeatability	NA	NA	NA
Reproducibility	NA	NA	mean bias 13.9% [j]
Resolution	*0.254* [a] *or 0.2794* [c] *or 0.3 mm/tip* [d] 2.5 ± 0.08 mL/tip, R^2 = 0.98 [f]	*0.2 or 0.02 mm* [e]	*0.010 mm*
Response time	NA	NA	NA
Sensitivity to environment	NA	NA	NA
Maintenance needs	NA	*After 7 to 10 years the lens will need to be replaced.*	*check the filter and the drain holes from time to time*
Longevity	> 1 year [g]	> 1 year [i]	> 3 months [k]

[a] According to user manual of WS-2080 page 35.

[b] On the website of RG-15, manufacturer writes “Field accuracy will vary”.

[c] In datasheet of SEN-15901: the original text is “Each 0.2794 mm of rain causes one momentary contact” in English.

[d] In datasheet of SEN-15901: the original text is “Each 0.3 mm of rain causes one momentary contact closure” in Chinese.

[e] In the website of RG-15, “Depending on option selected” written by manufacturer.

[f] Coloch Tahuico (2021) checks the resolution of WH-SP-RG by pouring a known volume of water inside it and then counting the tips.

[g] Tai *et al.* (2017) use WS-2080 at northern Lake Tahoe.

[h] Steele *et al.* (2014) compare RG-11 with manual rain gauge (typically are cylindrical and totalize the rainfall accumulated between visits to the field site).

[i] Moore *et al.* (2020) use RG-11 in Zadko Obervatory.

[j] Benoit *et al.* (2018) evaluate the performance of eight Pluvimates.

[k] Michelon *et al.* (2020) claim that Pluvimate is a low-cost sensor, and they use 12 Pluvimates in the Swiss Alps for three months.

WH-SP-RG appears as part of weather station kits WS-2080. Coloch Tahuico (2021) increases its collector area from 55 cm^2 to 314 cm^2 (calculated from design drawing, he describes it in the text as 1000 cm^2, maybe a mistake). And then he pours 1.6 to 1000 mL water and the sensor output 1 to 434 tips. he concludes that sensor resolution is 2.5 ± 0.08 mL/tip (R^2 = 0.98). The authors of this review do not think this a correct dynamic calibration method because pouring much water into the tipping bucket rain gauge means always simulating an unrealistic heavy rainfall and it seems that a curve function is much suitable in his calibration chart. Coloch Tahuico (2021) does not mention any in field test results. Tai *et al.* (2017) use WS-2080 at northern Lake Tahoe for one year and did

not mention any running problems. According to the user manual of WS-2080, WH-SP-RG has an accuracy of 10% and a resolution of 0.254 mm, but according to the datasheet of WH-SP-RG, its resolution is 0.2794 or 0.3 mm/tip in different languages.

About RG-15, its appearance is similar to RG-11. Steele *et al.* (2014) report that the average absolute percent deviation of RG-11 from a manual rain gauge is 86.9% and linear regression produces an R^2 of 0.75. They find that RG-11 tended to overestimate large rainfall events and underestimate smaller rainfall events. Moore *et al.* (2020) used RG-11 for one year in the field to detect rainfall events without error which is a reference to the longevity of RG-15. The manufacturer indicates that its accuracy is ±10% but field accuracy will vary. It has a resolution of 0.2 or 0.02 mm depending on the selected option, and its maintenance need is only replacing the lens after 7 to 10 years.

About Pluvimate sensor, (Benoit *et al.*, 2018) report that after bias correction for rainfall intensities 5 to 20 mm/h, the measurement uncertainties of seven Pluvimates sensors are less than 5% and one was slightly exceeding this value. For its reproducibility, they pass a known amount of water through the funnel and compare the recorded water depth to the known input (i.e., static calibration). The measured bias of eight sensors ranges from 2.8% to 23% with a mean bias of 13.9%. Michelon *et al.* (2020) do a dynamic calibration of a Pluvimate and report that the calibration curve is $p = -0.00059P^2 + 0.92P + 0.89$, $R^2 = 0.998$, where P is the generated rainfall intensity and p is the measured rainfall intensity in mm/h, which means that the measuring uncertainty is below 5 % for 0 to20 mm/h generated rainfall intensity and reach -10% of error at 60 mm/h and -15% at 150 mm/h. They used it in the field for 3 months. The manufacturer indicates a resolution of 0.010 mm and a maintenance need include checking its filter and drain hole.

In general, rain gauges WH-SP-RG and RG-15 deserve further tests. The drawbacks of WH-SP-RG are (i) a small collection area (only 55 cm^2), and (ii) in case of heavy rainfall events, water tends to splash because it has no visible cone or funnel (Coloch Tahuico, 2021). So WH-SP-RG needs to be adapted or transformed to be used in the field. The resolution of WH-SP-RG needs more investigation. It needs to check and clean every month to avoid drain hole blockage. For optical rain gauge RG-15, the point is to test whether it can really deliver the performance claimed by the manufacturer. We think that it is better to check and clean the surface of RG-15 every month like pyranometers.

2.4 LOW-COST WATER QUANTITY SENSORS REVIEW

In this chapter, three water quantity parameters are selected for review: water level, flow, and soil moisture.

2.4.1 Water level sensors

Water level is one of the most important parameters when monitoring stormwater. The correct and timely monitoring of this quantity is also related to the ability to achieve satisfactory urban stormwater management. There are many types of water level measurement devices such as float system, pressure-measuring devices, capacitive devices, ultrasonic devices, radar devices, and radiation devices (Morris and Langari, 2016). When narrowing the range to low-cost sensors. according to available comparisons and wireless system design, two types of water level sensors are commonly used: non-contact ultrasonic sensors and contact pressure sensors.

There are many kinds of ultrasonic and pressure sensors reported in the literature. Five sensors commonly found in articles and communities are selected: HC-SR04 (Intharasombat and Khoenkaw, 2015; Nasution *et al.*, 2018; Shrenika *et al.*, 2017; Sumitra *et al.*, 2017), JSN-SR04T (Andang *et al.*, 2019; Cherqui *et al.*, 2020a; Dswilan *et al.*, 2021), MS5803-01BA (Cherqui *et al.*, 2020a; Kombo *et al.*, 2021; Shi *et al.*, 2021), Kingspan Watchman Anywhere Pro (Zhang *et al.*, 2019) and TL231 (or named TL-231, TL136, ASL-MP-2F) which has not been investigated in scientific papers. Their user manuals specifications are listed in Table 2-12. In addition, we noted that JSN-SR04T has different versions. In some papers, it may be the original version while the version indicated in Table 2-12 is the version 2.0 with higher specifications. Kingspan Watchman Anywhere Pro is a complete off-the-shelf solution with ultrasonic transducer, control board, communication module, battery and housing. Table 2-13 gives a summary of the performance of the low-cost water level sensors given by manufacturer and tested by scientific studies.

Table 2-12. Specifications of low-cost water level sensors.

Model	HC-SR04	JSN-SR04T	Kingspan…Pro	MS5803-01BA	TL231
Principle	ultrasonic	ultrasonic	ultrasonic	pressure	pressure
Type	module	waterproof module	waterproof kit	module	waterproof module
Installation	above water	above water	above water	under water	under water
Size (mm)	45×20×15	42×29×12	NA	NA	100×280
Weight (g)	~ 5	~ 20	NA	~ 3	577
Range (cm)	2 to 400	20 to 600	12 to 400 [a]	0 to 1200	0 to 500
Power supply	5 V DC	3 to 5.5 V DC	fitted batteries [b]	1.8 to 3.6 V DC	24 V DC
Working frequency	40 kHz	40 kHz	NA	NA	NA
Output	digital (voltage)	digital (voltage)	NA	I^2C or SPI	4 to 20 mA
Price range (€)	< 5	< 10	< 200	< 30	~ 50
Performance tested in scientific literature	Yes	Yes	Yes	Yes	No [c]

[a] Based on a measurement to a flat liquid target of size 30 cm^2.

[b] 4 of Type C LR14 Alkaline 1.5V.

[c] Trueness of TL231 given by manufacturer is 0.2 but unit is not specified.

Table 2-13. A summary of performance characteristics of low-cost water level sensors.

Model	HC-SR04	JSN-SR04T	Kingspan…Pro	MS5803-01BA
Trueness	Mean error = 0.97 %, RMSE = 0.36 cm [a] Average accuracy = 96.6 % [b]	*10 mm* Error < 5 mm, error rate = 0.74 % [c] Expected accuracy < 10 mm [d]	*20 mm* r_s > 0.97, MAE < 1.12 mm [e]	*2.5 mbar (to 25 mm)* ±5 mm [d] Errors from -36.7 to 33.8 mm [f]
Repeatability	NA	7 mm [d]	NA	3 mm [d]
Reproducibility	NA	NA	NA	0.72 mbar (~ 7.2 mm) [d]
Resolution	NA	*1 mm*	*10 mm*	*0.012 to 0.065 mbar (About 0.12 to 0.65 mm)*
Response time	NA	< 250 ms [d]	< 15 mins	< 150 ms [d]
Sensitivity to environment	NA	Mandatory to correct according to air temperature, there should be no obstacles surrounding the sensor [d]	Spider nests interference and vandalized by somebody, rainfall events make output noisy [e]	Not impacted by sediment loads, some moisture uptakes in the sensor white gel that can lead to sensor drift. [f]
Maintenance needs	NA	Limited [d]	No [e]	Calibrated every two weeks [f]
Longevity	NA	> 300,000 measures [d]	> 2 years [e]	> 1 year [f]

[a] Sumitra *et al.* (2017) test HC-SR04 comparing to manually measurement in a distance to water surface less than 0.2 m.

[b] Nasution *et al.* (2018) test HC-SR04 comparing to manually measurement in a distance to water surface I the range 0.8 to 1.3 m.

[c] Andang *et al.* (2019) test JSN-SR04T by measuring the water level of a river compared with the manual distance measurement results.

[d] Cherqui *et al.* (2020) test the performance of JSN-SR04T and MS5803-01BA in lab in a water level range 0 to 2 m using an automatic system they developed with a reference sensor OTT PLS pressure transducer that has an accuracy <= ± 2mm.

[e] Zhang *et al.* (2019) compare the output of four Kingspan Watchman Anywhere Pro with nearby hydrometric station for one month and use nine along River Dodder.

[f] Shi *et al.* (2021) test MS5803-01BA in lab for two months and in field (pipe) for one year comparing with a HACH probe.

About HC-SR04, Sumitra *et al.* (2017) report that its mean error is 0.97% but they only record data in centimeter and do not describe the calculation details of water level from echo time. Nasution *et al.* (2018) do a lab test and report that the average accuracy is 96.6 % (they define accuracy as measurement value / reference value) but in their test, measurement value is always lower than true value, we think there may be a systematic error that is not corrected, and they also do not describe the calculation details.

About JSN-SR04T, Andang *et al.* (2019) use $D = 170T$ where D is the distance in metre and T is the echo time in seconds and they assume that sound speed is always 340 m/s. They report that the errors between JSN-SR04T and reference are always less than 5 cm in a range 0 to 200 cm and that the error rate is 0.74%. Cherqui *et al.* (2020) report that its distance measure range is 0.225 to1.9 m, expected accuracy can be less than 10 mm when adjusting the speed of sound for the correct temperature and humidity (error can increase up to 130 mm with a 40 °C difference and increase to 23 mm with a 100% relative humidity difference), its repeatability is 7 mm and it should be installed far from obstacles because it has a wide beam (70 degrees). During the laboratory experiment JSN-SR04T recorded a total of more than 300,000 values without fault or drift. The maximum measurement time is 250 ms (includes the measurement itself, processing of the measure by the micro-controller and transfer to the computer to be stored via serial). They believe that ultrasonic sensor needs little maintenance because it is not in contact with water so that it will be not fouled by sediment, debris or algal growth. According to the datasheet of JSN-SR04T, its resolution is 1 mm.

About Kingspan Watchman Anywhere Pro, Zhang *et al.* (2019) report that during their four units in field comparison in a water level in the range 0 to 1.2 m, Spearman's rank correlations between Kingspan sensor and reference outputs are 0.9907, 0.9893, 0.9736, 0.9786 respectively, and mean absolute errors are 0.92, 0.76, 1.12, 0.74 mm respectively. They conclude that "the low-cost remote sensor measurements are very close to the reference DCC (Dublin City Council) stations." But the authors of this review find that in their comparison chart of the unit which has mean absolute error 0.74 mm, at many reference water levels, Kingspan sensor's output has a deviation around 50 mm. Zhang *et al.* (2019) also report that throughout the duration the deployment in field for more than two years with sample rates of 15 min, there is no field maintenance need, but one sensor is influenced by spider nests and two sensors are destroyed by somebody.

About liquid pressure sensor MS5803-01BA， Cherqui *et al.* (2020) report that it includes a temperature compensation, but that there is a need to use a second sensor to measure atmospheric pressure to calculate the relative pressure. They report that for two MS5803-01BA sensors (one under water and one above water), trueness is ±5 mm and repeatability is 3mm when measuring water level ranging from 0 to 1.9 m. During their test, like JSN-SR04T, MS5803-01BA can also output more than 300,000 measurements without fault or drift and maximum measurement time is 150 ms. Shi *et al.* (2021) also use two MS5803-01BA to measure water level. They report that MS5803-01BA drifts clearly in water and they think this is because of water uptakes in the layer of white gel protection in the sensor. Facing this drawback, Shi *et al.* (2021) report that during manual re-calibration, for three test sensors, absolute errors can decrease from -20.6 to 34.4 mm to -8.4 to 2.3 mm in the lab. In their field test, they install the reference sensor 76 mm higher than low-cost sensor because that reference sensor is impacted by sediment loads and low-cost sensor is not, but do not explain why. With automated recalibration every 14 days, absolute errors decrease from -18.1 to 110.8 mm to -36.7 to 33.8 mm. They find that even without calibration, MS5803-01BA can still "adequately detect the water level trend" (almost same results as the reference with $R^2 \sim 1$). They also report that two MS5803-01BA have 0.72 mbar difference in air which is an indicator of reproducibility. According to the datasheet, trueness is about 25 mm and resolution is about 0.12 to 0.65 mm.

Complete solutions like Kingspan Watchman Anywhere Pro with reasonable price allows for rapid deployment. In this way, end users can focus on data collection and processing. For ubiquitous sensor networks, non-contact ultrasonic sensors HC-SR04 and JSN-SR04T installed above water have almost no maintenance needs except spider nest interference and man-made damage. But sensor outputs will be noisy in case of events. It is important to correct sound velocity by air temperature (correction for air relative humidity is less important because this parameter has a more reduced impact on sound velocity than air temperature). HC-SR04 is not waterproof, which means additional development work is required. JSN-SR04 is waterproof but its maximum accurate measurement range is limited to 2 m. Contact pressure sensors installed under water can avoid human damage and situations where water level cannot be monitored from above (e.g., presence of vegetation). However, Shi *et al*. (2021) report that MS5803-01BA experiences a drift issue in water due to water absorption of the sensor's white protective layer so that MS5803-01BA needs to be re-calibrated at least every two weeks to achieve "accuracy" ±10 mm. TL231 is a sensor worth testing: although slightly expensive, it provides waterproof metal housing and possible manufacturer calibration.

2.4.2 Water flow sensors

Water flow monitoring is crucial for hydrological monitoring. In this review, water flow (discharge) sensors are sensors that can measure velocity of water in a river, a stream, or a sewer. Low-cost flow sensors currently off-the-shelf are relatively scarce.

The most frequent type of sensors are Doppler velocity radars. We identified two representative works. Alimenti *et al.* (2020) propose a prototype of a low-cost continuous wave (CW) Doppler radar sensor, able to monitor the surface flow velocity of rivers. Their field results show a residual velocity standard deviation of 0.07 m/s compared to a commercial handheld radar sensor Decatur SVR. There are some 24 GHz radar module off-the-shelf such as CDM324 (or named IPM165), SEN0306 (SKU, from DFRobot), and 10 GHz module HB100. We cannot find papers describing in detail the usage of these sensors for water flow monitoring. Fulton *et al.* (2020) use a Doppler velocity radar QCam to measure surface velocities and river discharge. Compared to conventional stream gauging methods, percent differences were 0.3%, 2.5%, −10.4%, 7.3% and −18.8% in five flights. They thought QCam was relatively inexpensive (compared to traditional radar sensors) but still costed about 6000 €. In addition, some papers reported the use of the low-cost flow sensor YF-S201 (or other similar models such as G1/2), initially designed for pipelines, to measure flow rate in open channels or natural watercourses (Jegadeesan and Dhamodaran, 2018; Koshoeva *et al.*, 2021; Yuniarti *et al.*, 2021). However, these papers are poorly informative for our review. The specifications of YF-S201 are given in Table 2-14.

Table 2-14. Specifications of YF-S201 low-cost discharge sensor.

Parameter	Description
Principle	Hall-effect
Size (mm)	63×36×35
Weight (g)	43
Range	1 to 30 L/min
Resolution	NA
Power supply	4.5 to18 V DC
Output	5V TTL[a]
Longevity	300,000 cycles
Price range (€)	< 5
Trueness	±10%
Repeatability	NA
Reproducibility	NA
Resolution	0.13 L/min
Response time	NA
Sensitivity to environment	Working environment: -25 to +80°C, 35% to 80% RH, water pressure < 2.0 MPa
Maintenance needs	NA
Longevity	> 300,000 cycles

[a] Flow rate pulse characteristic: frequency (Hz) = 7.5×flow rate (L/min). Output duty cycle: 50% ±10%. Output rise time: 0.04 μs. Output fall time: 0.18 μs. 450 pulses per litre.

In general, water flow monitoring does not have low-cost solutions. Image-based methods (e.g. Giordan *et al.*(2018); Koutalakis *et al.* (2019); Patalano *et al.* (2017); Sanyal *et al.* (2014); Zhu and Lipeme Kouyi, (2019)) may be low-cost in the future thanks to advances in electronics and artificial intelligence technology. It seems unrealistic to send all the images to a centralized service for processing: images need to be processed locally. Flow rate information can then be sent to a server by means of a low-power wide-area network (LPWAN) and checked photos can be sent only in case of high flow rates. There are some sensors off-the-shelf based on Doppler velocity radar, but they are still too expensive to be used on a large scale (Fulton *et al.*, 2020). Given this situation, it may be feasible to develop a water flow velocity measurement system using commercially available Doppler radar modules such as CDM324 and SKU: SEN0306 which cost about 50 euros. But we cannot estimate the workload required to have a fully operational equipment. An alternative option is using pipeline water flow sensor like YF-S201 to develop an immersed water flow monitoring system. However, we did not find peer-reviewed literature about this solution.

Another interesting work is focusing on the presence or absence of water flow. Moody and Martin (2015) use resistor type instruments to develop overland flow detectors (OFD). Hinrich Kaplan *et al.* (2019) use time-lapse imagery, electric conductivity (EC) and stage measurements to check the presence of streamflow. Chamber *et al.* (2020) use EC sensors (soil moisture sensors in fact) to develop their autonomous OFD.

Assendelft and van Meerveld (2019) chose electrical resistance (ER) sensors, temperature sensors, float switch sensors, and flow sensors like YF-S201 to monitor temporary streams. They define the percentage of correct state data (the percentage of the state data derived from the sensor data that corresponded to the state data derived from time-lapse photos) and the percentage of correctly timed state changes (the percentage of the state changes derived from the sensor data that corresponded in timing with the state changes derived from time-lapse photos) to assess the performance of sensors. They conclude that ER sensors (99.9% correct state data and 90.9% correctly timed state changes) and flow sensors (99.9% correct state data and 90.5% correctly timed state changes) perform best.

EC and ER sensors are presented in the next section dedicated to soil moisture sensors.

2.4.3 Soil moisture sensors

As mentioned just above, soil moisture sensors can work as OFD. Of course, the objectives of soil moisture monitoring are more numerous: large scale soil moisture sensing networks can provide information about rainfall, runoff, water cycle and ecosystems (Robinson *et al.*, 2008). Due to the important use of soil moisture sensors in agriculture, there is a large number of off-the-shelf sensors now and some are cheap. In the field of science, the most frequent expression of soil moisture is volumetric water content (VWC) whose definition is volumetric soil content (%) = [volume of water (cm^3)/volume of soil (cm^3)] × 100.

There are several methods to measure VWC, e.g., gravimetry, time domain reflectometry (TDR), and time domain transmission (TDT). Two methods are usually low-cost (less than 100 euros approximately): electrical resistance and capacitance methods (Adla *et al.*, 2020).

Resistive soil moisture sensors, which are extremely cheap, have been reported as inaccurate. Saleh *et al.* (2016) report that resistive soil moisture sensor EC-5 show an average percent error rate above 10% and is corroded after one month of use, which is a severe problem for continuous monitoring. Adla *et al.* (2020) tested resistive soil moisture sensor YL69 and YL100 with reference to a secondary standard sensor Delta-T ThetaProbe ML3 and concluded YL69 and YL100 are also not accurate (MAE, RMSE, and RAE of YL69 were 4.13%, 5.54%, and 0.41; MAE, RMSE, and RAE of YL100 were 3.51%, 5.21% and 0.37 respectively) and they cannot work as standalone sensors.

As for capacitive soil moisture sensors, Adla *et al.* (2020) recommended SM100. There are also SKU: SEN0193 (DFRobot, Shanghai, China) (Akhter *et al.*, 2018; López *et al.*, 2022; Nagahage *et al.*, 2019; Placidi *et al.*, 2020, 2021) and 10HS (Mittelbach *et al.*, 2011; Panjabi *et al.*, 2018), and a low-cost TDR sensor VH400 (Bitella *et al.*, 2014; Tebbs *et al.*, 2019) which are reported which are reported. It is also worth mentioning the Chameleon sensor developed and commercialized by the Commonwealth Scientific and Industrial Research Organization (CSIRO) for agriculture in low-income countries (Mdemu *et al.*, 2020). Specifications of all above sensors are given in Table 2-15.

Table 2-15. Specifications of low-cost soil moisture sensors.

Model	SEN0193	SM100	10HS	VH400	Chameleon
Principle	capacitive	capacitive	capacitive	TDR	resistivity
Size (mm)	98×23	60×20×3	160×33×8	93.8×7	NA
Weight (g)	15	NA	NA	NA	NA
Range	NA	0 VWC to saturation	0 to 57% or 69% [b] VWC	NA	0 to >50 kPa [e]
Operating voltage (V DC)	3.3 to 5.5	3 to 5	3 to 15	3.5 to 20	NA
Interface	PH2.0-3P	2.5 mm stereo pin	NA	NA	NA
Output	0 to 3 V DC	analog voltage [a]	0.3 to 1.25 V [c]	0 to 3 V [d]	Colors [e]
Price range (€)	< 10	< 100	< 200	< 60	~ 50
Performance tested in scientific literature	Yes	Yes	Yes	Yes	No

[a] Proportional to excitation voltage (0.5 to 1.5 V for a 3 V excitation).

[b] Mineral soil calibration: 0 to 57% VWC, Soilless media calibration: 0 to 69% VWC.

[c] Independent of excitation voltage.

[d] Related to moisture content.

[e] Measuring soil water suction: Blue 0-20 kPa (wet), Green 20 to 50 kPa (moist) and Red > 50 kPa (dry).

According to the manufacturer, the Chameleon sensor measures how hard the roots of plants must suck (the tension required) to extract moisture. So that it does not need to be calibrated for different soil types. The sensor can provide a quantitative measure (based on resistance measurement) but for irrigation application in agricultural production, a qualitative measurement is proposed (it can only report if the soil is wet, moist, or dry). *Mdemu et al.* (2020) reported large increases in yields of green maize by using tools like Chameleon sensors and implementing other changes, but they did not assess the performance of the Chameleon sensor.

Table 2-16 gives a summary of the performance of the low-cost soil moisture sensor SEN0189, SM100, 10HS and VH400 modules given by manufacturer and tested by scientific studies.

Table 2-16. A summary of performance characteristics of low-cost soil moisture modules.

Model	SEN0193	SM100	10HS	VH400
Trueness	RMSE = 5 % VWC [f] Max error = 6.2%, 4.3%, R^2 = 0.76, 0.73 [g]	*3% VWC* [a] average r_s = 0.94, MAE = 1.67%, RMSE = 2.36%, RAE = 0.21 [h] RMSE = 0.91%, 1.03% [i]	*3% VWC* [b] R^2 = 0.93 [j]	*2% VWC* [c] R^2 = 0.89, RMSE = 2.61, NRMSE = 0.09 [k] R^2 > 0.90 [l]
Repeatability	NA	average $s_{r,p}$ = 0.41 %	NA	NA
Reproducibility	"Significant sensor-to-sensor variability" [f]	NA	NA	NA
Resolution (VWC)	NA	*0.1%*	*0.08%* [d]	NA
Response time	NA	NA	*10 ms*	*400 ms* [e]
Sensitivity to environment	"Not sensitive to high mineral content soil" [f] "Affected by bulk density, not affected by temperature and depth" [g]	"Predicted and corrected positive temperature effect, not sensitive to changes in salinity" [h]	NA	"Sensitive to temperature changes in wet conditions (in water) and small changes in water content" [k] "The response of VH400 was significantly affected by soil texture" [l]
Maintenance needs	NA	NA	NA	NA
Longevity	> 6 months [g]	NA	> 2 years [j]	NA

[a] EC <8 mS/cm.

[b] with standard calibration equation, typical in mineral soils that have solution electrical conductivity <10 dS/m.

[c] unit not specified.

[d] in mineral soils from 0 to 50% VWC.

[e] power on to output stable.

[f] Nagahage *et al.*, (2019) calibrate SKU: SEN0193 compared with gravimetric VWC.

[g] Akhter *et al.* (2018) test SKU: SEN0193 in two difference sites.

[h] Adla *et al.* (2020) test five SM100 with reference to gravimetric weight and ThetaProbe soil moisture sensor in fluid and 4 kinds of repacked soils.

[i] Salman *et al.* (2021) compare soil moisture measurements by the gravimetric method and SM100 readings in two sites.

[j] Panjabi *et al.* (2018) do a soil-specific calibration for 10HS in lab.

[k] Bitella *et al.* (2014) test VH400, in lab in three kinds of non-saline soils.

[l] Payero *et al.* (2017) test VH400 in four soil texture types (loamy sand, sandy clay, sandy clay loam and sandy loam) with the reference of gravimetric VWC and output of VH400 was measured by FLUKE 117 electrician multimeter.

Nagahage *et al.* (2019) report four SEN0189 sensors have significant sensor to sensor variability according to analysis of variance (ANOVA). It is not sensitive to high mineral content soil. They suggest this is because SEN0189 sensors "operate in low frequencies and are thereby more sensitive to effects of soil textural variances and salinity". The calibration function of SEN0193 for organic-rich soil is $P = 13.248 - 2.576 \times 10^{-3}p + 1.726 \times 10^{-7}p^2 - 3.839 \times 10^{-12}p^3$ where P is gravimetric soil water content and p is mean raw analog to digital counts output of two SEN0193 with R^2 = 0.98. After calibration, at a gravimetric water content of 60 to 80%, the RMSE of SEN0189 is 5 % VWC. Akhter *et al.* (2018) reported that after site-specific calibration (linear calibration function, R^2 > 0.98), in six months, the max errors are 6.2%, 4.3% and correlation coefficient are 0.76, 0.73 between reference value (oven-dry method) and reading of SEN0189 for two sites respectively. They also

use one-way ANOVA test (Tukey's multiple range test) to check sensitivity to environment and report that soil temperature and measuring depth had no significant effect on the SEN0193 output. But the output of SEN0189 increases with an increase of the bulk density (if the bulk density is either higher than 1.3 g/cm^3 or lower than 0.9 g/cm^3), resulting in statistically significant differences (p-value < 0.05).

About SM100, Adla *et al.* (2020) report that using the manufacturer calibration equation, average Spearman's rank correlation coefficient (r_s) between sensor readings and the actual VWC is 0.94. The average comparison of precision performance of SM100 is 0.41%. Using a piecewise linear equations calibration function (R^2 = 0.94), MAE = 1.67%, RMSE = 2.36%, RAE = 0.21. It follows an expected positive temperature effect (at the actual VWC values of 7.63% and 18.38%, respectively, an increase of 30℃ resulted in an increase of estimated VWC by 7% and 2.99%) and is not sensitive to changes in salinity (R^2 = 0.85). Salman *et al.* (2021) report that after site-specific calibration at one site, the RMSE values for SM100 changed from 2.68% before calibration to 0.91%. At another site, the RMSE values changed from 3.09% to 1.03%. According to datasheet, resolution is 0.1 % VWC.

Panjabi *et al.* (2018) report that their calibration function of 10HS is $P = 0.001p^2 - 0.2063p + 12.226$ with R^2 of 0.9299, where P is the soil moisture content in % by volume, p is the 10HS reading in mV. They use it in field for about 2 years, but do not discuss data validation. According to datasheet, resolution is 0.08% VWC and response time is 400 ms.

About VH400, Bitella *et al.* (2014) report that for all soil texture types, three parameters logistic model fits data (VH400 output and volumetric water content getting from gravimetric water content) "very well" (R^2 = 0.89), training RMSE = 2.63, validation RMSE = 2.61, and NRMSE = 0.09 in cross-validation (leave-one-out method). They also test its sensitivity to environment, report that its output increases by 70 mV between 3 and 50 °C and that it is sensitive small changes in water content but without details. Payero *et al.* (2017) report that VH400 responds linearly to changes in VWC for four soil types (R^2 > 0.90). An analysis of co-variance (ANCOVA) shows that soil texture has a highly significant effect (p <0.001) on the output of VH400.

In general, resistive type soil moisture sensors are reported as "inaccurate" and "easy to be corroded by water". Capacitive sensor SKU: SEN0193 is cheap but shows significant sensor-to-sensor variability. There is also a soil moisture development board named HiGrow including SKU: SEN0193, microcontroller, and DHT11 on the same board, which is reported of poor quality (Flashgamer, 2019). Low-cost capacitive sensor SM100, 10HS and TDR

sensor VH400 are worth trying. It is absolutely required to conduct a site-specific calibration before deploying these sensors because soil moisture sensors are impacted by many environment quantities such as soil texture, bulk density, temperature and salinity. Another worth trying sensor is Chameleon which claims no need to be calibrated thanks to its measurement principle.

2.5 LOW-COST WATER QUALITY SENSORS REVIEW

As all sensors cannot be reviewed here, five water quality parameters are selected for review: pH, conductivity, turbidity, nitrogen, and phosphorus. By monitoring these parameters, water quality professionals gain a comprehensive understanding of physical, chemical, and biological aspects of water quality. This information guides decision-making processes related to water resource management, pollution prevention, and protection of aquatic ecosystems and public health.

We note that producers and sellers of water quality sensors usually categorize their products in two types: laboratorial usage and industrial usage. We cannot find any unambiguous definition of this categorization. Usually, laboratory usage requires sensors with high quality and accuracy, operated under strict controlled conditions. Industrial usage requires monitoring in a more demanding environment (temperature, pressure, electromagnetic compatibility, resistance to shocks, lightning shield, etc.) and robust sensors which deliver data continuously over weeks, months and years with online transmission to a control room. Industrial usage is closer to what is expected in the field of *in situ* stormwater monitoring. In addition, we find low-cost water turbidity sensors which are originally used in household appliances such as washing machines and dishwashers. Therefore, in this chapter, we propose three categories: laboratory, industry and household appliances.

2.5.1 PH sensors

There is an extensive literature (e.g. Alam *et al.*, 2020; Qin *et al.*, 2018; Zhou *et al.*, 2017) describing the development of low-cost pH meters based on optical fiber, metal oxides, and micro-electro-mechanical system (MEMS) techniques. Their works are, however, only in the laboratory development stage and not related to low-cost commercial products yet available on the market.

Commonly used pH sensors in low-cost water quality monitoring system are SKU:SEN0161 and SKU:SEN0169 from DFRobot (Harun *et al.*, 2018; Ilyas *et al.*, 2021; Kelechi *et al.*, 2021; Nasution *et al.*, 2020; Saha *et al.*, 2018), pH sensor from Atlas Scientific (Bartos *et al.*, 2018; Demetillo *et al.*, 2019b; Faustine *et al.*, 2014; Faustine and Mvuma, 2014; Shamsi *et al.*, 2020; Zakaria and Michael, 2017), pH sensor from Phidgets (Nazer *et al.*, 2018; Rao *et al.*, 2013), and pH sensor from SensoreX (al Haji and al Odwani, 2015; Lambrou *et al.*, 2014; Sun *et al.*, 2016).

Some papers only states brand but no model. Common models in reviewed papers are ENV-40-pH from Atlas Scientific (Faustine *et al.*, 2014; Faustine and Mvuma, 2014; Zakaria and Michael, 2017). . Alumno et al., (2021); Baéz Rodríguez, and Rodríguez Jarquin, (2019) use PC2121-5M from Phidgets. Specifications of the above models are given in Table 2-17. Table 2-18 gives a summary of the performance of the low-cost water PH sensor modules given by manufacturer and tested by scientific studies.

Table 2-17. Specifications of low-cost water pH sensors

Model	SEN0161	SEN0169	ENV-40-pH	PC2121-5M
Range of use	laboratory	industry	laboratory	industry
Size (mm)	NA	NA	150.6 ×12	160 × 29.3
Weight (g)	NA	NA	25	NA
Detection range (pH)	0 to 14	0 to 14	1 to 14[c]	0 to 14
Power supply (V DC)	3.3 to 5.5[b]	3.3 to 5.5[b]	3.3 to 5[c]	4.5 to 5.3[e]
Output	analog voltage[d]	analog voltage[d]	UART & I^2C[c]	NA
Probe connector	BNC	BNC	Male SMA/BNC	BNC
Price range (€) [a]	~ 30	~ 60	~ 130	~ 130
Performance tested in scientific literature	Yes	Yes	Yes	Yes

[a] Including interface circuit board.

[b] With meter pro kit V2 interface adapter.

[c] With EZO™ pH circuit.

[d] 0 to 3 V on meter pro kit V2.

[e] With pH/ORP adapter.

Table 2-18. A summary of performance characteristics of low-cost water pH modules.

Model	SEN0161	SEN0169	ENV-40-pH	PC2121-5M
Trueness	*± 0.1 pH* [a] Deviation = 0.02 to 0.26 pH [f] ~ 0.1 pH [g] Error = 0.02 to 0.12 pH [l]	*± 0.1 pH* [a] Absolute error ≤ 0.1 pH [i] Average deviation = 0.0766 pH, max deviation = 0.16 pH [j]	*± 0.002 pH* [b] Max deviation = 0.60 pH, R^2 = 0.9731 [k]	*± 0.09 pH* [c] Errors = -0.5, -1.86 pH [m]
Repeatability	NA	NA	NA	NA
Reproducibility	NA	NA	NA	NA
Resolution	NA	NA	*0.001* [b]	*0.018* [c]
Response time	*< 2 min*	*≤ 1 min*	*95% in 1 s*	*< 10 s*
Sensitivity to environment	"May not be effective to be continuously immersed" [h]	NA	NA	NA
Maintenance needs	NA	NA	*~ 1 year before recalibration*	*Recommend to store in a storage solution.*
Longevity	*> 6 months* [d]	*> 6 months* [e]	*> ~ 30 month*	NA

[a] At 25 °C, with meter pro kit V2 interface adapter.

[b] With EZO™ pH circuit.

[c] With pH/ORP adapter.

[d] Depending on the frequency of use.

[e] 7 × 24 hours, depending on the water quality.

[f] Nasution *et al.* (2020) compare the reading of SKU: SEN0161 in a fishpond with handheld pH meter.

[g] Yuzhakov *et al.* (2021) do a three-point calibration and compare SEN0161 with OHAUS Starter 3100 stationary pH meter.

[h] AKHIR (2021) calibrated SEN0161 and tested it in shrimp pond for 5 days.

[i] Moyón Rivera and Ordóñez Berrones (2019) compare SEN0169 to pH metro consort C562.

[j] Saputra *et al.* (2017) compare SEN0169 to pH meter PH-009(I) in three types of pH buffer solution.

[l] Mahardika *et al.* (2021) calibrate SEN0161 comparing to a pH meter.

[m] Baéz Rodríguez and Rodríguez Jarquin (2019) test PC2121-5M in buffer solutions.

Nasution *et al.* (2020) use the function P=(7-output)/59.16 where *P* is the pH value and *output* is the SEN0161 output in mV. This formula has been first established by Shahrulakram and Johari (2016). In Nasution *et al.* (2020)'s field test, the deviation between SEN0161 output and a handheld pH meter is 0.02 to 0.26 pH at around 8.0 pH. But they do not provide calibration details. Yuzhakov *et al.* (2021) report that its calibration function is $P = a + bp$, where P is the measured pH and p is the measured voltage in mV, with $a = -7.17652 \pm 0.13704$ and $b = 7.89417 \pm 0.07516$. But using this calibration function, for a change of 1 pH unit, only a voltage of approximately 0.12 to 0.13 mV would be necessary. SEN0161 therefore seems highly susceptible to electrical interferences. A possible explanation could be that Yuzhakov *et al.* (2021) in fact use volt to record SEN01610 output. In addition, the number of digits in *a* and *b* is too high for measuring pH with an accuracy of ± 0.1 pH according to the supplier. After calibration, its reading was "similar" to stationary pH meter OHAUS Starter 3100 which had a ± 0.01 pH measurement error. Mahardika *et al.* (2021) use ADS1115 to measure its output

voltage and report that its calibration function is $P = 13.57p - 17.53$ where P is the measured pH and p is the measured voltage in mV. After calibration, the error is from 0.02 to 0.12 and the average error is 0.068. AKHIR (2021) reports that using manufacturer calibration function, in 3 hours immersing test, the error rate increases from 1.11% to 5.45%. In the five days *in situ* test, outputs pH of SEN0161 are from 7.15 to 11.27. AKHIR (2021) indicates that "SEN0161 can only be effectively performed in the range of pH 6 to 8 so that the sensor is not in optimal working condition" but does not give any further explanation and test results. According to the datasheet, response time is less than 2 minutes and longevity is more than 6 months but depends on the frequency of use.

About SEN0169, Moyón Rivera and Ordóñez Berrones (2019) report that its absolute error is ±0.1pH, but they do not give the calibration equation. Saputra *et al.* (2017) report that compared to a reference, the average deviation is 0.0766 pH. The maximum deviation is 0.16 pH, but their reference sensor has less valid numbers than SEN0169 and they also do not give calibration equation of SEN0169. The authors of this review think the researchers mentioned above use manufacturer's Arduino code and calibration equation. According to the datasheet, response time is less than 1 minute, and a longevity is more than 6 months with 7 × 24 hours use but depends on the water quality.

Demetillo *et al.* (2019) report that their Atlas Scientific pH sensor ENV-40-pH output p shows "good" results comparing to reference sensor output P: $P = 0.1662p + 6.4617$ with $R^2 = 0.9731$. In their test, the maximum difference is 0.60 pH at around 8 pH. They deploy their WSN system in two creeks for two weeks and do not mention any operation problem. The datasheet of ENV-40-pH indicates that resolution is 0.001, response time is 1 s and calibration should be done every year.

About the PC2121-5M, Baéz Rodríguez and Rodríguez Jarquin (2019) use analog to digital converter of Arduino to read its output and DS18B20 to account for temperature compensation. When using buffer solutions of respectively pH 8.86 and pH 9.7, the value measured were pH 7.00 and 9.2. They think these errors are due to improper calibration but do not give any further results. According to the datasheet, trueness is ± 0.09 pH, resolution is 0.018 and response time is less than 10 s. This sensor has many usage cautions, and it is recommended to store in a storage solution.

There are already some low-cost off-the-shelf pH probes and interface circuits with Arduino and other open-source hardware. According to the available literature, after calibration, at least all these sensors can indicate the acidity

or alkalinity of the tested liquid. But most reviewed papers do not report the influence of temperature on pH measurement. Further research could focus on the following points: (i) the true performance of ready to use pH sensors with open-source hardware. For example, trueness is reported very differently for different sensors, e.g. 0.1 pH for SEN0161 and 0.002 pH for ENV-40-pH, which is meaningless for sensors based on the same measuring principle; (ii) can these sensors be suitable for submersion measurements in stormwater for months? (iii) can these sensors perform at the expected performance with as little maintenance as possible? It is worth mentioning that there are some on-going projects on the subject such as Setier project (Prost-Boucle *et al.*, 2022).

2.5.2 Conductivity sensors

Measuring the electric conductivity (EC) of water can indirectly provide information on the water quality condition or identify a specific water source (rainwater or groundwater for example) in relation to increase or decrease of conductivity. In addition, total dissolved solids (TDS) concentration has an approximately proportional relationship with water conductivity (Rusydi, 2018).

Commonly used low-cost conductivity sensors are SKU: DFR0300 from DFRobot (Alimorong *et al.*, 2020; Nazer *et al.*, 2018; Saha *et al.*, 2018), and conductivity sensor from Atlas Scientific (Bartos *et al.*, 2018; Faustine *et al.*, 2014; Lockridge *et al.*, 2016; Othaman *et al.*, 2021; Shamsi *et al.*, 2020; Siyang and Kerdcharoen, 2016). A commonly used TDS sensor is SKU: SEN0244 (Mahardika *et al.*, 2021; Ula, 2020).

There are many segmented models of conductivity sensors from Atlas Scientific. The model commonly used in fresh water is ENV-40-EC-K0.1. We also found industry level water conductivity probes E201WM and 208DH. Specifications of above models are given in Table 2-19. Table 2-20 gives a summary of the performance of the low-cost water conductivity sensor modules given by manufacturers and tested by scientific studies.

Table 2-19. Specifications of low-cost conductivity sensors.

Model	DFR0300	ENV-40-EC-K0.1	E201WM EC	208DH	SEN0244
Type	EC	EC	EC	EC	TDS
Range of use	laboratory	laboratory	industry	industry	laboratory
Range	0 to 20,000 µS/cm [b]	0.07 to 50,000 µS/cm	0 to 19,990 µS/cm [e]	0 to 199,900 µS/cm [e]	0 to 1000 ppm [f]
Size (mm)	NA	145.5×12	85 (length)	165×26×26	NA
Weight (g)	NA	25	41	41	NA
Power supply (V DC)	3.0 to 5.0 [c]	3.3 to 5.5 [d]	3.0 to 5.0 [c]	3.0 to 5.0 [c]	3.3 to 5.5 [f]
Probe connector	BNC	Male SMA/BNC	BNC	BNC	XH2.54-2P
Output	0 to 3.4 V [c]	UART & I^2C [d]	0 to 3.4 V [c]	0 to 3.4 V [c]	0 to 2.3 V [f]
Price range (€) [a]	~ 70	~ 200	~ 70	~ 70	~ 10
Performance tested in scientific literature	Yes	Yes	No	No	Yes

[a] Including interface circuit board.
[b] Recommended detection range: 1,000 to 15,000 µS/cm.
[c] With DFRobot Signal Conversion Board (Transmitter) V2.
[d] With EZO™ Conductivity Circuit.
[e] Another type has a range 0 to 1999 µS/cm and a resolution 1 µS.
[f] With DFRobot Signal Transmitter Board, at 25 °C.

Table 2-20. A summary of performance characteristics of low-cost water conductivity sensor modules.

Model	DFR0300	ENV-40-EC	E201WM EC	208DH	SEN0244
Trueness	*±5%* [a] Average deviation = 2.1 ppm, max deviation = 6 ppm [f] Error rate = 9.5 % [g]	*±2%* [b] < 0.02 % [h] Error ~ 10 %, RMSE = 1.35 ppt, R^2 = 0.96 [i]	*±1.5%+2 digits*	*±1.5%+2 digits*	*± 10%* [c] Average error = 4.896 ppm [j] Average error rate = 3.59% [k]
Repeatability	NA	NA	NA	NA	NA
Reproducibility	NA	NA	NA	NA	NA
Resolution	NA	NA	*100 or 1 µS* [d]	*100 or 1 µS* [d]	NA
Response time	NA	*90% in 1 s*	NA	NA	NA
Sensitivity to environment	NA	"Proportional to the temperature" [h] "Instrument biofouling making sensor drift" i	NA	NA	NA
Maintenance needs	NA	Clean every month in summer [i]	NA	NA	NA
Longevity	*> 6 months* [e]	*~ 10 years*	NA	NA	NA

[a] With DFRobot Signal Conversion Board (Transmitter) V2.
[b] With EZO™ Conductivity Circuit.
[c] With DFRobot Signal Transmitter Board, at 25 °C.
[d] Depend on range (range 0 to 19,990 µS/cm has a resolution of 100 µS, range 0 to 1999 µS/cm has a resolution of 1 µS).
[e] Depending on the frequency of use.
[f] Saputra *et al.* (2017) compare the reading of DFR0300 with the measurement result of a TDS meter.
[g] Rozaq *et al.* (2020) calibrate DFR0300.
[h] Othaman *et al.* (2021) calibrate ENV-40-EC-K10 using 12880 µS/cm and 150000 µS/cm standard buffer solutions in temperature range 5 to 50 °C in lab.
[i] Lockridge *et al.* (2016) compare ENV-40-EC-K1.0 with YSL6600 for 55 hours at Dauphin Island Sea Lab.
[j] Mahardika *et al.* (2021) calibrate SEN0244 comparing to a TDS meter.
[k] Ula (2020) compare SEN0244 with TDS meter.

About DFR0300, Saputra *et al.* (2017) report that in 27 minutes measurement and around 650 ppm, comparing to reference, deviation is from 0 to 6 ppm and average deviation is 2.1 ppm, but they do not give calibration details. Rozaq *et al.* (2020) report that the calibration equation of DFR0300 is $P = 0.003p - 0.4175$ with $R^2 = 0.9587$ where P is salinity value and p is ADC counters of Arduino Due. Using this calibration equation, the error rates are from 5.7% to 17.6% and average error rate of DFR0300 was 9.5 %. But they do not divide calibration and validation dataset and their reference values are integer and DFR0300 outputs are with two decimal places. According to the datasheet, longevity is more than 6 months but depends on the frequency of use.

Othaman *et al.* (2021) report that for ENV-40-EC all the percentage differences between measured EC and manufacturers' suggested values are less than 0.02% and EC values are directly proportional to temperature ($R^2 \sim 1$). Lockridge *et al.* (2016) report that compared to reference, RMSE is 1.35 parts per thousand, approximately 10 % of the observed salinity range and outputs of ENV-40-EC-K1.0 and reference are "highly correlated" ($R^2 = 0.96$). They think this deviation is a slight offset/bias that is likely of a physical nature such as the distance between them (0.5 m). They also report that instrument biofouling is a significant issue during the summer in the field test, and commonly results in sensor drift after 3 to 4 weeks of deployment. Manufacturer claims that trueness is ±2%, response time is 1 s and longevity is 10 years.

About SEN0244, Mahardika *et al.* (2021) use ADS1115 to read its output voltage and report that its calibration function is $P = 352.7p - 42.76$ where P is the output of TDS meter and p is output of SEN0244 in mV. After calibration, its error is from 0.18 to 12.9 ppm in a range from 400 to 700 ppm and average error is 4.896 ppm. But they do not divide calibration and validation datasets. Ula (2020) reports that at about 820 ppm, error rate of SEN0244 is from 2.54% to 0.24% and average error is 1.89%; at about 400 ppm, error rate is from 5.12% to 8.29% and average error is 6.00%; and at about 170 ppm, error rate is from 0.47% to 7.39% and average error is 2.90%. But he does not provide the calibration details. The average error rate of three experimental samples is 3.59%.

There are two other interesting works we identified: Geetha and Gouthami (2016) used a resistive soil moisture YL-69 to measure water conductivity, but it is doubtful how long this resistance sensor can work continuously in water as aforementioned YL-83 and EC-5 are easily oxidated (Dias, 2019; Saleh *et al.*, 2016). Shi *et al.* (2021) built a DIY (do it yourself) water conductivity sensor using two small stainless-steel rods with a simple voltage divider circuit (a resistor 100 ohms and water as another resistor) and calibrate it comparing to HANNA meter

(linear calibration function in 0 to 10 mS/cm with R^2 = 0.9871). At four sites test, they claim that their DIY EC sensors has “highly linear correlation” with a HANNA meter even though relative uncertainties are from 17.42% to 31.12%. And they do not give temperature compensation details in test results and the longevity of their DIY EC sensor.

In general, *in situ* water conductivity measurement appears promising in terms of performance. Some low-cost sensors off-the-shelf and DIY sensors can give useful water quality information. It is mandatory to compensate EC readings with water temperature and DS18B20 is a commonly used waterproof temperature sensor. Like water pH sensor, the long-term performance of immersed EC sensor is also unstable because of e.g., biofouling, so that a self-clean or self-maintenance system is necessary.

2.5.3 Turbidity sensors

Turbidity is an optical determination of water clarity and total suspended solids (TSS) is a total quantity measurement of solid material per volume of water. These two parameters are related but not in a simple linear relationship. Turbidity is usually reported in nephelometric turbidity units (NTU).

We found four low-cost optical turbidity sensors in scientific papers. They are SKU: SEN0189 from DFRobot (Ammari *et al.*, 2019; Gusri and Harmadi, 2021; Hakim *et al.*, 2019; Hendri *et al.*, 2019; Iskandar *et al.*, 2019; Kelechi *et al.*, 2021; Mwemezi, 2020), TSD-10 and TSW-10 from Amphenol (Camargo, 2017; Faisal *et al.*, 2016; Nguyen and Rittmann, 2018; Valenzuela *et al.*, 2018), and TS-300B (Angdresey *et al.*, 2021; Yuan *et al.*, 2018). Specifications of above models are given in Table 2-21. Table 2-22 gives a summary of the performance of the low-cost turbidimeter modules given by manufacturers and tested by scientific studies.

Table 2-21. Specifications of low-cost water turbidity sensors.

Model	SEN0189	TSD-10	TSW-10	TS-300B
Principle	optical principle			
Range of use	household appliances			
Size (mm)	44×30×34	30×30×34	30×30×34	38.6×22.1
Weight (g)	30	NA	NA	NA
Range (NTU)	0 to 4000	0 to 4000	0 to 2000	0 to 1000 ±30
Operating voltage (V DC)	5	5	5	5
Voltage differential (V)	NA	3.0 ± 20%	1.3 ± 20%	NA
Output	two models [a]	analog voltage	analog voltage	two models [a]
Price range (€)[1]	~ 10	~ 10	~ 10	~ 10
Performance tested in scientific literature	Yes	Yes	Yes	No

[a] With adapter, analog output: 0 to 4.5 V, digital Output: High/Low level signal (can adjust the threshold value by adjusting the potentiometer) with an adapter board.

Table 2-22. A summary of performance characteristics of low-cost turbidimeter modules.

Model	SEN0189	TSD-10	TSW-10
Trueness	R^2 = 0.9762 [b] Average error rate = 7.7% [c]	R^2 = 0.99, average error rate = 6.51% R^2 = 0.997, average error rate = 9.35%	R^2 = 0.9961, average relative error = 3.86% [g]
Repeatability	NA	NA	NA
Reproducibility	*Output 4.1±0.3 V when NTU < 0.5* "Everyone needed to be individually calibrated" [d]	NA	NA
Resolution	NA	3.91 NTU/ADC count [e]	NA
Response time	*< 500 ms*	NA	NA
Sensitivity to environment	"The effect of temperature was not significant, influenced by ambient IR" [d] *<10%* [a]	Not sensitive in low NTU [e f] Influence by high intensity of light [f]	NA
Maintenance needs	Need clean regularly because of fouling [d]	NA	NA
Longevity	~ 7 months [d]	NA	NA

[a] In low temperature, thermal shock, damp heat, vibration tests, its output deviation is less than 10%.

[b] Hakim *et al.* (2019) calibrate SEN0189 referencing to water NTU calculated from weight of sediments in portable water.

[c] Gusri and Harmadi (2021) compare SEN0189 with Lutron TU-2016 meter.

[d] Trevathan *et al.* (2020) modify SEN0189 and only retain its original LED and IR phototransistor. They calibrate the modified sensor with Hach turbidimeter (relative error < 0.5%) using Formazin calibration samples. And then they deploy the sensors in various water bodies for several months.

[e] Faisal *et al.* (2016) calibrate and compare TSD-10 with a Hach 2100N.

[f] Angraini *et al.* (2016) compare TSD-10 with a turbidimeter and test it in a river.

[g] Valenzuela *et al.* (2018) calibrate TSW-10 with a reference T-100.

About SEN0189, Hakim *et al.* (2019) report that at 25 °C, the calibration function in the range 0 to 1000 NTU is $P = 4999.25 - 1250p$ where P is the turbidity of water in NTU and p is the output voltage of SEN0189 in V, with R^2 = 0.9762 but they do not validate the relation between water NTU and the weight of sediment in water. Gusri and Harmadi (2021) report that at 1 NTU, the error rate of SEN0189 is 31.37%; at 55 NTU, the error rate is

6.28%, and other error rates are less than 3.5 % from 75 to 228 NTU. Average error rate is 7.7 % but they do not give details about their calibration function. Trevathan *et al.* (2020) report that the performance of original LED and IR phototransistor of SEN0189 are different so that it should be calibrated one by one. About their modified sensor, they believe that it is "accurate for all turbidity levels", the actual changes due to temperature are "not that significant" but do not give any details data such as calibration function and RMSE. In their 7 months in field test, they find that their sensor is influenced by ambient IR and in some water bodies, sensor needs to be cleaned regularly because of fouling. According to the datasheet, output deviation is less than 10% in low temperature, thermal shock, damp heat, vibration tests, and response time is less than 500 ms.

Faisal *et al.* (2016) report that at the range 0 to 700 NTU, the TSD-10 calibration curve is $P = 2277 - 500p$ where P is the turbidity of water in NTU and p is the output voltage of TSD-10 in V, with R^2 = 0.99. After calibration, its average measurement error is 6.51% but measurement error is 24.63% when measuring at 37.8 NTU. They think this low sensitivity to low NTU is due to the fact that the range 0 to 4000 NTU is mapped to over 0 to 1023 digital counts and the IR phototransistor of TSD-10 is not sensitive enough. Angraini *et al.* (2016) calibrated TSD-10 in the range 169 to 771 NTU. The calibration equation was $P = 2298.89 - 0.619p$ where P is the turbidity of water in NTU and p is the output voltage in mV, with $R^2 = 0.997$. After calibration, the average relative error is 9.35%, and the error is large at low NTU (24.77% at 169 NTU). But they also do not separate calibration and validation dataset. In their field test, they find that at a point, sensor output NTU is abnormal lower than others and think this is because the light intensity at this point is higher than others.

About TSW-10, Valenzuela *et al.* (2018) report that in the range 0 to 180 NTU, the calibration equation is $P = 139.73p^3 - 1161.1p^2 + 2411.8p$, where P is the turbidity of water in NTU and p is the output voltage in V, with $R^2 = 0.9961$. After calibration, all the relative errors in 50 samples are in a range from 2.0% to 5.0% and average relative error is 3.86%. Camargo (2017) reported the calibration equation in datasheet is $P = 261.05p^2 - 2607.5p + 6367$ where P is the turbidity of water in NTU and p is the output voltage in V.

Four sensors are originally used in washing machines (and thus already widely used): SKU: SEN0189, TSD-10, TSW-10 and TS-300B. Because their principles are same, and appearances are similar, we can discuss them together. Dedicated case by case calibration functions (linear to cubic depending on the NTU range of interest) are absolutely necessary. The reproducibility appears as rather poor, maybe due to the difference performance of the

LED and IR phototransistor inside them. Their resolution depends on the analog to digital converter (ADC) that is used to read their voltage output so that an additional analog-to-digital converter such as ADS1115 is necessary. Their response time is sufficient for every second monitoring. They are sensitive to ambient infrared light interference and temperature compensation is not mandatory. They should be cleaned regularly because of fouling. Their longevity depends on the remodeling work because they are not designed for field operation.

2.5.4 Nitrogen and phosphorus sensors

We identified three commercially available technologies to monitor nutrients in water: optical (UV) sensors (>15,000 €), wet-chemical sensors (> 10,000 €), and ion-selective electrodes (ISE) (<1,000 €). It seems that only ISE could be a choice for ubiquitous low-cost sensors networks. ISE advantages are easy use, fast response, no influence of color or turbidity, availability for both ammonium and nitrate. Disadvantages are low resolution, accuracy and precision, ionic interferences, high instrument drift, and limited shelf life (Pellerin *et al.*, 2016).

Kotamäki *et al.* (2009) used a s::can spectrometer probe. Wollheim *et al.* (2017) used a submersible ultraviolet nitrate analyzer from SUNA. Jones *et al.* (2020) used Hach Nitratax SC Plus to measure nitrate in water continuously. All sensors are optical (UV) sensors which are not low-cost. Wade *et al.* (2012) used Systea Micromac C to determine the Total Reactive Phosphorus (TRP), nitrite and ammonium. Yu *et al.* (2021) used Sigmatax sampler combined with a Phosphax Sigma auto analyzer to measure total phosphorus (TP) and Amtax combined with a Filtrax automatic sampler to measure ammonium. The devices mentioned above are large cabinets and thus are also not low-cost. It is expensive to use a colorimetric method to measure phosphates in water and low-cost microfluidic and electrochemical methods to determine phosphorus in water are still in their lab development phase.

Therefore, in terms of nutrient monitoring in water, the only current comparatively low-cost option are ISE probes to monitor nitrate or ammonia. Some ISE sensors are used: nitrate and ammonia ISE from Vernier (Abu-Baker *et al.*, 2016; Rossi *et al.*, 2015), Cooking Hacks (Ramadhan, 2020), HYDRA (Menon *et al.*, 2017), and Thermo Scientific (El-deen *et al.*, 2018). Specifications of above models are given in Table 2-23. Table 2-24 gives a summary of the performance of the low-cost nitrogen sensors given by manufacturers and scientific literatures.

Table 2-23. Specifications of some water nitrogen ISE probes.

Brand	**Vernier**	**Vernier**	**Cooking Hacks**	**HYDRA**	**Thermo**
Detection	nitrate ion	ammonium ion	nitrate ion	nitrate or ammonium ion	ammonia ion
Range of use	laboratory	laboratory	laboratory	industry	laboratory
Size (mm)	155×12	155×12	NA	148×23.8	150×12
Range (mg/L)	1 to 14,000	1 to 18,000	0.6 to 31,000 [a]	0.1 to 14,000	0.01 to 17,000
Electrode slope (mV/decade at 25°C)	+56±4	+56±4	NA	NA	NA
Price range (€)	~ 300	~ 300	NA	~ 500	~ 600
Performance tested in scientific literature	No	No	No	No	No

[a] Linear range.

Table 2-24. A summary of performance characteristics of the above water nitrogen ISE probes.

Model	**Vernier**	**Vernier**	**Cooking Hacks**	**HYDRA**	**Thermo**
Detection of	nitrate ion	ammonium ion	nitrate ion	nitrate or ammonium ion	ammonia ion
Trueness	"Within the range of the government agency results" [e]		"Showed good agreement with laboratory results" [f]	*±3%* [a]	"Similar mentioned in user guide" [g]
Repeatability	*±10%* [b]	*±10%* [b]	NA	NA	NA
Reproducibility	NA	NA	NA	NA	*±2%*
Resolution	NA	NA	NA	NA	NA
Response time	NA	NA	NA	*T_{90} 1 minute*	NA
pH range	*2 to 11*[c]	*4 to 7.5*[c]	*2 to 11*	NA	*> 11*
Temperature range (°C)	*0 to 40*[d]	*0 to 40*[d]	*5 to 50*	*0 to 50*	*0 to 50*
Flow rate (m/s)	NA	NA	NA	*0.1 to 3.0*	NA
Interfering ions	*ClO_4^-, I^-, ClO_3^-, CN^-, BF_4^-*	*K^+*	*Br^{-1}, Br^2, NO_2^{-1}, NO_2^7, OH^{-1}, OH^8, AcO^{-2}, AcO^2*	NA	NA
Immersion	*2.8 cm*	*2.8 cm*	NA	NA	NA
Maintenance needs	NA	NA	NA	NA	NA
Longevity	NA	NA	> 10 days [f]	*4 to 6 months*	NA

[a] Of reading, dependent on calibration.

[b] Of full scale (calibrated 1 to 100 mg/L).

[c] No pH compensation.

[d] No temperature compensation.

[e] Abu-Baker *et al.* (2016) use Vernier nitrate and ammonium ISE probes to test water samples from the Muskingum River.

[f] Ramadhan (2020) connect Cooking Hacks ISE probe with ESP8266 and test it in lab and then use in five water station 24 hours a day for 10 days.

[g] El-deen *et al.* (2018) design interface circuits to use Thermo Scientific ammonia ISE probe with an Arduino Nano, calibrated the probe by Orion/mV benchtop meter and test his system on a fish tank.

About the Vernier nitrate and ammonium ISE probes, Abu-Baker *et al.* (2016) report that outputs within the range of the Environmental Protection Agency (EPA) results, but do not give details of comparison. According to the datasheet, repeatability is ±10% of reading, but depends on calibration. About sensitivity to environment, the nitrate ion probe works in pH range 2 to 11, the ammonium ion probe works in pH range 4 to 7.5, both work in

temperature range 0 to 40 °C and do not have pH and temperature compensation. Datasheet does not indicate working flow rate and we think they can only work in stable water, and both interfere with some other ions.

About Cooking Hacks nitrate ISE probe, Ramadhan (2020) report that its readings are in a range 10.5 to 11.7 mg/L in lab test and this results "show good agreement with laboratory results" but did not give any comparison details. The system is equipped with a sensor that was "functioning correctly" over ten days *in situ* tests. According to datasheet, it works in a pH range of 2 to 11 and a temperature range of 5 to 50 °C and interferes with many other ions. Manufacturer does not mention the water condition when use it.

About HYDRA nitrate or ammonium ISE probe, Menon *et al.* (2017) do not mention any performance assessment. Manufacturer claims that trueness is ±3%, response time is 1 minute, working temperature is 0 to 50 °C, that it can measure flow velocity from 0.1 to 3.0 m/s, and that its longevity is 4 to 6 months.

About the Thermo ammonia ISE probe, El-deen *et al*. (2018) claim that the performance of their own interface circuits is "similar" to Orion/mV benchtop meter. They use three segments of linear functions to represent the relation between the electrode output potential in mV and the logarithm of the NH3 concentration and claim that this curve is "similar to direct calibration curve mentioned in Thermo Scientific user guide" but do not give comparison details. In their fish tank test, the ammonia probe is output 0 and they think this is due to the fact that there is no ammonia in the fish tank. Manufacturer indicates that reproducibility is ±2 %, samples and standards must be adjusted to above pH 11, and temperature range is 0 to 50 °C.

In conclusion, there are some low-cost ISE probes to determine nitrate and/or ammonia concentrations, but no true low-cost option exists today to measure phosphorus in water. ISE probes are designed for specialized equipment, and there is therefore need for extra work to combine them with open-source hardware such as Arduino and Raspberry Pi. This undoubtedly requires a certain amount of specialized hardware knowledge. It is possible that some commercial pH probe adapter boards as discussed in low-cost pH sensor part can also work with nitrate ISE probe.

2.6 CONCLUSION

In this review on low-cost sensors ready for ubiquitous stormwater sensing networks, we included off-the-shelf low-cost sensors referred to by open-source communities and scientific literature as systematically as possible.

Various low-cost sensors, using different devices and methods in different environments, have been tested. There is to date no existing literature review dedicated to low-cost stormwater monitoring with a unified metrological framework considering numerous parameters and providing feedbacks from commercially available sensors. Performances of off-the-shelf low-cost sensors are summarized by means of six indicators: (i) trueness, (ii) repeatability, (iii) reproducibility, (iv) resolution, (v) response time, and (vi) sensitivity to environment, maintenance needs and longevity.

Of course, when building a node of a sensing network, according to the experience of authors of this review, there are many other aspects that must be considered. For example, the built-in real time clock of some Arduino boards is easy to drift over time. Most open-source hardware does not have shielding, which means that they are easily disturbed by external interferences. Energy efficiency is also essential for outdoor autonomous systems. However, the global performance of a sensing node is mainly governed by the sensors it uses.

The present review is nevertheless positive in the sense that several low-cost sensors and solutions already exist. Low-cost sensors have been identified to measure continuously and *in situ* several quantities of interest for urban hydrology (research) and stormwater management (operation), including meteorology and water quantity. There are many low-cost sensors for monitoring air humidity, wind speed, solar radiation, rainfall, water level and soil moisture. But many of their performances and their uncertainty still need to be better quantified by means of further tests and evaluations. Water flow monitoring needs more creative sensor modules and system design, but they are not far away from giving relatively reliable results.

Compared to meteorological and water quantity, water quality monitoring by means of low-cost devices is more knowledge intensive, and users clearly need specific skills, with adaptation to the water matrix of interest (stormwater in this paper, but this could be drinking water, river water, etc.). Reviewed papers do not sufficiently report repeatable examples with references to metrology literature and methods. For example, comparison between sensors, even a traditional more expensive one used as reference, is not equivalent to a true calibration.

To a higher degree compared with traditional sensors, the quality of data generated by low-cost sensors not only depends on the sensors themselves, but also on the user and his/her knowledge, skills and metrological practice.

This is why users of low-cost sensors and monitoring systems should not only have skills in electronics and informatics. They must be trained in metrology, including measuring principles, indispensable periodic calibration and verification of both sensors, and measuring chains and systems, uncertainty assessment, etc.

Regarding the trueness of low-cost sensors, it seems that every metric in Table 3 can be used to describe this parameter. There are several discussions about its assessment: (i) Many papers do not consider the trueness of reference sensors when they test low-cost sensors and give their results. (ii) Many papers do not distinguish calibration and validation datasets when they test low-cost sensors. (iii) Very different to traditional sensors, the output of low-cost sensors is frequently very primitive. Many low-cost sensors identified in this review deliver output voltage signal such as pyranometers, soil moisture and water quality sensors. It is better to use high performance analog to digital converter (ADC) such ADS1115 (Texas Instruments, 2018) to read their output. Using the build-in ADC of Arduino will introduce a higher system error (for example, Arduino Nano has a build-in 10-bit ADC while ADS1115 is a 15-bit ADC, which means that ADS1115 provides a resolution 32 times better). (iv) As the output of low-cost sensors is very primitive, there are almost no manufacturer calibration to adapt the output, which gives users more freedom but also involves more preparatory work in using the sensors. The trueness of low-cost sensors really depends on building a reliable calibration equation by users. For example, the output of ultrasonic water level sensors is the echo time. Users can improve the trueness by compensating the change of wind speed by temperature and humidity. (v) Some users use unsuitable methods to calibrate low-cost sensors: for example, pouring too much water into rain gauge means simulating an unrealistic heavy rainfall event.

Regarding the repeatability and reproducibility of low-cost sensors, some papers use pooled relative standard deviation and analysis of variance to check them. But many papers ignore these two important criteria. Almost no paper checks reproducibility of low-cost sensors intentionally. In fact, this should be the manufacturer's duty to ensure each sensor is calibrated in factory. But low-cost sensors often involve no guarantee of repeatability and reproducibility, and this is the buyer's duty to verify it. For example, the Pluvimate rain gauge has a mean bias of 13.9 % in the reproducibility test even though we are skeptical of the test method. Specific tests of every low-cost sensor are mandatory before usage (as it should also be the case for any sensor), but this introduces another problem: when we plan to use hundreds of low-cost sensors, testing all of them one by one is too costly and developing automated testing systems may facilitate this task but remains expensive.

In many cases, users cannot test the resolution of low-cost sensors because they do not have the required equipment. There is a risk of uninformed use of low-cost sensors if users only rely on information provided by manufacturers. Indeed, some datasheets of low-cost sensors are of poor quality (insurance quality and reliability are costly). For example, the datasheet of the weather station kit SEN-15901 gives different resolution values in different languages, as discussed in wind speed and rainfall sensors subsections. There is another issue as many low-cost sensors only deliver voltage: using an ADC with more bits can increase the resolution in theory but requires a case-by-case adaptation. However, more importantly, the original analytical performance of some of the low-cost sensors is low constrained by its principle such as low-cost turbidimeter. In addition, some low-cost sensors have a higher resolution than the reference sensors used to test them. For example, the optical rain gauge RG-15 has a theoretical resolution of 0.02 mm.

Regarding the response time, it appears that reviewed low-cost sensors can afford measuring every minute. In some cases, it may be better to read output signal every several seconds and then compare to reference for calibration, or to calculate mean or median values to improve repeatability.

Rare information is given about sensitivity to environment, maintenance needs and longevity of low-cost sensors. Some papers use an analysis of variance (ANOVA) to check sensitivity to environment. Indeed, most low-cost sensors need retrofit to make them suitable for *in situ* application: enclosure, coating, etc. This is not only related to low-cost sensors themselves. For example, air humidity and water level sensors with waterproof housing should have longer longevity. We speculate that all the low-cost water quality sensors discussed in this review will be fouled when immersing in stormwater and/or wastewater for months, which will (i) require frequent cleaning and (ii) reduce longevity. It would be valuable to develop a plumbing system that can automatically sample water and clean water quality sensors.

Based on this literature review, we have investigated low-cost meteorological sensors (see Chapter 3). A special attention has been devoted to rainfall monitoring (Chapter 4) and water level monitoring (Chapter 5).

CHAPTER 3: LOW-COST SENSOR ASSESSMENT METHODS AND TEST SITES

3.1 INTRODUCTION

This chapter presents the methods and sites used in this thesis to assess the performance of low-cost sensors. It is organized in two main sections: The first section gives the definition of Enlarged Uncertainty (EU), Coverage Interval (CI), and Correctness Rate (CR); and presents the correlation method applied to compare low-cost sensors with reference sensors. The second section describes the test sites: the Green ROOF (GROOF) platform and the "Porte des Alpes" stormwater management site.

3.2 SENSOR ASSESSMENT METHODS

As described in Table 2-2, major indicators for low-cost sensors performance assessment include trueness, repeatability, reproducibility, resolution, response time, sensitivity to environment, maintenance needs and longevity. Among these parameters, trueness, repeatability, and reproducibility are used to evaluate the sensor accuracy, which is important for end-users. This section gives the definitions of enlarged uncertainty, coverage interval and correctness rate to quantitatively characterize the accuracy of tested low-cost sensors. Tested sensor resolution and response time have not been assessed due to lack of adapted equipment. Sensitivity to environment, maintenance needs, and longevity are highly influenced by sensor location, local climate, maintenance frequency and so on. They are therefore described qualitatively in this thesis.

3.2.1 Enlarged uncertainty and coverage interval

In this research work, we faced the difference between on the one hand accuracy used in commercial practice and documents without explicit definition, and on the other hand academic recommendation and international standards. In academic recommendation and international standards, sensor accuracy is expressed by trueness, repeatability, and reproducibility which characterize distinct aspects of sensors (Table 2-2). But in their

commercial documents, most sensor manufacturers use “accuracy” directly in datasheets to “guarantee” their sensor performance, such as datasheet screenshots shown in Figure 3-1 and Figure 3-2.

3. Technical Specification:

Model	DHT22
Power supply	3.3-6V DC
Output signal	digital signal via single-bus
Sensing element	Polymer capacitor
Operating range	humidity 0-100%RH; temperature -40~80Celsius
Accuracy	humidity +-2%RH(Max +-5%RH); temperature <+-0.5Celsius
Resolution or sensitivity	humidity 0.1%RH; temperature 0.1Celsius
Repeatability	humidity +-1%RH; temperature +-0.2Celsius
Humidity hysteresis	+-0.3%RH
Long-term Stability	+-0.5%RH/year
Sensing period	Average: 2s
Interchangeability	fully interchangeable
Dimensions	small size 14*18*5.5mm; big size 22*28*5mm

Figure 3-1. Tested low-cost sensor DHT22 datasheet including “accuracy” specifications. Source: Sparkfun.com (accessed: 29 March 2023).

Specifications

Spectral Range	360 to 1120 nm (wavelengths where response is 10% of maximum)	Sensitivity	5 mV/Wm^{-2}
Measurement Range	0 to 2000 W/m^2 (full sunlight ≈1000 W/m^2)	Calibration Factor	5 W/m^2/mV
Absolute Accuracy	±5% for daily total radiation	Cosine Correction Error	±5% at 75° zenith angle; ±2% at 45° zenith angle
		Temperature Response	0.04 ± 0.04% per °C

Figure 3-2. Reference pyranometer CS300 datasheet including “absolute accuracy”. Source: campbellsci.com (accessed: 29 March 2023).

According to Bertrand-Krajewski *et al.* (2021), for any measured or calculated quantity Y, there are three steps in uncertainty assessment:

(1) Estimation of the true value of Y.

(2) Estimation of the standard uncertainty of Y noted $u(Y)$.

(3) Estimation of the coverage interval (CI) of Y for a given level of probability α (typically 95%):

$$[Y - ku(Y), Y + ku(Y)] \quad \text{Equation 3-1}$$

where k (-) is the enlargement factor and $ku(Y)$ is the enlarged uncertainty, sometimes also noted $U(Y)$

The coverage interval is usually interpreted, in a simplified way, as "the true value of the quantity Y has an approximately 95% probability to lie between [$Y - ku(Y)$, $Y + ku(Y)$]".

The value of k depends on ν, the number of degrees of freedom in the data set used to estimate $u(Y)$ and is given by the Student t distribution. If ν is large, typically higher 30 to 50, then k becomes close to 1.96, which corresponds to the Gaussian distribution that is the limit of the Student t distribution when ν tends to infinite. For lower values of ν, k increases and may reach 12.71 in the worst case where ν = 1 (details are given e.g., in (Bertrand-Krajewski *et al.*, 2021)). In the absence of a clear definition, one may interpret the "accuracy" given by sensor manufacturers as combining and/or likely confusing trueness, repeatability, and reproducibility. Sensor manufacturers frequently give accuracy with a plus and minus sign which has same format as enlarged uncertainty. But the level of probability α is not given, which makes the interpretation ambiguous. In the following chapters of this thesis, one assumes that (i) accuracy given by manufacturers is equal to the enlarged uncertainty, (ii) that the corresponding level of probability is 95 % and/or the enlargement factor k is 1.96.

3.2.2 Correctness rate

In Chapters 4, 5, and 6, low-cost sensors are compared with nearby reference sensors. The proposed correctness rate aims to assess the percentage of measured quantity values delivered by a low-cost sensor that are in agreement with the reference quantity values given by the corresponding reference sensor used under the same *in situ* conditions. Every sensor should be given with its enlarged uncertainty by its manufacturer. In case of reference sensors, the manufacturers usually provide the enlarged uncertainty. However, not all manufacturers of low-cost sensors provide the sensor enlarged uncertainty (and they sometimes provided doubtful values, as discussed later in the thesis).

When enlarged uncertainty is available for both low-cost and reference sensors, a correct output from a low-cost sensor corresponds to an overlap between the low-cost coverage interval and the reference coverage interval. For

example, Table 3-1 presents the air humidity measurement results obtained by a low-cost sensor (enlarged uncertainty ± 5 %RH) and a reference sensor (enlarged uncertainty ± 3 %RH).

Table 3-1. Low-cost and reference air humidity sensor output example.

Timestamp	Low-cost sensor output (%RH)	Reference sensor output (%RH)
2022-04-26 00:00:00	60	47
2022-04-26 00:00:01	51	52
2022-04-26 00:00:02	54	51
2022-04-26 00:00:03	47	54
2022-04-26 00:00:04	46	57

Table 3-2 provides the output coverage interval [sensor output – enlarged uncertainty, sensor output + enlarged uncertainty] for both sensors, and the last column indicates if the two coverage intervals overlap.

Table 3-2. Low-cost and reference air humidity sensor output coverage interval example.

Timestamp	Low-cost sensor output coverage interval (%RH)	Reference sensor output coverage interval (%RH)	Do the two coverage intervals overlap?
2022-04-26 00:00:00	[55,65]	[44,50]	No
2022-04-26 00:00:01	[46,56]	[49,55]	Yes
2022-04-26 00:00:02	[49,59]	[48,54]	Yes
2022-04-26 00:00:03	[42,52]	[51,57]	Yes
2022-04-26 00:00:04	[41,51]	[54,60]	No

As shown in the last column of Table 3-2, in five comparisons, low-cost and reference sensor output coverage intervals overlap for three measurements, the low-cost sensor output correctness rate is thus defined as the percentage of measurements for which both coverage ranges overlap:

$$Correctness\ rate = \frac{Number\ of\ measurements\ with\ overlapping\ coverage\ ranges}{Total\ number\ of\ measaurements} = \frac{3}{5} = 60\ \% \qquad \text{Equation 3-2}$$

One assumes that enlarged uncertainty of most low-cost sensors is unknown or doubtful. Therefore, the correctness rate is calculated for different hypothetical values of their enlarged uncertainty and both information (enlarged uncertainty and correctness rate) is provided together. It is worth mentioning that increasing the enlarged

uncertainty value will, by definition, increase the correctness rate. The enlarged uncertainty corresponding to 95% correctness rate is proposed in this thesis as a way to assess the low-cost sensor performance.

3.2.3 Correlation method

To compare a low-cost sensor with a reference sensor, evaluating the correlation function between their respective data sets is a useful approach. This section describes how this is applied in this thesis.

3.2.3.1 Material and methods

Assuming the reference sensor delivers "reference values" of the quantity of interest, a correlation function is determined for each corresponding low-cost sensor:

$$y = f(b, x) = \sum_{i=1}^{j+1} b_{ji}\ x^{\,i-1} \qquad \text{Equation 3-3}$$

where f is the correlation function, b is the vector of the parameters b_{ji} of the correlation function, x is the value given by the reference sensor, and y is the value measured by the low-cost sensor. Equation 3-3 is the generic equation, which is tested successively for degrees j = 1 to 3, and for cases without and with intercept ($b_{j1} = 0$ and $b_{j1} \neq 0$ respectively).

Ordinary least squares regression is used to calculate the correlation equation. The tested correlation functions are first to third order polynomial functions, as detailed in section 7.6.4 of Benisch *et al*. (2021). Calculations have been carried out by using the "Sensor Calibration/ Correlation" option of the UDMT (Urban Drainage Metrology Toolbox) online application (link: http://coudlabs.alisonen.com/, accessed 29 March 2023) developed in the Co-UDlabs project (Bertrand-Krajewski and Lepot, 2022).

Figure 3-3. UDMT user interface.

3.2.3.2 Example of application with the WH-SP-WS01 data set

Let consider the low-cost anemometer WH-SP-WS01 output quantity values compared with reference anemometer output quantity values as an example (results are summarised in section 4.3.2.1). The dataset imported to UDMT is shown in Figure 3-4 (csv file with ";" separator).

	A	B	C	D	E
1	Time	reference_wind_speed_m_s	u_reference	low_cost_wind_speed_tips_min	u_low_cost
22269	2021-07-18 11:07:00	2.258	0.5	183	0
22270	2021-07-18 11:08:00	2.8	0.5	217	0
22271	2021-07-18 11:09:00	1.137	0.5	114	0
22272	2021-07-18 11:10:00	1.6	0.5	159	0
22273	2021-07-18 11:11:00	4.025	0.5	287	0
22274	2021-07-18 11:12:00	4.138	0.5	310	0
22275	2021-07-18 11:13:00	3.1	0.5	291	0
22276	2021-07-18 11:14:00	3.937	0.5	283	0
22277	2021-07-18 11:15:00	3.712	0.5	264	0
22278	2021-07-18 11:16:00	3.475	0.5	287	0
22279	2021-07-18 11:17:00	1.45	0.5	138	0
22280	2021-07-18 11:18:00	2.046	0.5	143	0
22281	2021-07-18 11:19:00	2.9	0.5	280	0
22282	2021-07-18 11:20:00	4.5	0.5	330	0
22283	2021-07-18 11:21:00	1.912	0.5	205	0

Figure 3-4. Screenshot of the data to import into UDMT with the following columns: (1) date and time, (2) reference sensor outputs, (3) standard uncertainty of reference sensor output, (4) tested sensor outputs, (5) tested sensor standard uncertainty (the uncertainty columns are not accounted for in this standard regression method but are needed to meet the format requirement).

After importing data by clicking “Select” button in the area “Import data”, choose “Correlation”, “Ordinary least squares” with “Force to 0” to correlate reference and tested sensor data with zero intercept as shown in Figure 3-5. Uncertainties in measured values are not accounted for in this ordinary least square regression.

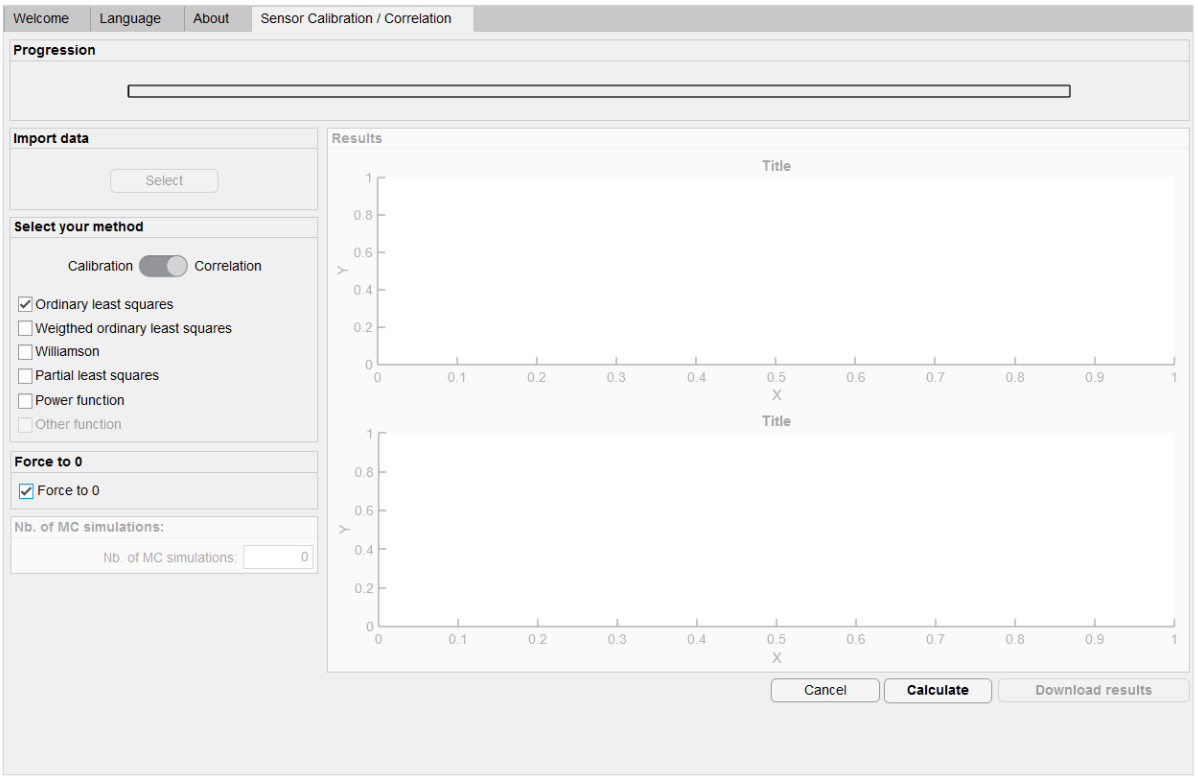

Figure 3-5. UDMT options to conduct an ordinary least squares correlation with zero intercept.

Results are shown in Figure 3-6.

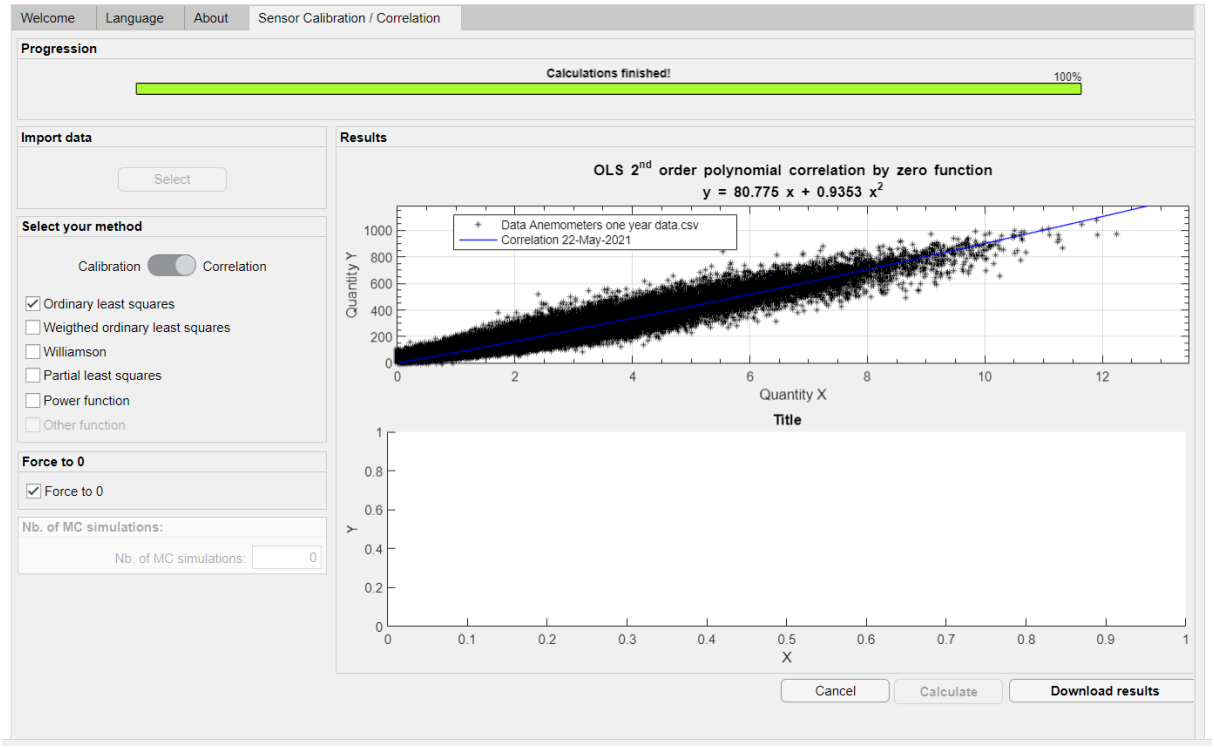

Figure 3-6. Correlation results given by UDMT.

The correlation graph in Figure 3-6 indicates that the optimal degree, based on a variance analysis, is the second order degree. But the user is not forced to accept this suggestion and can apply the function of his choice, e.g., in this case the first order polynomial function.

Quantitative results can be downloaded by clicking the “Download results” button on the right bottom corner of Figure 3-6. Same steps are conducted to correlate with free intercept by not selecting “Force to 0” option. All correlation results with or without zero intercept and their explanations are shown in Table 3-3.

Table 3-3. Correlation results and comments of reference and tested anemometer outputs.

Parameter	Results with zero intercept	Results with free intercept	Explanation
Time	2021-05-22 00:00	2021-05-22 00:00	Data set start time stamp
DegOpt	2	2	Recommended optimal order of the polynomial function
deg_1	1	1	Following lines are for the first order polynomial function $y = b_{11} + b_{12}x$
b11	0	10.0196	Regression coefficient b_{11}
b12	84.5610	81.0321	Regression coefficient b_{12}
u_b11	0	0.0855	Standard uncertainty in b_{11}
u_b12	0.0324	0.0436	Standard uncertainty in b_{12}
var_b11_b12	0	-0.0026	Covariance (b_{11}, b_{12})
ResVar1	926.0974	873.6885	Residual variance
deg_2	2	2	Following lines are for the second order polynomial function $y = b_{21} + b_{22}x + b_{23}x^2$
b21	0	18.3433	Regression coefficient b_{21}
b22	80.7750	67.3751	Regression coefficient b_{22}
b23	0.9353	2.6496	Regression coefficient b_{23}
u_b21	0	0.0965	Standard uncertainty in b_{21}
u_b22	0.0689	0.0952	Standard uncertainty in b_{22}
u_b23	0.0151	0.0166	Standard uncertainty in b_{23}
var_b21_b22	0	-0.0068	Covariance (b_{21}, b_{22})
var_b21_b23	0	0.0009	Covariance (b_{21}, b_{23})
var_b22_b23	-0.0009	-0.0014	Covariance (b_{22}, b_{23})
ResVar2	910.7501	786.6616	Residual variance
deg_3	3	3	Following lines are for the third order polynomial function $y = b_{31} + b_{32}x + b_{33}x^2 + b_{34}x^3$
b31	0	22.8652	Regression coefficient b_{31}
b32	79.8384	53.4502	Regression coefficient b_{32}
b33	1.4440	8.8414	Regression coefficient b_{33}
b34	-0.0536	-0.6080	Regression coefficient b_{34}
u_b31	0	0.1043	Standard uncertainty in b_{31}
u_b32	0.1244	0.1651	Standard uncertainty in b_{32}
u_b33	0.0582	0.0628	Standard uncertainty in b_{33}
u_b34	0.0059	0.0060	Standard uncertainty in b_{34}
var_b31_b32	0	-0.0125	Covariance (b_{31}, b_{32})
var_b31_b33	0	0.0035	Covariance (b_{31}, b_{33})
var_b31_b34	0	-0.0003	Covariance (b_{31}, b_{34})
var_b32_b33	-0.0067	-0.0096	Covariance (b_{32}, b_{33})
var_b32_b34	0.0006	0.0008	Covariance (b_{32}, b_{34})
var_b33_b34	-0.0003	-0.0004	Covariance (b_{33}, b_{34})
ResVar3	910.4290	752.3868	Residual variance

The mean error ε is the square root of the residual variance: in this case, the mean error of the six evaluated correlation functions shown in Table 3-3 are summarized in Table 3-4.

Table 3-4. Mean errors of the six evaluated correlation functions.

	Function with zero intercept	**Function with free intercept**
Mean error of first order function	30.4318	29.5582
Mean error of second order function	30.1786	28.0475
Mean error of third order function	30.1733	27.4297

As shown in Table 3-4, the mean error of second order function is slightly, but not very much, lower than the first order function. In this thesis, except in particular cases and for the sake of simplicity in the interpretation of correlation functions in terms of bias (intercept different from zero) and sensitivity (slope different from 1), we only show and compare first order regression results with or without zero intercept in tables like Table 3-5, when the second or third order does not provide significant reduction of the mean error.

Table 3-5. Regression results for the low-cost anemometer.

Parameter	**With 0 intercept**	**With free intercept**	**Explanation**
b11	0	10.0196	b_{11} of function $y = b_{11} + b_{12}x$
b12	84.5610	81.0321	b_{12} of function $y = b_{11} + b_{12}x$
u(b11)	0	0.0855	Standard uncertainty in b_{11}
u(b12)	0.0324	0.0436	Standard uncertainty in b_{12}
cov(b11, b12)	0	-0.0026	Covariance (b_{11}, b_{12})
ResVar1	926.0974	873.6885	Residual variance
IC95 b11	0	[9.8521, 10.1812]	95% coverage interval of b_{11}
IC95 b12	[84.4975, 84.6245]	[80.9467, 81.1175]	95% coverage interval of b_{12}
Standard error	30.4318	29.5582	Square root of the residual variance

As the number of correlation data pairs is much higher than 30 (28960 pairs in the above example), the distribution of regression coefficients b is usually assumed to be Gaussian (Bertrand-Krajewski *et al.*, 2021). In this case, k = 1.96 for a given level of probability α = 95%. Therefore, for the first order function with free intercept,

according to Equation 3-1 , the 95% coverage interval of the bias b11 is [b11 - 1.96 u(b11), b11 + 1.96 u(b11)] = [9.8521, 10.1812], which is different from 0. Therefore, the first order function with free intercept is selected to correlate two anemometers' outputs. As the range of low-cost anemometer output tips per minute are approximately 0 to 1000 as shown in Figure 3-6, the coefficients of correlation function are used with only two significant digits. The correlation function of low-cost and reference anemometers can therefore be expressed as:

$$y = 10 + 81\,x \qquad \text{Equation 3-4}$$

with a standard error ε = 30.

3.2.4 Sensor assessment sites

3.2.5 Green roof platform

Low-cost sensors described in Chapters 4 and 5 are tested in the GROOF (Green ROOf Facility) experimental platform. This platform is installed on one roof of INSA Lyon (Villeurbanne, France) by the DEEP (Déchets, Eaux, Environnement et Pollutions) laboratory. This platform was built to conduct research on the hydrological functioning of vegetated roofs used for urban stormwater management. In the long-term, the objective of this experiment is to evaluate the evapotranspiration capacities of different vegetated roofs thanks to continuous measurements of their mass, and to develop, if necessary, a correction model of the measured masses to consider the ambient meteorological conditions. The GROOF platform is composed of six pilot facilities designed to accommodate pilot green roofs as shown in Figure 3-7. (Deplette *et al.* 2021)

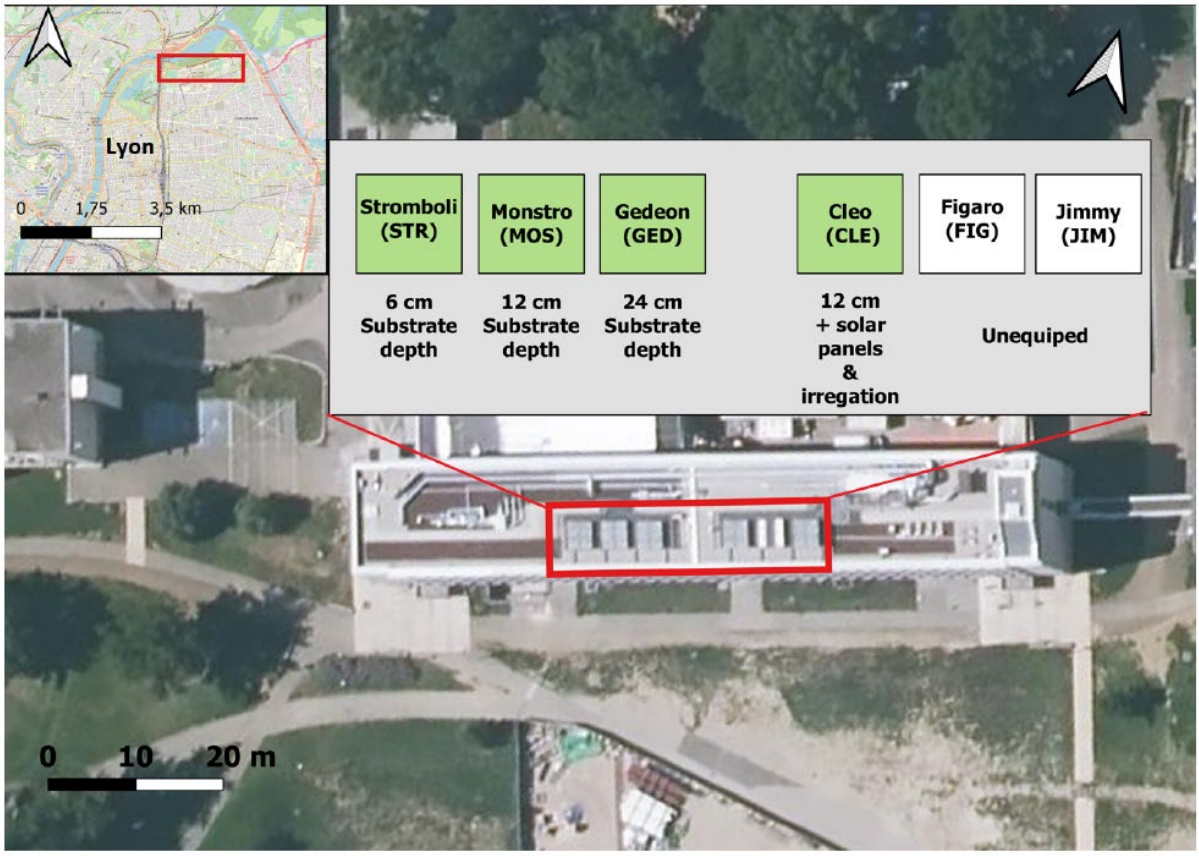

Figure 3-7. Location and configuration of the GROOF experimental platform at INSA Lyon, France. Source: Johnsen *et al*. (2023).

3.2.5.1 Reference meteorological sensors on the GROOF platform

To measure weather conditions, the GROOF experimental platform is equipped with a weather station including a Tipping Bucket Rain Gauge (TBRG, model: Précis Mécanique® 3029), a Weighing Rain Gauge (WRG, model: OTT pluvio²L from OTT HydroMet®), a wind speed and direction sensor (model: Campbell Scientific® 03002-L), an air temperature and relative humidity sensor (model: Campbell Scientific® CS215), and a pyranometer (model: Campbell Scientific® CS300). These sensors are described in the following subsections.

3.2.5.1.1 Rain gauges OTTPluvio²L and Précis Mécanique 3029

As described in Chapter 2, tipping-bucket rain gauges (TBRG) and weighing rain gauges (WRG) with improved dynamic stability and short step response are the most accurate gauges for one-minute rainfall intensity

measurements, providing the lowest measurement uncertainty with respect to the assumed working reference (Lanza and Vuerich, 2009).

(1) Weighing rain gauge OTTPluvio²L

The weighing rain gauge OTTPluvio²L (Figure 3-8) measures rainfall intensity by continuously recording the water mass inside its tank. The characteristics given by its manufacturer (OTT HydroMet, 2023a) are shown in Table 3-6.

Figure 3-8. Picture of the OTTPluvio²L rain gauge. Source: ott.com (accessed: 29 March 2023).

Table 3-6. Characteristics of the OTTPluvio²L reference rain gauge. Source: OTT HydroMet (2023).

Sensor name	**OTTPluvio²L**
Type	Weighing rain gauge
Size	Diameter ~ 45 cm, height ~ 70 cm
Weight	~ 1600 g
Measurement range	0 to 3000 mm/h
Power supply	5.5 to 28 V DC, typical value 12 V DC
Output	SDI-12, RS-485 [a]
Enlarged uncertainty	±6 mm/h or ±1% of the measured value (-25 to 45°C) [b]
Resolution	0.01 mm/h
Response time	1 minute
Sensitivity to environment	NA
Maintenance needs	NA
Longevity	NA

[a] SDI-12: Serial Digital Interface at 1200 baud (SDI-12 Support Group, 2009).

[b] "précision" in the datasheet in French.

The weighing rain gauge has been tested by Deplette *et al.* (2021). They pour, every 2 or 5 minutes, known quantity of water and then comparing this water quantity with the value recorded by the rain gauge (by reading the data recorded by the data acquisition unit). They conclude that, for this calibration, volumes of 5 and 10 mL of water, corresponding respectively to heights of 0.12 and 0.25 mm of water, are poured. The device detects the correct quantities of water introduced with a delay of 5 minutes, which is consistent with the technical manual of the supplier (acquisition in slightly delayed time). But they do not give details and conduct uncertainty assessment.

(2) Tipping bucket rain gauge Précis Mécanique 3029

The tipping bucket rain gauge Précis Mécanique 3029 (Figure 3-9) measures rainfall intensity by recording the number of tips per time unit. Its characteristics are summarized in Table 3-7.

Figure 3-9. Picture of the Précis Mécanique 3029 rain gauge.

A static calibration was done for the tipping bucket rain gauge. It concludes that the actual bucket tipping volume of the rain gauge V is 10.64 mL instead of the theoretical 10 mL (Deplette *et al.*, 2021). According to manufacturer (Precis Mécanique, 2023), the funnel area of Précis Mécanique 3029 is 40,000 mm^2 and the radius R of the Précis Mécanique 3029 circle funnel area is 113 mm according to our measurement.

The definition of tipping bucket rain gauge resolution r (mm/tip) is (Humphrey *et al.*, 1997):

$$r = \frac{V}{S} = \frac{V}{\pi R^2} \qquad \text{Equation 3-5}$$

with V the volume of water per tip in mm^3/tip and S the rain gauge collecting area in mm^2. One gets that Précis Mécanique 3029 has a resolution 0.265 mm/tip.

Using the resolution 0.265 mm/tip, one compares the cumulative rainfall depth reported by Précis Mécanique 3029 and the weighing rain gauge OTTPluvio²L cumulative from 31 March 2022 to 28 July 2022 (weighting rain gauge ends function on this date due to power supply interruption), results are shown in Figure 3-10 (a). Assuming that weighting rain gauge gives true values, a correction factor is calculated by the least square method to get lowest root mean square error. One gets that the correction factor is 0.88, i.e., the tipping bucket rain gauge Précis Mécanique 3029 has a corrected resolution $0.265 \times 0.88 = 0.233$ mm/tip (Johnsen *et al.*, 2023). The TBRG Précis Mécanique 3029 outputs with resolution 0.233 mm/tip conform well with WRG OTTPluvio²L as shown in Figure 3-10 (b). According to WMO (2008), tipping bucket rain gauge has a typical relative enlarged uncertainty

10%. The dynamic calibration of the tipping bucket rain gauge Précis Mécanique 3029 has not been done yet and is planned.

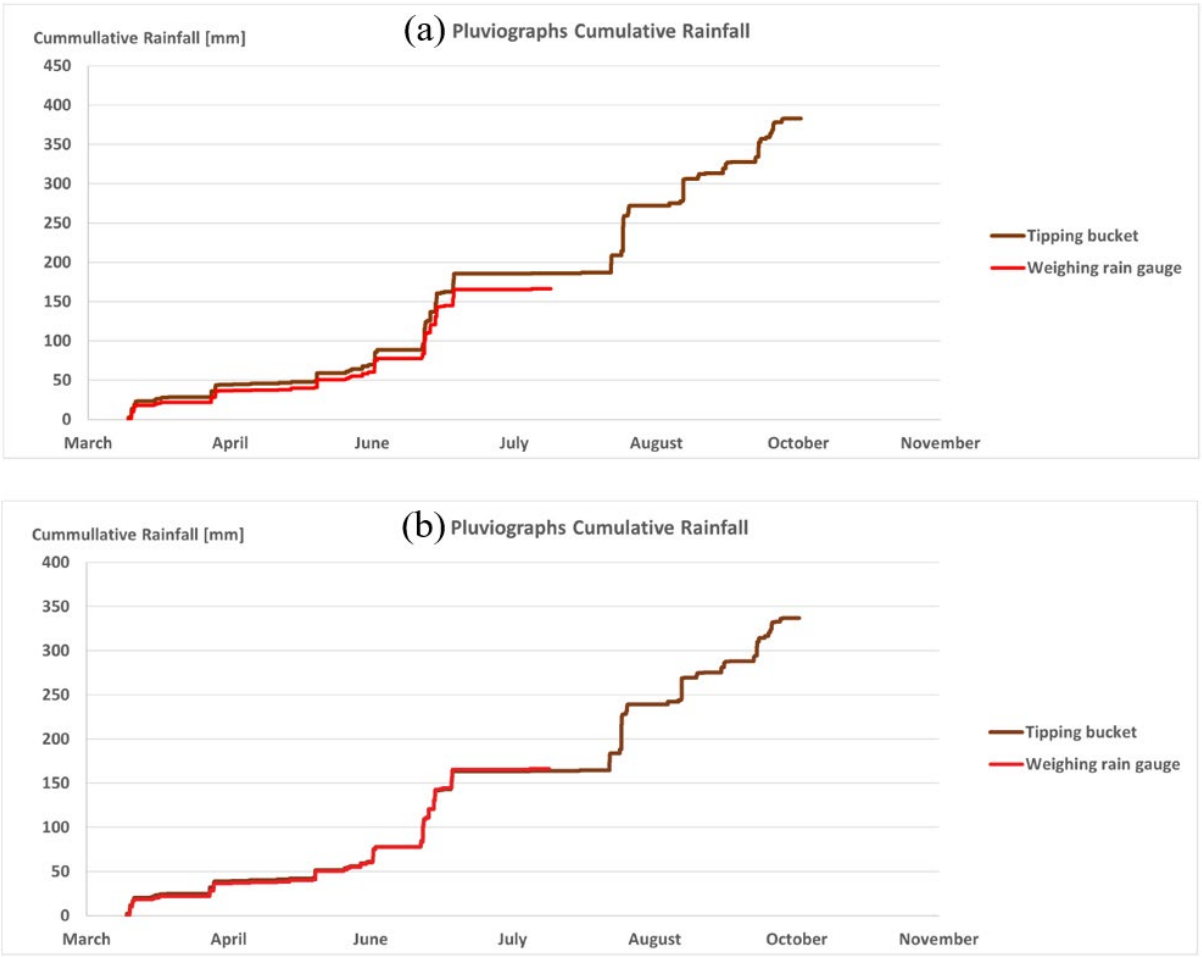

Figure 3-10. Pluviographs of TBRG and WRG cumulative rainfall depth from 31 March 2022 to 28 July 2022. (a) TBRG has a resolution 0.265 mm/tip, (b) TBRG has a resolution 0.233 mm/tip. Source: Johnsen *et al*. (2023).

Table 3-7. Characteristics of the Précis Mécanique 3029 rain gauge.

Sensor name	**Précis Mécanique 3029**
Type	Tipping bucket rain gauge
Size	Diameter ~ 22.5 cm, height ~ 70 cm
Weight	NA
Measurement range	NA
Power supply	NA
Output	NA
Enlarged uncertainty	±10%
Resolution	0.233 mm/tip
Response time	NA
Sensitivity to environment	NA
Maintenance needs	NA
Longevity	NA

3.2.5.1.2 Wind speed and direction Campbell Scientific 03002-L

The Campbell Scientific 03002-L device (Figure 3-11) is used as reference wind speed and direction sensor. Its characteristics (Campbell Scientific, 2020) are shown in Table 3-8 and Table 3-9 respectively for anemometer and anemoscope sensors.

Figure 3-11. Picture of the Campbell Scientific 03002 device. Source: campbellsci.com (accessed: 29 March 2023).

The Campbell Scientific 03002-L anemometer measures wind speed by processing the alternating current sine wave which has an amplitude proportional to the cup rotation speed.

Table 3-8. Characteristics of the Campbell Scientific 03002-L anemometer. Source: Campbell Scientific (2020).

Sensor name	**Campbell Scientific 03002-L**
Type	Three cups anemometer
Size	diameter ~ 12 cm
Weight	113 g
Measurement range	0 to 50 m/s, starting threshold 0.5 m/s
Power supply	NA
Output	NA
Enlarged uncertainty	± 0.5 [a] m/s
Resolution	0.75 m/s per Hz
Response time	NA
Sensitivity to environment	NA
Maintenance needs	NA
Longevity	NA

[a] "Accuracy" in the data sheet.

There is a potentiometer inside the Campbell Scientific 03002-L anemoscope. Its resistance is proportional to the azimuth angle of the wind direction and is measured by applying the precision excitation voltage on it.

Table 3-9. Characteristics of the Campbell Scientific 03002-L anemoscope. Source: Campbell Scientific (2020).

Sensor name	**Campbell Scientific 03002**
Type	Resistance anemoscope
Size	Vane length ~ 22 cm
Weight	170 g
Measurement range	Mechanical range 360°, output range 352° (8° open) [a]
Power supply	NA
Output	Voltage, starting threshold 1.8 m/s with 5° displacement
Enlarged uncertainty	±5° [b]
Resolution	NA
Response time	NA
Sensitivity to environment	NA
Maintenance needs	NA
Longevity	Life expectancy is 50 million revolutions

[a] The user manual (Campbell Scientific, 2022) explains: "The wind vane is coupled to a 10 kΩ potentiometer, which has a 8-degree electrical dead band between 352 and 360 degrees. A 1 MΩ resistor between the signal and ground pulls the signal to 0 mV (0 degrees) when wind direction is in the dead band (between 352 and 360 degrees)".

[b] "Accuracy" in the data sheet.

3.2.5.1.3 Air temperature and relative humidity sensor Campbell Scientific CS215-L

The air temperature and humidity sensor Campbell Scientific CS215-L (Figure 3-12) is used as reference. Its characteristics (Campbell scientific, 2023) are shown in Table 3-10.

According to manufacturer (Campbell Scientific, 2023a), this sensor is based on the Sensirion SHT75 sensor which can also be connected to Arduino directly.

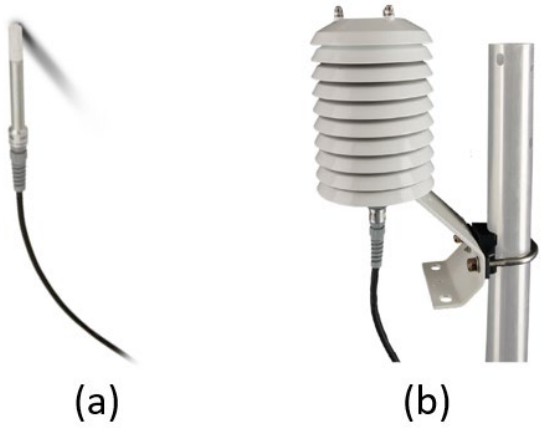

Figure 3-12. Picture of the Campbell Scientific CS215-L device: (a) probe, (b) probe in a metal protective housing. Source: campbellsci.com (accessed: 29 March 2023).

Table 3-10. Characteristics of the Campbell Scientific CS215-L sensor. Source: Campbell Scientific (2023).

Sensor name	**Campbell Scientific CS215-L**
Type	Air temperature and humidity sensor kit
Size	Diameter ~ 12 cm at sensor tip, length ~ 18 cm
Weight	~ 150 g
Measurement range	-40° to +70°C, 0 to 100% RH (-20° to +60°C)
Power supply	7 to 28 V DC
Output	SDI-12
Enlarged uncertainty	Air temperature: ±0.3°C (at 25°C) ±0.4°C (5° to 40°C) ±0.9°C (-40° to +70°C) Air humidity: ±2% (10% to 90% range) at 25°C ±4% (0% to 100% range) at 25°C [a]
Resolution	0.01°C, 0.03% RH
Response time	Air temperature < 120 s, air humidity < 20 s.
Sensitivity to environment	NA
Maintenance needs	NA
Longevity	NA

[a] "Accuracy" in the data sheet.

3.2.5.1.4 Pyranometer Campbell Scientific CS300

The CS300 pyranometer used as reference sensor is shown in Figure 3-13 and its characteristics are given in Table 3-11. According Campbell Scientific (2020), the CS300 sensor uses a silicon photovoltaic detector mounted in a

cosine-corrected head to provide solar radiation measurement. It is calibrated against a Kipp & Zonen CM21 thermopile pyranometer (REF). Characteristics of CS300 given by manufacturer are shown in Table 3-11.

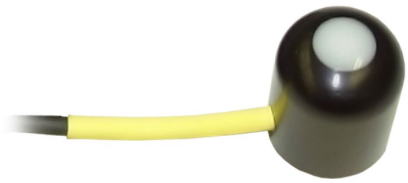

Figure 3-13. Picture of the Campbell Scientific CS300 pyranometer. Source: campbellsci.com (accessed: 29 March 2023).

Table 3-11. Characteristics of the Campbell Scientific CS300 pyranometer. Source: Campbell Scientific (2020).

Sensor name	**Campbell Scientific CS300**
Type	Silicon photovoltaic detector to measure solar radiation
Size	Diameter ~ 2.4 cm, height ~ 2.5 cm
Weight	65 g
Measurement range	0 to 2000 W/m^2
Spectral coverage	360 to 1120 nm [a]
Power supply	No need
Output	Voltage
Enlarged uncertainty	±5% for daily total radiation [b]
Resolution	0.2 mV/W/m^2
Response time	< 1 ms
Sensitivity to environment	NA
Maintenance needs	Check and clean every month
Longevity	Long-term stability < 2% per year

[a] "Wavelengths where response is 10% of maximum" explained by manufacturer.

[b] "Absolute accuracy" in the datasheet.

3.2.5.2 Data logger

All reference meteorological sensors are connected to a Campbell Scientific CR1000 data logger to collect monitoring data. CR1000 sends data to a desktop running loggerNet every minute. The desktop is remotely controlled by the DWService portal to monitor system operation, to setup the system and to get data conveniently. Figure 3-14 shows the reference data logger structure. In fact, measurements are taken every 5 seconds but only one value is recorded after processing of 12 measurements every minute. Table 3-12 gives details about how reference data are recorded.

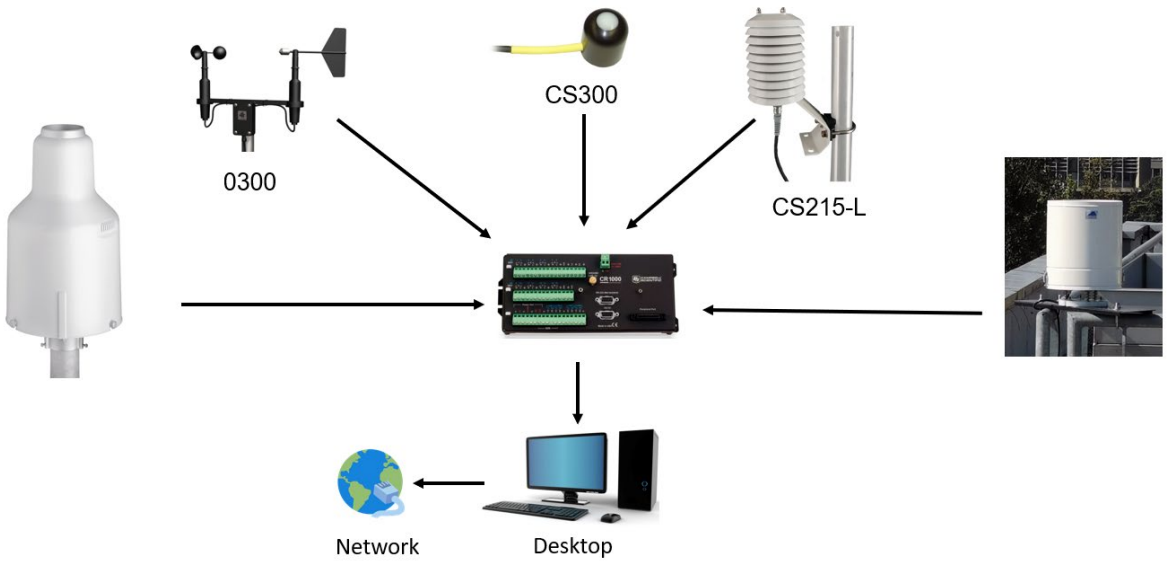

Figure 3-14. Structure of the reference data logger.

Table 3-12. Summary of recording measurements of reference sensors.

Sensor type	Sensor name	Measurement recording
Weighing rain gauge	OTTPluvio²L	Instantaneous mass measurement at timestamp
Tipping bucket rain gauge	Précis Mécanique 3029	Sum of tips per minute
Anemometer	Campbell Scientific 03002-L	Average, minimum and maximum wind speed of 12 measurements per minute
Anemoscope		Instantaneous wind direction measurement at timestamp
Air temperature sensor	Campbell Scientific CS215-L	Average of 12 measurements per minute
Air humidity sensor		Instantaneous measurement at timestamp
Pyranometer	Campbell Scientific CS300	Average of 12 measurements per minute

3.2.6 “Porte des Alpes” site

The low-cost water level monitoring station tested in Chapter 6 is installed along one of the lakes at Porte des Alpes in Lyon, France. The “Porte des Alpes” facility was built in 1996 as a multipurpose stormwater management infrastructure, with a cascade of storage and infiltration tanks, a park with permanent wetlands, aquatic ecosystems and original nature-like landscapes. Three lakes collect stormwater from the adjacent Technology Park district. Figure 3-15 below presents in a schematic way how stormwater control measures are operating in Portes des Alpes.

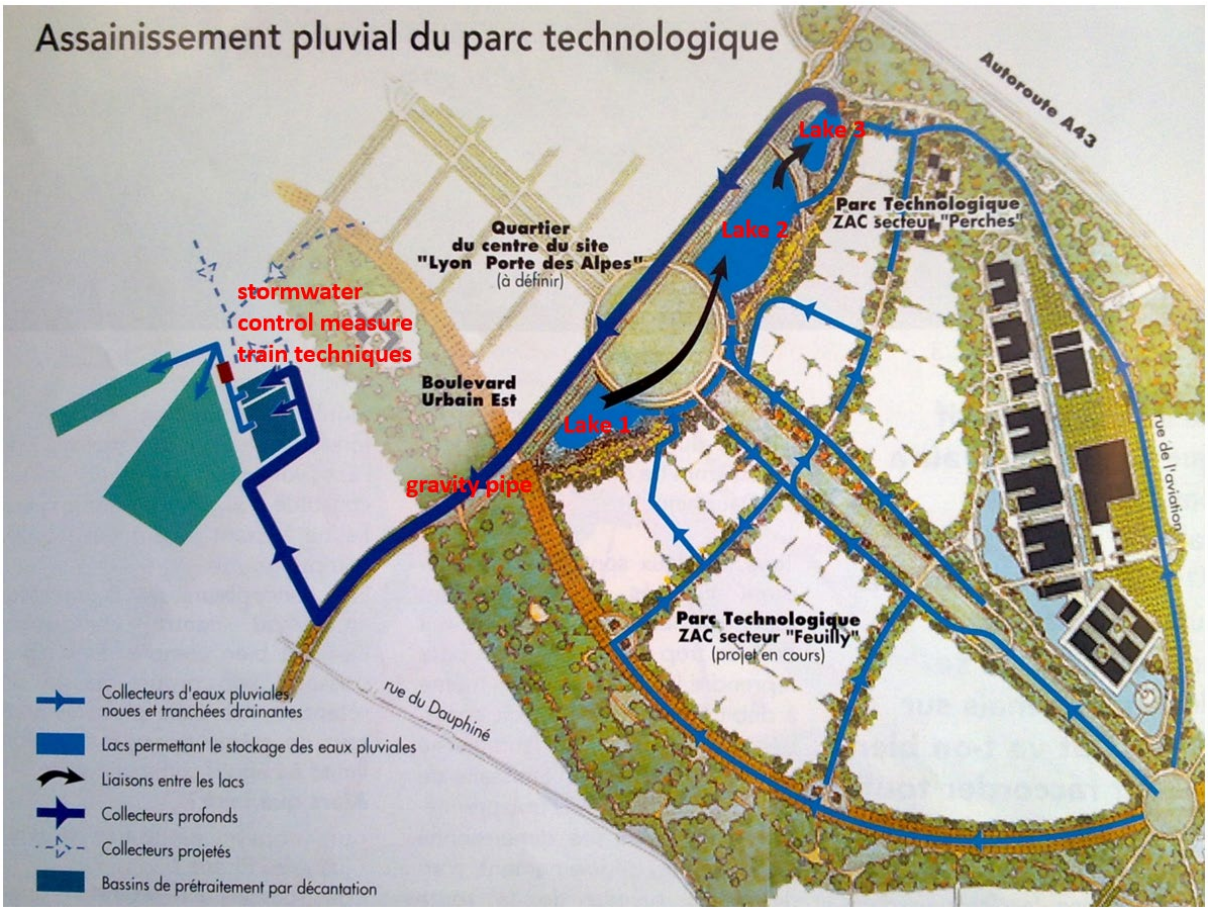

Figure 3-15. Stormwater control measures installed at Portes des Alpes, Lyon, France. Runoff from the “Parc Technologique” district is collected in swales and trenches and conveyed to the three lakes. Lake 1 (in the center) overflows into lakes 2. Lake 2 then overflows into lake 3 (smaller lake on top). Water from lake 3 is conveyed using a large gravity pipe to stormwater control measure train techniques (left of the image). Source: Greater Lyon.

The lakes have been monitored during the first years of installation and after more than 20 years the Lyon Metropolis was interested in monitoring the water level in the three lakes. The Lyon Metropolis has hired a company to install water level monitoring systems (with one measurement every hour) and we have taken the opportunity to install in parallel a low-cost water level monitoring system in each lake.

CHAPTER 4: LOW-COST METEOROLOGICAL SENSORS PERFORMANCE ASSESSMENT

4.1 INTRODUCTION

This chapter reports testing the possibility to use low-cost meteorological sensors in a weather station in the specific context of green roofs monitoring, measuring the following parameters: air temperature and humidity, wind direction and speed, rainfall and solar radiation. The data obtained are compared with those provided by reference meteorological sensors whose performance is known.

This chapter is organized in two main sections. Section 4.2 describes tested low-cost sensors and their reference instruments, design and implementation of sensor output data loggers, and some sensor data processing methods. Section 4.3 provides the operation details of low-cost sensor performance experiment activity and for most low-cost sensors, the results of a one-year period performance assessment, and their discussion.

Note: rain gauges are briefly introduced here: they will be presented and discussed separately in details in Chapter 5.

4.2 MATERIALS AND METHODS

4.2.1 Tested low-cost sensors

After literature review, open-source community communication and market research, several types of low-cost meteorological sensors are selected for analysis. Reference sensors are installed and operated by a technician on the same roof, nearby the tested low-cost sensors. Table 4-1 indicates the low-cost and reference sensors used for each measurement parameter and their respective prices.

Table 4-1. Tested low-cost sensors and the reference sensors with their commercial name and price range.

Measured quantity	Low-cost sensors	Price range	Reference sensors	Price range
Rainfall intensity	WH-SP-RG	~ 15 €	OTTPluvio²L Précis Mécanique 3029	~ 4250 € ~ 750 €
Wind speed	WH-SP-WS01	~ 20 €	Campbell Scientific 03002-L	~ 750 €
Wind direction	WH-SP-WD	~ 20 €		
Air temperature and humidity	BME280 DHT22	~ 5 € ~ 5 €	Campbell Scientific CS215-L	~ 280 €
Solar radiation	JXBS-3001-ZFS Si1145	~ 100 € ~ 10 €	Campbell Scientific CS300	~ 300 €

Low-cost tipping bucket rain gauge WH-SP-RG, anemometer WH-SP-WS01 and anemoscope WH-SP-WD are parts of the low-cost weather station kit SEN-15901 (Offset Electronics, 2023) which also contains mounting hardware and housing for air temperature and humidity sensor.

The description of each low-cost sensor is given hereafter, while the reference rain gauges are presented in section 3.2.5.1.

4.2.1.1 Tipping bucket rain gauge WH-SP-RG

Rainfall monitoring is particularly important for urban drainage systems management. Chapter 5 will be dedicated to rain fall monitoring with a detailed analysis of the WH-SP-RG rain gauge and an optical rain gauge.

4.2.1.2 Anemometer WH-SP-WS01

WH-SP-WS01 is made of low-density polyethylene. The output of WH-SP-WS01 is generated by a reed switch and a magnet. The reed switch inside the tested WH-SP-WS01 is normally closed. When the rotating mechanism turns a full rotation, the reed switch is opened two times by the magnet. WH-SP-WS01 has two pins and could be considered as a button when processing its signal. The structure of WH-SP-WS01 is shown in Figure 4-1.

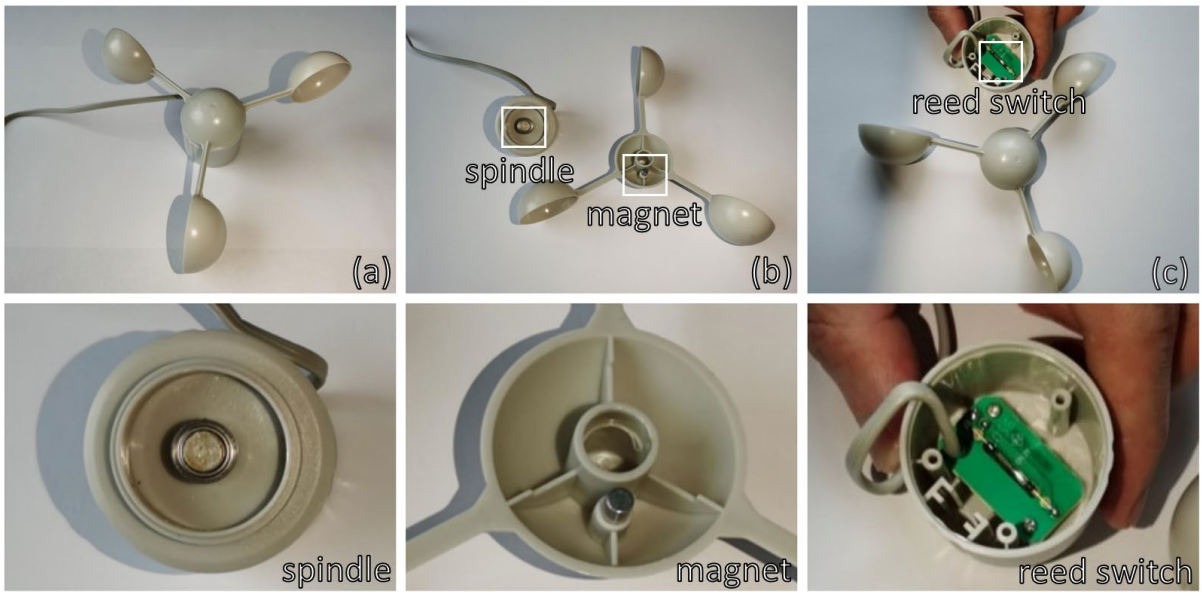

Figure 4-1. Internal and external structure of WH-SP-WS01: (a) appearance and three cup rotating mechanism (b) Spindle of rotating mechanism and the magnet. (c) internal circuit and reed switch. Enlarged images of spindle, magnet and reed switch are below.

The user manual of WH-SP-WS01 (Offset Electronics, 2023) indicates “a wind speed of 2.4 km/h (0.67 m/s) causes the switch to close once per second.” in English and “a wind speed of 0.33 m/s causes the switch to close once per second.” in Chinese. And in fact, at least for the WH-SP-WS01 tested, the reed switch is not closed but opened when the magnet is passing near it. Characteristics of WH-SP-WS01 are given in Table 4-2.

Table 4-2. Characteristics of WH-SP-WS01, adapted from Chapter 2. Source: Offset Electronics (2023).

Sensor name	WH-SP-WS01
Type	Three cups anemometer
Size	~ 7 ×10 ×10 cm
Weight	~ 45 g
Operating range	NA
Power supply	No need
Communication	As a button to controller
Enlarged uncertainty	NA
Resolution	0.67 or 0.33 m/s wind speed make the switch to close once per second.
Response time	NA
Sensitivity to environment	NA
Maintenance needs	NA
Longevity	NA

NA stands for not available.

4.2.1.3 Anemoscope WH-SP-WD

WH-SP-WD is made of low-intensity polyethylene. According to the user manual (Offset Electronics, 2023) and dismantling analysis, WH-SP-WD has four pins but only two pins are useful (black and white pins) and could be considered as a variable resistor when processing its signal. Resistance between the two other pins is always infinity. The structure of WH-SP-WD is shown in Figure 4-2.

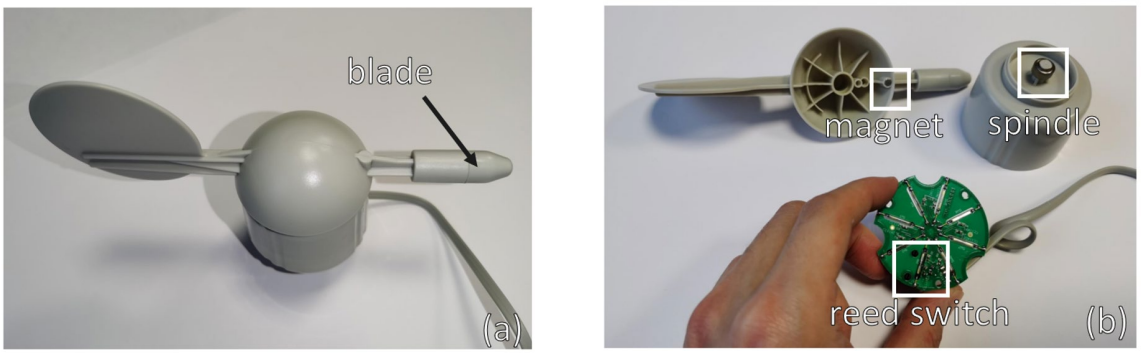

Figure 4-2. Internal and external structure of WH-SP-WD. (a) appearance (b) internal magnet, spindle, and circuit.

It has eight reed switches inside it, and each switch is connected with different values resistors. The blade's magnet can close two switches simultaneously, allowing 16 different wind directions to be indicated. Scheme given by the manufacturer is shown in Figure 4-3.

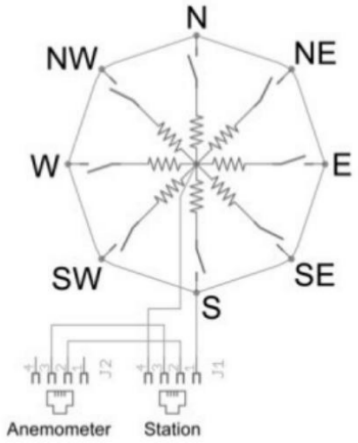

Figure 4-3. Function scheme of WH-SP-WD given by manufacturer. Source: sparkfun.com (accessed: 14 February 2023).

Characteristics of WH-SP-WD are given in Table 4-3.

Table 4-3. Characteristics of WH-SP-WD.

Sensor name	**WH-SP-WD**
Type	Anemoscope
Size	~ 19 × 10 cm
Weight	~ 90 g
Operating range	NA
Power supply	No need
Output	As a variable resistor to controller
Enlarged uncertainty	NA
Resolution	NA
Response time	NA
Sensitivity to environment	NA
Maintenance needs	NA
Longevity	NA

4.2.1.4 Temperature and relative humidity BME280, DHT22

4.2.1.4.1 BME280

A bare circuit module of low-cost resistive air temperature, humidity, and pressure sensor BME280 is tested (Figure 4-4).

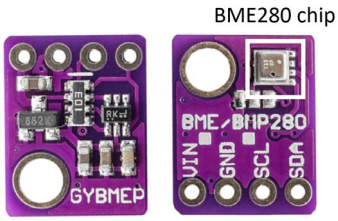

Figure 4-4. Pictures of BME280 bare circuit module. (The sensor is located in the upper right corner of the right picture). Source: Sparkfun.com (accessed 14 February 2023).

Characteristics of tested BME280 module given by manufacturer (BOSCH, 2018) are shown in Table 4-4.

Table 4-4. Characteristics of BME280, adapted from Chapter 2. Source: BOSCH (2018).

Sensor name	**BME280**
Type	Resistive air temperature, humidity, and pressure sensor
Size	1.4 ×1.1 × 0.25 cm
Wight	~ 1 g
Operating range	-40 to 85 °C, 0 to 100 % RH
Power supply	3.3 or 5 V DC
Output	I^2C or SPI protocol [a]
Enlarged uncertainty	± 0.5 ℃ (0 to 65 ℃), ± 1.25 ℃ (-20 to 0 ℃) and ± 1.5 ℃ (-40 to -20 ℃) [b], ±3 %RH (20 to 80 %RH, 25 ℃) [c]
Resolution	0.01 ℃, 0.008 %RH
Response time	1 s
Sensitivity to environment	NA
Maintenance needs	NA
Longevity	NA

[a] I^2C: Inter-Integrated Circuit (Gasperi and Hurbain, 2010), SPI: Serial Peripheral Interface (Wootton, 2016).

[b] The datasheet (BOSCH, 2018) writes: “absolute accuracy temperature”, “Temperature measured by the internal temperature sensor. This temperature value depends on the printed circuit board temperature, sensor element self-heating and ambient temperature and is typically above ambient temperature”.

[c] The datasheet (BOSCH, 2018) writes: “absolute accuracy tolerance, including hysteresis.”

4.2.1.4.2 DHT22

A second low-cost air temperature and humidity sensor has been tested: DHT22 (Figure 4-5).

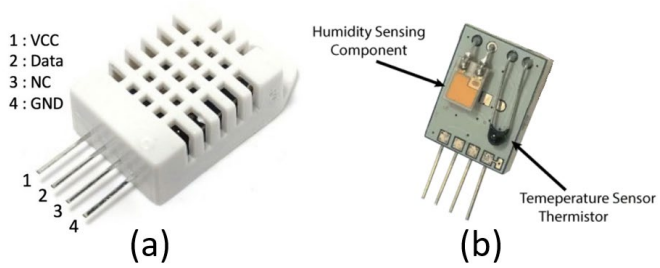

Figure 4-5. Pictures of DHT22 module: (a) appearance with its pin definition, (b) separate humidity and temperature sensing components inside the enclosure. Source: espruino.com, howtomechatronics.com (accessed 14 February 2023).

Characteristics of tested DHT22 given by manufacturer (Aosong Electronics, 2023) are shown in Table 4-5.

Table 4-5. Characteristics of DHT22, adapted from Chapter 2. Source: Aosong Electronics, (2023).

Sensor name	**DHT22**
Type	Capacitive humidity sensor
Size	~ 2.5 × 1.5 × 0.8 cm
Weight	~ 1 g
Operating range	-40 to 80 °C, 0 to 100 %RH
Power supply	3.3 to 6 V DC
Communication	Digital signal via single bus
Enlarged uncertainty	< ± 0.5 °C, ± 2 %RH (max ± 5 %RH) [a]
Resolution	0.1 °C, 0.1 %RH
Response time	Average 2 s
Sensitivity to environment	NA
Maintenance needs	NA
Longevity	NA

[a] Accuracy parameter in the datasheet.

4.2.1.5 Pyranometer JXBS-3001-ZFS

A low-cost pyranometer JXBS-3001-ZFS is tested (Figure 4-6). According to the manufacturer (WeihaiJingxun Electronic, 2020), JXBS-3001-ZFS is a total solar radiation (transmitter) sensor. Its core device is a photosensitive

element, and the quartz glass cover is installed outside the inductive element. Characteristics of JXBS-3001-ZFS given by manufacturer are shown in Table 4-6.

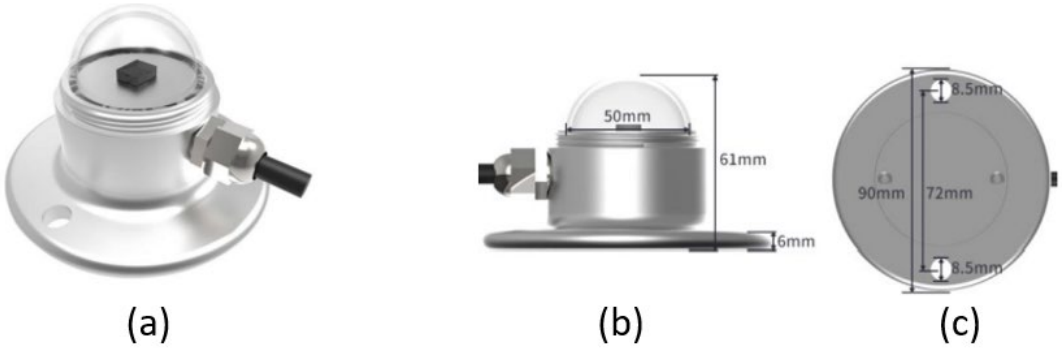

Figure 4-6. JXBS-3001-ZFS appearance (a) and size (b) (c). Source: WeihaiJingxun Electronic, (2020).

Table 4-6. Characteristics of JXBS-3001-FS. Source: Aosong Electronics (2023).

Sensor name	**JXBS-3001-ZFS**
Type	Total solar radiation sensor
Size	6.1 × 9 cm
Weight	~ 266 g
Measuring range	0 to 1500 W/m^2
Spectral coverage	300 to 3000 nm
Power supply	9 to 24 V DC
Output	Communication RS485 [a]
Enlarged uncertainty	NA
Resolution	1 W/m^2
Response time	≤ 5 s
Sensitivity to environment	Working environment -45 to 85 °C, 0 to 100 %RH
Maintenance needs	NA
Longevity	NA

[a] RS485: 2-wire, half-duplex, point-to-multiple master-slave communication (Buchanan, 2004).

4.2.1.6 Light sensor Si1145

One low-cost bear circuit Si1145 module (Figure 4-7) was tested from May 2022 to July 2022. The supplier (Adafruit, 2023) writes Si1145 Arduino library to printout the "counts" that proportional to visible light, infrared light intensity and ultraviolet light index but they do not give calculation details and guarantee the Si1145 performance. Characteristics of tested Si1145 given by supplier are shown in Table 4-7.

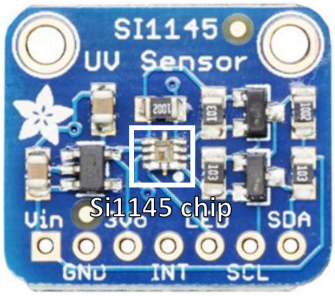

Figure 4-7. Picture of tested Si1145 module. Source: adafruit.com (accessed: 14 February 2023).

Table 4-7. Characteristics of tested Si1145 module, adapted from Chapter 2. Source: Adafruit (2023).

Sensor name	**Si1145**
Type	Light sensor
Size	~ 2 ×1.8 ×0.2 cm
Weight	~ 1.4 g
Measuring range	1 to 128 kilolux
Spectral coverage	400 to 1000 nm
Power supply	3 to 5 V DC
Output	"Counts" correspond to visible light intensity, infrared light intensity and ultraviolet light index at I^2C address 0x60 (7-bit)
Enlarged uncertainty	NA
Resolution	100 microlux
Response time	NA
Sensitivity to environment	NA
Maintenance needs	NA
Longevity	NA

4.2.2 Full scale deployment

In order to ensure independent measurement between the low-cost and reference sensors and to avoid interference between them, two distinct data loggers have been installed. Reference sensor data logger has been described in Chapter 3 section 3.2.5.

As shown in Figure 4-8, the core of the low-cost sensor data logger is an Arduino Nano (Arduino Documentation, 2023). Arduino Nano output low-cost sensors' measurements in real-time to a laptop using a serial connection. The laptop runs CoolTerm software (Roger Meier, 2023) to save the measurements to a text file. Roughly every minute: Arduino Nano (i) records the number of switches output by the low-cost tipping bucket rain gauge WH-SP-RG and the anemometer WH-SP-WS01 during the last minute, (ii) records the shared voltage of the low-cost anemoscope WH-SP-WD and convert it to wind direction, (iii) asks the low-cost pyranometer JXBS-3001-ZFS, light sensor Si1145, air humidity sensor BME280 or DHT22 to report their measurements. JXBS-3001-ZFS and

Arduino Nano communicate through RS485 to UART converter. In addition, Arduino Nano informs the laptop each time that WH-SP-RG has a tip (by sending a number “1” to the computer, see Figure 4-12 below).

For this installation, and to focus exclusively on the sensors performance, we decided to have the system always plug to a computer to avoid the risks related to the use of batteries. As the computer is connected to the INSA Lyon internal network, the system can be remotely checked.

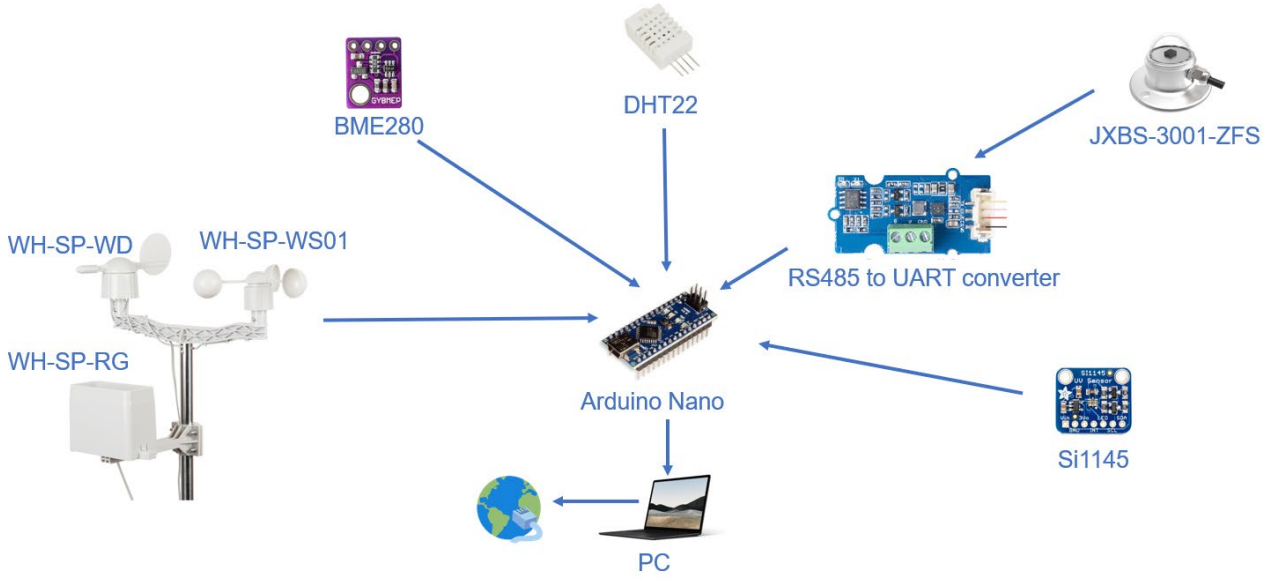

Figure 4-8. Structure of the data logger system dedicated to the low-cost sensors.

The connection design and hardware of the main control board of the low-cost data logger are given in Figure 4-9. It should be noted that there is an additional 5 V power supply coming from a 220 V power adapter in addition to the connection between the Arduino Nano and laptop to make the system more stable. The low-cost pyranometer JXBS-3001-ZFS needs an additional 12 V power supply to make it work. The real circuit board is shown in Figure 4-10.

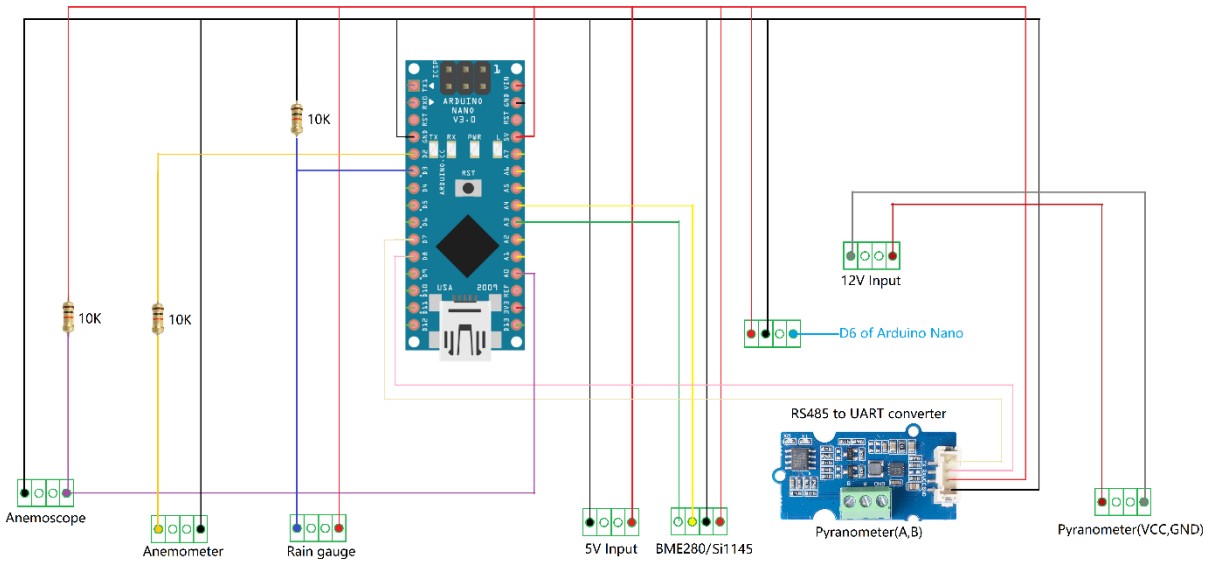

Figure 4-9. Circuit diagram of the data logger dedicated to low-cost sensors.

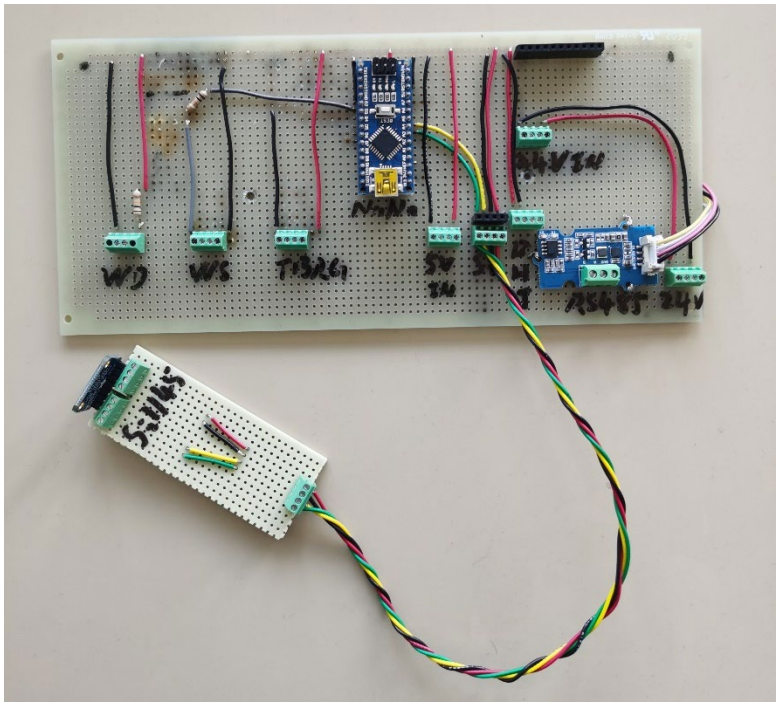

Figure 4-10. Real circuit board of low-cost sensors data logger.

Especially for wind direction data processing, a test is conducted to check the Arduino analog pin reading voltage in different wind blade position. Results are shown in Figure 4-11.

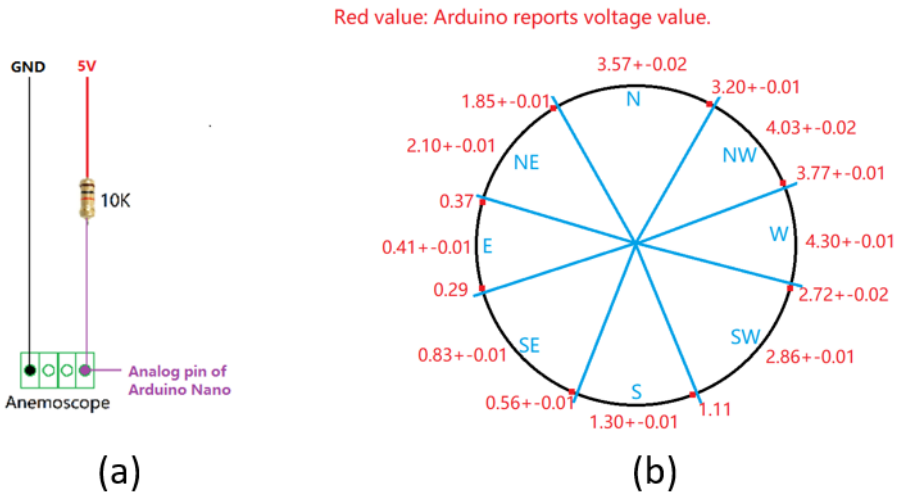

Figure 4-11. (a) Low-cost anemoscope test circuit. (b) Input voltage of Arduino analog pin in different wind direction.

As shown in Figure 4-11 (b), There are 16 possible voltage readings. Eight readings are detected when blade is at a specific position (red point on the black circle of Figure 4-11 (b)) and eight values are detected when blade is in a range of two specific positions (for example, when blade is at “S” position range on the bottom of Figure 4-11 (b), Arduino aways reads 1.30± 0.1 V). Eight positions are ignored and Arduino identifies eight wind directions range by the input voltage range i.e., north (N), northwest (NW), west (W), southwest (WS), south (S), southeast (SE), east (E), northeast (NE).

Figure 4-12 presents a screenshot of the text file generated by CoolTerm. The timestamps of measurement data are added by CoolTerm software i.e., the timestamp is the time when laptop acquires the output string from Arduino Nano. The timestamp corresponds to the measurement time because the communication between the Arduino Nano and the computer is immediate, and this system ensures to always have the correct timestamp (the computer is automatically synchronized thanks to its internet connection).

```
2021-09-08 05:56:43  ;20.90°C; 69.70%; 65W/m2;  0tR/min; 101tW/min; NE; 1,3,2,0,65,120,116,; V1.80
2021-09-08 05:57:43  ;20.90°C; 69.60%; 64W/m2;  0tR/min; 126tW/min; NE; 1,3,2,0,64,185,180,; V1.80
2021-09-08 05:58:44  ;20.90°C; 69.70%; 69W/m2;  0tR/min; 121tW/min; E; 1,3,2,0,69,121,183,; V1.80
2021-09-08 05:59:44  ;20.90°C; 69.60%; 78W/m2;  0tR/min; 103tW/min; E; 1,3,2,0,78,56,112,; V1.80
2021-09-08 05:59:59  1;
2021-09-08 06:00:44  ;20.90°C; 69.80%; 84W/m2;  1tR/min; 76tW/min; E; 1,3,2,0,84,185,187,; V1.80
2021-09-08 06:01:44  ;20.90°C; 69.90%; 90W/m2;  0tR/min; 107tW/min; E; 1,3,2,0,90,56,127,; V1.80
2021-09-08 06:02:44  ;21.00°C; 70.00%; 93W/m2;  0tR/min; 115tW/min; NE; 1,3,2,0,93,121,189,; V1.80
2021-09-08 06:03:44  ;21.00°C; 69.80%; 97W/m2;  0tR/min; 125tW/min; E; 1,3,2,0,97,121,172,; V1.80
2021-09-08 06:04:44  ;21.10°C; 69.70%; 97W/m2;  0tR/min; 153tW/min; NE; 1,3,2,0,97,121,172,; V1.80
2021-09-08 06:05:44  ;21.10°C; 69.40%; 100W/m2;  0tR/min; 84tW/min; NE; 1,3,2,0,100,185,175,; V1.80
2021-09-08 06:06:44  ;21.10°C; 69.40%; 99W/m2;  0tR/min; 140tW/min; NE; 1,3,2,0,99,248,109,; V1.80
```

Figure 4-12. Screenshot of low-cost sensor data logger output file.

As shown in Figure 4-12, a measurement data string is recorded every minute. Every line from left to right contains successively: timestamp generated by CoolTerm, air temperature and relative humidity instantaneous measurement outputs by DHT22, solar radiation instantaneous measurement output by JXBS-3001-ZFS, number of tips output by TBRG WH-SP-RG during the last minute, number of times the read switch opens during the last minute output by anemometer WH-SP-WS01, wind direction measurement output by anemoscope WH-SP-WD, raw RS-485 string output by JXBS-3001-ZFS, and code version. When there is a tip coming from the rain gauge, a number '1' is recorded directly with timestamp. How the measurements are recorded is summarized in Table 4-8. Arduino Nano code is shared in GitHub (Qingchuan ZHU, 2023).

Table 4-8. Summary of recording measurement of low-cost sensors.

Sensor type	Sensor module	Measurement recording
Rain gauge	WH-SP-RG	Sum of tips per minute and real time of every tip
Anemometer	WH-SP-WS01	Sum of switch open number per minute
Anemoscope	WH-SP-WD	Instantaneous measurement at timestamp time
Air temperature sensor Air humidity sensor	BME280/DHT22	Instantaneous measurement at timestamp time
Pyranometer	JXBS-3001-ZFS	Instantaneous measurement at timestamp time
Light sensor	Si1145	Instantaneous measurement at timestamp time

4.2.3 Installation

All the sensors are installed on the green roof test bench (GROOF) on the roof of a building in the INSA Lyon campus in Villeurbanne as shown in Figure 4-13. The GROOF platform is described in section 3.2.5.

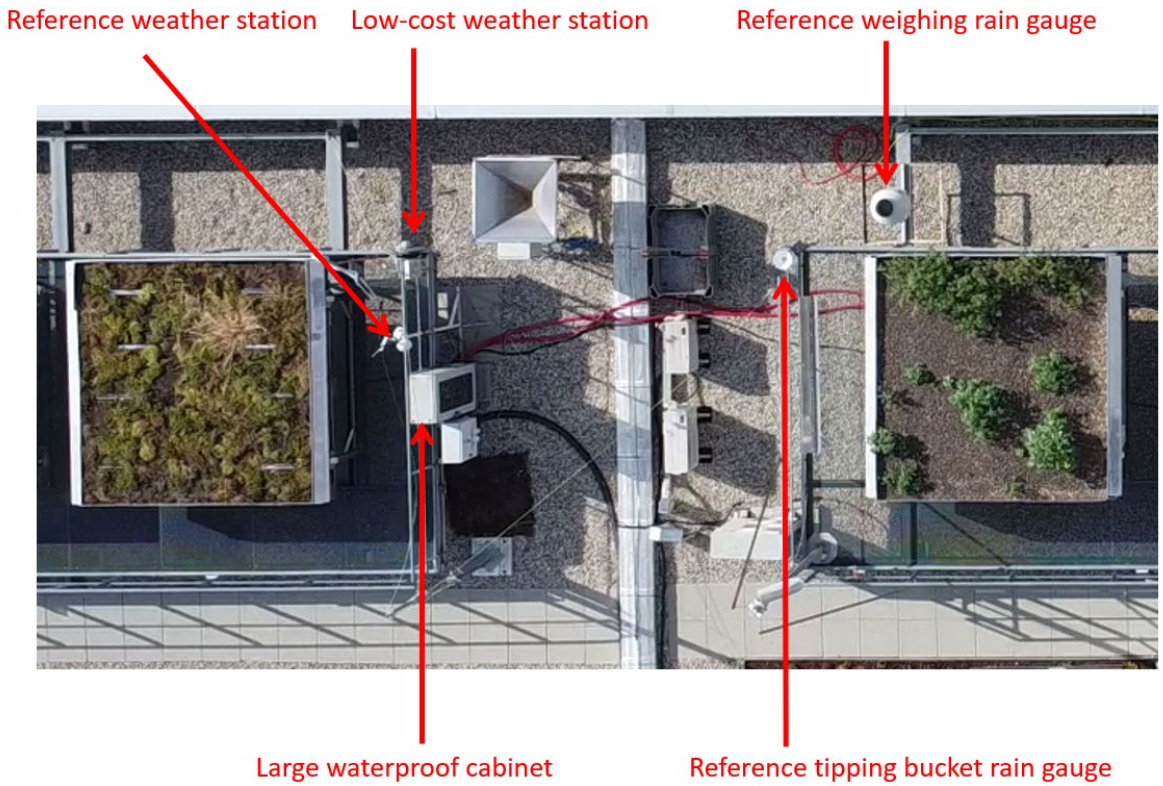

Figure 4-13. Aerial view of the GROOF platform with the location of the sensors.

4.2.3.1 Experimental setups

Figure 4-14 shows from left to right: the large waterproof cabinet that contains the laptop for the low-cost data logger and the desktop computer for the reference data logger; the reference weather station, from top to bottom: wind sensors, pyranometer, and air temperature and humidity sensor; and low-cost weather station: from top to bottom: wind sensors, tipping bucket rain gauge, air temperature and humidity sensors, transparent waterproof box containing the main control board (Arduino Nano and associated circuits). The two reference rain gauges are shown in Figure 4-15.

Figure 4-14. One side view of low-cost and reference meteorological sensors installation with the waterproof cabinet (A), the reference weather station (B), and the low-cost weather station (C).

Figure 4-15. Another side view of low-cost (A) and reference (B) meteorological sensors and two reference rain gauges (C: weighing rain gauge, D: tipping bucket rain gauge).

4.2.3.2 Enclosure for the air humidity sensors

BME280 and DHT22 are installed in a cylindrical plastic housing as shown in Figure 4-16. The housing is well ventilated, and several inspections revealed that there is no water accumulation.

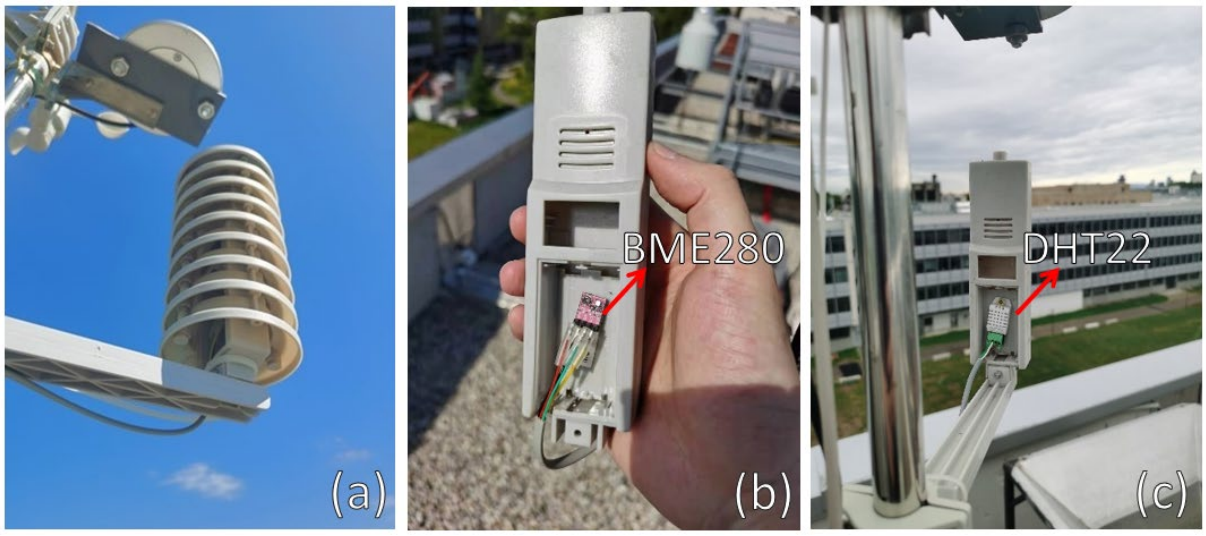

Figure 4-16. Installation of low-cost air sensors BME280 and DHT22: (a) protective housing. (b) BME280 inside housing. (c) DHT22 inside housing.

4.2.3.3 Low-cost light sensor

Si1145 is installed in a box with a transparent lid together with the main control board of the low-cost data logger (Figure 4-17). According to Burgt (2020), the light transmission properties of this kind of transparent box are more than 90% within the spectral response of Si1145. We have not checked if this was correct or not.

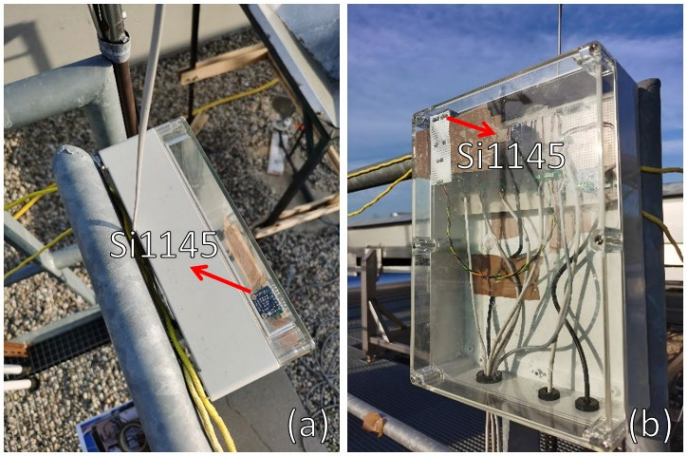

Figure 4-17. Installation of Si1145: (a) top view. (b) side view.

We also tried to connect Si1145 to an Arduino MKR WAN 1310 which provides a practical and cost-effective solution to add LoRa® connectivity to projects (Arduino Documentation, 2023b). However, the I^2C address of Si1145 and LoRa® chip of Arduino MKR WAN 1310 are conflicting and leading to unstable communication.

4.2.4 Preparation of sensor assessment

This one-year experiment mainly assesses the accuracy and behavior of low-cost meteorological sensors. The terminology and performance assessment methods used are described as follows.

4.2.4.1 Timestamp difference

As shown in Figure 4-12, as there is no real time clock module connected to Arduino Nano and the time function of Arduino is not stable (typical drift of boards with resonator clock is 0.8 second per 100 seconds according to Arduino Forum, 2016), the seconds number of low-cost sensor measurement data timestamp is not exactly 0 and changes during the operation. On the contrary, the seconds number of reference sensor measurement data timestamp is exactly 0. This means that low-cost and reference sensors do not measure exactly at the same time. The time difference is less than one minute in our experiments.

Before comparing with reference sensors, linear interpolation is used to process the output of low-cost anemometer WH-SP-WS01, air temperature and humidity sensor BME280, DHT22, pyranometer JXBS-3001-ZFS and light sensor Si1145 to make their data have the same timestamp as reference sensor. This undoubtedly introduces errors, but we hypothesize that the measured quantities should not change abruptly over the course of a minute.

4.2.4.2 Anemoscopes comparison

The following issues should be considered when comparing the output of low-cost and reference anemoscopes: (i) low-cost data logger can only save eight wind directions whereas reference anemoscope can output degrees, (ii) reference anemoscope has 8° output open (its output is only from 0 to 351.6 degrees in real data), (iii) reference anemoscope has a startup threshold 1.8 m/s with a displacement of 5 degrees and its enlarge uncertainty is 5 degrees (iv) the distance between the two anemoscopes is approximate 1 meter (see Figure 4-14) and winds could have quite high spatial variability because of surroundings obstacles.

Therefore, the wind direction output distributions of the two anemoscopes are compared under the following premises: (i) reference anemoscope output is converted to eight directions: north, northeast, east, southeast, south, southwest, west, and northwest as the output of low-cost anemoscope, (ii) the output dead band of the reference anemoscope has no influence on the results due to that when wind direction is in the dead band (between 352 and 360 degrees), sensor output is 0 degree (Campbell secientific, 2023), this wind direction is still identified to be north, (iii) only comparing the output between low-cost anemoscope WH-SP-WD and reference anemoscope when wind speed is more than 1.8 m/s reported by reference anemometer, (iv) in the results and discussion, only wind direction distribution (i.e., percentage of specific wind direction output over all wind direction output) is compared and discussed.

4.2.4.3 Total daily radiation comparison

Even though in the test, measurement is taken every minute, the manufacturer of reference pyranometer CS300 only guarantee its performance in total daily radiation as shown in Table 3-11 and the manufacturers of low-cost sensor JXBS-3001-ZFS and Si1145 do not give any accuracy parameters as shown in Table 4-6 and Table 4-7. In the results and discussion, total daily radiation is calculated to assess low-cost pyranometers performance:

$$R = \sum_{n=1}^{1440} r_n \Delta t \qquad \text{Equation 4-1}$$

Where R is total daily radiation in Wh/m^2, n is from 1 to 1440 because pyranometer output is recorded every minute and there are 1440 minute per day, r_n is the nth measurement output value in W/m^2 for CS300 and JXBS-3001-ZFS or "counts" for Si1145 and Δt is time interval of measurement in hour, i.e., $\Delta t = 1/60 \ = 0.017$ hour.

4.3 RESULTS AND DISCUSSION

4.3.1 Operation

Test experiment runs from 10 March 2021 to 21 July 2022. Details about low-cost sensors testing periods are given in Figure 4-18.

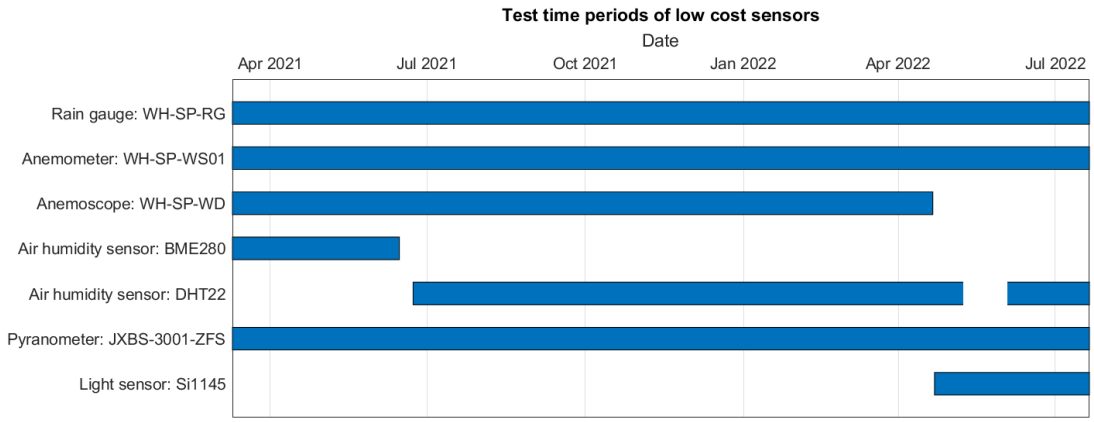

Figure 4-18. Gantt chart of low-cost sensors testing periods.

Three sensors WH-SP-RG, WH-SP-WS01 and WH-SP-WD are installed from May 2021 to July 2022, but after May 2022, WH-SP-WD is disconnected due to maintenance problems. Air humidity sensor BME280 is tested from March to May 2021, and then it has been removed because it was malfunctioning. Air humidity sensor DHT22 replaces BME280 in May 2021, and DHT22 is disconnect in June 2022 due to maintenance problems. Low-cost pyranometer JXBS-3001-ZFS is tested from March 2021 to July 2022 without any operation problem. Low-cost light sensor Si1145 is tested from May to July 2022.

Table 4-9 gives a summary of reasons why during some periods there are no data to be collected. Four kinds of reasons are classified as man-made, hardware failure, software failure and connection failure.

Table 4-9. Reasons of data acquisition failure of low-cost data logger.

Year	Month	Man-made	Hardware failure	Software failure	Connection failure
2021	4	\	\	Windows 10 update	\
	5	\	\	Windows 10 update	between laptop and Arduino Nano
	6	Install DHT22	Laptop shutdown	CoolTerm stops	\
	7	\	Laptop shutdown	\	\
	8	\	Laptop shutdown	\	\
	9	\	Laptop shutdown	\	\
	10	\	Laptop shutdown	\	\
	11	Test new system	\	\	\
	12	\	\	CoolTerm stops	\
2022	1	Forget saving in CoolTerm	\	\	\
	2	Test new system	\	\	\
	3	\	Laptop shutdown	\	\
	4	Install Si1145	\	\	\
	5	\	\	\	between laptop and Arduino Nano
	6	Fix DHT22 disconnection	\	\	\
	7	Forget saving in CoolTerm	Laptop shutdown	\	\

As shown in Table 4-9, the main weakest point of low-cost data acquisition was the laptop. At the beginning, Windows 10 updates interrupted the data saving. During summer, the laptop overheated and shutdown automatically to protect itself. Some power interruptions in the building have also led to shutdowns of the laptop. Reference sensors data are available from May 2021 to 2022. The reference sensor data were also unavailable during some periods due to system improvement and maintenance. Therefore, the longest continuous data for each month from May 2021 to July 2022 is selected to assess the performance of low-cost sensors, details are given in Table 4-10. The number of days of comparison is 37% of all days from May 2021 to July 2022.

Table 4-10. Low-cost sensors performance assessing periods.

Number	Year	Month	Low-cost sensors data available period	Reference sensors data available period	Selected comparing period	Comparison days per month
1	2021	5	4 to 31	21 to 31	22 to 31	9
2		6	25 to 30	1 to 31	26 to 29	3
3		7	9 to 31	15 to 31	16 to 30	14
4		8	1 to 10	1 to 26	2 to 9	7
5		9	21 to 28	8 to 30	22 to 27	5
6		10	1 to 21	1 to 31	2 to 20	18
7		11	1 to 15	1 to 10	2 to 10	8
8		12	9 to 29	1 to 31	11 to 28	17
9	2022	1	3 to 12	1 to 31	4 to 11	7
10		2	9 to 28	1 to 28	10 to 27	17
11		3	1 to 17	1 to 22	2 to 13	11
12		4	1 to 15	1 to 30	2 to 14	12
13		5	10 to 16	1 to 31	11 to 15	4
14		6	1 to 27	1 to 30	2 to 26	24
15		7	15 to 19	1 to 31	16 to 18	2

4.3.2 Low-cost sensor performance assessment

As written above in this chapter (Section 4.2.1.1), low-cost rain gauge results are presented and discussed in Chapter 5. The results of all other low-cost sensors are presented and discussed in the sections hereafter.

4.3.2.1 Anemometer WH-SP-WS01

In Figure 4-19, low-cost anemometer WH-SP-WS01 output numbers of reed switch open per minute are compared with reference anemometer output average wind speed in meter per second per minute. The adjacent time low-cost and the reference sensor output values are plotted are indicated above the plots.

As a first quick qualitative assessment of the low-cost sensor behavior for each test period, each graph displays respectively the experimental points, the slope of the line with zero intercept and the corresponding coefficient of determination.

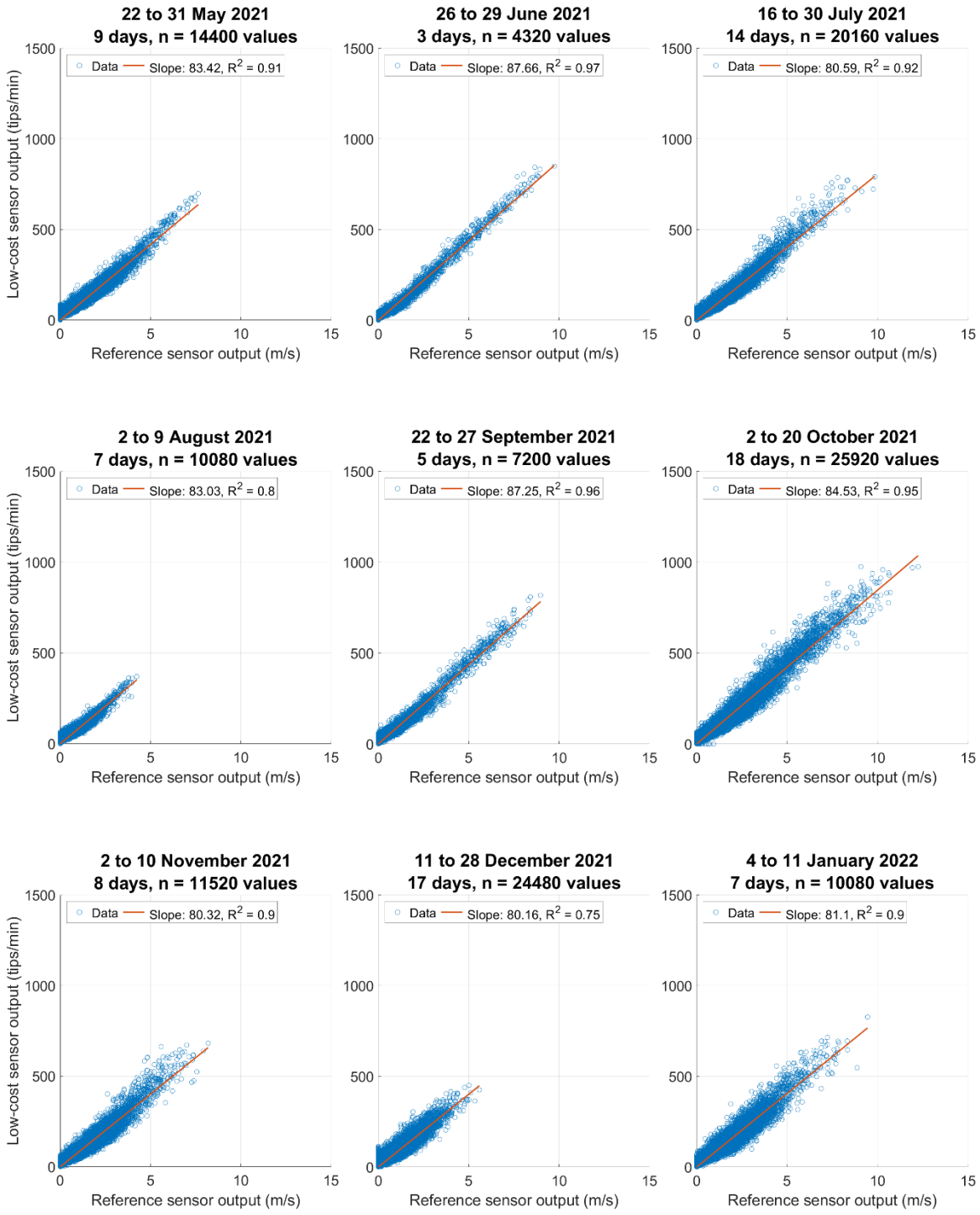

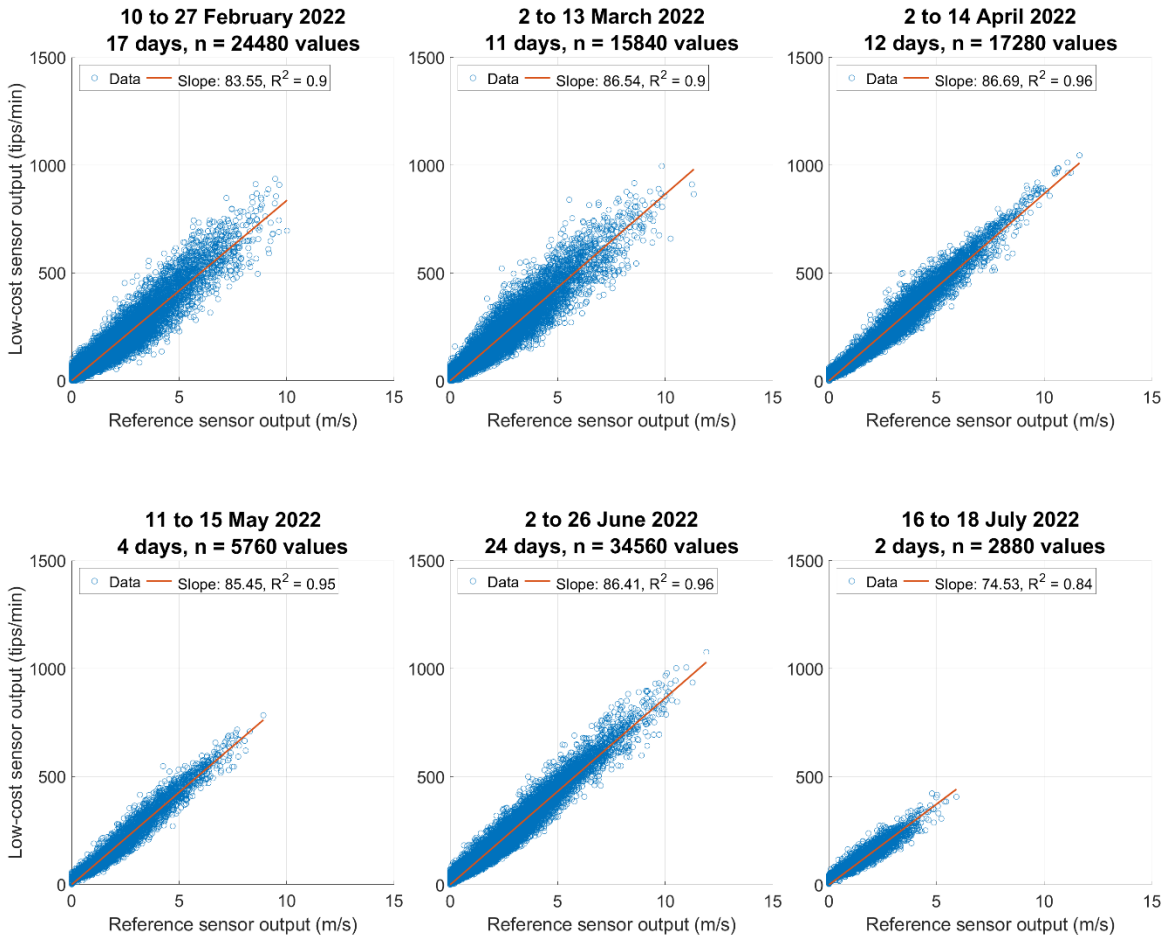

Figure 4-19. Low-cost and reference anemometer output comparison from May 2021 to July 2022.

The slope ranges from 74.53 (period 16 to 18 July 2022) to 87.66 (period 26 to 29 June 2021). From above graphs, one can conclude that the low-cost anemometer WH-SP-WS01 has a rather stable behavior over fifteen-months of operation.

Figure 4-20 shows all data over the 15 months test period. The regression results are given in Table 4-11.

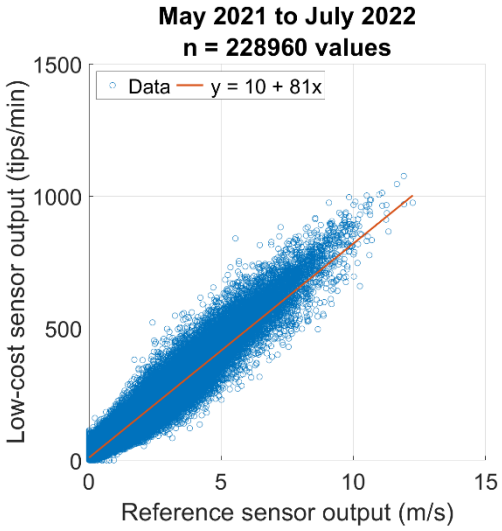

Figure 4-20. Low-cost and reference anemometer output comparison from May 2021 to July 2022. The correlation function has been selected from the regression results given in Table 4-11.

Table 4-11. Regression results for the low-cost anemometer (see section 3.2.3 for explanations).

Parameter	**With 0 intercept**	**With free intercept**
b11	0	10.0196
b12	84.5610	81.0321
u(b11)	0	0.0855
u(b12)	0.0324	0.0436
cov(b11, b12)	0	-0.0026
ResVar1	926.0974	873.6885
IC95 b11	0	[9.8521, 10.1812]
IC95 b12	[84.4975, 84.6245]	[80.9467, 81.1175]
Standard error	30.4318	29.5582

According to Table 4-11, the bias estimated with the free intercept regression is equal to 10.0196 and its 95% coverage interval [9.8521, 10.1812] is different from 0. Therefore, the selected correlation function, with two significant digits, is:

$$y = 10 + 81\,x \qquad \text{Equation 4-2}$$

with a standard error ε = 30.

The regression in Figure 4-20 and Table 4-11 indicate that when the wind speed is 1 m/s in one minute, the read switch inside WH-SP-WS01 opens approximately 91 times on average. In other words, based on all measurements, a wind speed $1/(b_{12}/60) = 0.66$ m/s corresponds to one switch open per second. Therefore, the value 0.66 m/s per tip per second is the anemometer resolution r. This value is close to 0.67 m/s per tip per second given by manufacturer.

Using reference anemometer enlarged uncertainty 0.5 m/s (given by manufacturer) and inverse function of Equation 3-4 to convert WH-SP-WS01 raw output to average wind speed per minute. Low-cost anemometer WH-SP-WS01 enlarged uncertainty corresponding to 90%, 95% and 99% correctness rates are given in Table 4-12. The enlarged uncertainty for a 95% correctness rate is 0.24 m/s.

Table 4-12. Enlarged uncertainty of the low-cost anemometer (see Chapter 3 for explanations).

Correctness rate	Enlarged uncertainty
90%	0.06 m/s
95%	0.24 m/s
99%	0.61 m/s

4.3.2.2 Anemoscope: WH-SP-WD

As explained in 4.2.1.3 and discussed in 4.2.4.2, after converting the reference anemoscope degree output to wind direction, the detected wind direction distribution of low-cost and reference anemoscopes for each period when wind speed is higher than 1.8 m/s is shown in Figure 4-21.

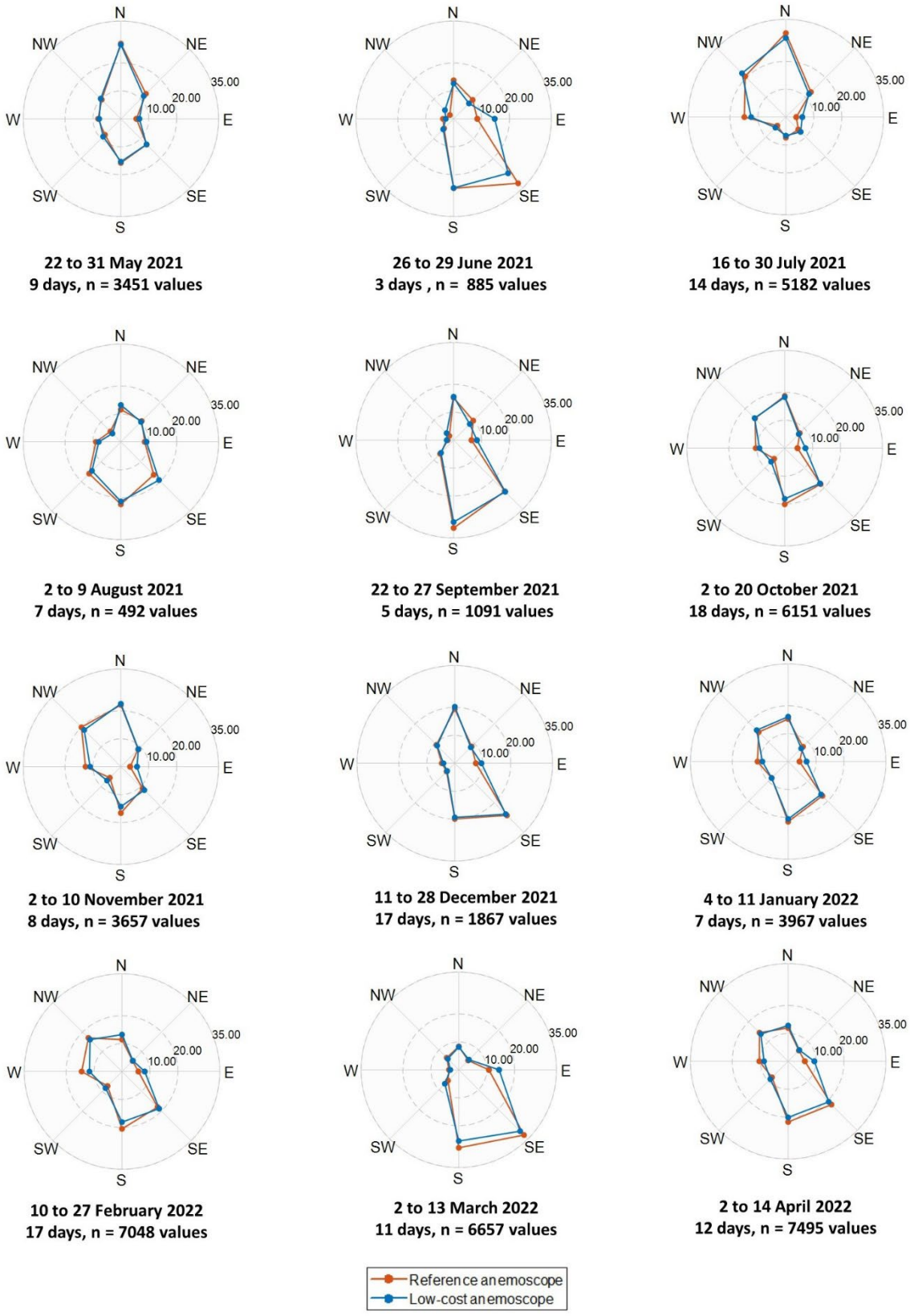

Figure 4-21. Low-cost and reference anemoscope output distributions from May 2021 to April 2022.

From above graphs, one can conclude that the low-cost anemoscope WH-SP-WD has similar wind direction identification as reference anemoscope over 12 months operation. The overall distribution of the 12 months data is shown in Figure 4-22 and given in Table 4-13.

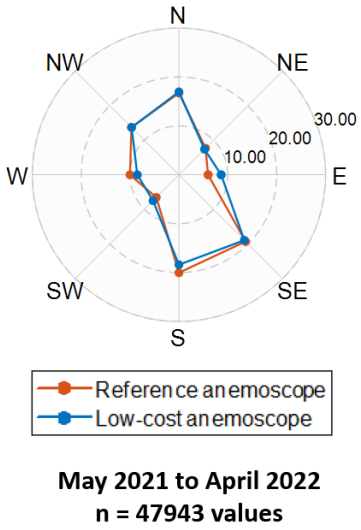

Figure 4-22. Low-cost and reference anemoscope total output distributions.

Table 4-13. Low-cost and reference anemoscope output distributions from May 2021 to April 2022.

Wind direction	North	Northeast	East	Southeast	South	Southwest	West	Northwest
Low-cost anemoscope output distribution （%）	16.96	7.40	8.64	18.92	18.39	7.49	8.51	13.70
Reference anemoscope output distribution （%）	16.72	7.69	5.96	19.29	20.03	6.54	10.02	13.74

According to Figure 4-22 and Table 4-13, the overall data shows that low-cost anemoscope WH-SP-WD has similar wind direction identification as reference anemoscope Campbell Scientific 03002. However, due to the restrictions discussed in Section 4.2.4.2 and the reference anemoscope has an enlarged uncertainty ± 5°, it is difficult to give a quantitative conclusion about the performance of WH-SP-WD such as its correlation function, enlarged uncertainty and startup threshold.

In practice, WH-SP-WD performance also depends on the system design, code, and installation. At least, different from the setup describe in Section 4.2.2, users should record low-cost sensor output as raw as possible, i.e., the

voltage shared by WH-SP-WD but not only eight different wind directions (as shown in Figure 4-12) for further data mining and possible additional correction.

4.3.2.3 Humidity BME280, DHT22

4.3.2.3.1 BME280

(1) Temperature measurements

BME280 was tested from March to May 2021 but there was no reference data in the first two months. Comparison between BME280 and reference sensor temperature outputs in May 2021 is shown in Figure 4-23. Correctness rate is calculated by enlarged uncertainty parameters given in Table 4-4 and Table 3-10.

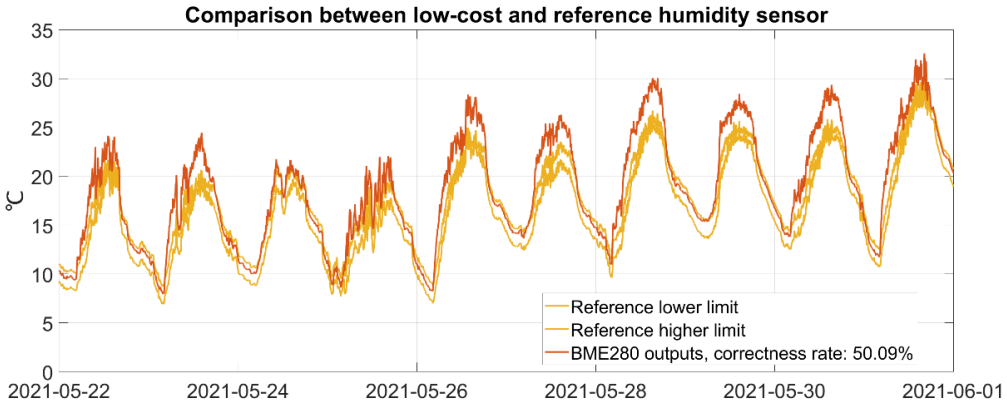

Figure 4-23. The air temperature measurements of BME280 and reference sensor in May 2021.

BME280 temperature outputs are often higher than reference sensor and correctness rate is 50% when trust accuracy parameters given by manufacturer, this phenomenon has explained by its manufacturer as the footnotes of Table 4-4. Figure 4-24 and Table 4-14 show regression results.

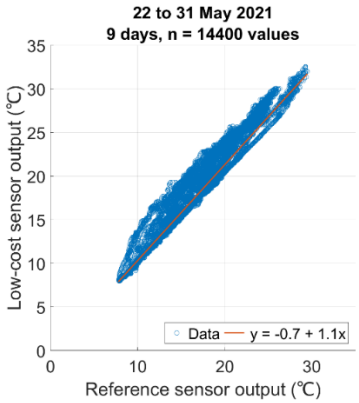

Figure 4-24. BME280 and reference sensor air temperature measurements comparison in May 2021. The correlation function has been selected from the regression results given in Table 4-14.

Table 4-14. Regression results for the BME280 temperature measurements.

Parameter	With 0 intercept	With free intercept
b11	0	-0.6974
b12	1.1033	1.1413
u(b11)	0	0.0393
u(b12)	0.0006	0.0022
cov(b11, b12)	0	-0.0001
ResVar1	1.6471	1.6120
IC95 b11	0	[-0.7745, -0.6203]
IC95 b12	[1.1021, 1.1044]	[1.1369, 1.1456]
Standard error	1.2834	1.2697

According to Table 4-14, the bias estimates with the free intercept regression is equal to -0.6974 and its 95% coverage interval [-0.7745, -0.6203] is different from 0. Therefore, the selected correlation function, with two significant digits, is:

$$y = -0.7 + 1.1x \qquad \text{Equation 4-3}$$

with a standard error ε = 1.3 °C.

Equation 4-3 indicates that BME280 overestimates air temperature of the reference value by approximately 10%. Using reference sensor enlarged uncertainty given by Table 3-10 and reverse function of Equation 4-3 to correct BME280 air temperature measurements. BME280 air temperature measurements enlarged uncertainty

corresponding to 90%, 95% and 99% correctness rates are given in Table 4-15. The enlarged uncertainty for 95% correctness rate is 2.0 ℃.

Table 4-15. Enlarged uncertainty of the BME280 air temperature measurements.

Correctness rate	Enlarged uncertainty
90%	1.6 ℃
95%	2.0 ℃
99%	2.5 ℃

(2) Humidity measurements

As shown in Figure 4-25, after installed in field for two months, the humidity reading of BME280 is often quickly over 100% and correctness rate is 35%. This is most likely because BME280 is not a sealed device and water condensates inside its package.

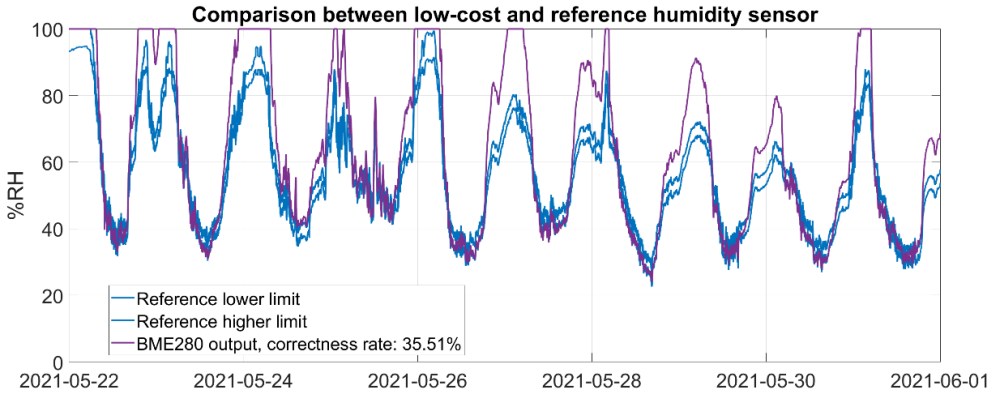

Figure 4-25. The air humidity measurements of BME280 and reference sensor in May 2021.

As shown in Figure 4-26, the measurement error increases with the humidity and the sensor seems better suited for relative humidity up to 60% or 70%.

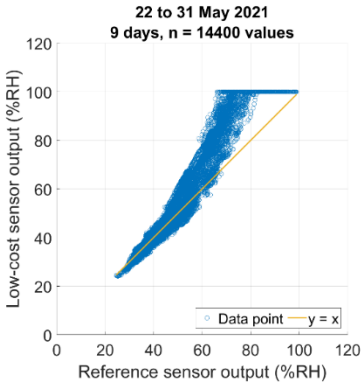

Figure 4-26. Low-cost and reference air humidity sensor outputs comparison in May 2021.

Due to the poor longevity of BME280, there is no need to conduct further data comparison. BME280 was replaced by DHT22 since May 2021, and we decided not to try another BME280 sensor.

4.3.2.3.2 DHT22

(1) Temperature measurements

The comparison of DHT22 and reference sensor outputs in each period is shown in Figure 4-27.

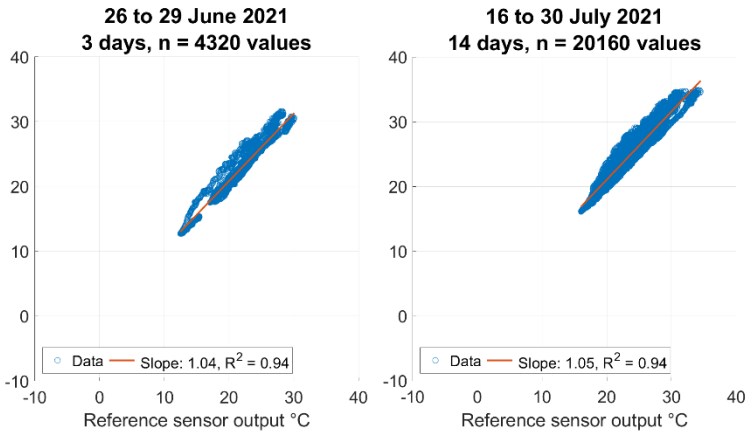

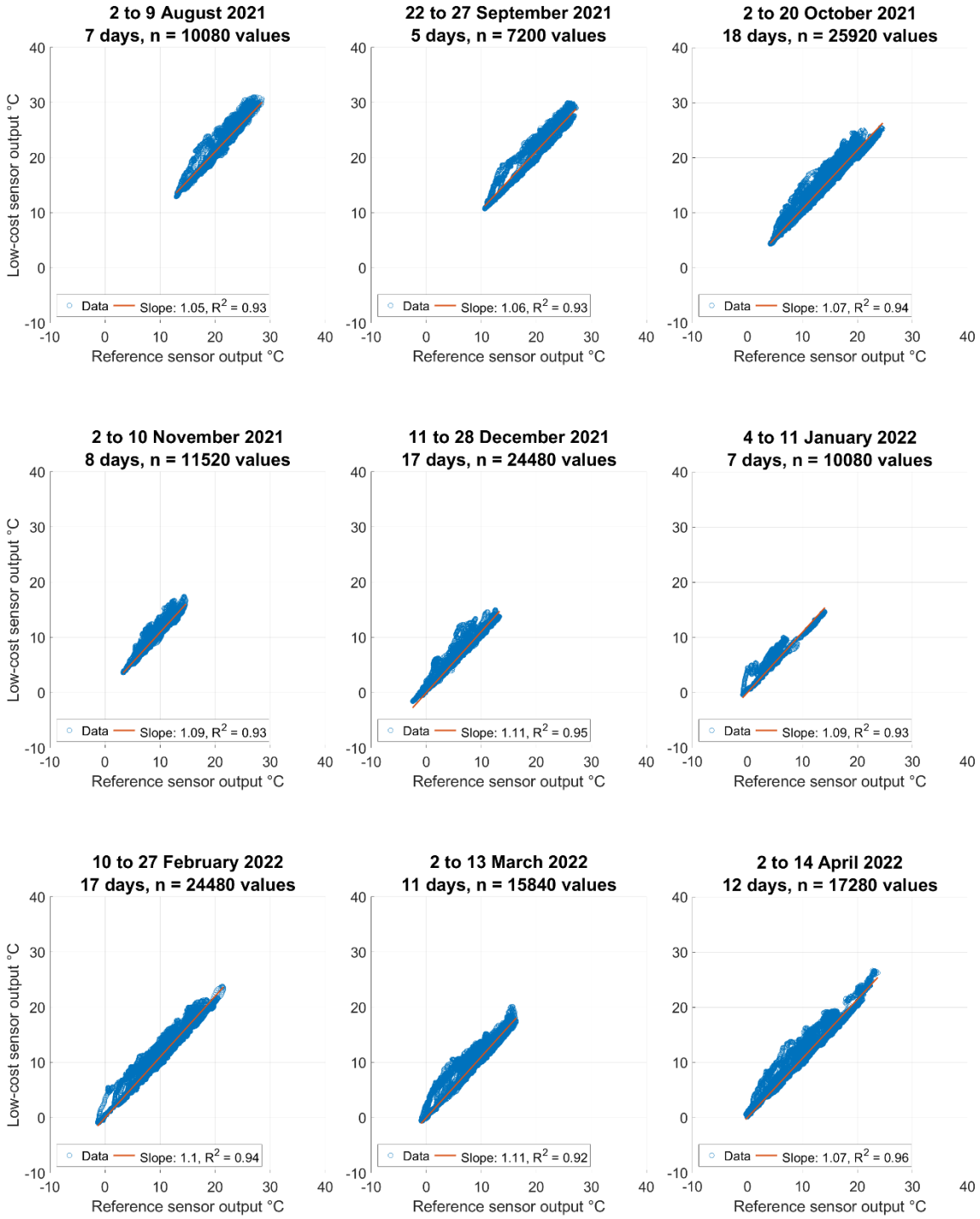

Figure 4-27. Comparison between DHT22 and reference sensor air temperature measurements in May and July 2022.

In above figures, the slopes are always higher than one ranging from 1.04 (16 to 18 July 2022) to 1.11 (11 to 28 December 2021) which indicates that DHT22 overestimates air temperature than reference sensor.

Figure 4-28 shows all data over 13 months test period. The regression results are given in Table 4-16.

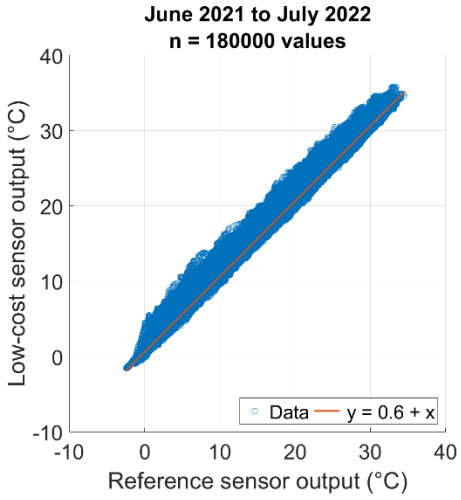

Figure 4-28. DHT22 and reference sensor air temperature measurements comparison from June 2021 to July 2022. The correlation function has been selected from the regression results given in Table 4-16.

Table 4-16. Regression results for DHT22 air temperature measurements.

Parameter	With 0 intercept	With free intercept
b11	0	0.5564
b12	1.0619	1.0291
u(b11)	0	0.0047
u(b12)	0.0002	0.0003
cov(b11, b12)	0	0
ResVar1	1.2454	1.1553
IC95 b11	0	[0.5472, 0.5656]
IC95 b12	[1.0615, 1.0623]	[1.0285, 1.0298]
Standard error	1.1160	1.0748

According to Table 4-16, the bias estimated with the free intercept regression is equal to 0.5564 and its 95% coverage interval [0.5472, 0.5656]. Therefore, the selected correlation function, with two significant digits, is:

$$y = 0.6 + x \qquad \text{Equation 4-4}$$

with a standard error ε = 1.1 ℃.

The regression in Figure 4-28 and Table 4-11 indicate that low-cost sensor DHT22 air temperature measurements are approximately 0.6 ℃ higher than the reference sensor.

Using reference sensor enlarged uncertainty given by Table 3-10 and reverse function of Equation 4-4 to correct DHT22 air temperature measurements. DHT22 air temperature measurements enlarged uncertainty corresponding to 90%, 95% and 99% correctness rates are given in Table 4-17. The enlarged uncertainty for 95% correctness rate is 2.3 ℃.

Table 4-17. Enlarged uncertainty of the DHT22 air temperature measurements.

Correctness rate	Enlarged uncertainty
90%	1.7 ℃
95%	2.3 ℃
99%	3.2 ℃

The DHT22 is housed in a plastic case and the SHT75 reference sensor in a metal case, and the two sensors have a distance of about one meter. Although they both use thermistors to measure temperature, the DHT22 has separate humidity and temperature sensing modules, whereas SHT75 is fully integrated. It is therefore difficult to explain the difference in air temperature measurement, as it could be due to spatial heterogeneity of temperature or the fact that the different housings induce different responses to temperature changes.

(2) Humidity measurements

Figure 4-29 give the comparison between DHT22 and reference sensor air humidity measurements.

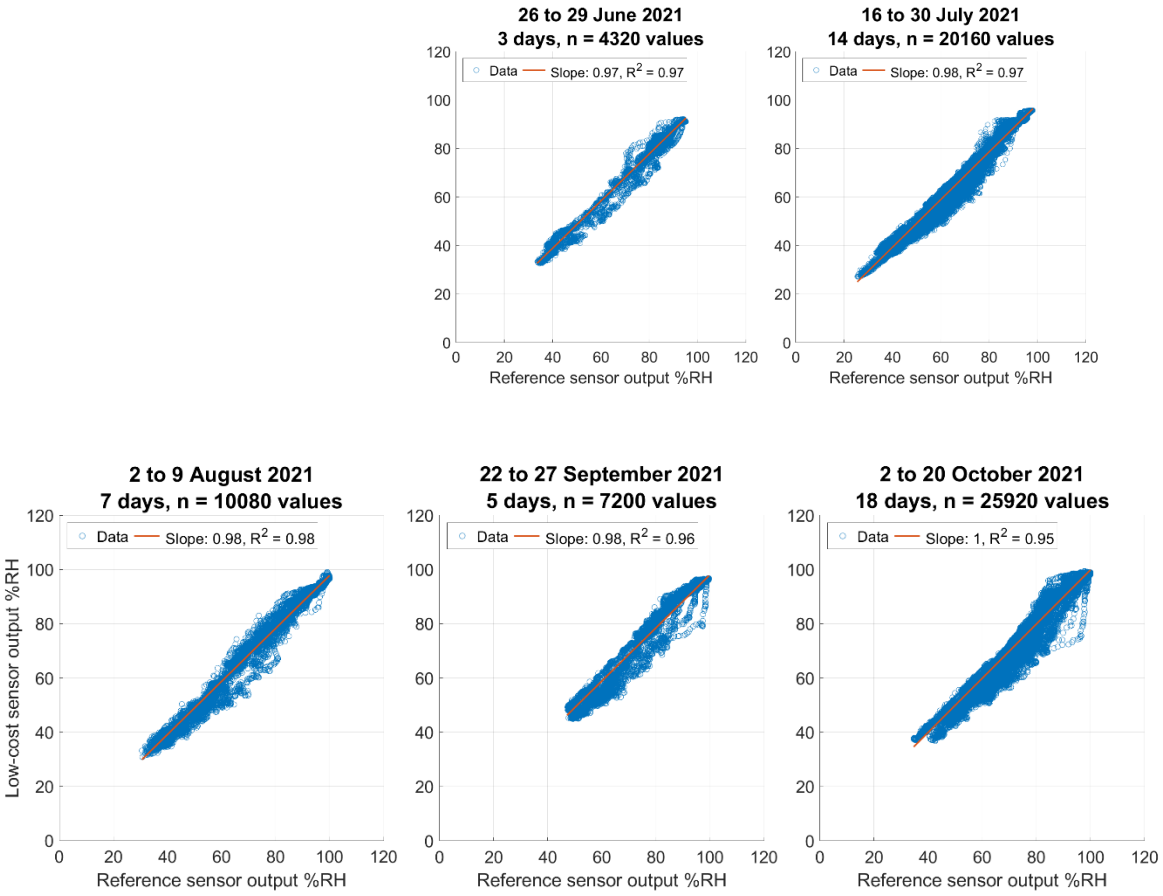

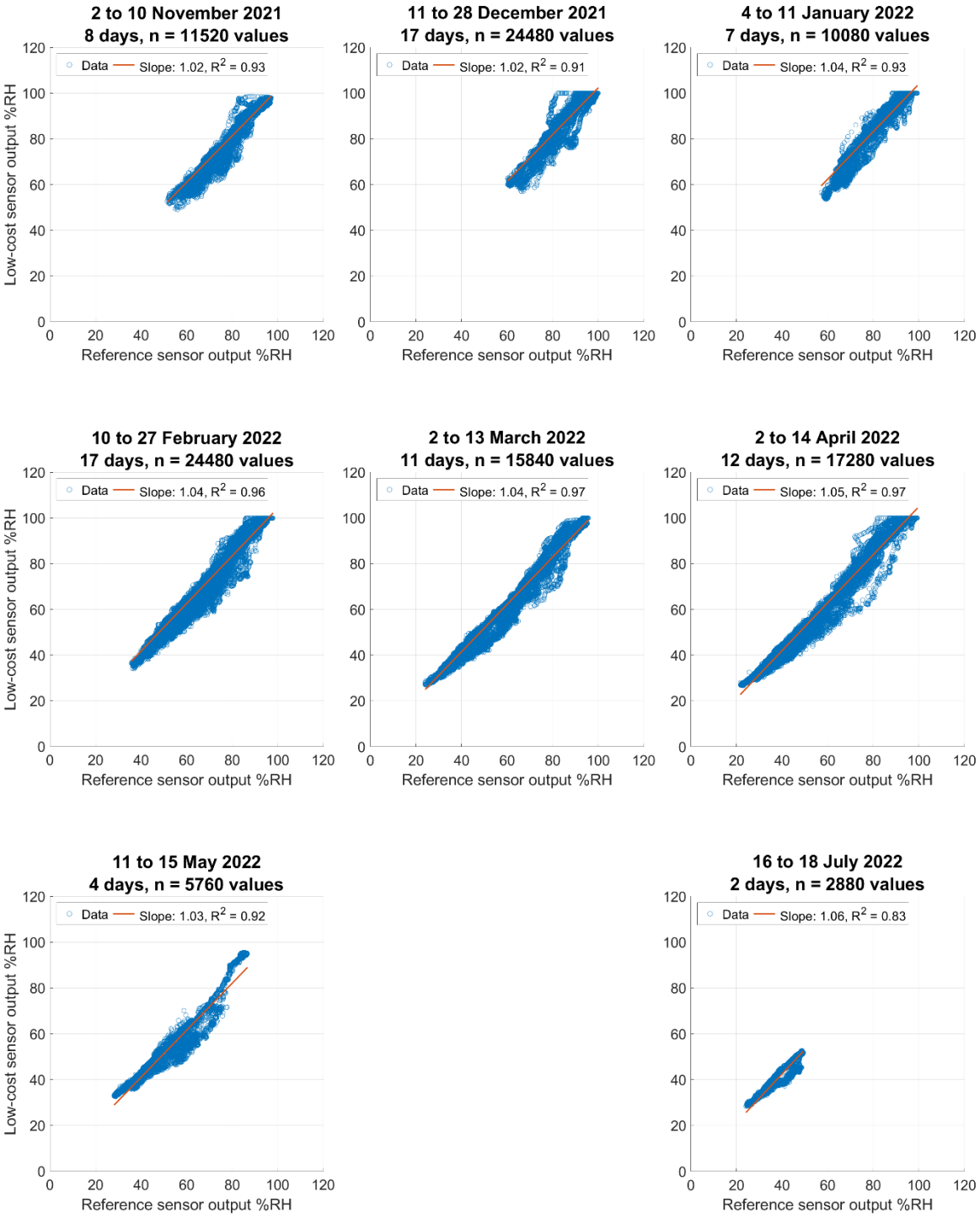

Figure 4-29. Comparison between DHT22 and reference sensor air humidity measurements from June 2021 to July 2022.

As shown in Figure 4-29, the slopes are around one, one can conclude that DHT22 has a rather stable air humidity measuring behavior over 13-months operation. Figure 4-30 shows all data over the 15 months test period. The regression results are given in Table 4-18.

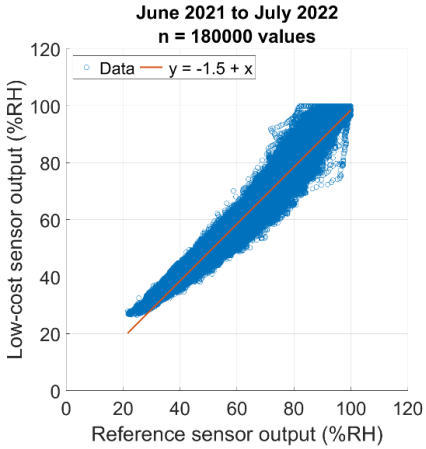

Figure 4-30. Comparison between DHT22 and reference sensor air humidity measurements from June 2021 to July 2022. The correlation function has been selected from the regression results given in Table 4-18.

Table 4-18. Regression results for DHT22 air humidity measurements.

Parameter	With 0 intercept	With free intercept
b11	0	-1.5489
b12	1.0159	1.0357
u(b11)	0	0.0352
u(b12)	0.0001	0.0005
cov(b11, b12)	0	0
ResVar1	14.0449	13.8951
IC95 b11	0	[-1.6178, -1.4800]
IC95 b12	[1.0157, 1.0162]	[1.0348, 1.0366]
Standard error	3.7476	3.7276

According to Table 4-18, the bias estimated with free intercept regression is equal to -1.5489 and its 95% coverage interval [-1.6178, -1.4800] is different from 0. Therefore, the selected correlation function, with two significant digits, is:

$$y = -1.5 + x \qquad \text{Equation 4-5}$$

with a standard error ε = 3.7 %RH.

The regression in Figure 4-30 and Table 4-18 indicate that DHT22 slightly underestimates air humidity by approximately 1.5 %RH than reference sensor. Using reference sensor enlarged uncertainty given by Table 3-10 and inverse function of Equation 4-5 to correct DHT22 air humidity measurements, DHT22 air humidity measurements enlarged uncertainty corresponding to 90%, 95% and 99% correctness rates are given in Table 4-19. The enlarged uncertainty for a 95% correctness rate is 5.7 %RH.

Table 4-19. Enlarged uncertainty of DHT22 air humidity measurements.

Correctness rate	Enlarged uncertainty
90%	4.4 %RH
95%	5.7 %RH
99%	8.4 %RH

It should be noted that low-cost and reference sensors are not exactly at same location and in the same enclosure (as discussed previously when analyzing the temperature measurements from the DHT22).

4.3.2.4 Pyranometer JXBS-3001-ZFS

The comparison of low-cost sensor JXBS-3001-ZFS and reference sensor measurements of solar radiation is shown in Figure 4-31.

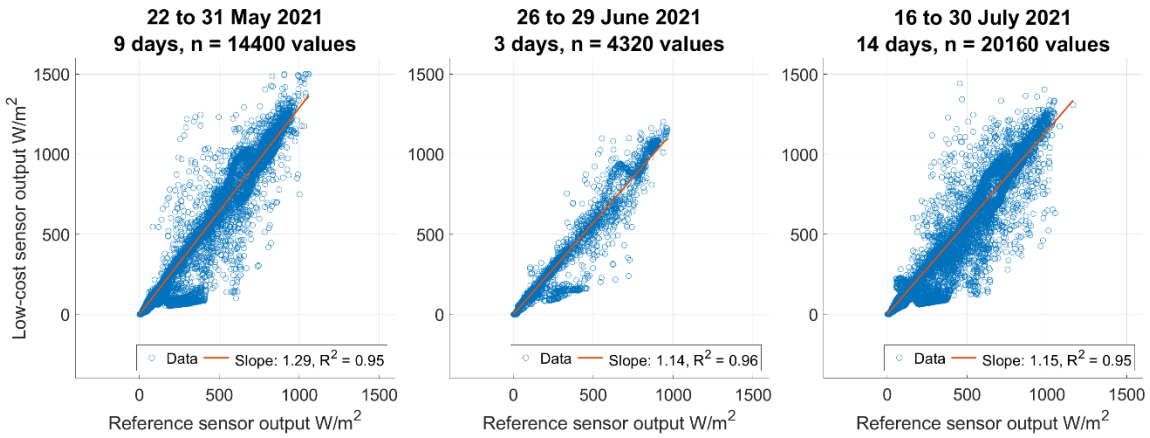

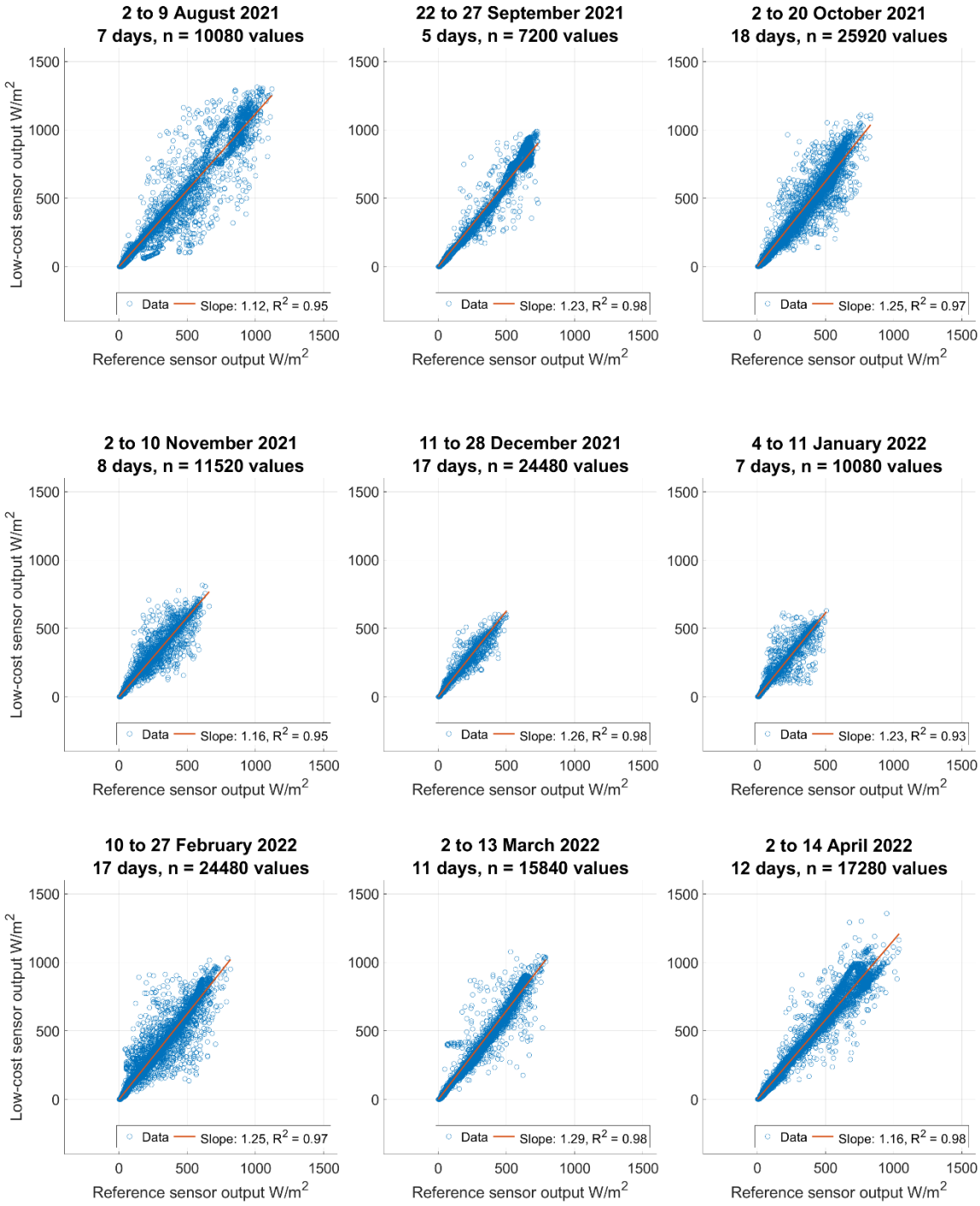

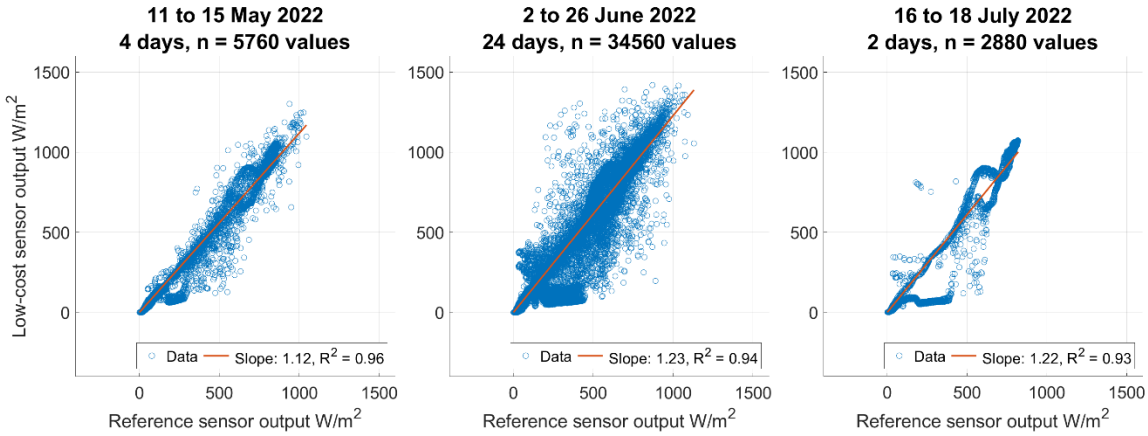

Figure 4-31. Comparison between JXBS-3001-ZFS and reference sensor air humidity measurements from May 2021 to July 2022.

Figure 4-31 shows that JXBS output per minute is frequently higher than reference pyranometer. As described in Section 4.2.4.3, total daily radiation is calculated to compare two pyranometers performance.

Figure 4-32 shows all total daily radiation over 15 months test period. The regression results are given in Table 4-20.

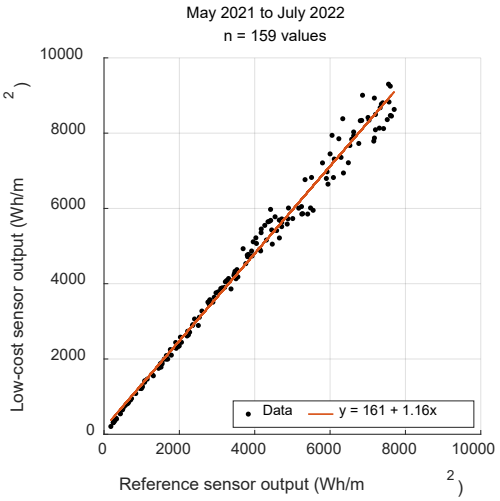

Figure 4-32. Total daily radiation output by two pyranometers.

Table 4-20. Regression results for pyranometer JXBS-3001-ZFS.

Parameter	With 0 intercept	With free intercept
b11	0	161.0194
b12	1.1894	1.158
u(b11)	0	43.6439
u(b12)	0.0052	0.0099
cov(b11, b12)	0	-0.3721
ResVar1	83231.8095	77079.3072
IC95 b11	0	[75.4774, 246.5613]
IC95 b12	[1.1793, 1.1996]	[1.1386, 1.1773]
Standard error	288.4992	277.6316

According to Table 4-20, the bias estimated with the free intercept regression is equal to 161.0194 and its 95% coverage interval [75.4774, 246.5613] is different from 0. Therefore, the selected correlation function, with three significant digits, is:

$$y = 161 + 1.16\,x \qquad \text{Equation 4-6}$$

with a standard error ε = 278 Wh/m^2.

The regression in Figure 4-32 and Table 4-20 indicate that JXBS-3001-ZFS output total daily radiation is 16% higher than reference sensor CS300.

Using reference sensor enlarged uncertainty 5 % (given by manufacturer as shown in Table 3-11) and inverse function of Equation 4-6 to correct JXBS-3001-ZFS output to calculate correctness rate. Low-cost pyranometer JXBS-3001-ZFS enlarged uncertainty corresponding to 90%, 95% and 99% correctness rates are given in Table 4-21. The enlarged uncertainty for a 95% correctness rate is 227 Wh/m^2.

Table 4-21. Enlarged uncertainty of the low-cost pyranometer JXBS-3001-ZFS total daily radiation output.

Correctness rate	Enlarged uncertainty
90%	133 Wh/ m^2
95%	227 Wh/m^2
99%	422 Wh/m^2

4.3.2.5 Light sensor Si1145

Low-cost light sensor Si1145 has 3 outputs: visible light intensity, infrared light intensity and ultraviolet light index. Figure 4-33 compares the three different outputs of Si1145 with the reference pyranometer outputs from May to July 2022.

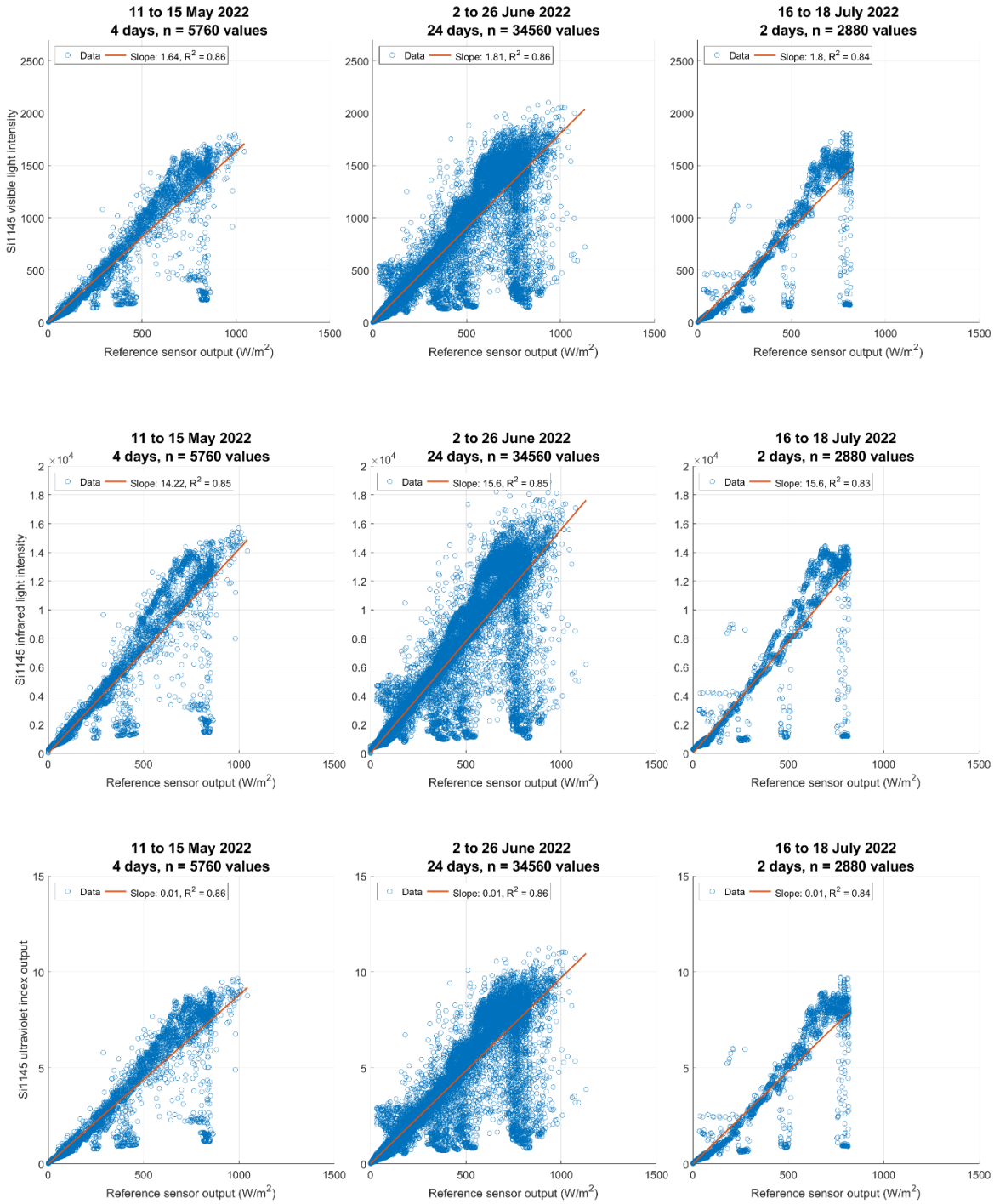

Figure 4-33. Comparison between Si1145 visible light measurement, infrared light measurement and ultraviolet index output and reference pyranometer output from May to July 2022.

As shown in Figure 4-33, the three Si1145 outputs are similar in shape. Therefore, the next discussion is only focused on the Si1145 visible light intensity which has a moderate size slope (around 1.7) to reference sensor output values. Figure 4-34 displays reference pyranometer and Si1145 visible light intensity outputs from 2 to 26 June 2022.

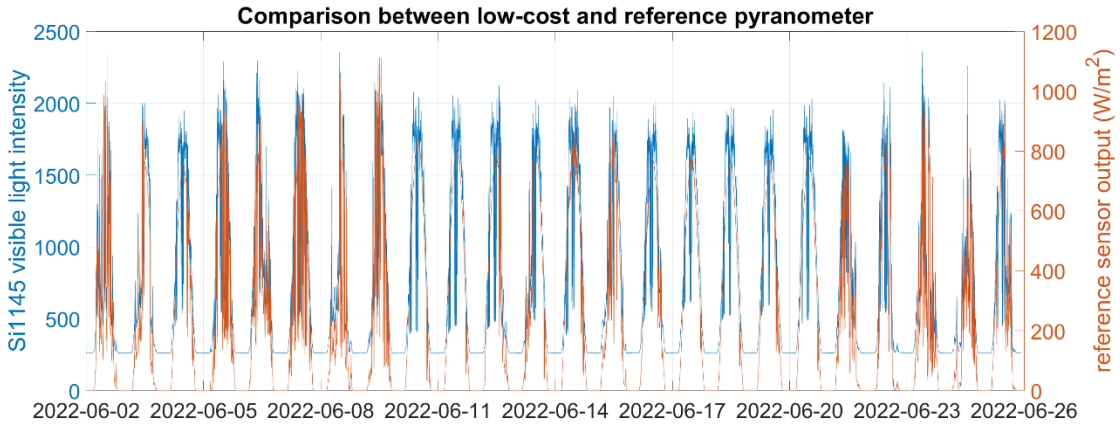

Figure 4-34. Reference pyranometer and Si1145 visible light intensity outputs from 2 to 26 June 2022.

As shown in Figure 4-34, Si1145 can reasonably track the change of light intensity, but it always output approximately 260 at night. In addition, Si1145 always has lower output values in the morning and midday every day, which is due to the shade over it according to *in situ* investigation.

Figure 4-35 show total daily radiation over 3-months test period. The regression results are given in Table 4-22.

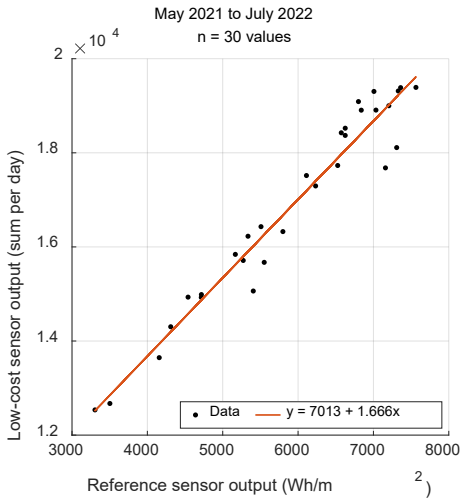

Figure 4-35. Total daily radiation output by Si1145 and reference pyranometers.

Table 4-22. Regression results for Si1145.

Parameter	With 0 intercept	With free intercept
b11	0	7013.4035
b12	2.8041	1.6658
u(b11)	0	447.0967
u(b12)	0.0451	0.0740
cov(b11, b12)	0	-32.4434
ResVar1	2224282.3196	235358.5311
IC95 b11	0	[6137.0939, 7889.7130]
IC95 b12	[2.7157, 2.8924]	[1.5207,1.8109]
Standard error	1491.4028	485.1378

According Table 4-22, the bias estimated with the free intercept regression is equal to 7013.4035 and its 95% coverage interval [6137.0939, 7889.7130] is different from 0. Therefore, the selected correlation function, with four significant digits, is:

$$y = 7013 + 1.666\,x \qquad \text{Equation 4-7}$$

with a standard error ε = 485.1.

Reverse function of Equation 4-7 gives a way to estimate the total daily radiation by Si1145 visible light intensity output.

Using reference sensor enlarged uncertainty 5% (given by manufacturer as shown in Table 3-11) and inverse function of Equation 4-7 to estimate the total daily radiation by Si1145 visible light intensity output. Low-cost light sensor Si1145 enlarged uncertainty corresponding to 90%, 95% and 99% correctness rates are given in Table 4-23. The enlarged uncertainty for a 95% correctness rate is 303.7 Wh/m^2.

Table 4-23. Enlarged uncertainty of Si1145 total daily radiation measurements.

Correctness rate	Enlarged uncertainty
90%	107.1 Wh/ m^2
95%	303.7 Wh/m^2
99%	399.0 Wh/m^2

4.4 CONCLUSION

In this chapter, six low-cost meteorological sensors have been tested and compared with reference sensors installed nearby. Data have been collected with a measurement frequency of one minute over a period of 15 months. Main findings of this campaign are summarized in Table 4-24 and Table 4-25.

Table 4-24. Summary of comparison between low-cost and reference sensors

Sensor name	Measured quantity	Correlation equation [a]	Enlarged uncertainty [b]
WH-SP-WS01	Wind speed	$y = 10 + 81\,x$	0.24 m/s
WH-SP-WD	Wind direction	NC [c]	NC
BME280	Air temperature	$y = -0.7 + 1.1x$	2.0 ℃
	Air humidity	NC [d]	NC
DHT22	Air temperature	$y = 0.6 + x$	2.3 ℃
	Air humidity	$y = -1.5 + x$	5.7 %RH
JXBS-3001-ZFS	Total solar radiation	$y = 161 + 1.16\,x$	227 Wh/m^2
Si1145	Total solar radiation	$y = 7013 + 1.666\,x$	303.7 Wh/m^2

[a] y is low-cost sensor measurements, x is reference sensor measurements.

[b] In the calculation of low-cost sensor correctness rate, low-cost sensor measurements are corrected by the reverse function of correlation equation. The enlarged uncertainty in this column corresponds to 95% correctness rate.

[c] NC: not calculated, WH-SP-WD cannot output wind direction angles like reference sensor, which makes it difficult to give a quantitative result.

[d] Tested BME280 module has poor longevity in air humidity measurement, which makes it meaningless.

Table 4-25. Comments about using tested low-cost sensor in urban hydrology.

Sensor name	Application in urban hydrology?	Comments
WH-SP-WS01	possible	In 15-months test, the performance of this sensor is stable and quantifiable.
WH-SP-WD	reserved	Although this sensor is stable in our performance, it cannot give wind direction in angles.
BME280	not recommended	The longevity of the sensor tested is very poor: after three months, the measurements are inconsistent.
DHT22	possible	In 15-months test, the performance of this sensor is stable and quantifiable.
JXBS-3001-ZFS	reserved	This sensor is already more than 100 euros, but its manufacturer does not give any accuracy parameters which indicates the manufacturer is less specialized.
Si1145	reserved	This sensor cost only a few euros and can be used to estimate total daily radiation as traditional pyranometer which costs several hundred euros. But end user needs to design an enclosure for it.

According to our tests, there is a low-cost alternative for the measurement of most weather parameters. These sensors offer an interesting price to performance ratio and seem to have a longevity of more than a year. As previously discussed, the next chapter will focus on rainfall measurement.

CHAPTER 5: LOW-COST STAND-ALONE RAIN GAUGE STATION PERFORMANCE ASSESSMENT

5.1 INTRODUCTION

This chapter reports the testing of low-cost rain gauges in a standalone rainfall monitoring station to observe precipitation intensity and depth. In the first step, low-cost rain gauges are chosen. Then, a low-cost rainfall monitoring system that could run automatically is designed and built. In the third step, calibration protocols are introduced. In the last step, tests are carried out and performances of the low-cost rain gauges sensors and of the whole system itself are presented and discussed based on four months data collection in the winter season.

5.2 MATERIAL AND METHODS

5.2.1 Tested low-cost sensors

After literature review (see Chapter 2), open-source community communication and market research, Optical Rain Gauge (ORG) RG-15 and Tipping Bucket Rain Gauge (TBRG) WH-SP-RG low-cost sensors were selected for testing. Both low-cost sensors are presented hereafter, while the reference rain gauges are presented in section 3.2.5.1.

5.2.1.1 Optical rain gauge RG-15

According to the manufacturer (Hydreon Corporation, 2023), the optical rain gauge RG-15 (Figure 5-1) generates infrared light that is directed within the lens to detectors. When water drops hit the outside surface of the lens, some of the infrared beam escape. The sensor detects the change in beam intensity and determines the size of the rain drop that caused the change. The characteristics of RG-15 given by the manufacturer are shown in Table 5-1.

(a) (b) (c)

Figure 5-1. (a) Low-cost ORG RG-15 appearance, (b) RG-15 circuit board, (c) RG-15 internal structure and measuring principle. Source: hydreon.com (accessed: 20 February 2023).

Table 5-1. Characteristics of RG-15, adapted from Chapter 2. Source: Hydreon Corporation (2023).

Sensor name	**RG-15**
Type	Optical rain gauge
Size	~ 12 ×7 ×5.5 cm
Weight	~ 155 g
Operating range	NA
Power supply	5 to 15 V or 3.3 V [a]
Communication	RS232 [b] at 3.3 V
Enlarged uncertainty	±10% [c]
Resolution	0.2 mm or 0.02 mm
Response time	NA
Sensitivity to environment	It should not be exposed to rapidly varying light levels. Specifically, avoid conditions where an anemometer can cast shadows on the lens
Maintenance needs	Maintenance-free, after 7 to 10 years the lens will need to be replaced
Longevity	NA

[a] 5-15 V DC on J1 (reverse polarity protected to 50V), or 3.3V DC through pin 8 on J2.

[b] RS232: a standard for serial communication transmission of data.

[c] "Nominal accuracy" with footnote "field accuracy will vary" given by manufacturer.

5.2.1.2 Tipping bucket rain gauge WH-SP-RG

The WH-SP-RG (Figure 5-2) low-cost tipping bucket rain gauge is made of low-density polyethylene. Its measurement principle is a magnet attached to its bucket which closes a reed switch generating a pulse signal when the bucket tips. Therefore, the WH-SP-RG can be considered as a button when processing its signal. As described in section 2.3.4, this sensor is part of the weather station kit WS-2080 (Ambient Weather, 2011) and SEN-15901

(Offset Electronics, 2023). It has been used by some researchers (Coloch Tahuico, 2021; Tai *et al.*, 2017) but we cannot find systematic performance assessment. The characteristics of RG-15 are shown in Table 5-2.

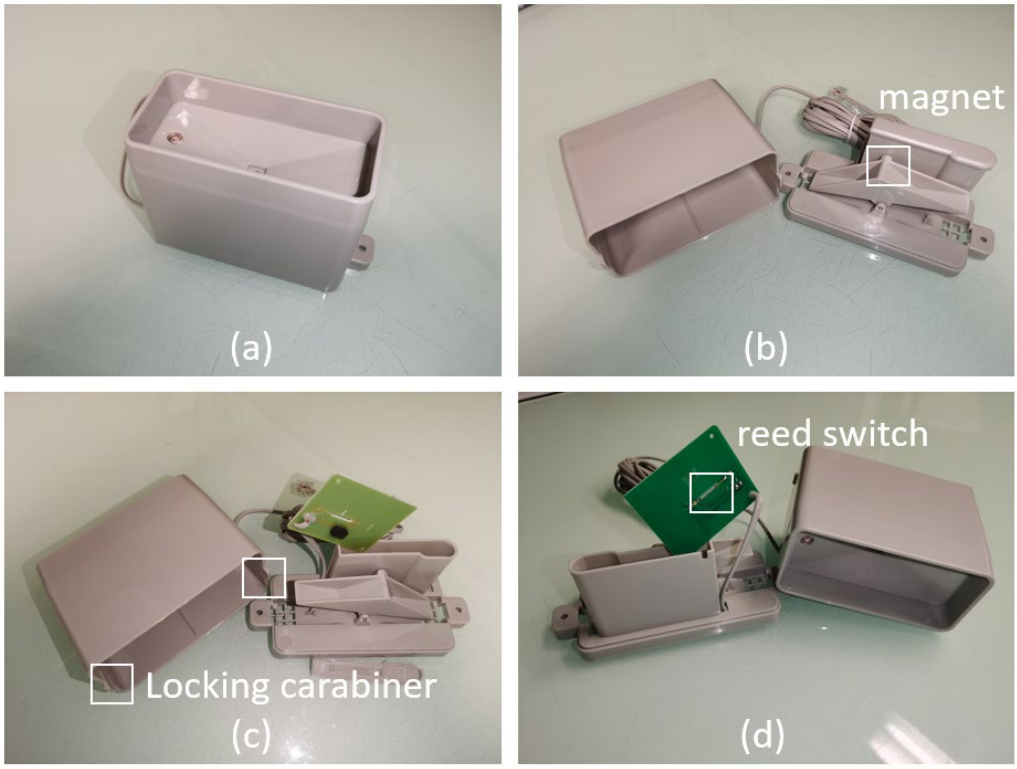

Figure 5-2. External and internal structure of WH-SP-RG: (a) appearance and water collection funnel, (b) internal tipping bucket and magnet, (c) two locking carabiners to attach the funnel and the base part together, (d) other side of the circuit board and the reed switch.

Table 5-2. Characteristics of WH-SP-RG, adapted from Chapter 2. Source: Offset Electronics (2023).

Sensor name	**WH-SP-RG**
Type	Tipping bucket rain gauge
Size	~ 11 ×5.5×9.5 cm
Weight	~ 160 g
Operating range	0 to 155 mm [a]
Power supply	No need
Communication	As a button to controller
Enlarged uncertainty	±10% [a]
Resolution	0.254 [a] or 0.2794 [b] or 0.3 [c] mm/tip
Response time	NA
Sensitivity to environment	NA
Maintenance needs	NA
Longevity	NA

[a] According to user manual of WS-2080 page 35.

[b] In datasheet of SEN-15901: the original text is “Each 0.2794 mm of rain causes one momentary contact” in English.

[c] In datasheet of SEN-15901: the original text is “Each 0.3 mm of rain causes one momentary contact closure” in Chinese.

5.2.2 *In situ* installation

5.2.2.1 Low-cost data logger

Different from the data logger described in Chapter 4 for the other meteorological low-cost sensors, the low-cost data logger developed for the low-cost rainfall sensors is a stand-alone system. It includes a self-contained low-power wide area network connection, a real time clock, data storage and batteries for dozens of days self-power. This system together with the rain gauges is called the low-cost the rainfall monitoring station in this thesis.

5.2.2.1.1 Components

After preliminary tests, the following modules were chosen to build the low-cost rainfall monitoring station. Their names, functions and approximate prices are given in Table 5-3.

Table 5-3. Modules used in the low-cost rainfall monitoring station.

Module name	Function	Approximate price
Arduino MKR WAN 1310	Main control board and communication	~ 30 €
Arduino MKR Mem Shield	Save data in Secure Digital (SD) card	~ 20 €
DS3231	Real time clock	~ 5 €
LiPo Rider Pro	Operate solar panel and LiPo battery, power the system	~ 15 €
RG-15	Low-cost optical rain gauge	~ 80 €
WH-SP-RG	Low-cost tipping bucket rain gauge	~ 20 €

The whole station costs less than 250 € including two different rain gauge systems, one SD card, a solar panel and a LiPo battery. It has a surface smaller than 2 square decimeters.

The hardware schematic of the connections between modules is shown in Figure 5-3.

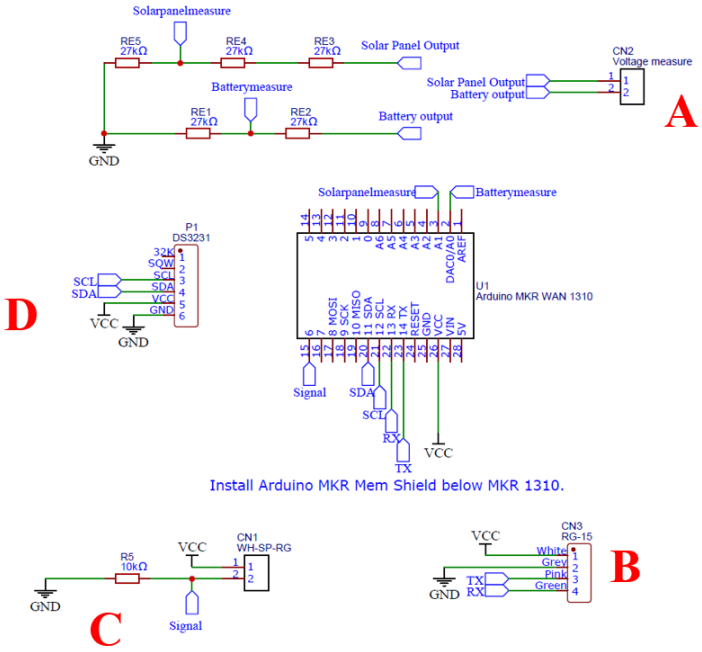

Figure 5-3. Hardware schematic of the low-cost rainfall monitoring station.

As shown in Figure 5-3, clockwise from top to bottom:

(A) Solar panel and battery output voltage measurement circuit. Three 27,000 ohms resistors divide the output voltage of the solar panel and two 27,000 ohms resistors divide the output voltage of the battery because the voltage measurement range of the Arduino MKR WAN 1310 (abbreviated as Arduino in the following) internal Analog to Digital Converter (ADC) is 0 to 3.3 V, and the solar panel and battery output voltage could rise to 6.5 V and 4.2 V respectively, as shown in the results (see section 5.3.4.1).

(B) Optical rain gauge RG-15 interface. RG-15 is powered by 3.3 V from Arduino. RG-15 and Arduino communicate by Universal Asynchronous Receiver/Transmitter (UART).

(C) Low-cost tipping bucket rain gauge WH-SP-RG interface. One pin of WH-SP-RG is connected to Arduino 3.3 V output. Another pin of WH-SP-RG is connected to Arduino digital read pin and pull down to 0 V by a 10,000 ohms resistor. When a tip occurs, the read voltage of Arduino pin changes from 0 V to 3.3 V and then goes back to 0 V.

(D) Real Time Clock (RTC) module DS3231 interface. DS3231 is connected to Arduino by Inter-Integrated Circuit (I^2C).

Assembling and connections are shown in Figure 5-4.

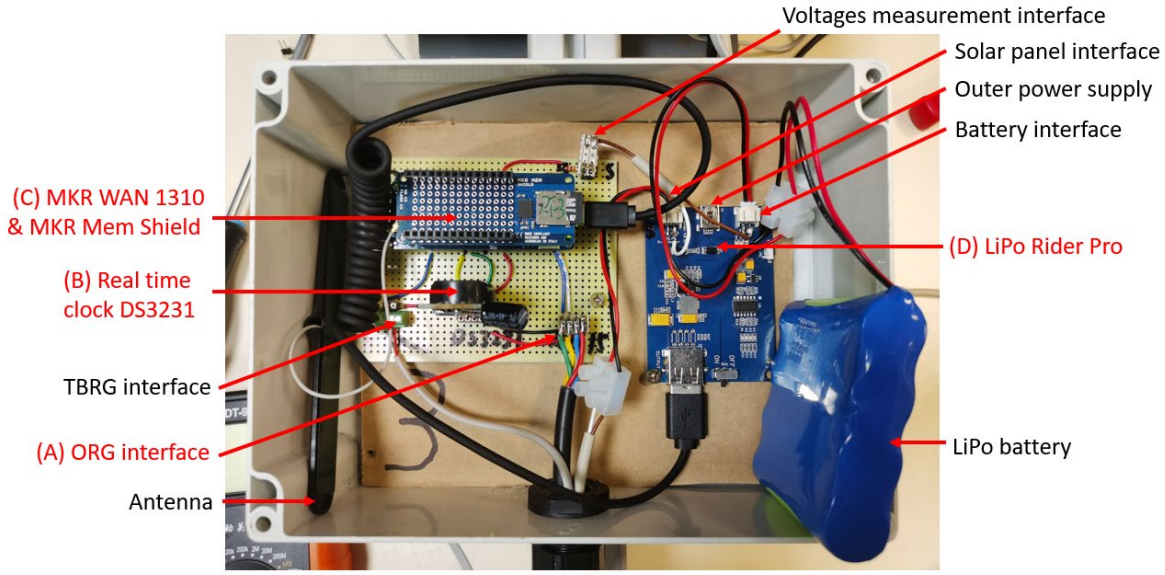

Figure 5-4. Components in the hardware containing box, items identified by letters are presented in the main text.

As shown in Figure 5-4, clockwise from left to right, the following points should be noted in particular:

(A) The optical rain gauge RG-15 is sold without connecting cable. Users need to open the lens and make the cable and interface by themselves, and this undoubtedly introduces a risk of damaging the sensor.

(B) There is a big capacitor across the coin cell battery which powers the RTC module DS3231. If not, this kind of RTC module is easy to reset by itself.

(C) The Arduino MKR Mem Shield is installed on Arduino to operate the SD card.

(D) Solar panel, outer power supply and battery interfaces of LiPo Rider Pro are used in the field. The entire system has two power supply methods by this way. The outer power supply is powering the system and the battery is always full in normal times. If the outer power supply is interrupted, the system can still run for dozens of days powered by the solar panel and the battery except in winter with low temperature conditions (results shown in 5.3.4.1). A USB cable is used to connect the LiPo Rider Pro and Arduino.

5.2.2.1.2 Programming

(1) Arduino programming

The Arduino operation codes are written in Arduino IDE language (close to C++). The software flow chart is shown in Figure 5-5.

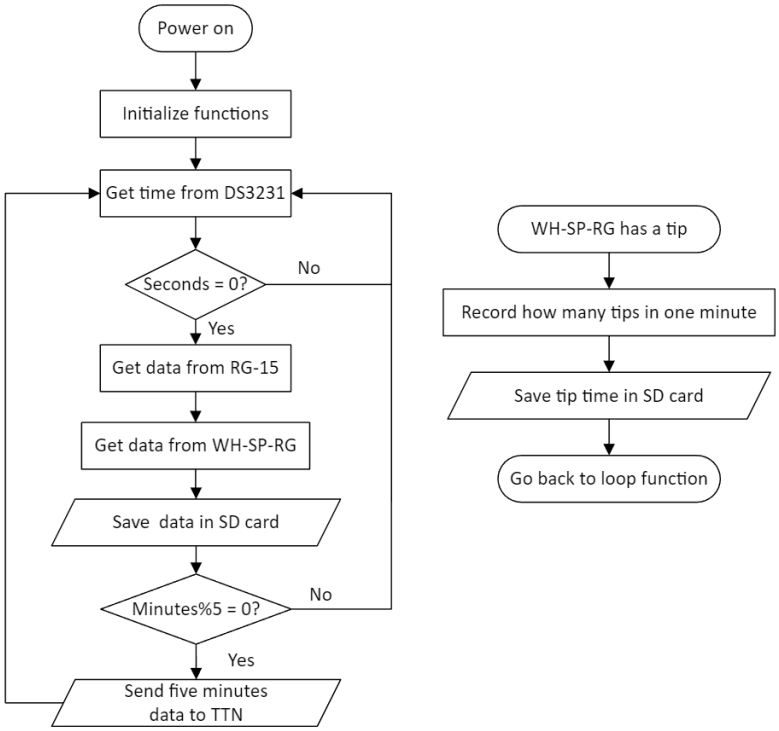

Figure 5-5. Software flowchart of the Arduino code of the low-cost rainfall monitoring station.

The core of the system behavior control is the time number output of the RTC module. Data are saved in the SD card every minute and sent online every 5 minutes. When the tipping bucket rain gauge WH-SP-RG outputs a tip, the tip time in Unix time format in seconds is saved directly in the SD card. Other details are given in section 5.2.2.1.3 describing the data acquisition process.

A software switch debounce is implemented in the interrupt code for reading the output of WH-SP-RG. After one tip, the system cannot read another tip in the same one second. According to the best estimated low-cost TBRG resolution as discussed in section 5.3.3, the TBRG monitoring maximum value that could potentially be measured is 800 mm/h, which is far beyond any realistic rainfall intensity to be expected in Lyon.

A software watch dog function is used to make the system can handle exception autonomously.

The last version of the software developed for this thesis is shared in GitHub (Zhu, 2023a). All rainfall monitoring stations used in this study are uploaded with the same software except the identification string to link them to the online platform.

(2) Online platform programming

The Things Network (The Things Network, 2023) platform is used to receive data sent by Arduino through Long-Range Radio (LoRa) network (LoRa Alliance, 2023). But The Things Network platform does not provide data storage service. The data in Message Queueing Telemetry Transport (MQTT) (Hillar, 2017) format is forwarded to custom Node-RED (Hagino, 2021) server to parse and store.

It should be noted that we used three same rainfall monitoring stations to test three same pairs of TBRG and ORG low-cost sensors, one station is an end device and all of them are in the same application in The Things Network as shown in Figure 5-6.

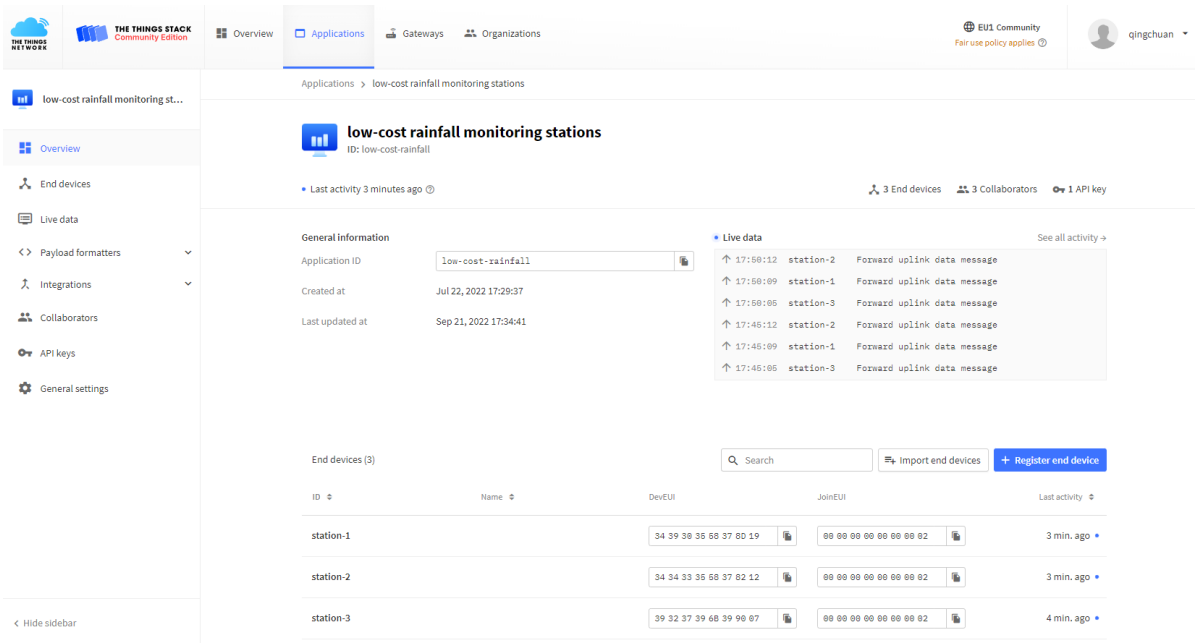

Figure 5-6. Screenshot of The Things Network platform.

The custom JavaScript formatter code is shared in GitHub (Zhu, 2023b).

(3) Node-RED programming

A custom Node-RED server was built by a technician of INSA laboratory DEEP because Node-RED provides a browser-based editor and a flow-based programming that make it user-friendly.

We use the laboratory Node-RED server to process rainfall monitoring data. The design is shown in Figure 5-7.

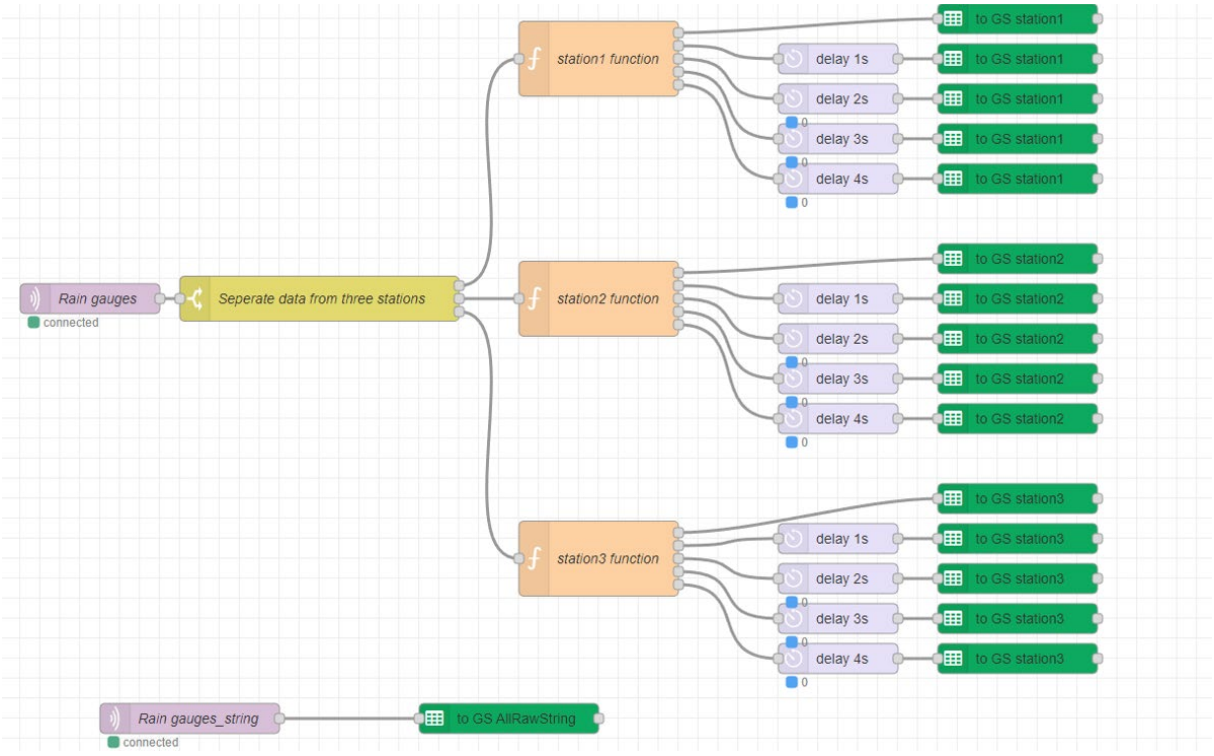

Figure 5-7. Screenshot of Node-RED programming.

As shown in Figure 5-7, two “MQTT in” nodes (shown on the left side in dark purple color) receive the same MQTT string output from The Things Network platform.

One MQTT string is sent to a switch node (shown in yellow color) to separate different station MQTT strings by their end device identification (“station-1”, “station-2”, and “station-3” as shown in the bottom of Figure 5-6). And then, a function node (shown in orange color) is used to parse the information of interest. A delay node (shown in light purple color) is used to write the data in Google Sheet line by line as shown and explained in Figure 5-11 by “G Sheet” node (shown in green color).

The same MQTT string is also received by another “MQTT in” node (shown in the bottom of Figure 5-7) and saved directly in Google Sheet as a backup for further possible operation problem investigation.

The Node-RED programming shown in Figure 5-7 is shared in GitHub (Zhu, 2023c).

5.2.2.1.3 Data acquisition

Thanks to the system design and the components selection, there are two ways to collect data: (i) store all data locally in the SD card, or (ii) store the data online in Google sheet. Details are given in Table 5-4.

Table 5-4. Monitoring data categories, types, sources, acquisition frequencies and directions.

Category	Data type	Source	Acquisition frequency	Save on SD card?	Send online?
Monitoring	Date and time number (time stamp)	RTC	every minute	yes	yes
	Cumulative rainfall depth of last minute	ORG	every minute	yes	yes
	Total tips of last minute	TBRG	every minute	yes	yes
	Unix time of every tip	TBRG and RTC	when it happens	yes	no
Maintenance	Battery output voltage	ADC of Arduino	every minute	yes	yes
	Solar panel output voltage	ADC of Arduino	every minute	yes	yes
	Air temperature in the box	RTC	every minute	yes	yes
	SD card saving flag (success: 1, failure: 0)	Arduino	every minute	no	yes
	System reset time	Arduino watch dog function	when it happens	yes	no

(1) SD card data

There are up to six separate csv files in the SD card to record as much details as possible for allowing further operation problem investigation. These six files with different objectives are:

- DATA.CSV to save every minute data as shown in Table 5-4.

- BAK.BAK to backup DATA.CSV.

- TTNSUM.CSV to save the data sent online every five minutes.

- ORGRAW.CSV to save output string of low-cost optical rain gauge RG-15 every minute.

- TBRGRAW.CSV to save the Unix time in seconds of every tip output of tipping bucket rain gauge WH-SP-RG.

- WDT.CSV to save the system reset time once the watch dog function is operating. This file will not be created when there is no system reset initiated by the watchdog function.

Data is recorded with as much detail as possible on the SD card. Screenshots of the above-mentioned documents are given in Figure 5-8 to Figure 5-10. All details of the system operation are saved in this way on the SD card for future analysis.

Station	Count	DS3231 (UTC)	RG-15 (mm/min)	TBRG Acc (tips/min)	Battery Voltage (V)	Solar Panel Voltage (V)	Temperature (Celsius)	Code version
2	0	2022-11-01 10:18:00	0	0	4.18	4.67	18	1 November 2022
2	1	2022-11-01 10:19:00	0	0	4.18	4.67	18	1 November 2022
2	2	2022-11-01 10:20:00	0	0	4.19	4.66	18	1 November 2022
2	3	2022-11-01 10:21:00	0	0	4.18	4.66	18	1 November 2022
2	4	2022-11-01 10:22:00	0	0	4.19	4.67	18	1 November 2022
2	5	2022-11-01 10:23:00	0.41	0	4.19	4.66	18	1 November 2022
2	6	2022-11-01 10:24:00	0	0	4.18	4.67	18	1 November 2022
2	7	2022-11-01 10:25:00	0	0	4.19	4.66	18	1 November 2022
2	8	2022-11-01 10:26:00	0	0	4.19	4.68	18	1 November 2022
2	9	2022-11-01 10:27:00	0	0	4.2	4.69	18	1 November 2022

Figure 5-8. Screenshot of DATA.CSV file in SD card.

Station	Count	DS3231 (UTC)	RG-15 Acc (mm/5min)	TBRG counts (tips/5min)	Battery Voltage (V)	Solar Panel Voltage (V)	Temperature (Celsius)
2	0	2022-11-01 10:20:00	0	0	4.19	4.66	18
2	1	2022-11-01 10:25:00	0.41	0	4.19	4.66	18
2	2	2022-11-01 10:30:00	0	0	4.2	4.68	19
2	3	2022-11-01 10:35:00	0	0	4.2	4.71	19
2	4	2022-11-01 10:40:00	0.01	0	4.2	4.71	19
2	5	2022-11-01 10:45:00	0	0	4.19	6.55	19
2	6	2022-11-01 10:50:00	0	0	4.18	6.32	19
2	7	2022-11-01 10:55:00	0	0	4.18	6.13	19

Figure 5-9. Screenshot of TTNSUM.CSV file in SD card.

Station	Count	DS3231 (UTC)	RG-15 Raw String
2	0	2022-11-01 10:18:00	Acc 0.00 mm
2	1	2022-11-01 10:19:00	Acc 0.00 mm
2	2	2022-11-01 10:20:00	Acc 0.00 mm
2	3	2022-11-01 10:21:00	Acc 0.00 mm
2	4	2022-11-01 10:22:00	Acc 0.00 mm
2	5	2022-11-01 10:23:00	Acc 0.41 mm
2	6	2022-11-01 10:24:00	Acc 0.00 mm
2	7	2022-11-01 10:25:00	Acc 0.00 mm
2	8	2022-11-01 10:26:00	Acc 0.00 mm
2	9	2022-11-01 10:27:00	Acc 0.00 mm

(a)

Time of tips (/3600/24 + 25569) (UTC)
1667501424
1667501495
1667501655
1667501830
1667501901
1667501940
1667501996
1667502044

(b)

Time
2022-11-18 18:37

(c)

Figure 5-10. Screenshot of (a) ORGRAW.CSV, (b) TBRGRAW.CSV, and (c) WDT.CSV files in SD card.

(2) Online data

Online data are sent every five minutes only to save power and saved in Google Sheet as shown in Figure 5-11. If there is no loss of data during transmission, at the same timestamp time, online ORG output intensity (mm/min)

and TBRG output (tips/min) should be same as the DATA.CSV file in the SD card. At the time when the number of minutes in the timestamp is an integer multiple of five, other online data should be the same as in the DATA.CSV file on the SD card. I.e., if only relying on online data, rain gauges data are saved with a one-minute time step and other data are saved with a five-minute time step. This method aims to reduce the length of the communication string to meet the limitation of free LoRa WAN network but can still record the most interesting quantities in a one-minute time step.

TTN receive time (UTC)	Device ID	Count (send by system)	RTC output time (UTC)	ORG output intensity (mm/min)	TBRG output (tips/min)	RTC output temperature ( )	Battery output voltage (V)	Solar panel output voltage (V)	SD save flag (1:success, 0:fail)	RSSI
			2022-11-02 13:01:00	0	0					
			2022-11-02 13:02:00	0	0					
			2022-11-02 13:03:00	0	0					
			2022-11-02 13:04:00	0	0					
2022-11-02 13:05:13	station-2	65	2022-11-02 13:05:00	0	0	23	3.3	3.12	1	-97
			2022-11-02 13:06:00	0	0					
			2022-11-02 13:07:00	0	0					
			2022-11-02 13:08:00	0	0					
			2022-11-02 13:09:00	0	0					
2022-11-02 13:10:13	station-2	66	2022-11-02 13:10:00	0	0	23	3.28	3.06	1	-95
			2022-11-02 13:11:00	0	0					
			2022-11-02 13:12:00	0	0					
			2022-11-02 13:13:00	0	0					
			2022-11-02 13:14:00	0	0					
2022-11-02 13:15:13	station-2	67	2022-11-02 13:15:00	0	0	23	3.24	3.81	1	-97
			2022-11-02 13:16:00	0	0					
			2022-11-02 13:17:00	0	0					
			2022-11-02 13:18:00	0	0					
			2022-11-02 13:19:00	0	0					
2022-11-02 13:20:13	station-2	68	2022-11-02 13:20:00	0	0	23	3.24	3.78	1	-93

Figure 5-11. Screenshot of online data saving file in Google sheet.

Temperature in the containing box reported by the RTC, battery output voltage, and SD saving flag can be used to create an alarm in case the system is running abnormally.

5.2.2.2 Reference data logger

The reference data logger has been described in section 3.2.5.2.

5.2.2.3 System trial operation

From January 2022 to January 2023, the rainfall monitoring station has been tested in four locations on the GROOF platform (Figure 5-12). Choice of locations and corresponding observations are presented in the following sub-sections.

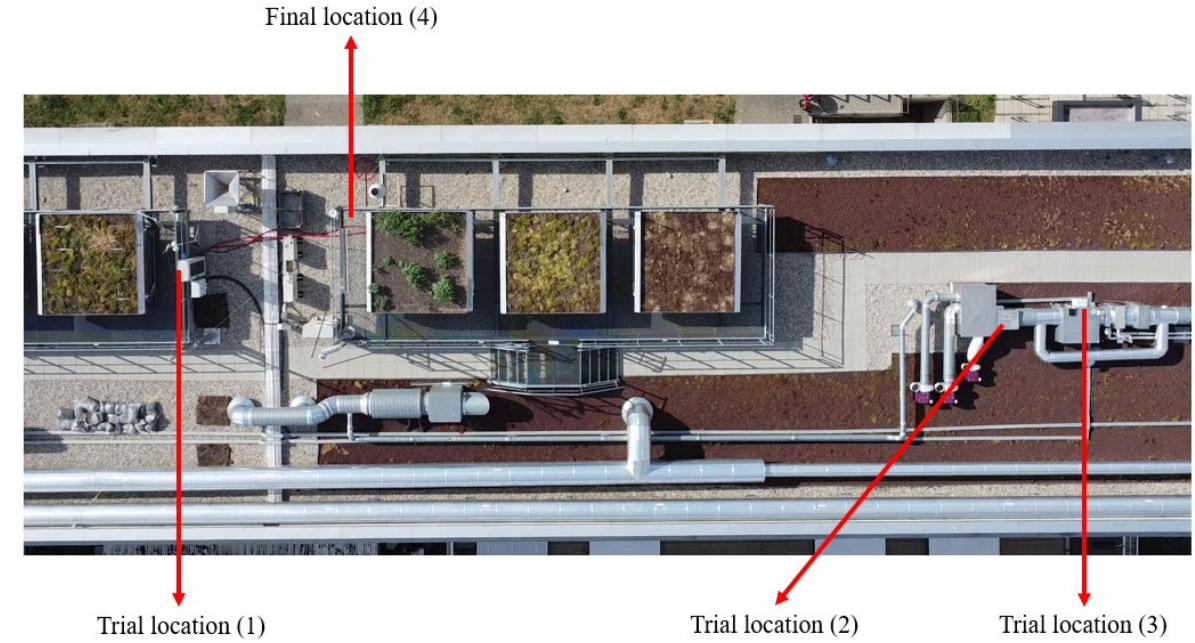

Figure 5-12. Four rainfall monitoring station test locations, final location in the top and trial locations in the bottom.

First location: above the electric cabinet from January to July 2022.

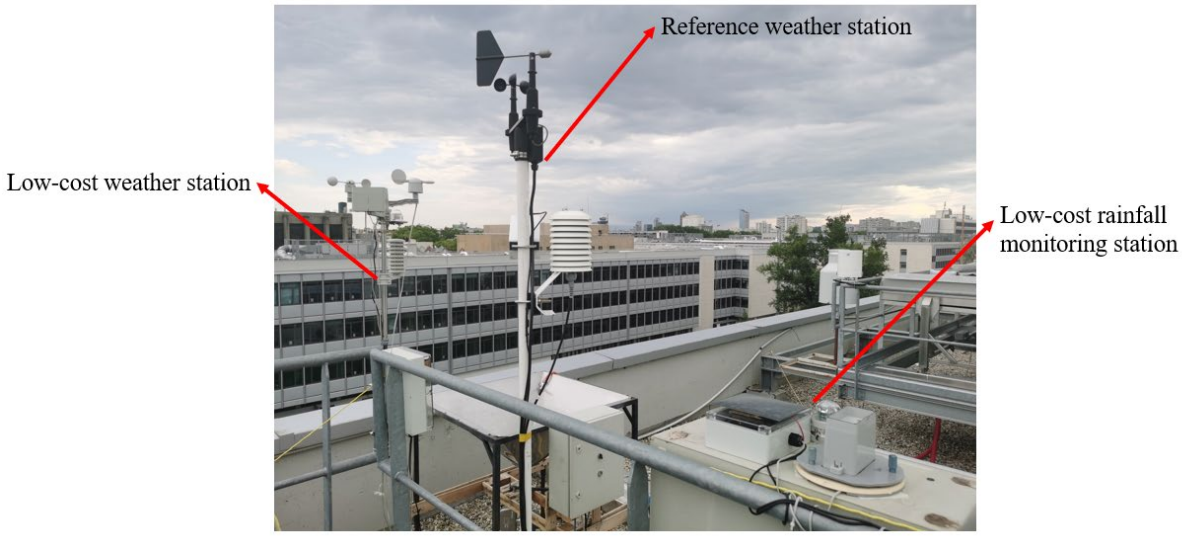

Figure 5-13. First low-cost rainfall monitoring station trial operation location. From left to right: low-cost weather station, reference weather station, low-cost rainfall monitoring station.

This location (Figure 5-13) has convenient power supply, and easy maintenance. But it has a fatal drawback as we found that the nearby reference weather station influenced the input of the optical rain gauge and the tipping bucket rain gauge by generating shadow and sheltering rainfall drops.

There are not so much valuable data collected during this period, which was mainly dry weather in Spring and beginning of Summer.

Second location: open area of the green roof, the box is mounted horizontally from July to August 2022.

Figure 5-14. Second low-cost rainfall monitoring station trial operation location: (a) Open area panorama, (b) Close up view of system installation.

This open area (Figure 5-14 (a)) appeared initially as an ideal location to test rain gauges. The low-cost tipping bucket rain gauge is far away from the optical rain gauge (Figure 5-14 (b)) to avoid shadow interference with the optical rain gauge. Unfortunately, rainwater entered the hardware containing box through the cable routing hole and the system stopped working during a heavy rainfall event. The rainfall monitoring station was then moved to the third location to solve this rainwater intrusion problem.

Third location: at open area of the green roof, the box is mounted vertically from August to September 2022.

Figure 5-15. Third low-cost rainfall monitoring station trial operation location.

The hardware containing box is mounted vertically and the cable routing hole is oriented downward to avoid rainwater entering the box (Figure 5-15). The system can operate for a long time with this design and installation. However, this location was not clearly authorized for our experiments, and we had to change once more.

Fourth location: on the GROOF platform barrier.

From September 2022, three similar low-cost rainfall monitoring stations were installed on the GROOF platform barrier (Figure 5-16) to test accuracy and reproducibility of tipping bucket rain gauge WH-SP-RG, optical rain gauge RG-15 and the whole rainfall monitoring station design.

Figure 5-16. Recent rainfall monitoring station installation: (a) Panorama, (b) Top view.

As shown in Figure 5-16, from left to right, the reference tipping bucket rain gauge is just beside the low-cost sensors. Three low-cost TBRG are installed in the middle of the bracket and three low-cost ORG are installed on the extremities of the bracket and slightly higher than the other components. Three similar low-cost rainfall monitoring stations (from top to bottom: No. 1, 2, 3) are in different containing boxes. To facilitate data processing, the low-cost ORG No.1 and low-cost the TBRG No.1 are connected to station No.1 and so on. After January 2023, the low-cost TBRG No. 4, 5, 6 are connected to stations No. 1, 2, 3 separately.

(a) (b)

Figure 5-17. Last rainfall monitoring station installation: (a) After increase of the funnel area, (b) Back view showing the three solar panels for three rainfall monitoring stations.

As shown in Figure 5-17, after November 2022, the TBRG rain collecting area has been tripled by means of an enlarged 3D printed additional funnel, with a radius of 7.02 cm and a height of 7.02 cm as shown in Figure 5-18. Adhesive tape is used to combine the additional funnel and the original low-cost TBRG. The increased funnel aimed to improve the resolution of the rain gauge (see results in section 5.3.3.3).

(a) (b)

Figure 5-18. Comparison of low-cost TBRG initial funnel and additional enlarged funnel.

(a) Top view, (b) Side view.

5.2.3 Optical rain gauge calibration

The low-cost optical rain gauge cannot be calibrated in laboratory with our available equipment, as it would require an artificial rainfall drops simulator to generate a rain event (with a real drop distribution and size) with known intensity on the sensor. Therefore, instead of a true calibration, the optical rain gauge will be compared in the field with reference sensors, as presented in section 5.3.2.

5.2.4 Tipping bucket rain gauge calibration

Due to the overfilling phenomenon, all tipping bucket rain gauges underestimate intensity in heavy rainfall events. The objective of the calibration aims to estimate and correct the systematic underestimation of the low-cost tipping bucket WH-SP-RG and check its repeatability and reproducibility (Bertrand-Krajewski *et al.*, 2021).

5.2.4.1 Setups and calibration protocol

Calibration setups are shown in Figure 5-19.

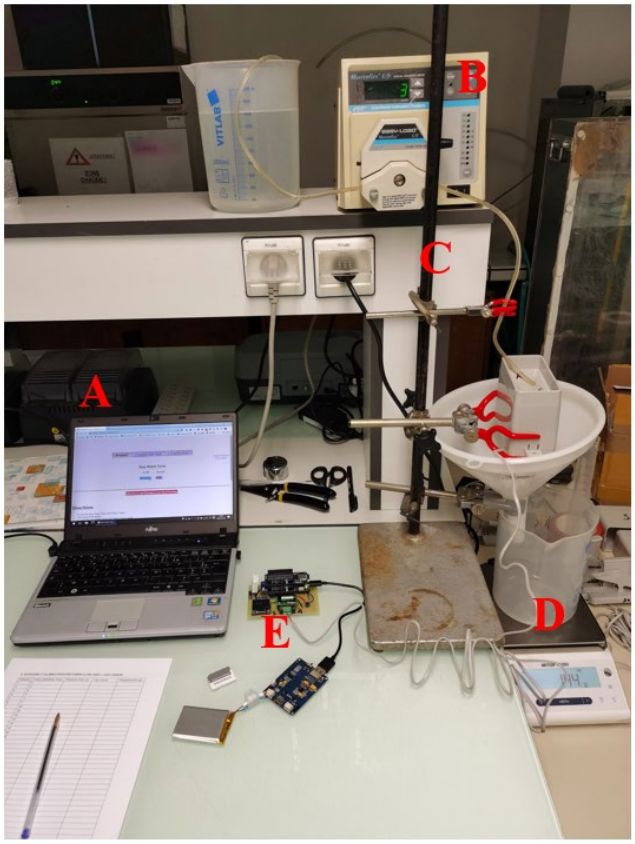

Figure 5-19. Low-cost tipping bucket rain gauge calibration setups. Clockwise from left to right: (A) laptop to run the timer to record the time duration *t* in second, (B) low-speed peristaltic pump to simulate rainfall intensities, (C) bracket to hold the low-cost tipping bucket rain gauge, (D) scale to weight the discharge water mass *m* in gram, and (E) DIY low-cost data logger to record the total number of tips *n* during one rainfall simulation.

The operating steps of calibration are the following ones:

At the beginning:

1) Open and clean the low-cost TBRG.

2) Make sure the low-cost TBRG is horizontal and installed stable.

3) Wet the whole benchmark at first (about 10 tips).

4) Power the low-cost system with full charge battery (reported by Lipo Rider Pro).

5) Install the SD card in the low-cost data logger.

6) Reset the timer to zero.

7) Reset the scale to zero.

Repeat measurement three times for each pump speed. Set the pump speed in turn to 3, 7, 10, 15, 20, 25, 30, 35, 40, 45, 50, 55, 60 mL/min.

At each pump speed:

1) Start the timer and the pump at the same time.

2) Run the experiment for about 50 ~ 60 tips and read the low-cost data logger screen.

3) Stop the timer and the pump at the same time just after the last tip.

4) Record duration time, number of tips and water mass discharged during the experiment.

5) Pour water into the pump suction bucket.

6) Reset timer, low-cost data logger and scale to zero.

5.2.4.2 Low-cost data logger

The low-cost data logger used for the tipping bucket rain gauge calibration is described by Figure 5-20.

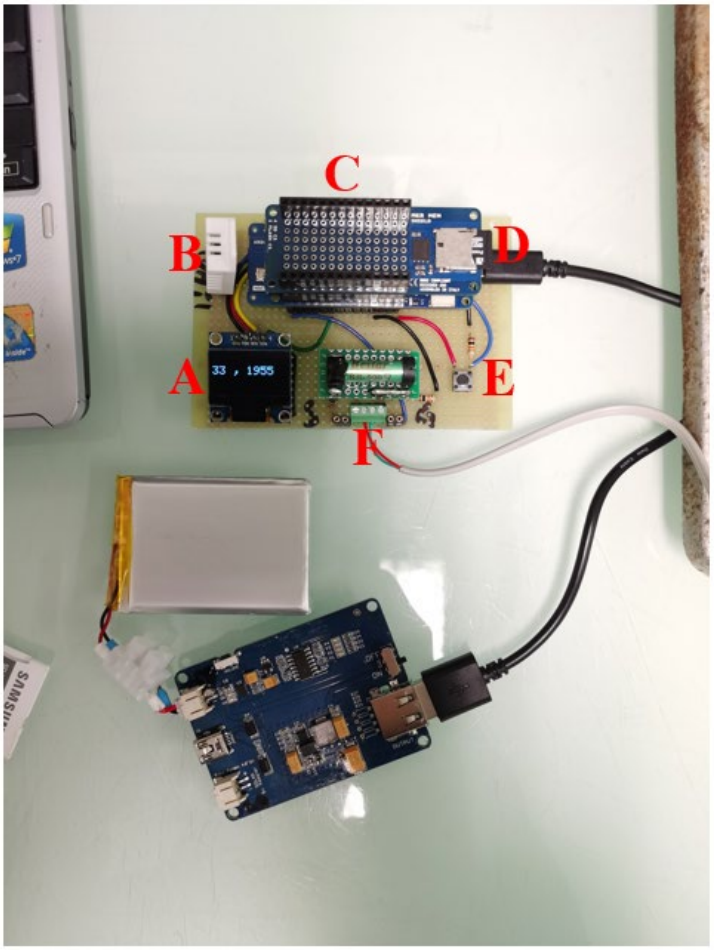

Figure 5-20. Low-cost TBRG calibration data logger.

The core of the DIY low-cost data logger is an Arduino MKR WAN 1310. As shown in Figure 5-20, the logger has:

(A) a screen to show current tips counting and total tips counting (current tips counting 33, total tips counting 1955),

(B) a DHT22 sensor to record air temperature and humidity during the experiment,

(C) a SD card module to save tip times in the SD card connected to the underlying Arduino,

(D) a battery and a Lipo Rider Pro module to charge it and avoid interference caused by unstable power supply,

(E) a press button to reset the current tips counting to 0,

(F) a TBRG interface,

The Arduino code of low-cost TBRG calibration data logger is shared in GitHub (Zhu, 2023d).

5.2.4.3 Calibration data processing

Three measurement quantities about tipping bucket rain gauge dynamic response are recorded: (i) total number of tips number n at each pump speed, (ii) discharged water mass m in gram, (iii) duration time t in second of the experiment.

One assumes that: (i) the water density is $\rho = 0.001$ g/mm^3, (ii) with additional enlarged funnel, the low-cost tipping bucket rain gauge collecting area is $s = 15482$ mm^2. For each pump speed, with the TBRG resolution r in mm/tip, the calibration rainfall intensity I_t (also named true intensity) in mm/h is:

$$I_t = 3600\frac{m}{\rho t s} \quad \text{Equation 5-1}$$

the measured rainfall intensity I_m in mm/h is:

$$I_m = 3600\frac{rn}{t} \quad \text{Equation 5-2}$$

The true bucket tipping depth r_t (also named tipping bucket resolution) in mm/tip is:

$$r_t = \frac{m}{\rho n} \quad \text{Equation 5-3}$$

The typical calibration function is a power function (Bertrand-Krajewski *et al.*, 2021):

$$I_t = b_1 {I_m}^{b_2} \quad \text{Equation 5-4}$$

5.2.5 Timestamp difference

In the comparison between low-cost and reference rain gauges, the timestamp difference problem is encountered because of the use of different real time clock modules. The difference is estimated to be less than 15 seconds. On the other hand, all the rain gauges having different sensitivity, one cannot expect that all of them respond within

the same exact minute. Therefore, even though data are collected with a one-minute time step, comparison between reference and low-cost rain gauges data is carried out every 5 minutes by summing every minute output.

5.3 RESULTS AND DISCUSSION

5.3.1 Operation

As described in section 5.2.2.3, three rainfall monitoring stations have been installed on the GROOF platform and data have been collected from 2022-09-26. Reference weighing rain gauge data are available from April to July 2022. The performance of the reference TBRG is corrected by comparing with the reference weighing rain gauge as described in section 3.2.5.1.1. Verified reference TBRG data are available from April 2022 to January 2023.

Three low-cost ORG No.1, 2, 3 and six low-cost TBRG No. 1 to 6 are tested. These nine rain gauges are not always in operation due to ORG repair and TBRG calibration. Details are given in Table 5-5.

Table 5-5. Sensor comparing periods and sensors in operation or not.

Number	1	2	3	4
Time begins	2022-09-28	2002-11-09	2022-12-17	2023-01-10
Time ends	2022-10-30	2022-12-04	2023-01-08	2023-01-31
Days	33	26	22	22
ORG 1	in operation	in operation	removed	in operation
ORG 2	in operation	in operation	removed	in operation
ORG 3	in operation	removed	removed	in operation
TBRG 1	in operation	in operation, WAF	in operation, WAF	removed
TBRG 2	in operation	in operation, WAF	in operation, WAF	removed
TBRG 3	in operation	removed	in operation, WAF	removed
TBRG 4	-	-	-	in operation, WAF
TBRG 5	-	-	-	in operation, WAF
TBRG 6	-	-	-	in operation, WAF

WAF: with additional funnel (used to triple the colleting area). Tipping bucket rain gauges (TBRG) 4, 5 and 6 were bought and installed to replace TBRG 1, 2 and 3.

As shown in Table 5-5, from 2022-09-28 to 2022-10-30, low-cost TBRG No.1 to 3 had no specific modifications and were used as bought. After 2022-11-09, the TBRGs were modified based on the initial results: additional enlarged funnel was added to each low-cost TBRG (No.1 to 3) to improve low intensity rainfall monitoring. From

2022-11-09 to 2022-12-04, the whole station 3 (TBRG 3 and ORG 3) was taken back to laboratory for calibration and to try to fix the problem that the ORG No.3 output was much lower (see section 5.3.2.3) than other rain gauges. From 2022-12-04 to 2022-12-17, all systems were taken back to the laboratory to add outer power supply capability because during winter the battery could not be sufficiently recharged by solar panel. From 2022-12-17 to 2023-01-08, the three stations were installed back *in situ* but without ORG: there was not enough time to reinstall also the ORGs before the campus close for holidays (2022-12-18 to 2023-01-07) and the objective was to reinstall as soon as possible not to miss any rain event. After 2023-01-10, new TBRG No. 4, 5, and 6 replaced TBRG No. 1, 2, 3 to check the reproducibility of new low-cost TBRG WH-SP-RG. TBRG No.1 and No. 3 have been tested *in situ* for more than one year and their locking carabiners of housing were damaged. Their funnel and bucket part were fixed together by tapes.

During the test period, output of reference TBRG is shown in Figure 5-21 with a one-minute time step. According to Figure 5-21, most of the time, all the low-cost rain gauges are tested with rainfall intensity less than 45 mm/h except one minute on 9 November 2022.

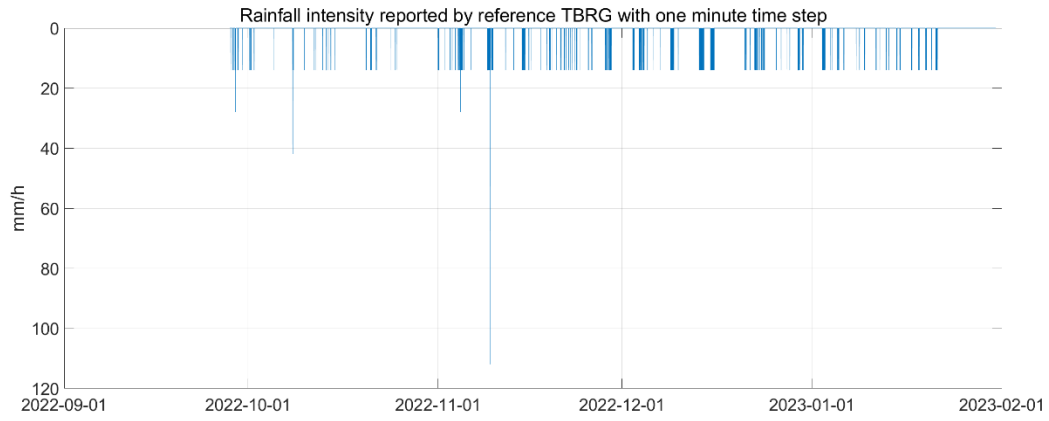

Figure 5-21. Rainfall intensity measured by the reference TBRG with one-minute time step.

5.3.2 Low-cost optical rain gauge RG-15 performance assessment

ORG No.1 was bought in June 2021 and installed intermittently from January 2022 to January 2023.

ORG No.2 was bought together with ORG No.1 and installed in September 2022.

ORG No.3 was bought in July 2022 and installed in September 2022.

5.3.2.1 ORG No.1

Output comparison between low-cost ORG No.1 and reference TBRG in three periods are given in Figure 5-22 to Figure 5-24. As a first quick qualitative assessment of the low-cost sensor behavior for each test period, each figure displays respectively, on the left graph: (i) the experimental points, (ii) the slope of the line with zero intercept and (iii) the corresponding coefficient of determination; on the right graph: the cumulative rainfall depths with coverage intervals (CI in figures).

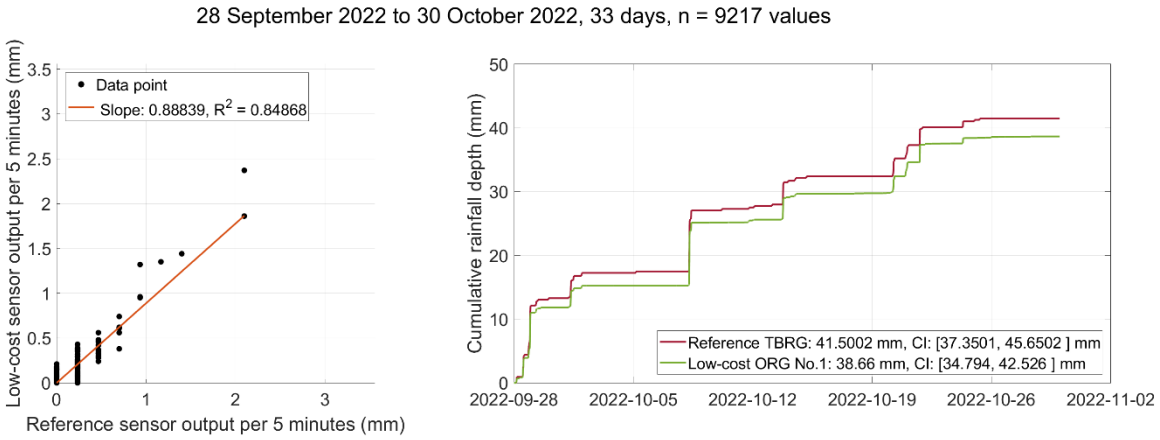

Figure 5-22. Comparison of low-cost ORG No.1 with reference TBRG from 28 September 2022 to 30 October 2022.

As shown in Figure 5-22, ORG No.1 has an acceptable performance, cumulative rainfall depths are similar to reference TBRG depths, under the hypothesis that they have a relative enlarged uncertainty of 10%.

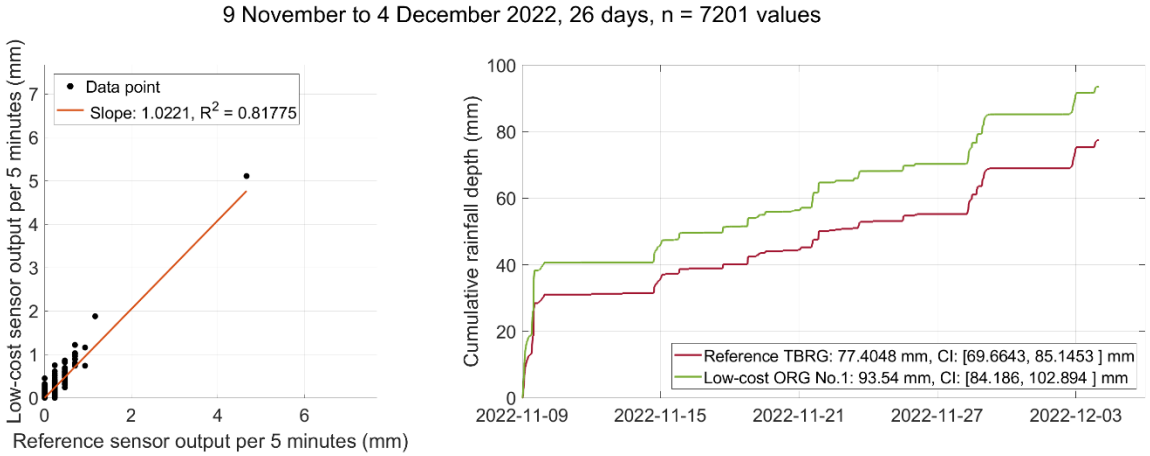

Figure 5-23. Comparison of low-cost ORG No.1 with reference TBRG from 9 November 2022 to 4 December 2022.

As shown in Figure 5-23, ORG No.1 output shows higher value than TBRG in the heavy rainfall event on 9 November 2022. Even so, there is still an overlap between the coverage interval of the two sensors. The linear regression appears as extremely dependent on the single point with the highest value, which is not satisfying.

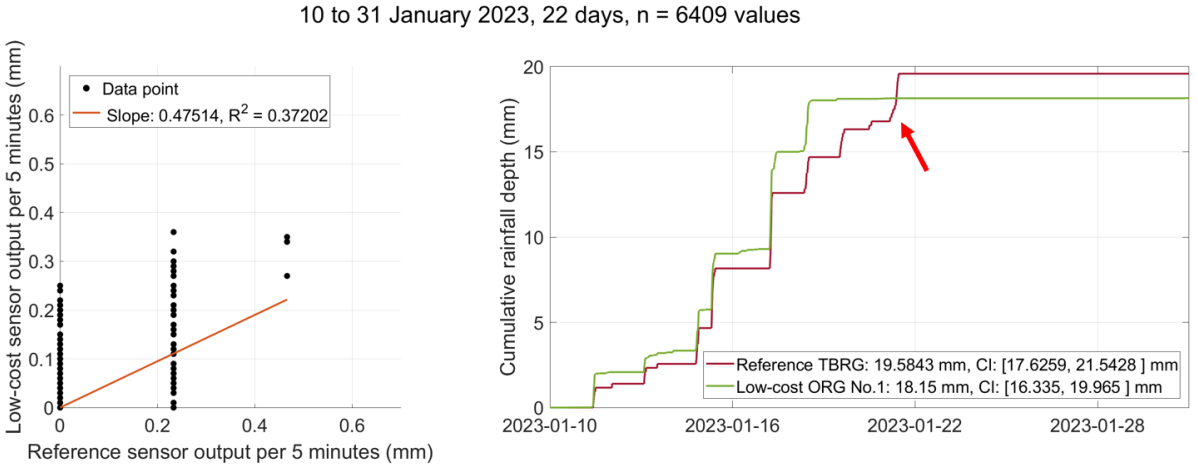

Figure 5-24. Comparison of low-cost ORG No.1 with reference TBRG from 10 to 31 January 2023. The red arrow indicates a snow period.

As shown in Figure 5-24, the least square regression is not appropriate for this case (R^2 = 0.37) due to the inadequate points distribution (left graph). The low-cost ORG slightly underestimates rainfall (right graph). This may be partly due to that there were snowfall during this period marked by red arrows on Figure 5-24.

As shown in the legends of Figure 5-22 to Figure 5-24, under the hypothesis that low-cost ORG No.1 and reference TBRG have relative enlarged uncertainty of 10%, their output coverage interval overlaps in three periods.

Data for all periods are shown in Figure 5-25. The regression results are given in Table 5-6.

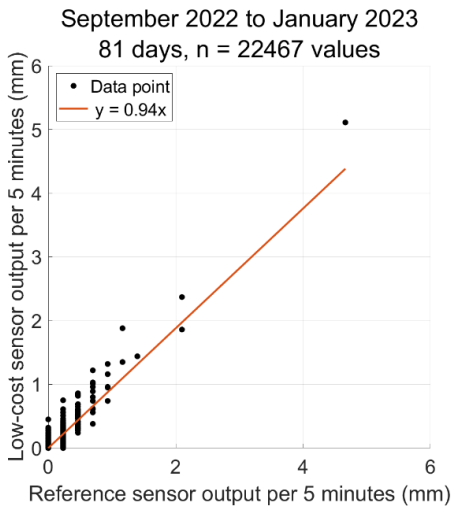

Figure 5-25. Ordinary least square regression results of ORG No.1 output from September 2022 to January 2023. The correlation function has been selected from the regression results given in Table 5-6.

Table 5-6. Regression results for the low-cost ORG No.1.

Parameter	With 0 intercept	With free intercept
b11	0	0.0009
b12	0.9431	0.9415
u(b11)	0	0.0002
u(b12)	0.0032	0.0032
cov(b11, b12)	0	0
ResVar1	0.0008	0.0008
IC95 b11	0	[0.0005, 0.0013]
IC95 b12	[0.9369, 0.9493]	[0.9352, 0.9477]
Standard error	0.0278	0.0277

According to Table 5-6, the bias estimated with the free intercept regression is equal to 0.0009 and its 95% coverage interval [0.0005, 0.0013] is very close to zero (standard errors are also not significantly different). Therefore, the selected correlation function, with two significant figures, is:

$$y = 0.94x \qquad \text{Equation 5-5}$$

with a standard error ε = 0.03.

The regression in Figure 5-25 and Table 5-6 indicate that low-cost ORG No.1 can measure rainfall events similarly to reference TBRG.

However, the low-cost ORG is set to resolution 0.02 mm and the reference TBRG has a resolution 0.233 mm/tip (see section 3.2.5.1.1). Data with five-minute time step is not appropriate for regression and to calculate the correctness rate. Daily cumulative rainfall depth for all periods is shown in Figure 5-26. The corresponding regression results are given in Table 5-7.

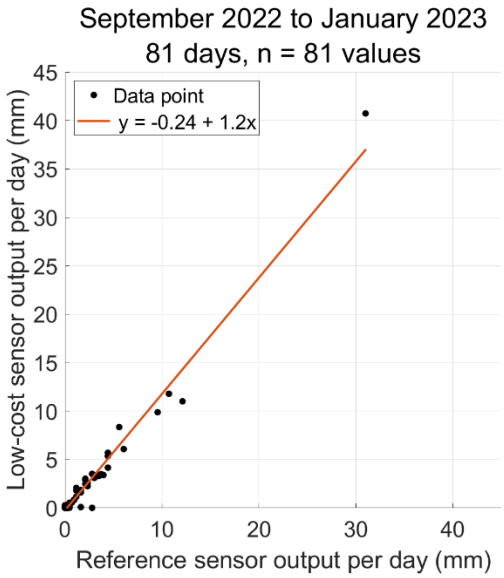

Figure 5-26. Ordinary least square regression results of ORG No.1 daily output from September 2022 to January 2023. The correlation function has been selected from the regression results given in Table 5-7.

Table 5-7. Regression results for the low-cost ORG No.1 daily output.

Parameter	With 0 intercept	With free intercept
b11	0	-0.2420
b12	1.2057	1.2272
u(b11)	0	0.0980
u(b12)	0.0212	0.0223
cov(b11, b12)	0	-0.0009
ResVar1	0.7017	0.6597
IC95 b11	0	[-0.4341, -0.0499]
IC95 b12	[1.1641, 1.2473]	[1.1834, 1.2710]
Standard error	0.8377	0.8122

According to Table 5-7, the bias estimated with the free intercept regression is equal to -0.2420 and its 95% coverage interval [-0.4341, -0.0499] is not including zero. Therefore, the selected correlation function, with two significant figures, is:

$$y = -0.24 + 1.23x \qquad \text{Equation 5-6}$$

with a standard error ε = 0.81.

The regression in Figure 5-26 and Table 5-7 indicates that the low-cost ORG No.1 daily output is approximately 20% higher than the reference TBRG. This is reasonable if one accounts for the fact that the optical rain gauge is more sensitive than the reference tipping bucket rain gauge.

When using the inverse function of Equation 3-4 to correct the low-cost ORG No.1 daily output, relative enlarged uncertainty of the resolution corresponding to 70%, 80%, 90%, 95%, 99% correctness rates are given in Table 5-8. Under the initial hypothesis of a relative enlarged uncertainty of 10% for the optical rain gauge, the correctness rate would be less than 70%, which is a poor performance. A relative enlarged uncertainty of 11% is a required assumption to reach a correctness rate of 70%. Increasing the correctness rate requires higher values of the relative enlarged uncertainty of the low-cost sensor. For example, the correctness rate is equal to 80% if one assumes a relative enlarged uncertainty of 20%. In other words, the low-cost optical rain gauge can provide results compatible with those of the reference rain gauge if one assumes that it has very high uncertainties. In such a case, the low-cost sensor cannot be considered as a satisfactory sensor.

Table 5-8. Relative Enlarged Uncertainty (EU) of the low-cost ORG No.1 daily output.

Correctness rate	Relative enlarged uncertainty	Comments
70%	11%	Close to the hypothesis relative enlarged uncertainty 10% to calculate coverage interval in Figure 5-22 to Figure 5-24.
80%	20%	\
90%	38%	\
95%	83%	Too big to be meaningful.
99%	NA	When relative enlarge uncertainty is 100%, correctness rate is 95.7%. The correctness rate cannot reach 100% due to two points on the x-axis in Figure 5-26.

5.3.2.2 ORG No.2

ORG No.2 gives comparable results compared with ORG No.1. Coverage Intervals (CI) of low-cost rain gauge ORG No.2 and reference TBRG cumulative outputs in three periods are given in Table 5-9. Regression results of low-cost rain gauge ORG No.2 and No.1 with time step five minutes and one day with corresponding enlarged uncertainty are summarized in Table 5-10. Details of ORG No.2 results are given in Appendix.

Table 5-9. Coverage Intervals (CI) of low-cost rain gauge ORG No.2 and reference TBRG cumulative outputs (assuming both have a relative enlarged uncertainty of 10%).

Period number	Time range	ORG No.2 output CI (mm)	Reference TBRG output CI (mm)	CI overlaps?
1	2022-09-28 to 2022-10-30	[39.20, 47.91]	[37.35, 45.65]	Yes
2	2022-11-09 to 2022-12-04	[89.02, 108.8]	[69.66, 85.15]	No
3	2023-01-10 to 2023-01-31	[14.54, 17.78]	[17.63, 21.54]	Yes

As shown in Table 5-9, CI of ORG No.2 and reference TBRG are overlapped in periods number 1 and 3 and the difference is only 4 mm during period number 2.

Table 5-10. Regression results for the low-cost rain gauge ORG No.2 and No.1.

Low-cost rain gauge ORG Number	2	1
Correlation function of data with a five-minute time step	$y = 0.93x$	$y = 0.94x$
Correlation function of daily cumulative outputs	$y = -0.32 + 1.33x$	$y = -0.24 + 1.23x$
Relative enlarged uncertainty for a 70% correctness rate	12%	11%

As shown in Table 5-10, Regression results of ORG No.1 and No.2 are similar numerically.

5.3.2.3 ORG No.3

ORG No.3 was bought one year after ORG No.1 and No.2. According to manufacturer's data, they have the same hardware composition and firmware version. But the output of ORG No.3 appears always very significantly lower than the reference rain gauge TBRG, as shown in Figure 5-27.

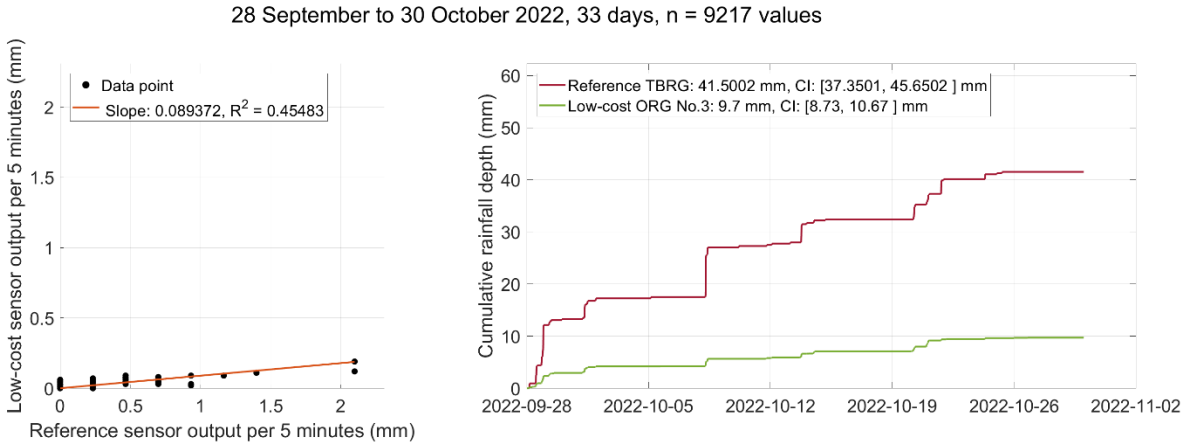

Figure 5-27. Comparison of low-cost ORG No.3 with reference TBRG from 28 September 2022 to 30 October 2022.

After investigation, the output of ORG No.3 is approximately 10 times smaller than the reference TBRG, whereas ORG No.1 and ORG No.2 are operating much better as shown in Figure 5-22 and Table 5-9. This problem could not be fixed despite resetting ORG No.3 several times: the output remained inexplicably still low as shown in Figure 5-28.

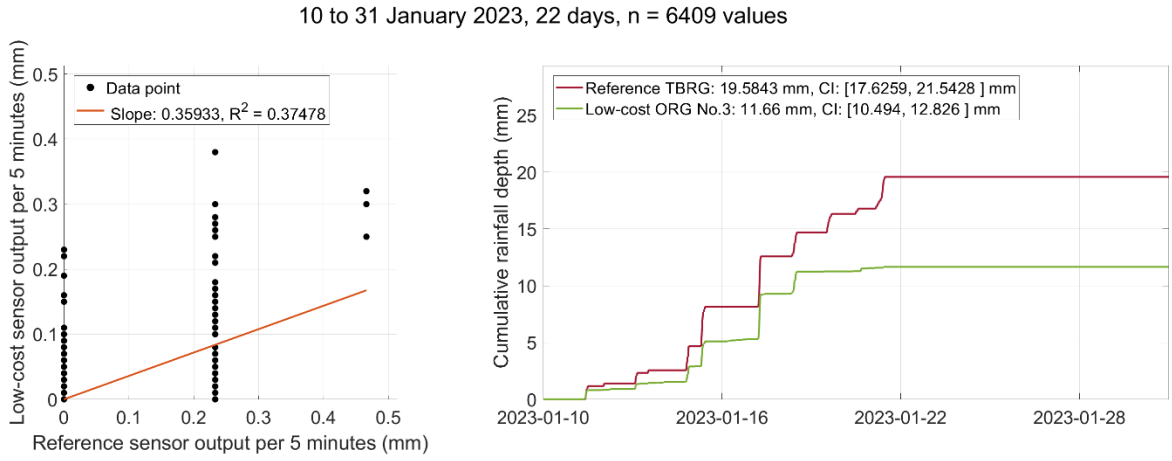

Figure 5-28. Comparison of low-cost ORG No.3 with reference TBRG from 10 to 31 January 2023.

As shown in the left graph of Figure 5-28, the least square regression is not appropriate for this case (R^2 = 0.37) due to the inadequate points distribution. The daily cumulative outputs of low-cost ORG No.3 and reference TBRG from 10 to 31 January 2023 are therefore compared in Figure 5-29. The regression results are given in Table 5-11.

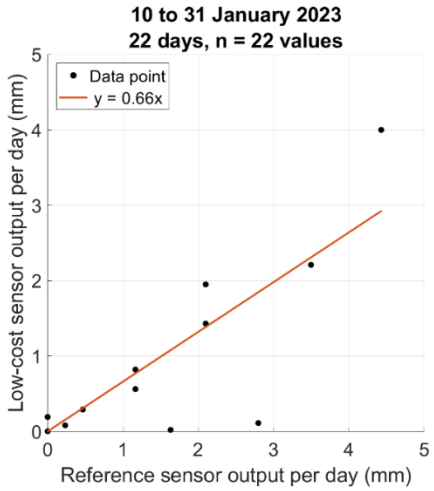

Figure 5-29. Ordinary least square regression results of ORG No.3 from 10 to 31 January 2023. The correlation function has been selected from the regression results given in Table 5-11.

Table 5-11. Regression results for the low-cost ORG No.3.

Parameter	With 0 intercept	With free intercept
b11	0	-0.0584
b12	0.6399	0.6610
u(b11)	0	0.1375
u(b12)	0.0707	0.0876
cov(b11, b12)	0	-0.0068
ResVar1	0.2709	0.2819
IC95 b11	0	[-0.3279, 0.2110]
IC95 b12	[0.5012, 0.7785]	[0.4895, 0.8328]
Standard error	0.5205	0.5309

According to Table 5-11, the bias estimated with the free intercept regression is equal to -0.0584 and its 95% coverage interval [-0.3279, 0.2110] is including zero and could be either positive or negative. Therefore, the selected correlation function is the zero intercept one, with two significant figures:

$$y = 0.64x \qquad \text{Equation 5-7}$$

with a standard error ε = 0.52.

The regression results indicate that the low-cost ORG No.3 output is approximately 36% lower than the reference TBRG. When using the inverse function of Equation 5-7 to correct the low-cost ORG No.3 daily output, the relative enlarged uncertainty corresponding to 70%, 80%, 90% correctness rates are given in Table 5-12. The relative enlarged uncertainty for a 70% correctness rate is 43%. Both the correctness rate and the enlarged uncertainty are poor.

Table 5-12. Relative Enlarged Uncertainty (EU) of the low-cost ORG No.3 daily output.

Correctness rate	Relative enlarged uncertainty
70%	43%
80%	44%
90%	Can not achieve

5.3.2.4 Discussion

The regression results of ORG No.1, 2, 3 low-cost sensors are summarized in Table 4-24.

Table 5-13. Summary of comparison between low-cost ORG and reference TBRG sensors.

ORG Number	Correlation equation [a]	Relative enlarged uncertainty [b]
1	$y = -0.24 + 1.2x$	11%
2	$y = -0.32 + 1.33x$	12%
3	$y = 0.66x$	43%

[a] y is low-cost ORG daily measurements, x is reference TBRG daily measurements.

[b] In the calculation of low-cost sensor correctness rate, low-cost sensor measurements are corrected by the inverse function of correlation equation. The relative enlarged uncertainty in this column corresponds to 70% correctness rate.

As shown in Table 4-24, the low-cost ORG No.1 and No.2 deliver acceptable data comparing to reference TBRG if one accepts a correctness rate of only 70%. Both overestimate rainfall depth approximately by 25% at daily scale under the test experimental conditions. It should be noted that the low-cost ORG No.1 has been tested *in situ* for one year with stable performance.

The low-cost ORG No.3 did not perform correctly. Its output is always about 10 times lower than other sensors at first glance. ORG No.3 was not purchased together with the other ones. Despite similar specifications are given by the manufacturer, it clearly performs unsatisfactorily, and it has not been possible to detect the cause of the problem. The manufacturer did not reply to our demand for technical support.

In conclusion, the low-cost optical rain gauge RG-15 delivers intermediate quality data under the test conditions of this research: 70% correctness rate only under the assumption of a relative enlarged uncertainty in the range of 10 to 12%, with a systematic overestimation in the range 20 to 33% for daily rainfall depth. Its performance must be systematically evaluated and quantified by comparison with a reference sensor. In addition, reproducibility is not ensured, as one among three tested sensors had a quite different behavior without any identifiable cause. Unfortunately, no test or use of this low-cost optical rain gauge was found in the literature for comparison with our results.

5.3.3 Low-cost tipping bucket rain gauge WH-SP-RG performance assessment

As shown in Table 5-2, the resolution of the low-cost TBRG WH-SP-RG given by manufacturer is confusing (three values: 0.254, 0.2794 and 0.3 mm/tip). The following work mainly aims to estimate the true resolution of WH-SP-RG.

5.3.3.1 Initial installation

TBRG No.1 was installed on the GROOF platform from March 2021 to January 2023. Before September 2022, it was part of the low-cost weather station. During this period, its output is speculated to be disturbed by wind as illustrated in Figure 5-30, where intensity values are given by TBRG No.1 in the absence of intensity measured by both WRG and TBRG reference sensors, to some extent when wind speed is significant (approximately above 10m/s).

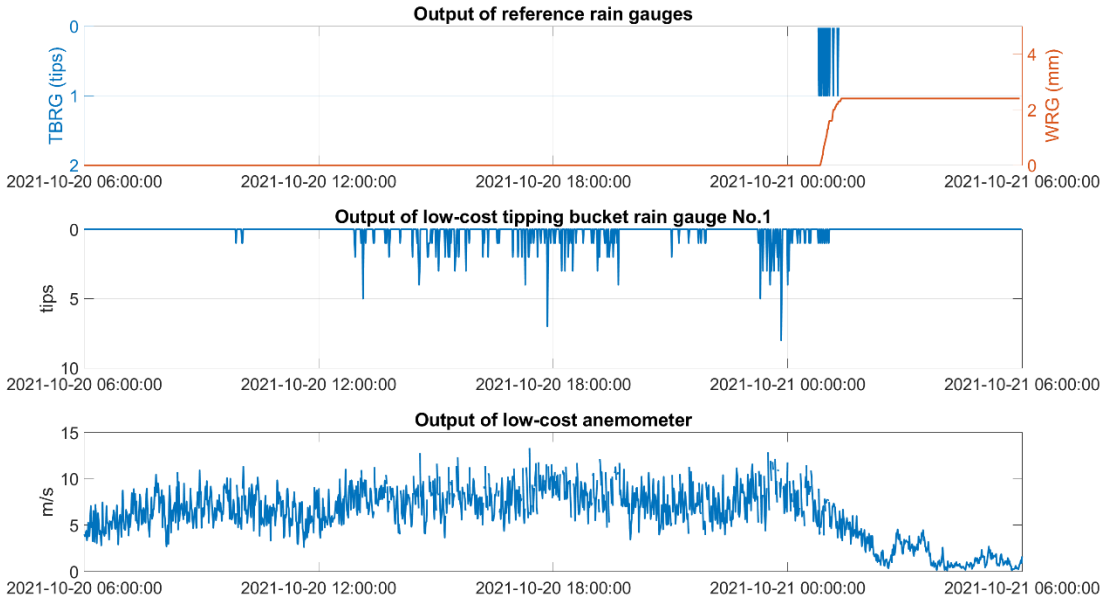

Figure 5-30. Data comparison between low-cost and reference rain gauges with wind speed detail for the 20 October 2021.

On 20 October 2021, there was only a slight rainfall event at midnight reported by both reference TBRG and WRG, but low-cost TBRG No.1 installed on the low-cost weather station reported a lot of fake tips. We suspect that this is due to the high wind speed at that day. This phenomenon is also found in the data of other periods. But we could not find papers or researchers reporting this phenomenon. Later, the low-cost TBRG WH-SP-RG was reinstalled differently, to avoid that high wind speed could generate movements of the bucket and thus possible fake tips.

5.3.3.2 Final installation with initial funnel

As described in sections 5.2.2.3 and 5.3.1, more reliable data are obtained from September 2022 to January 2023. And the fake tips problem due to high wind speed has been solved with the installation shown in Figure 5-13 to Figure 5-17.

5.3.3.2.1 TBRG No.1

From September to October 2022, there was no modification of the funnel area on low-cost TBRG as shown in Figure 5-16. Results are given in Figure 5-31.

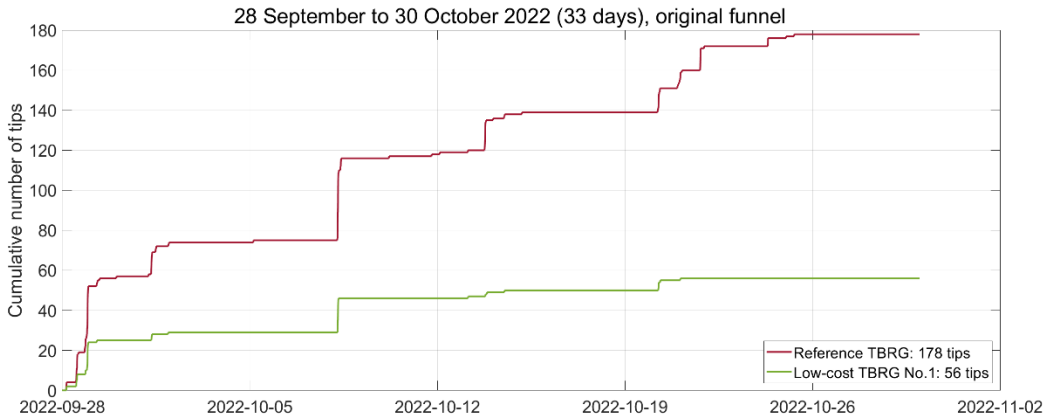

Figure 5-31. Low-cost TBRG No.1 performance from 28 September to 30 October 2022.

As shown in Figure 5-31, the low-cost TBRG No.1 could respond during rainfall events, but its output tips are approximately one third compared with the reference TBRG.

Figure 5-32 shows data from 28 September to 30 October 2022. The regression results are given in Table 5-14.

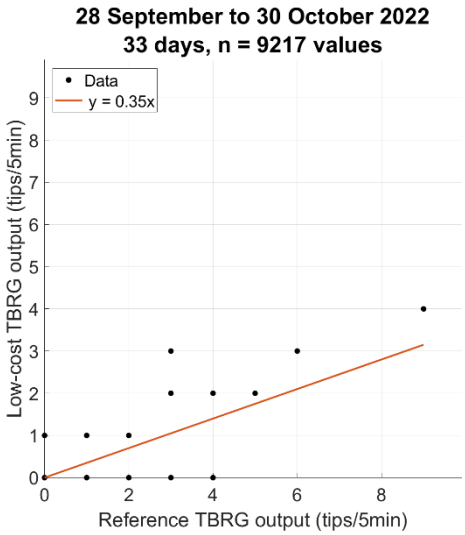

Figure 5-32. Low-cost TBRG No.1 and reference TBRG output comparison from 28 September to 30 October 2022. The correlation function has been selected from the regression results given in Table 5-14.

Table 5-14. Regression results for low-cost TBRG No.1 with original funnel.

Parameter	With 0 intercept	With free intercept
b11	0	-0.0008
b12	0.3541	0.3544
u(b11)	0	0.0008
u(b12)	0.0033	0.0033
cov(b11, b12)	0	0.0000
ResVar1	0.0052	0.0052
IC95 b11	0	[-0.0022, 0.0007]
IC95 b12	[0.3476, 0.3606]	[0.3478, 0.3609]
Standard error	0.0719	0.0719

According to Table 5-14, the bias estimated with the free intercept regression is equal to -0.0008 and its 95% coverage interval [-0.0022, 0.0007] is including 0. Therefore, the selected correlation function, with two significant digits, is:

$$y = 0.35x \qquad \text{Equation 5-8}$$

with standard error ε = 0.07.

The results shown in Figure 5-32 and Table 5-14 indicate that the low-cost TBRG No.1 with initial funnel has a resolution of approximately $1/\ b_{12} = 2.9$ times higher than the reference TBRG. The reference TBRG has a resolution of 0.233 mm/tip according to laboratory calibration, comparison with reference WRG as described in Chapter 3 section 3.2.5.1.1. One can conclude that, during this test period with initial funnel, the low-cost TBRG No.1 had a resolution of approximately $0.233/b_{12} = 0.67$ mm/tip.

Using the reference TBRG resolution of 0.233 mm/tip, a relative enlarged uncertainty of 10% and a low-cost TBRG resolution of 0.67 mm/tip, one can redraw Figure 5-31. Results are shown in Figure 5-33.

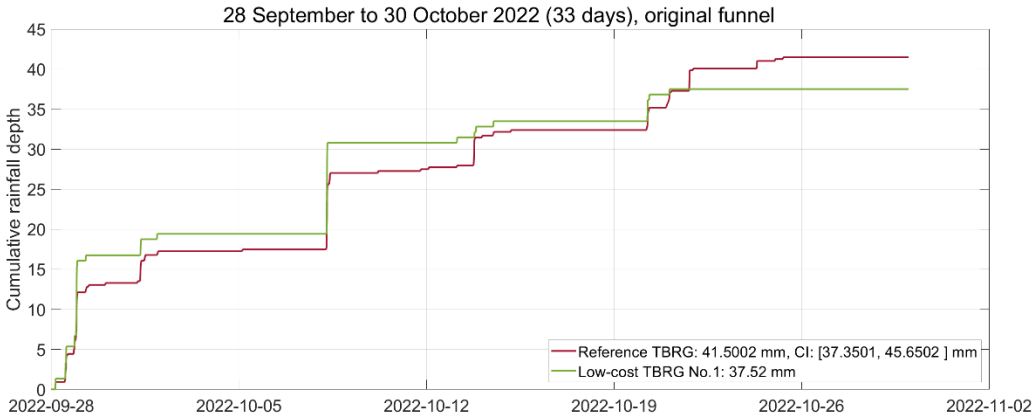

Figure 5-33. Revised low-cost TBRG No.1 performance from 28 September to 30 October 2022.

As shown in Figure 5-33, the low-cost TBRG No.1 can measure rainfall events similarly to TBRG. Due to its lower resolution, it is not as sensitive as the reference TBRG. The cumulative rainfall depth from 2022-09-28 to 2022-10-30 reported by low-cost TBRG No.1 (resolution 0.67 mm/tip) is 37.52 mm which is inside the output coverage interval of reference TBRG [37.3501, 45.6502].

5.3.3.2.2 TBRG No.2 and No.3 with initial funnel

The method used in section 5.3.3.2.1 is also used to assess the performance of low-cost TBRG No.2 and No.3 with initial funnel from 28 September to 30 October 2022. Details are given in Appendix.

5.3.3.2.3 Discussion and further work

Compared with reference TBRG, the resolution values of low-cost TBRG No.1, 2, 3 with initial funnel are summarized in Table 5-15.

Table 5-15. TBRG No.1 to No.3 regression results with initial funnel.

TBRG Number	Resolution	Cumulative rainfall depth	CI of reference TBRG
1	0.67 mm/tip	37.52 mm	
2	0.52 mm/tip	38.48 mm	[37.3501, 45.6502]
3	0.52 mm/tip	40.56 mm	

As shown in Table 5-15, when rainfall intensity is less than 45 mm/h, low-cost TBRG WH-SP-RG with initial funnel has a resolution around 0.60 mm/tip which is approximately twice the resolution given by the manufacturer as described in Table 5-2. This resolution is much larger than the World Meteorological Organization (WMO) recommendation that rain gauge resolution should not be greater than 0.2 mm/tip if detailed records are required (Lanza *et al.*, 2006). It was then decided to improve the resolution by enlarging the collecting area of the sensor by means of an additional 3D printed funnel installed above the initial funnel as shown Figure 5-18.

5.3.3.3 Final installation with enlarged additional funnel

5.3.3.3.1 TBRG No.1

The performance of TBRG No.1 with an additional enlarged funnel (as shown in Figure 5-17) is given in Figure 5-34 and Figure 5-35.

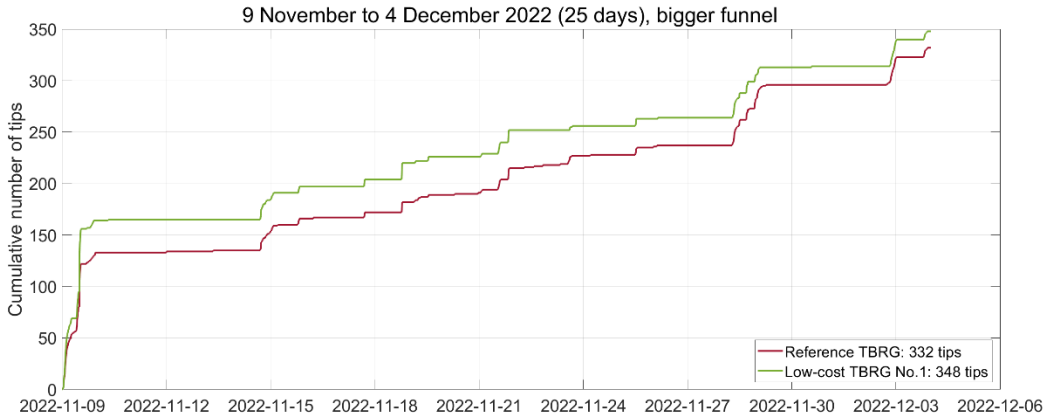

Figure 5-34. Low-cost TBRG No.1 performance from 9 November 2022 to 4 December 2022.

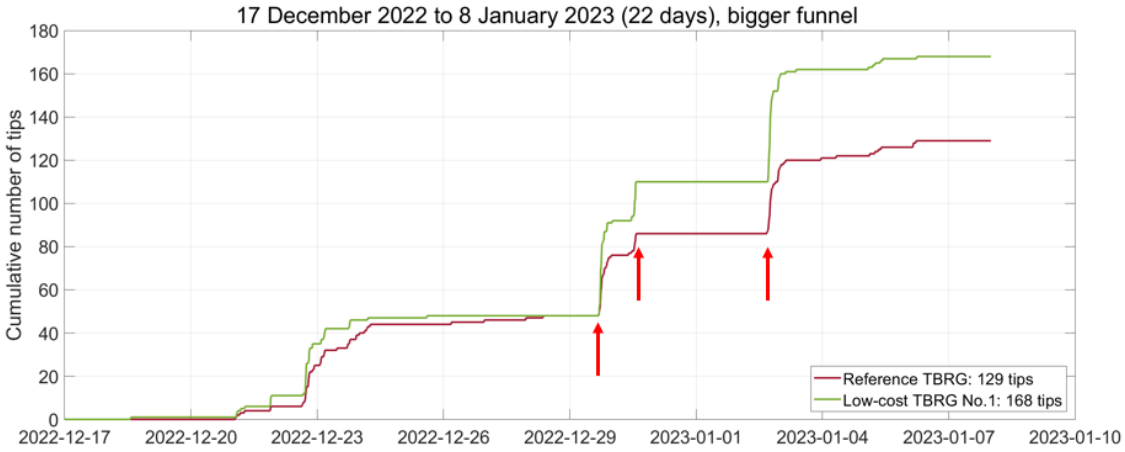

Figure 5-35. Low-cost TBRG No.1 performance from 17 December 2022 to 8 January 2023.

According to Figure 5-34 and Figure 5-35, the low-cost TBRG No.1 outputs a quite similar number of tips compared with the reference TBRG which indicates that they have a quite similar resolution. In Figure 5-34, the low-cost and reference number of tips are respectively 348 and 332, i.e., a relative difference of 4.8%, which is acceptable. In Figure 5-35, the relative difference is much higher and reaches 30.2%, mainly due to three events between 29 December 2022 and 3 January 2023 marked by red arrows.

Figure 5-36 shows all data from the two periods with enlarged funnel. The regression results are given in Table 5-16.

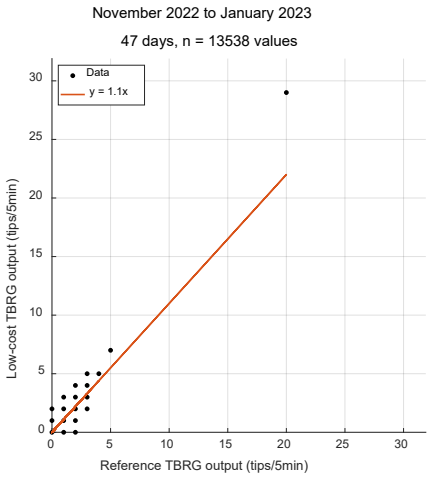

Figure 5-36. Low-cost TBRG No.1 and reference TBRG output comparison from November 2022 to January 2023. The correlation function has been selected from the regression results given in Table 5-16.

Table 5-16. Regression results for low-cost TBRG No.1 with additional enlarged funnel.

Parameter	With 0 intercept	With free intercept
b11	0	0.0012
b12	1.0853	1.0847
u(b11)	0	0.0017
u(b12)	0.0063	0.0064
cov(b11, b12)	0	0
ResVar1	0.0400	0.0400
IC95 b11	0	[-0.0022, 0.0046]
IC95 b12	[1.0728, 1.0977]	[1.0722, 1.0972]
Standard error	0.2001	0.2001

According to Table 5-16, the bias estimated with the free intercept regression is equal to 0.0012 and its 95% coverage interval [-0.0022, 0.0046] is including 0. Therefore, the selected correlation function, with one significant digit, is:

$$y = 1.1x \qquad \text{Equation 5-9}$$

with a standard error ε = 0.2.

The results shown in Figure 5-36 and Table 5-16 indicate that the low-cost TBRG No.1 with additional enlarged funnel has a resolution of approximately $0.233/b_{12} = 0.21$ mm/tip. This resolution is one third of the resolution with initial funnel, which corresponds very well to the fact that the collecting area has been tripled.

Enlarged uncertainties of the resolution corresponding to 70%, 80%, and 90% correctness rates are given in Table 5-17. The enlarged uncertainty for a 70% correctness rate is 0.02 mm/tip. This means that, with a resolution with a relative enlarged uncertainty of approximately 10%, the low-cost TBRG No.1 gives equivalent results compared to the reference TBRG for 70% of the values. Reciprocally, a 90% correctness rate implies an enlarged uncertainty of 0.08 mm/tip, which is a rather high value compared to the calculated resolution of 0.21 mm/tip.

Table 5-17. Enlarged uncertainty of the low-cost TBRG with additional enlarged funnel.

Correctness rate	Enlarged uncertainty
70%	0.02 mm/tip
80%	0.06 mm/tip
90%	0.08 mm/tip

5.3.3.3.2 TBRG No.1 to No.6 with additional enlarged funnel

The same method used in 5.3.3.3.1 is also used to assess the performance of low-cost TBRG No.2 to No.6 with additional triple area funnel from November 2022 to January 2023. Details are given in Appendix. All results are summarized in Table 5-18.

Table 5-18. TBRG No.1 to No.6 regression results with additional triple area funnel.

TBRG Number	Resolution (mm/tip)	Enlarged uncertainty (mm/tip) [a]
1	0.21	0.02
2	0.15	0.06
3	0.17	0.04
4	0.15	0.06
5	0.16	0.05
6	0.15	0.06

[a] Enlarged uncertainty of resolution corresponding to 70% correctness rates.

As shown in Table 5-18, all the six tested low-cost TBRG with additional tripled area funnel have a resolution around 0.17 mm/tip.

5.3.3.4 Calibration

The following sub-sections detail the results obtained based on the calibration protocol described in section 5.2.4.

5.3.3.4.1 TBRG No.1

The raw data of low-cost TBRG No.1 calibration is shown in Table 5-19.

Table 5-19. Raw data of low-cost TBRG No.1 calibration.

Pump speed (mL/min)	Duration time (s)	Number of tips	Water displacement (g)
7	1127.495	99	154
7	1962.941	172	268.74
7	1165.449	103	159.66
15	517.383	95	151.63
15	546.021	99	159.8
15	586.296	106	171.64
30	290.409	97	171.28
30	356.533	119	210.45
30	327.316	109	193.23
45	397.681	191	356.11
45	253.253	121	226.83
45	281.714	133	252.34
60	180.35	101	210.98
60	174.246	101	209.02
60	175.326	100	210.16
75	145.102	101	220.02
75	176.3	124	267.44
75	146.151	102	221.55

Assuming that the low-cost TBRG No.1 with additional enlarged funnel has a resolution 0.1 mm/tip, and according to Equation 5-1 to Equation 5-3, the calibration intensity I_t, measured intensity I_m and bucket depth r_t (see calibration protocol in section 5.2.4) are given in Table 5-20.

Table 5-20. Low-cost TBRG No.1 calibration data. (Grayed values is used to calculate enlarged uncertainty of resolution when real rainfall intensity is less than 45 mm/h)

Calibration intensity (mm/h)	Measured intensity (mm/h)	Bucket depth (mm/tip)
31.94203964	31.60989627	0.101050758
32.01707215	31.54450388	0.1014981
32.03755756	31.81606402	0.100696169
68.53770033	66.1019013	0.103684915
68.44220252	65.2722148	0.104856565
68.46334634	65.08657743	0.105188119
137.9282198	120.2442073	0.114706748
138.0402524	120.1571804	0.114883066
138.0587277	119.8841487	0.115160119
209.4140786	172.9024017	0.121116929
209.4606477	172.0019111	0.121778093
209.4759731	169.9596044	0.123250448
273.578327	201.6079845	0.135698161
280.5314615	208.6705003	0.134437528
280.324001	205.3317819	0.136522461
354.6053714	250.582349	0.14151251
354.7566942	253.2047646	0.140106642
354.5083845	251.246998	0.14109955

Regressing calibration intensity and measured intensity by Equation 5-4, results are given in Figure 5-37 and Figure 5-22.

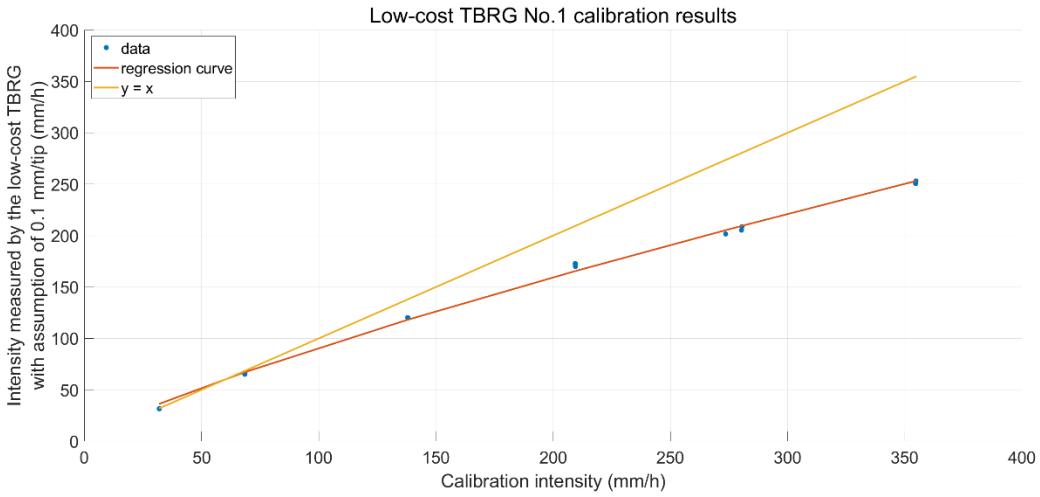

Figure 5-37. Low-cost TBRG No.1 calibration curve.

Table 5-21. Regression results low-cost TBRG No.1 calibration.

Parameter	**result**
b_1	2.2209
b_2	0.8066
$u(b_1)$	0.1692
$u(b_2)$	0.0137
IC95(b_1)	[1.8893, 2.5525]
IC95(b_2)	[0.7798, 0.8334]
cov(b_1, b_2)	$\begin{bmatrix} 0.0286 & -0.0023 \\ -0.0023 & 0.0002 \end{bmatrix}$
$MatCor$	$\begin{bmatrix} 1.0000 & -0.9972 \\ -0.9972 & 1.0000 \end{bmatrix}$

One gets, for the low-cost TBRG No.1 over a true rainfall intensity range of [0, 360] mm/h:

$$I_t = 2.2{I_m}^{0.81} \qquad \text{Equation 5-10}$$

As shown in Figure 5-37, the systematic underestimation of intensity due the bucket overfilling is clearly visible. But this phenomenon is not obvious when the true rainfall intensity is less than 45 mm/h. Below this rainfall intensity, 0.1 mm/tip is a reasonable resolution with an enlarged uncertainty of 0.0008 mm/tip. This "average" enlarged uncertainty of the three values with a grey background in Table 5-20 are calculated by means of the type A method for uncertainty assessment described in Bertrand-Krajewski *et al.*, 2021.

5.3.3.4.2 TBRG No.1 to No.6

The method used in 5.3.3.4.1 is also used to process the calibration data of low-cost TBRG No.2 to No.6 with additional tripled area funnel. Raw data are given in Appendix. Main results are summarized in Table 5-22.

Table 5-22. TBRG No.1 to No.6 calibration results with additional tripled area funnel when calibration rainfall intensity is less than 45 mm/h.

TBRG Number	Resolution (mm/tip)	Enlarged uncertainty (mm/tip) [a]
1	0.10	0.0008
2	0.10	0.0021
3	0.12	0.0086
4	0.10	0.0019
5	0.10	0.0012
6	0.10	0.0036

5.3.3.5 Discussion

Table 5-23 is a summary of Table 5-18 and Table 5-22. It shows the *in situ* and in calibration resolutions of low-cost TBRG No.1 to No.6 when true rainfall intensity is less than 45 mm/h.

Table 5-23. low-cost TBRG No.1 to No.6 resolutions. (All quantities have a unit mm/tip)

TBRG Number	*In situ* resolution	Enlarged uncertainty [a]	In calibration resolution	Enlarged uncertainty [b]
1	0.21	0.02	0.10	0.0008
2	0.15	0.06	0.10	0.0021
3	0.17	0.04	0.12	0.0086
4	0.15	0.06	0.10	0.0019
5	0.16	0.05	0.10	0.0012
6	0.15	0.06	0.10	0.0036

[a] Enlarged uncertainty of *in situ* resolution corresponding to 70% correctness rate.
[b] Enlarge uncertainty of the resolution in calibration.

As shown in Table 5-23, the *in situ* comparison with the nearby reference TBRG indicates that the low-cost TBRG should have a resolution around 0.17 mm/tip. However, the laboratory calibration results prove the low-cost TBRG have a resolution of 0.10 mm/tip. The performance of the reference TBRG, the calibration and the data processing methods have been rechecked several times to explain these diverging results. One speculates that this difference could be due to the fact that the low-cost TBRG WH-SP-RG has a shallow non-conical shape funnel as shown in Figure 5-38. *In situ* and during light rainfall events, the rainwater cannot flow smoothly through this shape funnel as in the reference TBRG. In calibration, the water is always dropped directly just above in the hole, which makes

this problem undetectable. To check this assumption, the phenomenon has been reproduced qualitatively in the laboratory as shown in Figure 5-38. One observes that (i) the slopes of the initial rectangular funnel are not sufficient to ensure all raindrops can slip toward the hole above the bucket, and (ii) the low-density polyethylene surface of the funnel is not as slippery as expected. Consequently, this water detention leads to a deficit of and/or to a delayed capture of rain drops, which itself may lead to an increase of the estimated resolution of the rain gauge as more rain is needed to generate tips.

Figure 5-38. Water drops cannot flow easily on WH-SP-RG. (a) TBRG No.1 with initial funnel, (b) TBRG No.4 with the first version of the additional enlarged funnel.

5.3.3.6 Additional experiment

To try to solve the problem illustrated in Figure 5-38, a new additional enlarged funnel has been designed as shown in Figure 5-39 and was tested *in situ* from 2023-03-23 to 2023-03-28 as shown in Figure 5-40.

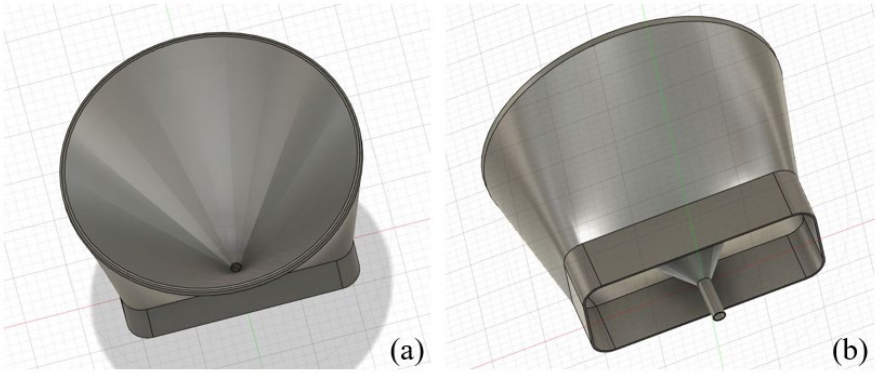

Figure 5-39. Screenshots of the new additional enlarged funnel design – The collecting area is the same as with the previous design (15482 mm^2): (a) Top view, (b) Bottom view.

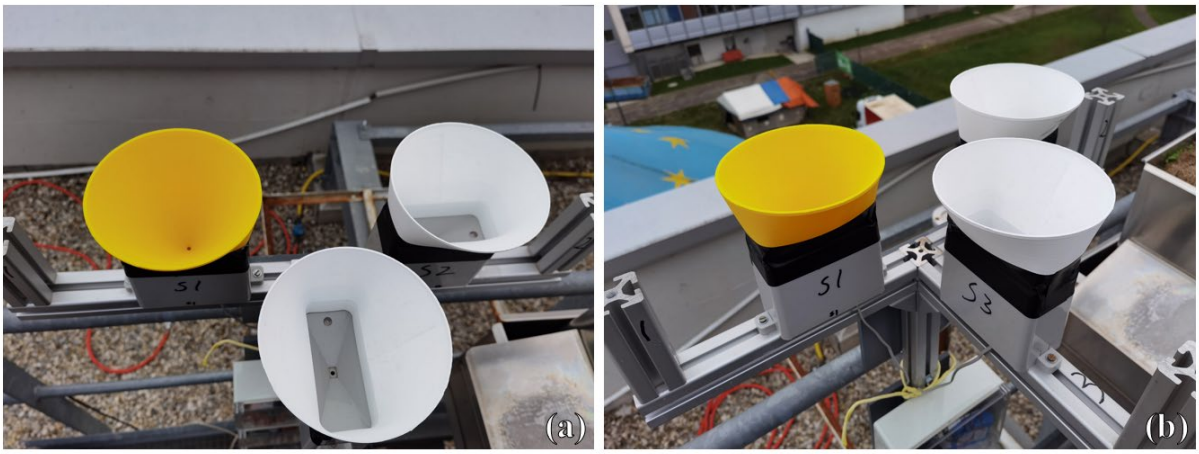

Figure 5-40. New test setups: new additional enlarged funnel in conical shape in yellow color installed on low-cost TBRG No.4 and old additional enlarged funnel in white color installed on low-cost TBRG No.5 and No.6. (a) Top view, (b) Side view.

During the 5-day test, unfortunately, the low-cost rainfall monitoring station No.2 with the low-cost TBRG No.5 could not give continuous data because the LiPo battery was not in place. Consequently, only results of both the low-cost TBRG No.4 with new additional enlarged funnel and the low-cost TBRG No.6 with old additional enlarged funnel comparing to reference TBRG are shown in Figure 5-41. A Teflon layer is sprayed to lubricate all funnels.

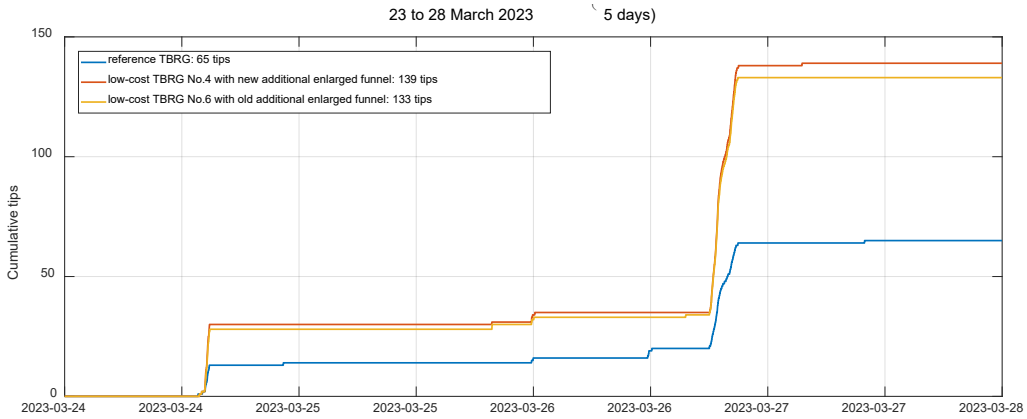

Figure 5-41. Low-cost and reference TBRG cumulative tips from 23 to 28 March 2023. TBRG No. 4 and 6 have funnels lubricated with Teflon spray.

From Figure 5-41, it is obvious that with the Teflon lubrication, the low-cost TBRG has a resolution in mm/tip approximately halved compared with the reference TBRG, as the number of tips over the test period is doubled for the same amount of rain. Using (i) a low-cost TBRG resolution of 0.10 mm/tip based on the calibration results (Table 5-22), and (ii) a reference TBRG resolution of 0.233 mm/tip to redraw Figure 5-41, results are shown in Figure 5-42.

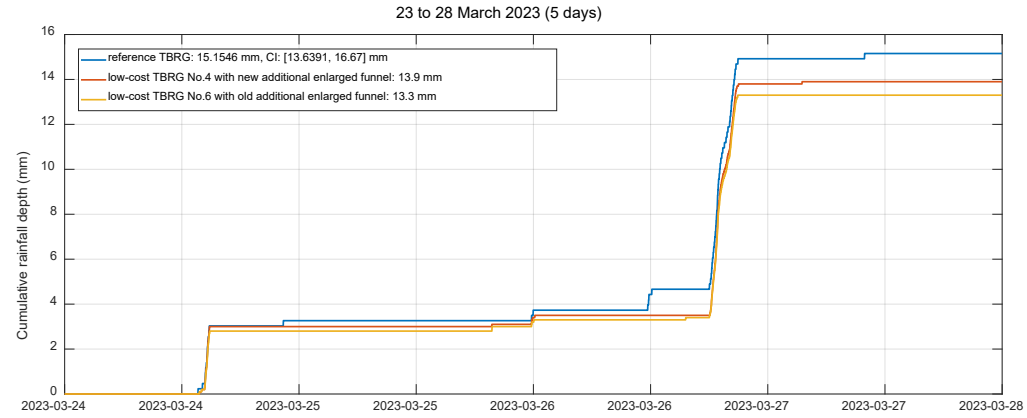

Figure 5-42. Low-cost and reference TBRG cumulative rainfall depth from 23 to 28 March 2023, with enlarged funnels and Teflon lubrication.

As shown in Figure 5-42, cumulative rainfall depth of the low-cost TBRG No.4 with the new additional enlarged funnel and a resolution of 0.1 mm/tip lies in the coverage interval of the reference TBRG. This proves a conical shaped additional enlarged funnel sprayed with Teflon is effective to retrofit/improve the low-cost TBRG WH-SP-RG. In addition, as indicated in the results of low-cost TBRG No.6 with old design additional enlarged funnel, funnel surface lubrication could fix the drawback of the initial funnel shape poor quality geometry and slipperiness.

5.3.4 Low-cost monitoring station assessment

The previous sections focus on the low-cost rain gauge sensor performance assessment. But the sensor performance is only one of the aspects of a low-cost monitoring system. It is also important to design a robust low-cost monitoring station that is self-powered by solar panel, able to save data locally continuously, and able to send data online continuously to reduce the consumption of human resource. This section discusses the performance of the low-cost rainfall monitoring stations, exampled with station No.2 data from 9 November to 8 December 2022. The two other stations have similar performance and are not presented here.

5.3.4.1 The ability of self-powering by solar panel

A low-cost monitoring station design that does not rely on outer power supply could be use in remote or off grid sites. We installed a large solar panel on the rainfall monitoring station as shown in Figure 5-17. During the system test operation, it could work with solar panel without power failure during summer and fall. But in winter, without outer power supply, it is difficult to recharge the battery only with the solar panel as illustrated in Figure 5-43.

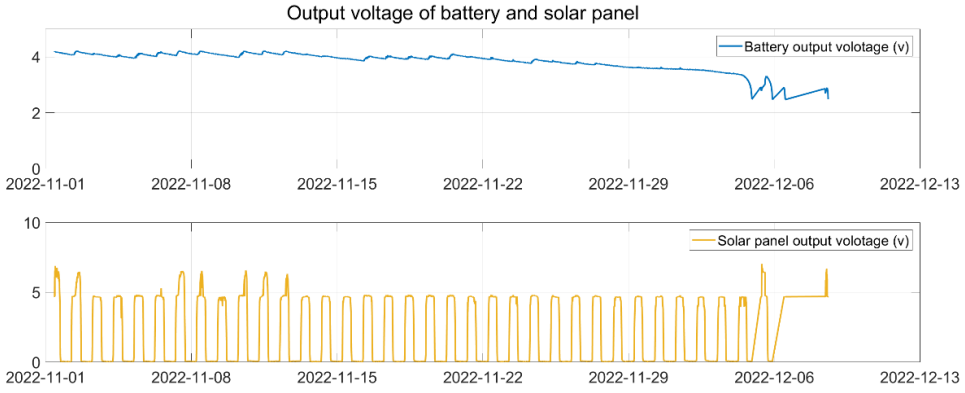

Figure 5-43. Battery and solar panel monitoring data in SD card of station No. 2.

Before 25 November 2022, the battery can be powered by the solar panel (the voltage is always in the range 3.7 to 4.3 V), and then, due to continuous rainy days, the battery drains continuously until the entire system stops operating. After 6 December 2022, the system restarts because the battery is partly recharged by the solar panel, but the system cannot run continuously. After 17 December 2022, an outer power supply is connected to the rainfall monitoring stations to ensure it works without power failure. A self-powering rainfall monitoring station will require to consider daily sun duration and intensity during the year, but also daily rainfall depth because more energy will be drawn when the system is recording tips. The design is thus strongly dependent on the location of the monitoring site.

5.3.4.2 The ability of continuously recording data locally

It is important that the monitoring station records the data with a defined time step, without error, data loss, duplicate, time drift, etc. To evaluate this performance, we check the continuity and regularity of timestamps recorded in the SD card. Some results are shown in Figure 5-44 from 2022-11-01 to 2022-12-13. The frequency is set to one data record per minute. Figure 5-44 shows deviations from this target value.

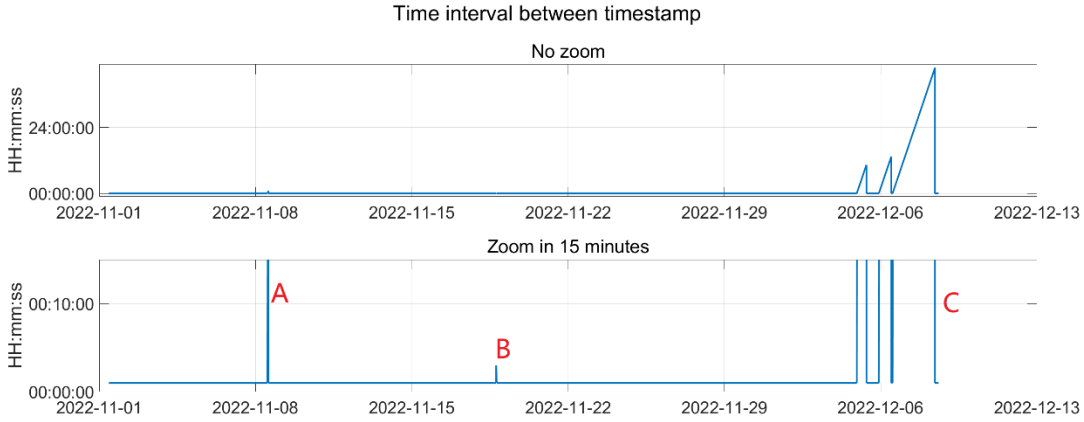

Figure 5-44. Time intervals between the timestamps of DATA.CSV file in SD card of station No.2 from 2022-11-01 to 2022-12-13. The first chart (above) provides the full range of intervals (y-axis) and the second chart is zoom on the interval range 0 to 15 minutes. A, B and C identify specific time intervals.

The interruption on 8 November 2022 (mark A in Figure 5-44, deviation is 57 minutes) is due to a man-made maintenance. The interruption on 18 November 2022 (mark B in Figure 5-44, deviation is 3 minutes) is due to unknown reason but the watch dog timer we implemented in the Arduino code operated properly at that time to

reset the monitoring system. A watchdog timer monitors program execution and triggers a reboot of the micro-controller if the program is out of control or stops (we have set a three-minute watchdog timer). The interruptions at the end of the period (mark C on Figure 5-44, deviations are up to 45 hours) are due to insufficient battery voltage and insufficient recharge by the solar panel. In summary, the designed rainfall monitoring station can record data correctly and continuously when there is no power failure, and the watch dog timer can handle unusual situation to present important data loss.

5.3.4.3 The ability of continuously sending data online

It is convenient to get online data and not need to go on site too frequently to ensure that the system is running smoothly. Data transmission reliability is therefore of key importance. But it seems the online data quantity is doubtful. Figure 5-45 shows the online data timestamp continuity when the SD card data timestamp is continuous from 19 November to 4 December 2022 with not fully charged battery. The frequency is set to send one data record every 5 minutes. It should be noted that the tested low-cost rainfall monitoring stations are approximately 200 meters away from the nearest LoRa network gateway to transfer data to our office and almost inline of sight.

Several deviations from the expected 5-minute period are visible in Figure 5-45, with several values reaching 10 minutes (one packet loss) and one case with 15 minutes (two consecutive packets lost). Data loss happened during wet weather leads to not reported tips and thus rainfall underestimation.

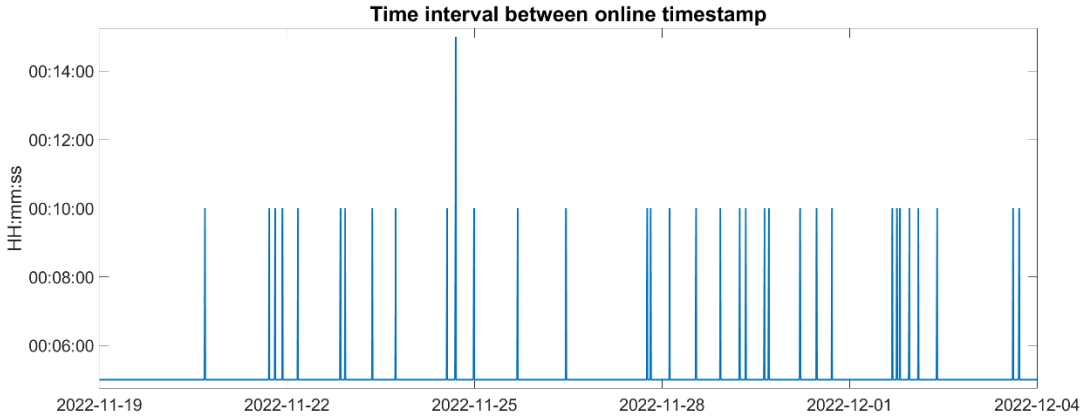

Figure 5-45. Online data transfer continuity of station No.2 from 19 November to 4 December 2022.

Online data transfer lost three tips (two tips during the rainfall event on 2022-11-22 and one tip during the rainfall event on 2022-11-29) as shown by the red arrows in Figure 5-46.

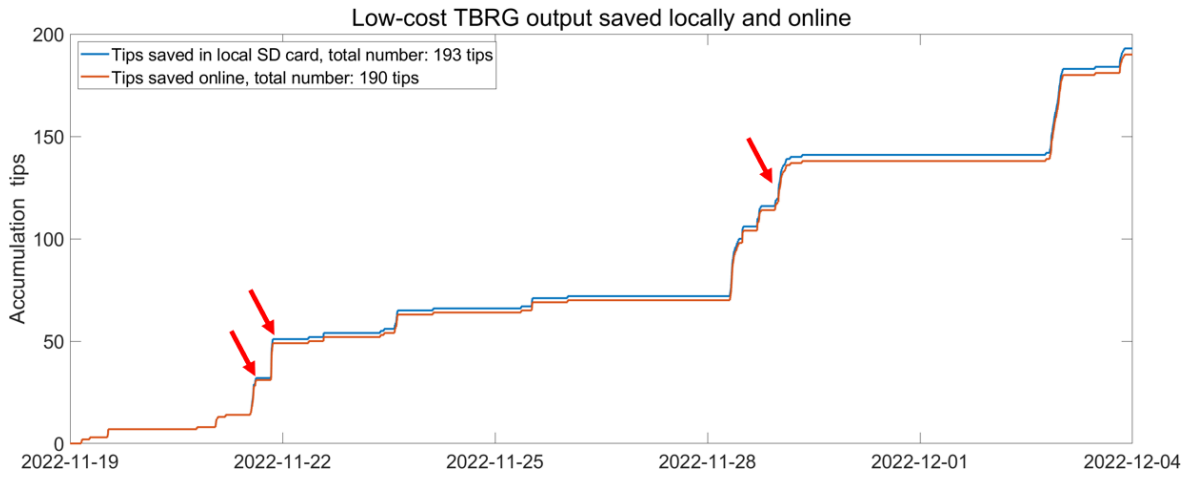

Figure 5-46. Accumulation tips of station No.2 SD card and online data from 19 November to 4 December 2022.

In summary, although the loss of online data is not critical in our test period, one cannot expect this phenomenon would not change in the future as it is highly dependent on wet weather period. This is an uncertainty that cannot be assessed or compensated. Online data transmission is very useful to check if the station is working satisfactorily, but a local data storage on SD card remains more reliable and must be implemented systematically. For information, all the rain gauge data comparisons in this chapter are based on SD card data.

5.4 CONCLUSION

In this chapter, a low-cost rainfall monitoring station was designed, built, installed, and tested. This station has (i) two power supply methods: output power and/or solar power, (ii) two kinds of low-cost rain gauges: optical rain gauge RG-15 and tipping bucket rain gauge WH-SP-RG, and (iii) two data recording methods: *in situ* SD card and/or online data transmission through LoRa network to The Things Network platform and then custom Node-RED server before finally transfer to a Google sheet. Most data are collected with a one-minute time step including timestamp, output of rain gauges, output of solar panel and battery and air temperature. After testing, the designed system could run independently and autonomously.

The Arduino board and code were developed progressively, from basic versions with elementary functionalities to more elaborated versions accounting for and solving all the problems discovered during the test periods, including improved RTC modules, watch dog timer, debouncing, online data format. In total, five versions of station hardware were developed, and 16 versions of the codes were written. The last hardware setup is shown in Figure 5-4 and the last versions of the codes are available in GitHub (Zhu, 2023a to 2023b).

A low-cost TBRG calibration data logger was designed and built with a screen to display the number of tips.

As the low-cost rainfall monitoring station trial operation was longer than expected (and rain was scarcer than expected), only four-month trusted data in the winter season are available to assess the performance of the low-cost optical rain gauge RG-15 and the low-cost tipping bucket rain gauge WH-SP-RG. Three RG-15 and six WH-SP-RG were tested during this period. Based on our tests and experience, the main findings and recommendations about these two rain gauges and the monitoring station are summarized in Table 5-24. In the future, more data will be generated by the three rainfall monitoring stations.

Table 5-24. Summary about using the tested low-cost rain gauge sensors in urban hydrology.

Sensor/system	Application in urban hydrology?	Comments / conditions of use
Low-cost optical rain gauge RG-15	reserved	The sensor is not out-of-the-box devices, a cable needs to be added by users which introduced potential risk of damage. The sensor must be placed in a location where there are no disturbances due to shade created by other devices especially anemometer and anemoscope. Frequent soft cleaning of the spherical surface is necessary to ensure there are no interferences. **Several months of use have shown a stable functioning and no drift.** **Experiment shows important sensor to sensor variance clearly.** **A systematic comparison with a reference sensor is necessary** to establish a correlation function to estimate possible bias and under/over estimation. With this correlation function, it is then possible to convert the RG-15 raw data into corrected rainfall depth per time step. One major difficulty is that this comparison must be done on site, and no classification method can be applied.
Low-cost tipping bucket rain gauge WH-SP-RG	reserved or possible depending on adaptations	The low-cost TBRG WH-SP-RG is disturbed by high wind speed and must therefore be rigidly attached to avoid vibrations which may lead to fake tips. **The reproducibility of this sensor is acceptable according to calibration.** **Several months of use have shown a stable functioning and no drift.** The sensor has a stable bucket part with approximately 1.5 mL volume, but it has a poorly designed funnel section compared to reference tipping bucket rain gauge. The shallow non-conical plastic funnel makes its original resolution at approximately 0.6 mm/tip, which is insufficient for research applications. **Users should not try this sensor without modify its funnel area firstly,** in particular enlarging the funnel (e.g., with a 3D printed funnel) to improve the resolution up to 0.1 mm/tip. **Users must also spray Teflon on the adapted funnel to ensure raindrops can slip to the bucket.** **A systematic laboratory calibration is required** (like for reference rain gauge) to check the functioning and determine the true resolution (mm/tip).
Low-cost DIY monitoring stations	reserved or possible depending on objective and knowledge	Low-cost DIY monitoring station is an opportunity to conduct stormwater monitoring activity with limited budget. This opportunity provides **unprecedented flexibility to researchers to develop their own instrument** by themselves. Even with the help of a growing community, time dedicated to components selection, hardware, software development work is a large part of the cost which needs to be estimated. **Researchers with clear monitoring objective and certain knowledge of hardware, software and metrology are more suitable to this kind of work.**

After having tested meteorological sensors in Chapter 4 and Chapter 5, the next chapter will describe our work about related to low-cost water level monitoring and more focus on low-cost monitoring station assessment.

CHAPTER 6: LOW-COST WATER LEVEL MONITORING SYSTEM DESIGN AND EVALUATION

6.1 INTRODUCTION

The main objective of this chapter is to test the deployment of a low-cost water level monitoring system, from the sensor selection to the field installation. The work in this chapter has been done jointly with one of my supervisors Frédéric Cherqui. The main contributions of the author of this thesis are experiment and prototype documentation, data collection, data analysis, interpretation, discussion, and writing. Based on the literature review, a water level sensor has been extensively tested in laboratory. After having successfully passed the lab testing to confirm that the low-cost sensor's performance was in accordance with our specifications, field testing was dedicated to assessing the long-term (more than one year) behavior of the sensor and the whole monitoring system. Field measurement performance assessment (including uncertainty analysis) was not in the scope of this study, as the primary objective of the field experiment was to confirm the possibility to use the sensor for more than one year. This chapter is organized as follows: the first section presents the material and methods including system design objectives, choice of the water level sensor, calibration methods, and full-scale deployment; the second section is dedicated to results and discussion including low-cost sensor calibration results and low-cost monitoring station *in situ* evaluation.

6.2 MATERIAL AND METHODS

6.2.1 Objectives

The planned water level monitoring system is designed to monitor the level of open water in a low-cost and convenient way. That is to say, in addition to reduce hardware cost, the objective is to save human resource by decreasing maintenance needs because "overall monitoring is costly in operational time" (Schellart *et al.*, 2021). To achieve this objective and to avoid the need for batteries change, the system should have a reduced electrical

consumption because there is no power supply on numerous monitoring sites. Electrical consumption could be compensated by a solar panel and thus lead to energy self-sufficiency. Site visit is only necessary when an alert (abnormal activity) has been triggered, such as abnormal water level, absence of data for more than one hour, or a too low battery voltage. The system should also be as small and inconspicuous as possible and installed in a location difficult to access for the public, to avoid incivilities. In summary, the designed system should: (i) have a total cost below 100 euros for the prototype components, (ii) be able to operate *in situ* autonomously for a long time without maintenance or with limited maintenance, and (iii) provide access to measurement data in real-time.

6.2.2 Selection of the low-cost water level sensor

6.2.2.1 Sensor choice

There are many applications for water level sensors such as process control for manufacturing, environmental monitoring, water supply, etc. which has given rise to different types of level sensor. Commonly available sensors employ fundamentally different methods to measure water level and offer acceptable measurement accuracy. Morris & Langari (2016) propose a list of these: float systems, pressure-measuring devices, capacitive devices, ultrasonic level gauge, radar (microwave) sensors, nucleonic (or radiometric) sensors, vibrating level sensors and laser methods. Image-analysis based sensors can also be added to the list (e.g., Jafari et al. (2021)). There are thus many types of water level sensor on the market that can achieve this and consequently deciding which sensor is most appropriate can be challenging.

The current study is limited to water level sensors appropriate for measuring open waters such as wetlands, lakes, basins, swales, or streams rather than tanks and closed vessels. Based on this objective, on cost-consideration, on previous experience (Cherqui *et al.*, 2020a) and on the most-used sensor types in urban hydrology, we have narrowed down the list to three types of sensors: pressure transducer, capacitive device, and ultrasonic sensor. Sensors based on image analysis are discarded because of the higher electrical consumption (either for on-board image analysis or for communication to transmit images to a server). Capacitance sensor is a weighted, sensing cable that bridges the air/water interface and measures the change of capacitance affected by surrounding water (Loizou and Koutroulis, 2016). Ultrasonic sensor is mounted above water and measures the distance down to the water surface (Cherqui *et al.*, 2020a). Pressure transducer is fixed underwater and measures the hydrostatic pressure of water, from which water depth can be calculated (Cherqui *et al.*, 2020a).

To finalize the selection of the type of sensor, several aspects were considered: (i) the fouling of the sensor leading to erroneous measurements, (ii) the measurement constraints linked to the presence of obstacles (vegetation, waste or other) on the water surface, (iii) the sensitivity to the external environment (leading to disturbance of the measurement) and (iv) the need for maintenance. These four aspects are detailed below and summarized in Table 6-1.

Concerning the fouling of the sensor, we consider the algal growth or the deposition of sediments when the sensor is under water. This applies to capacitive sensors and pressure transducers; however, only capacitive sensors will have their measurements affected by fouling. In the case of ultrasonic sensors, fouling may be due to the presence of dust in the air in certain situations, and the measurements could also be affected.

The measurement constraints due to the presence of obstacles only concern the ultrasonic sensor which is mounted on the surface above the water. The presence of vegetation on the surface or floating objects (rubbish or other) prevents the measurement of the actual distance between the sensor and the water. Similarly, the sensor may also be obstructed by vegetation or the presence of insects or spider nests.

Regarding environmental sensitivity, capacitive sensors are affected by the presence of high voltage lines which affect the nearby electric field. The ultrasonic sensor is also sensitive to its immediate environment since the speed of sound depends on the air temperature, and to a lesser extent on the relative humidity of the air (Cherqui *et al.*, 2020a). The pressure transducer may be affected by the temperature of the water and may requires compensation depending on water temperature range. In addition, pressure transducers need to be compensated for atmospheric pressure. There are at least three methods for this: (i) use a differential pressure transducer with one side vented to the atmosphere using a vent tube (most reliable method), (ii) install a second pressure sensor above water, (iii) where available, obtain data from existing local weather stations such as online governmental meteorology services (less reliable method).

Regarding the need for maintenance, we consider here the need to regularly clean the sensor (fouling for the capacitive sensor) or remove obstacles in front of the sensor (ultrasonic sensor). Maintenance related to data downloading is not considered since the system must send its data in real time. Maintenance also considers the ease of access to the system to make repairs or change parts: underwater systems are less accessible. Summary is given in Table 6-1.

Table 6-1. Water level sensors related to environment and maintenance needs.

	Capacitance	Ultrasonic	Pressure
Fouling impacts	Prone to fouling, lead to output error	Less prone to fouling, depend on air quality	Prone to fouling but it won't affect the measurement
Objects at surface impact	No impact	High impact	No impact
Sensitivity to environment	Sensitive to environment (electric field)	Sensitive to environment (air temperature and air relative humidity)	Need to compensate for water temperature and atmospheric pressure
Maintenance needs	High maintenance needs (frequent cleaning)	Average maintenance needs	Limited maintenance needs

Based on the above analysis, the pressure sensor was selected. The capacitive sensor was discarded because it is affected by fouling and the potential presence of high voltage lines near the measurement sites. The ultrasonic sensor was discarded because the chosen sites does not allow for installation above water.

6.2.2.2 Low-cost sensor YB-2J-F

Among different pressure transducers, ALS YB-2J-F (also named ALS-MPM-2F or TL231 or Gravity KIT0139[2]) is chosen because (i) it is commonly used and mass produced, (ii) it has a well-produced stainless steel housing ready to use, (iii) it has a differential pressure transducer and vent tube incorporated in the electrical cable sheath, (iv) its output (4 ~ 20 mA current signal proportioned to water level according to manufacturer) is easy to process with open-source hardware, (v) it is one of the cheapest ready-to-use pressure sensors (it costs around 50 euros). The ALS YB-2J-F is presented in Figure 6-1.

[2] https://www.gotronic.fr/art-capteur-de-pression-etanche-gravity-kit0139-32275.htm

Figure 6-1. Left: Appearance of low-cost pressure liquid sensor YB-2J-F. Below from left to right: Probe, sensor diaphragm protector. Source: Pro Powers Tools Store in Aliexpress.com (accessed: 31 March 2023). Middle: Screenshot of datasheet in Chinese. Right: Engraved parameters on sensor casing.

The characteristics of YB-2J-F given by manufacturer are summarized in Table 6-2.

Table 6-2. YB-2J-F specifications, translated from Figure 6-1.

Sensor name	**YB-2J-F**
Type	Pressure liquid probe
Size	10.5 × 2.5 cm
Weight	~ 580 g (including 5 m length cable)
Measurement range	-0.1 ~ 0 to 60 MPa [a] or 0 to 5 m [b]
Power supply	12 to 36 V DC typical value 24 V
Output	4 to 20 mA or 1 to 5 V DC [a], 4 to 20 mA [b]
Enlarged uncertainty	0.2 %, 0.5% [a], 0.03%FS/°C [c]
Resolution	NA
Response time	NA
Sensitivity to environment	Media temperature: -20 to 75 °C, Environment temperature: -30 to 80 °C Measurement media: Gases and liquids that are not corrosive to stainless steel Overload capacity: < 1.5 times measure range Temperature drift: 0.03%FS/°C
Maintenance needs	NA
Longevity	NA

[a] Written in datasheet.
[b] Engraved on the sensor casing.
[c] "Accuracy" in datasheet.

The enlarged uncertainty of this low-cost sensor is not clearly defined. Moreover, as this sensor can only output current or voltage signal, its performance is also dependent on the data logger and calibration function used. No information is provided regarding electrical consumption.

6.2.3 Reference sensors used for lab and field testing

Two reference sensors have been used. An OTT PLS water level sensor (OTT HydroMet, 2023b) was used for the lab testing. This reference sensor is part of a testing bench developed by Cherqui *et al.* (2020). For field tests, another sensor was available to serve as reference: a Paratronic CNR 5. A lab experiment was dedicated to the measurement performance of the low-cost sensor. After having successfully passed the lab testing (that is to say that the low-cost sensor's performance was in accordance with our specifications), field testing was dedicated to assessing the long-term (several months) behavior of the sensor and of the whole monitoring system. It was thus not focusing on field measurement performance itself. The characteristics of both OTT PLS and Paratronic CNR 5 sensors given by manufacturers are summarized in Table 6-3.

Table 6-3. Characteristics of OTT PLS and Paratronic CNR 5.

Sensor name	**OTT PLS**	**Paratronic CNR 5**
Type	Pressure liquid probe	Pressure liquid probe
Size	19.5 × 2.2 cm	17 × 2.1 cm
Weight	~ 300 g	180g + 50g per meter of standard cable
Measurement range	0 to 4 m	0 to 30 m
Power supply	9.6 to 28 V DC, typical value 12/24 V DC	6 to 38 V DC
Output	SDI-12 communication	4 to 20 mA
Enlarged uncertainty	±0.05 % FS [a]	< ±0.3 % FS [b]
Resolution	0.01 m	NA
Response time	NA	< 0.15 s
Sensitivity to environment	Operating temperature: – 25 °C to 70 °C, Protection type: P68	Temperature drift: (0°C to 40°C) ±0.02% FS/°C
Maintenance needs	NA	NA
Longevity	Long-term stability: (linearity and hysteresis): ≤ ±0.1 % / year FS	NA

[a] "Accuracy (linearity and hysteresis) SDI-12" in datasheet. FS: Full Scale.
[b] "Precision" in datasheet.

6.2.4 Laboratory test: measurement performance assessment

A testing bench has been developed to test various water level sensors (Cherqui *et al.*, 2020a), as shown in Figure 6-2. It consists of a 2-meter-high water column equipped with a reference OTT PLS pressure sensor and a pump

to automatically modify the water level; the measurements are verified with several manual readings during the experiment. The water level is decreased from 1.90 m to 0 m with steps of less than 0.03 m. For each step, the water level is measured with the reference sensor for 10 times and with the low-cost sensor for 1,000 times in alternation. Air temperature and relative humidity are monitored by a DHT22 low-cost sensor (see section 4.2.1.4.2), and the water temperature is monitored by both a DS18B20 sensor and by the reference OTT PLS sensor. Two webcams are installed to monitor the system remotely.

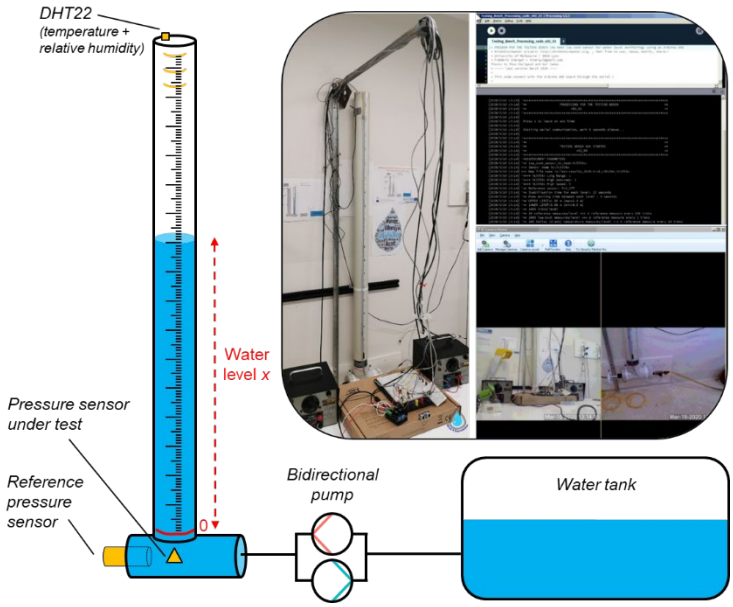

Figure 6-2. Water level sensor testing bench. The schematic drawing on the left shows the two-meter water column and the hydraulic equipment. The reference sensor OTT PLS and the low-cost sensor YB-2J-F on the bottom are represented in yellow. The pictures on the upper right corner show the water column, and screenshots of the interface and of the webcams used to monitor the system remotely (adapted from Cherqui *et al.*, 2020).

The OTT PLS sensor uses a SDI-12 connection to communicate with Arduino and is powered with an independent 12 V power supply. The low-cost sensor YB-2J-F is powered with a 12 V step-up voltage regulator U3V12F12 (Polotu, 2022) and its output is a 4-20 mA current signal. The 12 V step-up voltage regulator is also used for field measurements. To precisely measure the low-cost pressure sensor output, the 4-20 mA current is converted into a 1-5 V voltage using a 250 ohms high-precision resistor (RS, 2022), that is to say with a very tight tolerance

(±0.02%) and extremely low temperature coefficient of resistance (± 5 ppm/°C). The voltage is read out using an analog to digital converter DFR0553 (DFRobot, 2022), based on the ADS1115 chip (Texas Instruments, 2018), to convert the current signal to a voltage signal with a 16-bit resolution (which is better than the 10-bit resolution of the Arduino board). The circuits are shown in Figure 6-3 and the codes are shared in GitHub (Mind4stormwater, 2022). A calibration function is required to establish the relationship between the recorded voltage and the water level.

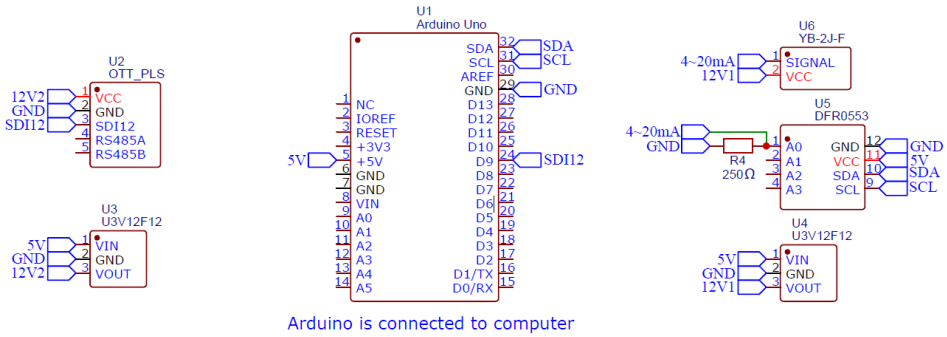

Figure 6-3. Circuit schematic for testing the low-cost water level sensor.

6.2.5 Full scale deployment

Aiming to design a real low-cost water level monitoring system, the development of the prototype and the field study were based on studying the following points:

- autonomy of the system from an energy point of view.

- easiness of implementation in the field in relation to encapsulation and longevity (sealing, protection of electronics).

- constraints related to available LPWAN (Low-Power Wide Area Network) providers: connection to the existing network, reliability of the communication, and consequence on the access to the data in real time.

- maintenance requirements and alerts in case of malfunction.

- implementation of a real-time data access platform and real-time water level monitoring possibilities.

6.2.5.1 System operation cycle

The system operation cycle, including (i) a measurement phase, (i) a sleep phase and (iii) a manually waking up, is shown in Figure 6-4 and reasons of this design are explained hereafter.

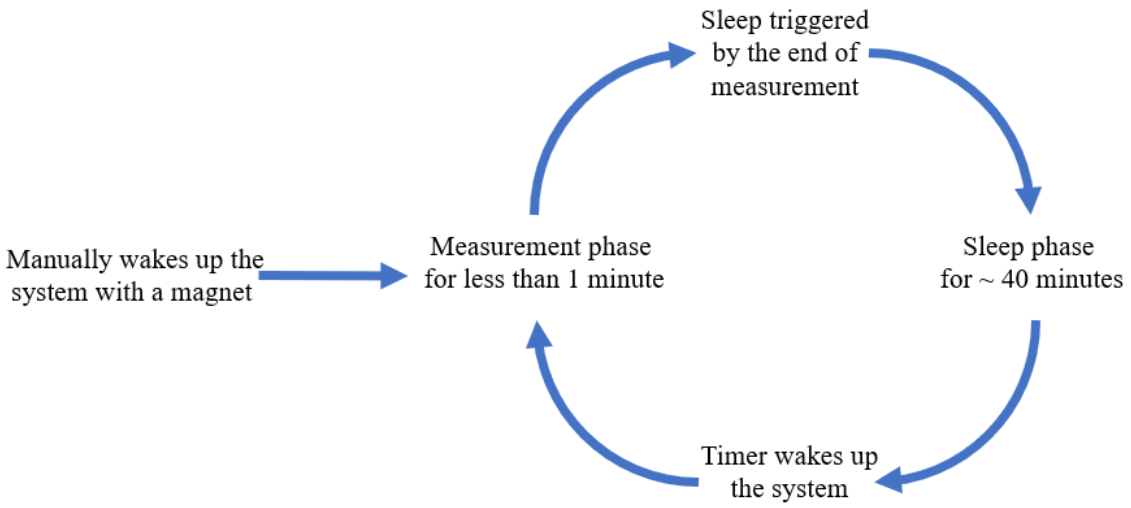

Figure 6-4. System operation cycle sketch.

As shown in Figure 6-4, during one cycle, the system will be on (measurement phase) for less than 1 minute and off for approximately 40 minutes (sleep phase). It should run on batteries and with a solar panel (0.5 W). It is thus critical to pay attention to power consumption. It is difficult to reduce the consumption during the measurement phase because it is mandatory to power the sensor and the micro-controller (including the communication chip). However, it is possible to drastically reduce the consumption during the sleep phase by powering off the entire system. During the sleep phase, the only component that needs to remain on is the timer used to restart the micro-controller. The TPL5110 module (SparkFun, 2022) is a nano-power consumption timer (approximately 35

nanoampere claimed by manufacturer) used (i) to turn on the whole system based on a set time interval, and then (ii) to turn off system after one measurement activity (when receiving a specific pulse from the micro-controller). By this way, there is almost no power consumption between measurements, that is to say more than 97% (40 min out of 41 min) of the time, and the monitoring system can run *in situ* for a long period with the solar panel.

It is also particularly important to be able to manually trigger a measurement on site. During the installation or maintenance, several measurements may be needed in a brief period of time (instead of one measurement per 40 minutes). A reed switch has therefore been installed: it allows to awake the system manually, with a magnet, to do a measurement and to send it online. The use of the reed switch reduces the leakage risk because the enclosure doesn't need to be drilled to add a physical button or open to push a button.

6.2.5.2 Design and prototyping

After iterative improvements during the development of the prototype, the final circuit was designed, as shown in Figure 6-5. One important objective of the development was to build a monitoring system as minimalist as possible and based on easy-to-buy components. To simplify at maximum the design, the system does not have any real-time clock component (to timestamp the measurement) and no SD card (to save locally the data). It relies entirely on the communication network for timestamping and online storage of measurements.

Each component presented in Figure 6-5 is dedicated to one or several specific functions.

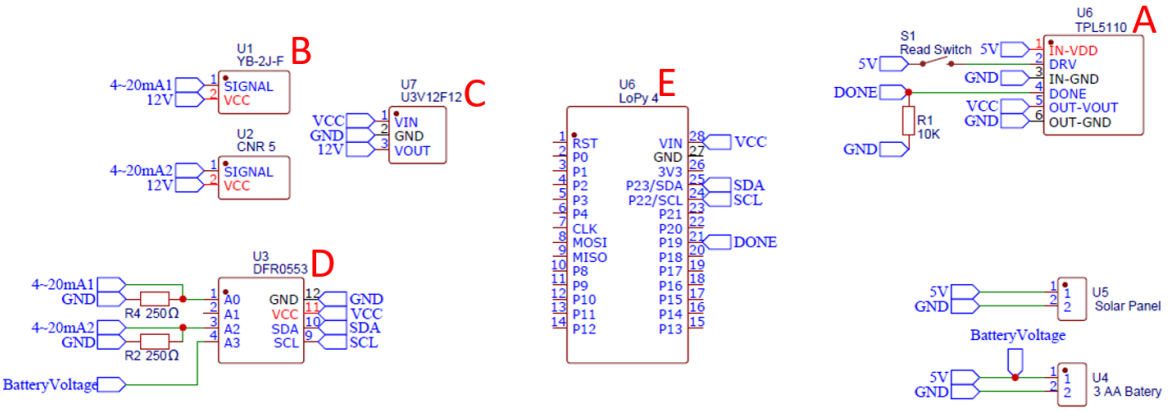

Figure 6-5. Hardware circuit design of the low-cost water level monitoring station.

In this design, the TPL5110 module (mark A) has been described in section 6.2.5.1. The low-cost sensor YB-2J-F and the reference sensor CNR 5 (mark B) are used in a same unit to make it easier to develop, install and compare. They are both connected to the same 12 V step-up voltage regulator U3V12F12 (mark C, also used for the laboratory test). Two high-precision resistors and an analog to digital converter DFR0553 (mark D) are dedicated to measure the current output of each sensor. Contrary to the laboratory setup, a LoPy 4 (mark E) (Pycom, 2022) module is used instead of an Arduino Uno. The LoPy 4 is a micro-controller with a communication chip that can work with both LoRaWAN and Sigfox Low-Power Wide Area Network (LPWAN). It enables to use the same device and switch from one network to another depending on the site coverage. Unfortunately, the Pycom company has been bankrupted in 2022 and recently bought by another group with, as of today, no clear vision on the continuity of the products. The actual prototype is shown in Figure 6-6.

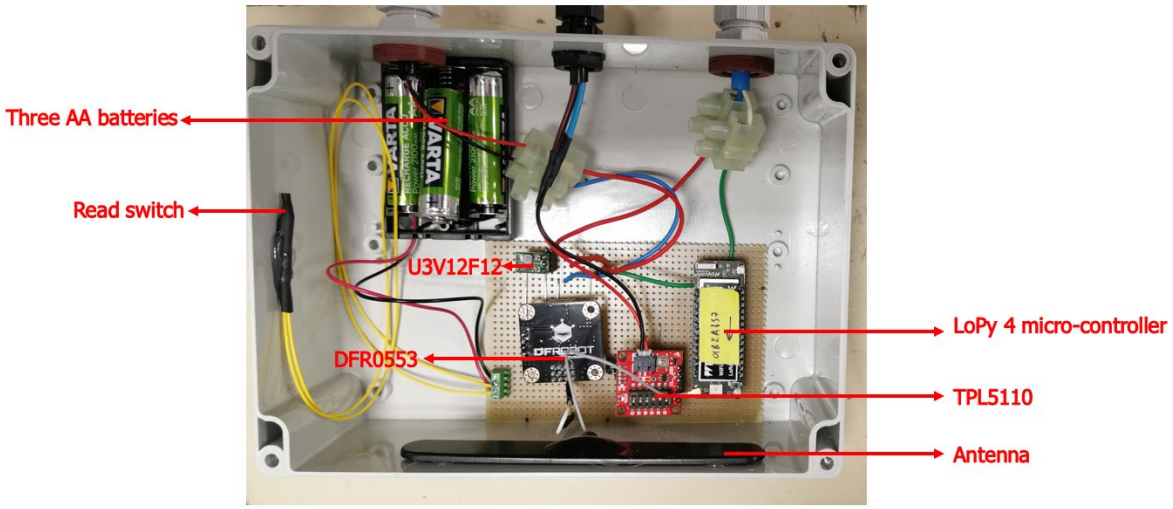

Figure 6-6. Picture of the prototype. Clockwise direction in the waterproof box (left): reed switch (with the yellow cables and glued to the enclosure), three AA batteries, LoPy 4 micro-controller and antenna (flat), TPL5110，DFR0553 and U3V12F12.

The communication of the designed system is based on the Sigfox network which cost less than 20 euros for a one-year subscription with a theorical maximum capacity of 140 messages per day, i.e., a maximum of one message every 10 minutes.

6.2.5.3 Remote monitoring and maintenance alerts

To reduce monitoring needs, it is important to have access in real-time to the battery level and to the signal strength. No regular maintenance of the system is planned (as the sensor is not affected by fouling) and alerts can be defined to be triggered when (i) the system stops sending new data, (ii) the battery level is too low meaning abnormal consumption or a problem with the solar panel, (iii) the water level exceeds a predefined threshold which may lead to the system being submerged, or (iv) when a specific number of measurements have been carried out and the sensor requires to be checked or re-calibrated. All these functions have been developed using the Google Sheet Apps Script, and later on redeveloped with the Node-RED editor. The Google Sheet user interface was used for convenient setup and maintenance as shown in Figure 6-7. A specific sheet is dedicated to on-site log with a smartphone (see Figure 6-16).

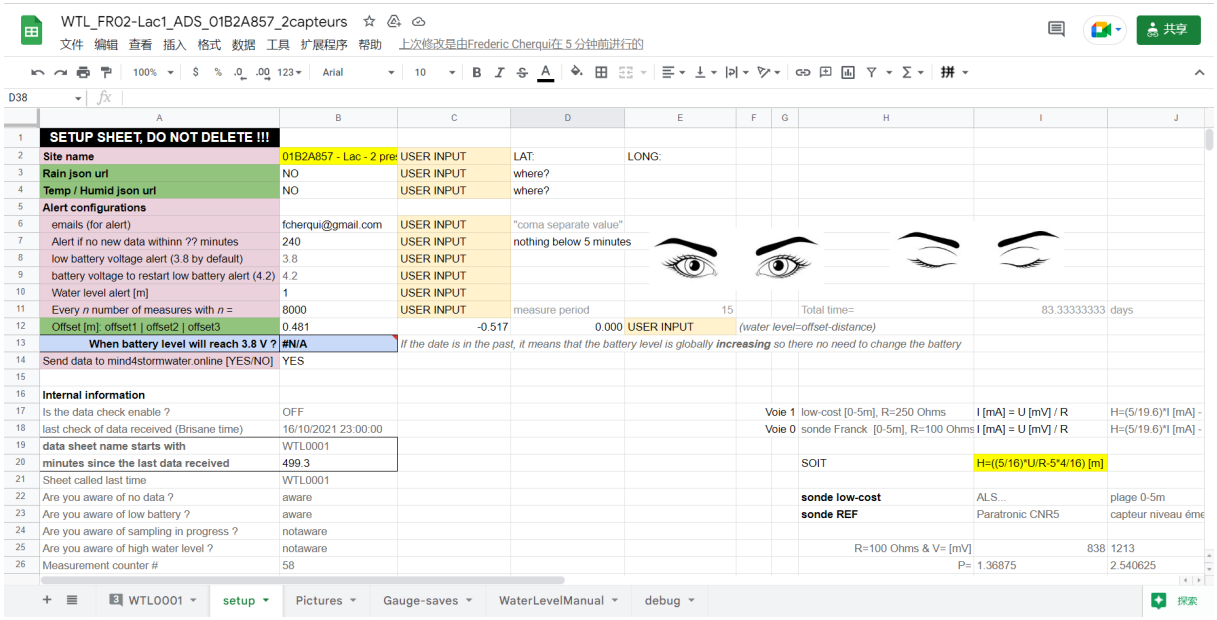

Figure 6-7. User interface created in Google Sheet.

As shown in Figure 6-7, the interface in Google Sheet is designed to provide the user with as much setting convenience and detailed information as possible. Open eyes and close eyes pictures on the right side correspond to starting or stopping the alert system. Alarm-related information setups are grouped in the pink area in the upper left corner (cells B6 to B11). From top to bottom, the user can set alerts for (i) sending email(s), (ii) maximum tolerated duration with no data time (240 minutes in the figure), (iii) low battery alarm voltage (3.8 V in the figure), (iv) low battery alarm reset voltage (4.2 V in the figure), (v) high water level alarm water level (1 m in the figure), (vi) maintenance alarm (every 8000 measurements in the figure), and (vii) whether to send data to the online platform (YES in the figure).

6.2.5.4 Access to the data in “near” real-time

During the deployment of the prototype, it was required to provide easy access to the raw data produced in order to regularly check the monitoring system. This was the initial reason for the development of a platform dedicated to data visualization. Each measurement is immediately pushed to the platform and shared in a website under development: http://mind4stormwater.online/opendataeau/see/ with many other monitoring stations data. Figure 6-8 shows the designed system location and data in real time.

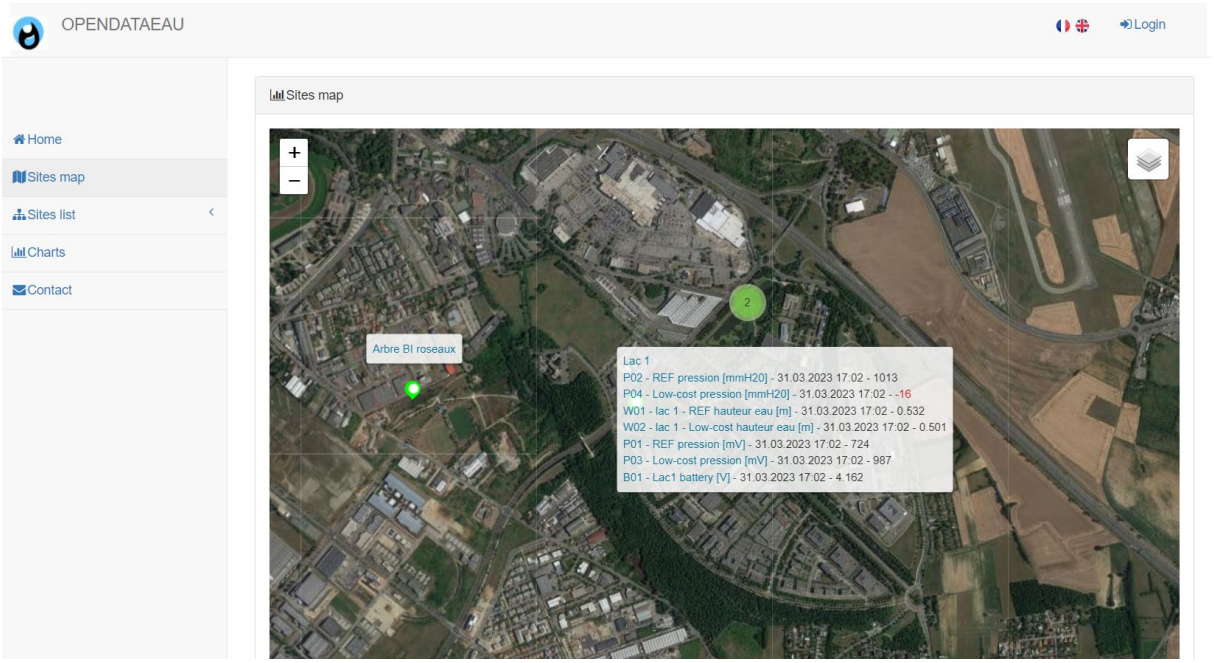

Figure 6-8. Screenshot of the map in the mind4stromwater website to show monitoring points. The system designed for this thesis is installed in “Lac 1” (in French *Lake 1*). A value out of predefined range appears in red and if the last data is older than 24 h, its date appears in red.

As shown in Figure 6-8, the platform can display the interface in French or in English. On the left, the online platform aims and terms of use are accessible in the “Home” tab. An interactive map with measurement points is available in the “Sites map” tab. All available measurements are available in the “Sites list” tab. In the “Charts” tab, data can be visualized for any specific range (see Figure 6-11 in the results section), and data can also be downloaded for further off-line analysis. The platform was first a deliverable of the Mind4Stormwater project: https://mind4stormwater.online/ (CORDIS, 2023). This open platform gathers and gives free access in real-time to environmental measurements produced by public research laboratories. It aims to communicate and to make available data on water systems to as many people as possible, especially on climatology, hydrology, and fluvial geomorphology.

This tool targets various stakeholders: local authorities, consultancy firms, researchers, non-profit organizations, and the general public. OpenDataEau has been further developed in the frame of the Cheap’Eau project (see section 1.2.1) with two objectives: (i) to give access to water-related data to everybody (researchers, professionals and

general public), and (ii) to help other researchers who are developing new monitoring systems to easily visualize their data.

6.2.5.5 Installation

The water level monitoring station prototype has been installed in the Porte des Alpes stormwater management facility (see section 3.2.6). Figure 6-9 shows how the system is installed in Lake 1. It is installed in a pit directly connected to the lake. Both pressure sensors are laying on the bottom of the pit (around 2-meter depth) and connected to the DIY datalogger on top (gray box). The enclosure is waterproof but not built to be submerged: it is installed higher than the known maximum water level. A grid closes the pit and protects the system from theft or vandalism. The cable that connects the data logger to the small solar panel (0.5W) is facing the lake to be as invisible as possible and to maximize the exposure to indirect solar radiation.

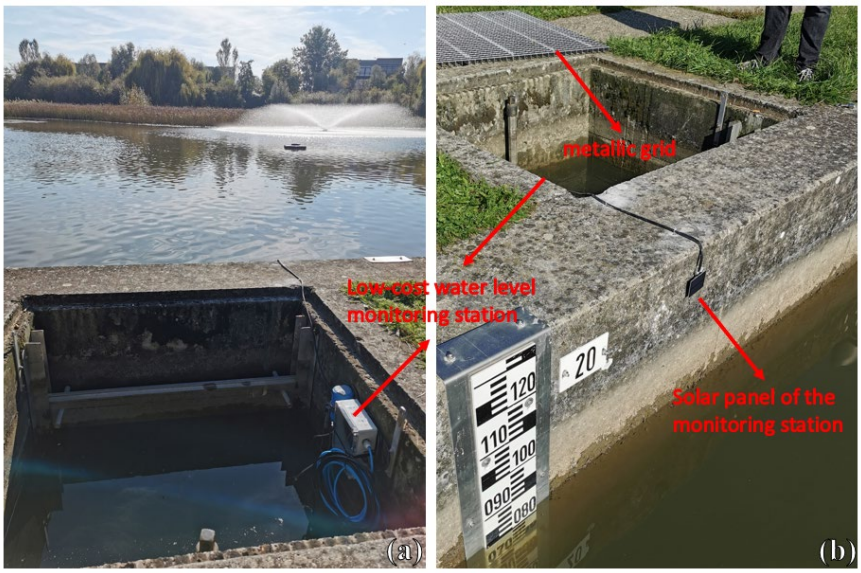

Figure 6-9. Installation of the water level monitoring station prototype. (a) Left side view: the gray box containing the monitoring system. The blue circular enclosure corresponds to another system installed by a company operating for Greater Lyon (with one measurement per hour), (b) Right side view: the metallic grid covers the pit under normal condition, and the 0.5 W solar panel used to power the entire system.

6.3 RESULTS AND DISCUSSION

6.3.1 Laboratory test: measurement performance

Low-cost sensor YB-2J-F and reference sensor OTT PLS are compared in the testbench described in section 6.2.4. During the experiment, water temperature ranges from 9.9 to 10.7 °C and air temperature ranges from 9.7 to 11.3 °C. Figure 6-10 shows all data. The regression results are given in Table 4-11.

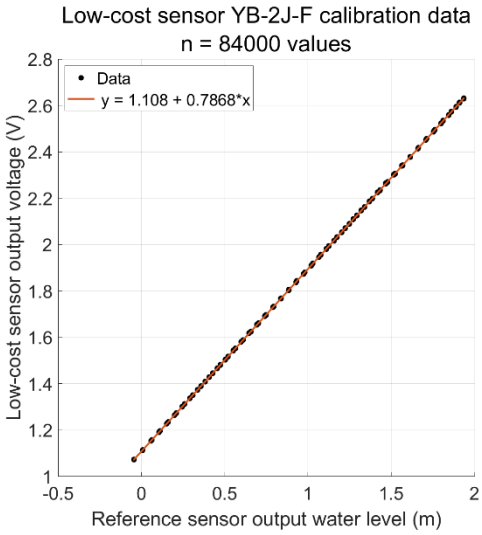

Figure 6-10. Low-cost sensor YB-2J-F calibration data. The correlation function has been selected from the regression results given in Table 4-11.

Table 6-4. Regression results for the low-cost water level sensor

Parameter	With 0 intercept	With free intercept
b11	0	1.108029
b12	1.641231	0.786791
u(b11)	0	0.000008
u(b12)	0.001761	0.000007
cov(b11, b12)	0	0
ResVar1	0.322789	0.000001
IC95 b11	0	[1.108013, 1.108045]
IC95 b12	[1.637780, 1.644682]	[0.786777, 0.786806]
Standard error	0.568145	0.001224

According to Table 6-4Table 4-11, the bias estimated with the free intercept regression is equal to 1.108029 and its 95% coverage interval [1.108013, 1.108045] is different from 0. Therefore, the selected correlation function, with four significant digits, is:

$$y = 1.108 + 0.7868\,x \qquad \text{Equation 6-1}$$

with a standard error ε = 0.0012.

The inverse function of Equation 6-1 could be the calibration function of YB-2J-F.

Assuming that the reference water level sensor has an enlarged uncertainty 0.05 % of full scale(see Table 6-3), the YB-2J-F low-cost water level sensor enlarged uncertainty corresponding to 90%, 95% and 99% correctness rates are given in Table 6-5. The enlarged uncertainty for a 95% correctness rate is 0.11 mm, which indicates that the YB-2J-F low-cost water level sensor with DIY data logger has a comparable performance as the reference water level sensor at a fiftieth of the price.

Table 6-5. Enlarged uncertainty of the low-cost water level sensor.

Correctness rate	Enlarged uncertainty
90%	0.08 mm
95%	0.11 mm
99%	0.16 mm

Another point to check is that the YB-2J-F sensor output 4 to 20 mA current signal corresponds to 0 to 5 m water level (as engraved on the sensor casing as shown Figure 6-1). The current signal in mA is converted to voltage in V by a 250 ohms precision resistor. Therefore, a theoretical two-point calibration dataset is shown in Table 6-6.

Table 6-6. Two-point theoretical water level sensor calibration dataset.

Water level (m)	Sensor theory output current (A)	Data logger theory record voltage (V)
0	0.004	1
5	0.020	5

From data in Table 6-6, one gets the theoretical correlation function:

$$y = b_1 + b_2 x = 1 + 0.8\,x \qquad \text{Equation 6-2}$$

where x is the real water level in meter, y is the output voltage of low-cost sensor in volt. Standard error, and standard uncertainties of b_1 and b_2 can be considered as negligible.

The real system response (Equation 6-1) is different form the theoretical system response (Equation 6-2). When the system records a sensor output voltage of 2 V, the inverse function of Equation 6-1 gives an estimated water level of 1.13 m, while the inverse function of Equation 6-2 gives an estimated water level of 1.25 m. The systematic errors generated by the theorical calibration function is 120 mm. This is due to several reasons including the imperfection of the sensor itself. It shows that a dedicated calibration of the low-cost water level monitoring system is mandatory before using it *in situ*. Because of the correctlinearity of the sensor's response at 0 to 2 m test water level as shown in Figure 6-10, a three-point calibration is sufficient to correct the systematic errors.

6.3.2 Field-test: longevity of the DYI monitoring system

Considering that the designed system outputs have a low enlarged uncertainty (Table 6-5), it has been decided to do one measurement when the system wakes up to decrease the power consumption. The total active cycle lasts less than 15 seconds: initialization, measurements of water level and battery voltage, communication and termination. The system was deployed in the field with the objectives detailed in section 6.2.1. Figure 6-11 presents the whole-time range online data of the system.

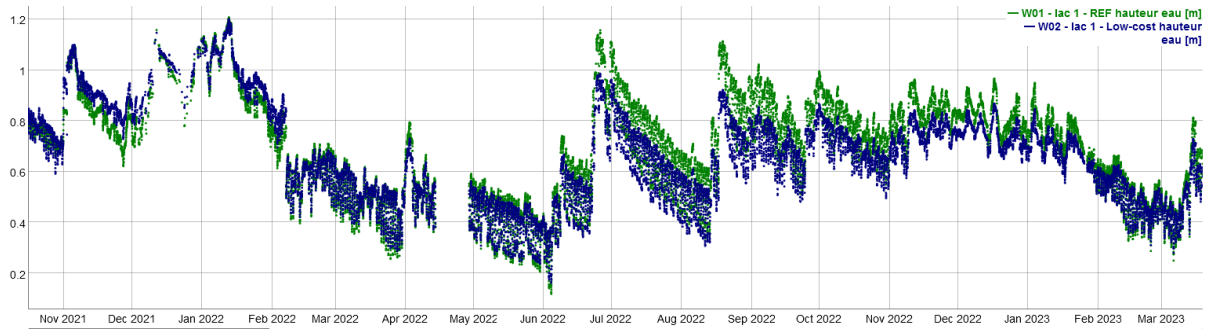

Figure 6-11. Low-cost (blue) and reference (green) water level sensors outputs in Lake 1 from 15 October 2022 to 18 March 2023, Porte des Alpes, France (extract from http://mind4stormwater.online/opendataeau/see/, accessed: 18 March 2023).

The last version of the monitoring system was installed *in situ* from 15 October 2021 to March 2023 with no need for reparation or replacement of any part (even batteries have not been changed). Prior to October 2021, several trials were carried out to improve the assembly of the measuring system, the position and orientation of the solar panel and, above all, the sealing of the system. No data was sent between 14 and 29 April 2022 because the Sigfox subscription (LPWAN provider) was not renewed in time. As the system does not have a local data backup, the measurements were lost for this period. In almost one year and a half of operation, three visits were made on site: on 2 November 2021, 10 December 2021, and 7 February 2022. During these three site visits, a manual reading of the water level was done and compared with the low-cost measurement, and, if necessary, the offset was corrected (to align the low-cost water level and the reference water level with the manual reading). Except theses visits (dedicated exclusively to check the water level), no other visit or intervention was done: the main objective was thus to assess the autonomy of the system (energy autonomy but also system longevity).

6.3.2.1 Low-Power Wide Area Network Communication

As shown in Figure 6-9, the system is installed in a pit covered by a metallic grid: the signal strength is very limited and close to the theorical minimum of -120 dB as shown in Figure 6-12. The Received Signal Strength Indicator (RSSI) is a common indicator of the power level being received by a gateway and is expressed with a negative

value and the closer to 0 the value is, the stronger the signal is. A RSSI around -130 dB is considered as the low limit, meaning that the signal cannot be received by the gateway.

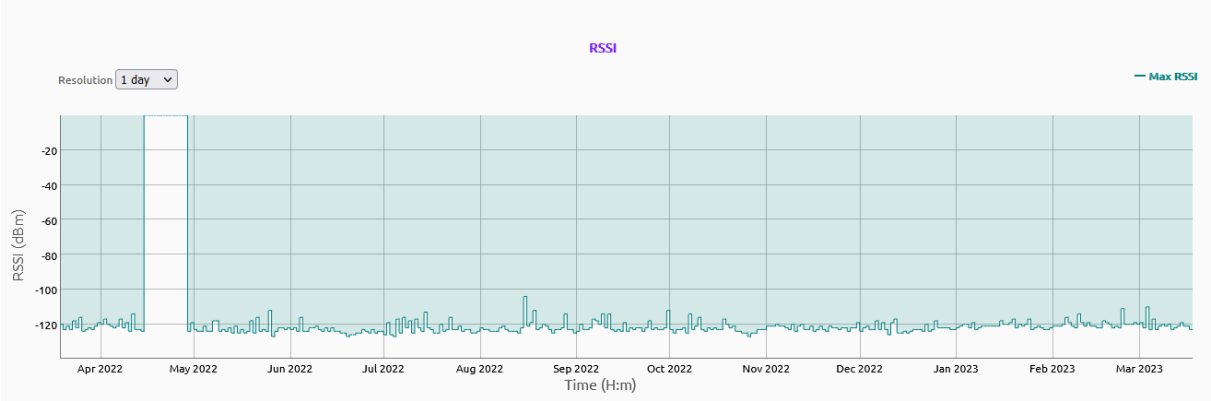

Figure 6-12. RSSI (Received Signal Strength Indicator) of the tested system from the Sigfox backend.

According to the data provided by the Sigfox network operator for our device, the signal remains stable during the whole period (however with important data loss as discussed below) despite the fact that the device is located in a pit and covered with a metallic grid. The signal strength is influenced by environmental parameters such as humidity, temperature, atmospheric pressure, and rain (Goldoni *et al.*, 2022).

The system is set to wake up and to send measurement data online with a time step of 40 minutes and the real time step is shown in Figure 6-13.

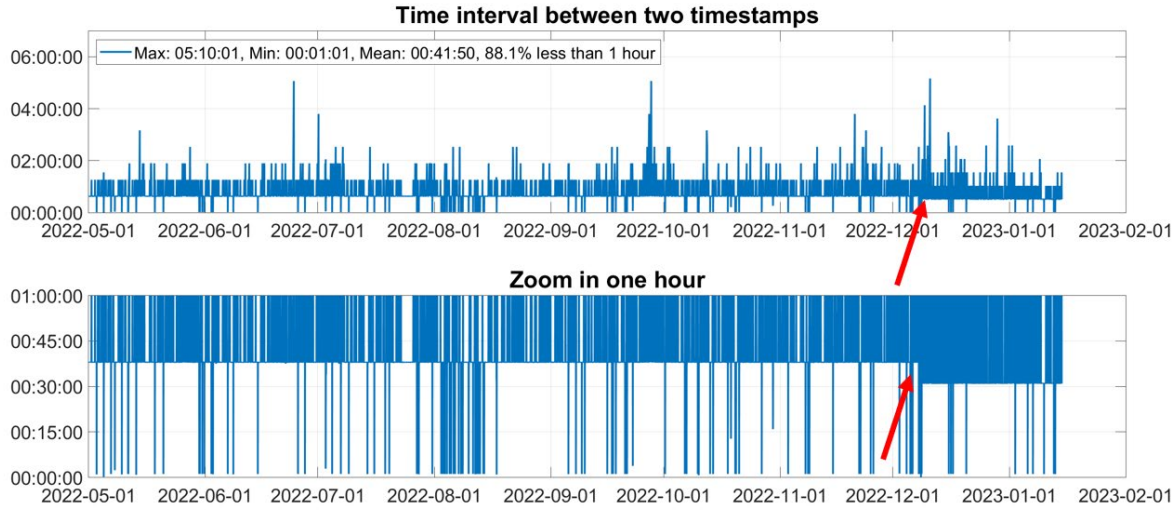

Figure 6-13. Time interval between two timestamps of online data from 2022-05-01 to 2022-12-01.

As shown in Figure 6-13, the average timestamp interval is 41 minutes which is close to the set time of 40 minutes, but the regularity of the timestamp is not satisfactory.

Before 2022-12-08 (mark red arrow in the figure), common timestamp intervals are: 1 minute, 38 minutes, 76 minutes, 114 minutes and higher values that are integer multiples of 38 minutes. We speculate that the timestamp interval 1 minute is due to the fact that the sleep is not triggered correctly after one measurement sometimes. The code has to be rechecked later. Timestamp intervals that are an integer multiple of 38 minutes reveal that the system sleep time is set to 38 minutes actually but not 40 minutes because the TPL5110 module described in section 6.2.5.1 cannot set sleep time accurately according to manufacturer (SparkFun, 2022). The timestamps interval of 76 minutes (twice 38 minutes) means one communication packet is lost due to limited signal strength. In the worst case, eight consecutive packets are lost and monitoring data are lost completely within five hours.

After 2022-12-08, the system condition is similar, but the system sleep time jumped to 30 minutes. No one reset the system around 2022-12-08. As shown in Figure 6-14, the battery output voltage has an outlier on 2022-12-08. We speculate that the TPL5110 module was reset due to this battery problem but identifying the true reason needs further investigation.

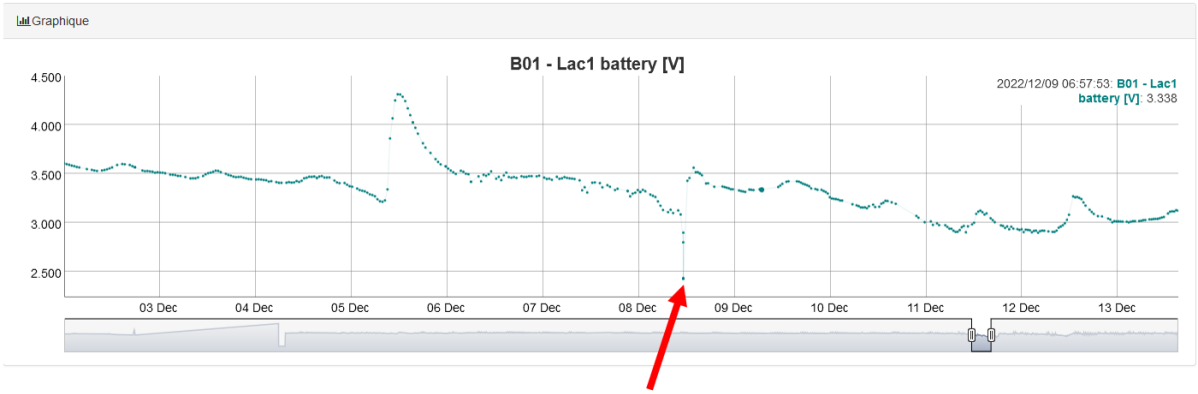

Figure 6-14. Battery output voltage from 2022-12-03 to 2022-12-13.

In summary, The TPL5110 module is not reliable and shouldn't be used when precise time steps are required. Within the Cheap'eau project, we have developed a system including real time clock and transistors providing a precise sleep duration (as it is directly based on the real-time clock module) and still low power consumption (only the real-time clock remains powered during the sleep period). It is recommended to install low-cost systems that need to send data online at a location with correct LPWAN signal. And, more important, it is highly recommended to store data locally, e.g., in a SD card.

6.3.2.2 Autonomy and energy consumption

The power supply part of the system is a 0.5 W solar panel as shown in Figure 6-9 and three AA rechargeable Nickel Metal Hybrid batteries of 2300 mAh each as shown in Figure 6-6. The batteries output voltages measured during the *in situ* test are shown in Figure 6-15.

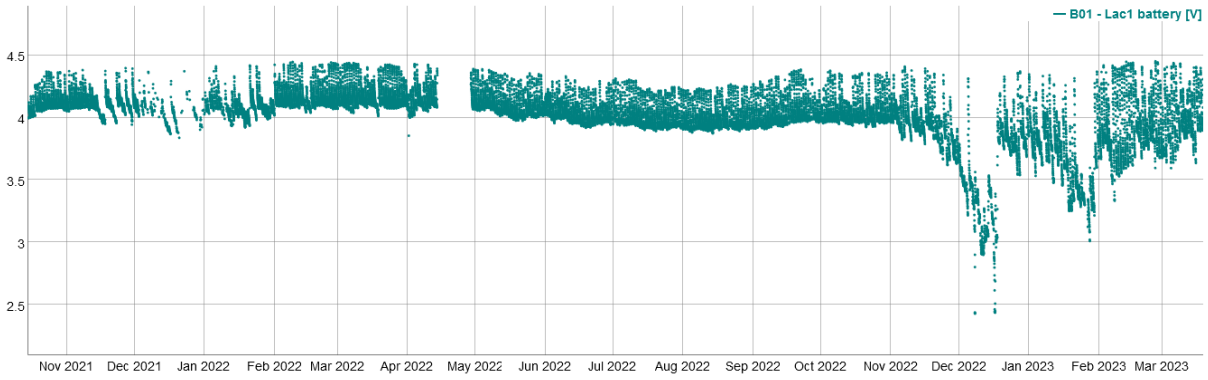

Figure 6-15. Batteries output voltage of the proposed system.

According to Figure 6-15, we can observe that the Nickel Metal Hybrid batteries have more than one year of longevity. The batteries output voltages were higher than 3.7 V from December 2021 to March 2022 but decreased from 4.5 V to 2.5 V from December 2022 to March 2023. The winter period can explain the more important drop of voltage because of the reduction of solar radiation (intensity and duration). However, we can also notice a more rapid drop of voltage since November 2022, meaning that the energy stored in the battery decreases over time. The system, and thus the batteries, remains outside all the time and was exposed to significant variations of temperature along the year. According to Lemaire-Potteau et al. (2009) “among all environmental factors, temperature is the most influential factor governing the power sources behavior (charge, discharge, self-discharge, lifetime)”. The low charging voltage (because of the small solar panel) preserves the battery and is sufficient for the system to continue to run. These results are very encouraging if we consider a required autonomy of at least one year, and it is thus possible to reduce the sleep time (maybe to 20 minutes or 15 minutes) and still provide at least one year of autonomy.

6.3.2.3 Maintenance practice

In theory, according to the specifications given in section 6.2.2, maintenance visits related to the YB-2J-F sensor itself can be avoid. But regular visits and calibration are highly recommended to ensure accurate data are delivered. During such maintenance visit, the following calibration steps have been conducted:

1) using a magnet to trigger an instantaneous measurement immediately as described in section 6.2.5.1,
2) manual reading of the water level from the gauge installed on site as shown in Figure 6-9,

3) accessing the spreadsheet with a smartphone to enter the manual reading of the water level,
4) the new offset is then calculated automatically (sensor reading obtained in step 1 minus manual reading obtained in step 3),
5) using again a magnet to trigger an instantaneous measurement immediately as described in section 6.2.5.1
6) compare the new measurement with the manual reading to confirm the new offset, and in case of difference between the measurement and the reading, repeat the calibration process.

Maintenance records in the spreadsheet are shown in Figure 6-16. Maintenance visits have been done at the start of the experiment (on 2 November 2021, 10 December 2021, and 7 February 2022, as discussed in the beginning of section 6.3.2) in order to verify the correct implementation and functioning of all steps of the data collection and transmission process.

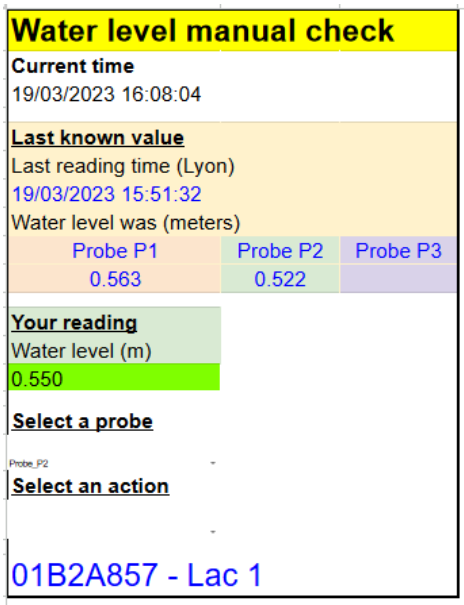

Figure 6-16. Interface accessible from a smartphone to save the water level manual readings (reference and low-cost) and to correct the offsets (probe P1: reference sensor and probe P2: low-cost sensor).

In addition, alerts described in section 6.2.5.4 have been successfully tested. Alert emails were received timely. Without regular visit during more than a year, the system (reference and low-cost sensors) has not been sufficiently

calibrated to consider assessing its measurement performance. However, we can guarantee that, except regular calibration, this system does not need any other maintenance visit to operate for more than a year without failure so severe that it stops operation. Figure 6-11 demonstrates the reliability of (i) the low-cost sensor as no abnormal low-cost measurement was reported), and (ii) the data logger as no abnormal reference measurement was reported. In this situation, an abnormal measurement is a physically impossible value (water level negative or higher than the pit), or a measurement appearing as inconsistent with previous and subsequent measurements. The monitoring system is therefore proven to be reliable for at least one year and a half.

6.4 CONCLUSION

The main work and findings of this chapter are summarized in Table 6-7.

Table 6-7. Summary about using the tested low-cost water level sensor and the system in urban hydrology.

Sensor/system	Application in urban hydrology?	Comments / conditions of use
YB-2J-F	Possible	The low-cost pressure water level sensor YB-2J-F is a robust sensor with a stainless-steel housing that has not sent any outliers during continuous *in situ* measurements lasting one year and a half. The sensor outputs a 4-20 mA signal. A signal processing circuit is necessary to be developed by users, including a precision resistor and a DFR0553 module based on an ADS1115 chip. This has proven to be effective. Calibration is mandatory when using this sensor, as for all sensors.
Low-cost DIY monitoring stations	Reserved to possible depending on the objectives	The low-cost DIY water level monitoring system developed in this chapter is designed to operate without maintenance or with limited maintenance. The system has three rechargeable AA batteries and a 0.5 W solar panel to power it. This method makes it work continuously for one year and half. The system did not have local data storage to be as simple as possible. However, the continuity of online data was not as reliable as expected, and data were lost because of network failures. The system was set to operate with a cycle: sleep for 40 minutes and measurement for less than one minute that is controlled by a timer. However, the observed average sleep time was 42 minutes. The regularity of the timestamp is not satisfactory because the system cannot sleep in time, as the TPL5110 timer module is not accurate enough, and the communication signal strength is limited. It is recommended to use our newly developed solution with the real-time clock and transistors to obtain a more regular measurement period. Additional work was done to assemble a convenient monitoring chain. In addition to monitoring station hardware and software, a platform to support data storage, data display and maintenance practice has been developed. The manufacturer of the control board used in our system is bankrupt. This reveals part of the potential risks that low-cost DIY monitoring station faces.

CHAPTER 7: GENERAL CONCLUSION AND PERSPECTIVES

This thesis aimed contributing to assess the assumption that the large-scale deployment of low-cost monitoring systems could have the potential to significantly change, or even revolutionize, the field of urban hydrology monitoring, bringing improved urban management and a better living environment. Even though low-cost sensors already emerged a few decades ago, versatile and cheap electronics like Arduino could nowadays give stormwater researchers like the author of this thesis a new opportunity to build their own monitoring systems to support their work, and to deploy them on large scale at very affordable costs. However, most of commercially available low-cost sensors were originally designed either for teaching purposes, or as small parts for other goods, or also for DIY (Do It Yourself) use by electronics enthusiasts. Their reliability for research and operation applications in urban hydrology was questionable. This question was addressed in this work.

In Chapter 2, a literature review was conducted to map the present knowledge and practice about using low-cost sensors to monitor (i) meteorological, (ii) water quantity, and (iii) water quality quantities. The review was positive in the sense that it showed that several low-cost sensors and solutions already exist to monitor continuously the quantities of interest. However, water quality monitoring by means of low-cost devices is more knowledge intensive, and users clearly need specific skills, that should also be adaptable to the water matrix of interest. In addition, reviewed papers do not sufficiently report repeatable examples with reference to metrology standards, literature, and methods. To a higher degree compared with traditional sensors, the quality of data generated by low-cost sensors not only depends on the sensors themselves, but also on the user and his/her knowledge, skills and metrological practice. Therefore, this thesis aimed at testing selected low-cost sensors in the context of stormwater source control measures.

In Chapter 3, a metrology framework was proposed. It proposes to base the low-cost sensor assessment on some key indicators, in particular “enlarged uncertainty” and “correctness rate”. Assuming that reference sensors deliver “reference values” of the quantities of interest, the correctness rate is defined to assess the percentage of measured

quantity values delivered by a low-cost sensor that agree with the reference quantity values given by the corresponding reference sensor used under the same *in situ* conditions. The correctness rate should be calculated with large data sets to be representative as small data sets cannot give robust results. A correlation function is also proposed to estimate the most likely true values (i.e., the reference values) of the quantities of interest from the values delivered by the low-cost sensors, accounting for offset and slope correction. Two low-cost sensor testing sites were also introduced in Chapter 3.

In Chapter 4, a 15-month comparison test of low-cost meteorological sensors with reference sensors has been performed. The performance of the low-cost anemometer WH-SP-WS01 was stable and quantifiable. The performance of the low-cost anemoscope WH-SP-WD was stable, but it cannot give wind direction in angles, only in sectors, which however may be sufficient for urban hydrology purposes. The low-cost air humidity sensor BME280 had only three-month longevity with poor performance. The low-cost air humidity sensor DHT22 had stable and quantifiable performance. The low-cost pyranometer JXBS-3001-ZFS systematically delivered higher values than the reference sensor. Lastly, the low-cost light sensor Si1145 was able to estimate the total daily radiation, provided some adaptation of the sensor is made.

In Chapter 5, low-cost and reference rain gauges were compared for four months. Three low-cost optical rain gauges RG-15 were tested. They showed a stable functioning without drift, but a significant and unexplained variability from sensor to sensor was observed. For RG-15, a systematic comparison with a reference sensor is necessary to establish a correlation function to estimate possible bias and under/over estimation. Six tipping bucket rain gauge WH-SP-RG were also tested. The reproducibility of this sensor is acceptable according to calibration. Several months of use have shown a stable functioning and no drift. But users should not use this sensor without modify its funnel area firstly to improve its resolution. Users also should spray Teflon on the adapted funnel to ensure raindrops can slip into the bucket. A systematic laboratory calibration is also required for this sensor.

Also in Chapter 5, a low-cost rainfall monitoring station prototype was designed, built, installed, tested and iteratively improved. This station has two power supply methods: output power and/or solar power, and two data recording methods: *in situ* SD card and/or online data transmission through LoRa network. The last version of this station performed to our satisfaction.

In Chapter 6, the low-cost water level pressure sensor YB-2J-F has been calibrated in laboratory firstly and then used *in situ* for one year and a half. Calibration is mandatory when using this sensor. On the one hand, the calibration function is needed to convert sensor output to water level measurement. On the other hand, the theoretical calibration function is far from reality and needs to be established for each sensor. This sensor has demonstrated excellent performance in calibration and has not sent any outliers during the whole testing period.

In this chapter, a low-cost water level monitoring system was designed to operate without maintenance or with very reduced maintenance. This system is only solar powered and does not have local data storage to avoid data fetch visit and to save power. However, the data quality of this system was not as reliable as expected and further improvements are needed.

At the end of Chapters 4, 5 and 6, based on the tests carried out during the thesis, a final assessment of all tested sensors and devices for potential use in urban hydrology is proposed, with detailed comments. This information can be used by other researchers or operators who would like to use these low-cost sensors.

In summary, even with the help of a growing community, the time to be dedicated to components selection, hardware design and assembling, software development work, systematic sensor calibration and comparison, is the largest part of the total cost which needs to be estimated when using low-cost sensors. It is commonly believed that low-cost sensors and low-cost monitoring systems have lower accuracy compared to standard more expensive monitoring equipment. But by quantifying the uncertainty of low-cost monitoring systems, hydrologist could rely on these systems to draw conclusions with known uncertainty.

In details, after testing, four low-cost sensors appear as usable for stormwater source control measures monitoring: wind speed sensor WH-SP-WS01 with enlarged uncertainty 0.24 m/s, air temperature and humidity sensor DHT22 with enlarged uncertainty 2.3 °C and 5.7 %RH, rain gauge WH-SP-RG whose collecting funnel area needs to be enlarged (original resolution is around 0.60 mm/tip), and pressure water level sensor YB-2J-F which requires a signal processing circuit to convert its output current to measurable quantity for open-source hardware. After dozens of software and hardware upgrades, a proven and reliable low-cost monitoring station has been tested and validated. In this station, an Arduino MKR WAN 1310 is used as main control board, a DS3231 module is used as real time clock, and a Lipo Rider Pro board is used as power management board. Data are saved locally in a SD

card by the Arduino MKR Mem shield and sent online through the LoRaWAN network. All details (hardware and software) of this monitoring station are given as open-source information.

This thesis lays the groundwork for large-scale low-cost monitoring. By referring to above recommendations, hydrologist could develop their own low-cost monitoring systems and networks.

There are still several questions in this domain and further work could include the following aspects:

- Continue to collect more data to better evaluate the long-term behavior and performance of these devices. The low-cost rainfall and water level monitoring stations developed during the thesis are still in operation and it will be interesting to monitor their ageing and longevity.
- Continue to make our work to be easily repeated / reproduced by others. For example, draw printed circuit boards and share this design, wrap code as an Arduino library, share 3D print design files, etc.
- Develop a software toolbox to calculate correctness rates with different enlarged uncertainty autonomously. Correctness rate is an appropriate tool to compare the outputs of tested sensor and reference sensor considering their respective enlarged uncertainty.
- Further check the sensitivity of the low-cost sensors to the environment. For example, the water temperature sensitivity of the low-cost water level pressure sensor YB-2J-F is presently checked by a collaborative team.
- Explore using low-cost water quality sensors (e.g., pH, conductivity, turbidity) to monitor stormwater *in situ* in real time. A preliminary work has been documented in the Appendix.
- Implement a spatially distributed network of low-cost sensors and stations at catchment scale to provide data and knowledge about various stormwater source control measures.
- As sensor networks grow in size, it is worthwhile to further investigate how to calibrate a large number of sensors automatically.

References

Abeledo, M.C., Bruschetti, F., Priano, D.A., Calbosa, D., Crubellier, R., Iriso, P. and Abete, E. (2016), "Application of wireless technology to determine optimum maturity in strains of Malbec vineyards for Argentine wine sectors", *CACIDI 2016 - Congreso Aergentino de Ciencias de La Informatica y Desarrollos de Investigacion*, Institute of Electrical and Electronics Engineers Inc., pp. 1–7, doi: 10.1109/CACIDI.2016.7785984.

Abu-Baker, S., Frazier, C., Frazier, N. and Ghaffari, S. (2016), "Engaging Freshman Undergraduate Students in Faculty Environmental Science Research: Testing the Local Surface Waters for Nitrate, Phosphate, and Ammonium Ions Using Two Affordable Methods as an Example", *Green and Sustainable Chemistry*, Vol. 06 No. 03, pp. 143–149, doi: 10.4236/gsc.2016.63014.

adafruit. (2023), "SI1145 Digital UV Index / IR / Visible Light Sensor", available at: https://www.adafruit.com/product/1777 (accessed 15 March 2023).

Adepoju, T.M., Oladele, M.O., Kasali, A.A. and Fabiyi, G.J. (2020), "Development of a Low-Cost Arduino-Based Weather Station", *FUOYE Journal of Engineering and Technology*, Vol. 5 No. 2, pp. 69–73, doi: 10.46792/fuoyejet.v5i2.508.

Adla, S., Rai, N.K., Karumanchi, S.H., Tripathi, S., Disse, M. and Pande, S. (2020), "Laboratory calibration and performance evaluation of low-cost capacitive and very low-cost resistive soil moisture sensors", *Sensors (Switzerland)*, Vol. 20 No. 2, doi: 10.3390/s20020363.

AKHIR, P. (2021), *Sistem Monitoring Kualitas Air Tambak Udang Berbasis Internet of Things (Iot)*, Doctoral dissertation, Politeknik Manufaktur Negeri Bangka Belitung.

Akhter, T., Ali, M., Cha, J., Park, S., Jang, G., Yang, K. and Kim, H. (2018), "Development of a Data Acquisition System for the Long-term Monitoring of Plum (Japanese apricot) Farm Environment and Soil", *Journal of Biosystems Engineering*, Vol. 43 No. 4, pp. 426–439.

Alam, A.U., Clyne, D., Jin, H., Hu, N.X. and Deen, M.J. (2020), "Fully Integrated, Simple, and Low-Cost Electrochemical Sensor Array for in Situ Water Quality Monitoring", *ACS Sensors*, Vol. 5 No. 2, pp. 412–422, doi: 10.1021/acssensors.9b02095.

Alimenti, F., Bonafoni, S., Gallo, E., Palazzi, V., Vincenti Gatti, R., Mezzanotte, P., Roselli, L., *et al.* (2020), "Noncontact measurement of river surface velocity and discharge estimation with a low-cost doppler radar sensor", *IEEE Transactions on Geoscience and Remote Sensing*, Institute of Electrical and Electronics Engineers Inc., Vol. 58 No. 7, pp. 5195–5207, doi: 10.1109/TGRS.2020.2974185.

Alimorong, F.M.L.S., Apacionado, H.A.D. and Villaverde, J.F. (2020), "Arduino-based Multiple Aquatic Parameter Sensor Device for Evaluating pH, Turbidity, Conductivity and Temperature", *2020 IEEE 12th International Conference on Humanoid, Nanotechnology, Information Technology, Communication and Control, Environment, and Management, HNICEM 2020*, pp. 3–7, doi: 10.1109/HNICEM51456.2020.9400145.

Al-Rubaei, A.M., Merriman, L.S., Hunt, W.F., Viklander, M., Marsalek, J. and Blecken, G.-T. (2017), "Survey of the Operational Status of 25 Swedish Municipal Stormwater Management Ponds", *Journal of Environmental Engineering*, Vol. 143 No. 6, p. 05017001, doi: 10.1061/(asce)ee.1943-7870.0001203.

Alumno, N.D.E.L., Tesis, D.E., Tesis, N.D.E.L.D.E., Tesis, C.D.E., Del, N. and Tesis, C.D.E. (2021), *Sistema De Monitoreo Remoto Con Resguardo En La Nube Para Un Reactor Anaerobio Hibrido De Lecho Fijo Y Lecho Fluidizado Inverso*, Doctoral dissertation, TecNM/Instituto Tecnológico de Orizaba.

Ambient weather. (2011), "Ambient Weather WS-2080 Wireless Home Weather Station User Manual", available at: http://ambientweather.wikispaces.com/ws2080 (accessed 16 March 2023).

Ammari, S., Wildian, W. and Harmadi, H. (2019), “Rancang Bangun Sistem Peringatan Dini Banjir Berdasarkan Tingkat Kekeruhan Air Hulu Sungai dengan Turbidity Sensor SEN0189 dan Transceiver nRF24L01+”, *Jurnal Fisika Unand*, Vol. 8 No. 3, pp. 240–244, doi: 10.25077/jfu.8.3.240-244.2019.

Andang, A., Hiron, N., Chobir, A. and Busaeri, N. (2019), “Investigation of ultrasonic sensor type JSN-SRT04 performance as flood elevation detection”, *IOP Conference Series: Materials Science and Engineering*, Vol. 550 No. 1, doi: 10.1088/1757-899X/550/1/012018.

Angdresey, A., Sitanayah, L. and Immanuel, T.M. (2021), “A Real-Time Water Quality and Quantity Monitoring System for Aquarium A Real-Time Water Quality and Quantity Monitoring System for Aquarium”, doi: 10.1145/3489088.3489090.

Angraini, L.M., Mardiana, L., Hadi, K. Al and Ahmawati, E. (2016), “Design Of The Measuring Instrument Of Turbidity Level Using Turbidity Sensor Based on SMS Gateway”, *Scientific Committee*, pp. 300–307.

Aosong Electronics. (2023), “Digital-output relative humidity & temperature sensor/module DHT22 (DHT22 also named as AM2302) Capacitive-type humidity and temperature module/sensor”.

Aqualabo. (2023), “Aqualabo - World leader in water monitoring and analysis”, available at: https://en.aqualabo.fr/ (accessed 2 April 2023).

Araújo, T., Silva, L. and Moreira, A. (2020), “Evaluation of Low-Cost Sensors for Weather and Carbon Dioxide Monitoring in Internet of Things Context”, *IoT*, Vol. 1 No. 2, pp. 286–308, doi: 10.3390/iot1020017.

Arduinio Forum. (2016), “[SOLVED] Accuracy of millis() for keeping time - Using Arduino / Project Guidance - Arduino Forum”, available at: https://forum.arduino.cc/t/solved-accuracy-of-millis-for-keeping-time/401399/7 (accessed 10 February 2023).

Arduino Documentation. (2023a), “Arduino® Nano”, available at: (accessed 15 March 2023).

Arduino Documentation. (2023b), “MKR WAN 1310 | Arduino Documentation | Arduino Documentation”, available at: https://docs.arduino.cc/hardware/mkr-wan-1310 (accessed 15 March 2023).

Arzoumanian, E., Vogel, F.R., Bastos, A., Gaynullin, B., Laurent, O., Ramonet, M. and Ciais, P. (2019), "Characterization of a commercial lower-cost medium-precision non-dispersive infrared sensor for atmospheric CO2 monitoring in urban areas", *Atmospheric Measurement Techniques*, Copernicus GmbH, Vol. 12 No. 5, pp. 2665–2677, doi: 10.5194/amt-12-2665-2019.

Assendelft, R.S. and Ilja van Meerveld, H.J. (2019), "A low-cost, multi-sensor system to monitor temporary stream dynamics in mountainous headwater catchments", *Sensors (Switzerland)*, Vol. 19 No. 21, doi: 10.3390/s19214645.

Azma Zakaria, N., Zainal Abidin, Z., Harum, N., Chen Hau, L., Salih Ali, N. and Azni Jafar, F. (2018), *Wireless Internet of Things-Based Air Quality Device for Smart Pollution Monitoring*, *IJACSA) International Journal of Advanced Computer Science and Applications*, Vol. 9.

Azouzoute, A., Merrouni, A.A., Bennouna, E.G. and Gennioui, A. (2019), "Accuracy measurement of pyranometer vs reference cell for PV resource assessment", *Energy Procedia*, Elsevier B.V., Vol. 157 No. 2018, pp. 1202–1209, doi: 10.1016/j.egypro.2018.11.286.

Baéz Rodríguez, L.A. and Rodríguez Jarquin, J.P. (2019), *Diseño de un sistema automatizado de control de pH para eficientar la producción de biogas en bioreactores*, Doctoral dissertation, TecNM/Instituto Tecnológico de Orizaba.

Bankar, S.P. and Sagat, S.P. (2020), "High resolution meteorological parameters measurement and analysis for quality weather forecasting", No. December, pp. 21–27.

Bartos, M., Park, H., Zhou, T., Kerkez, B. and Vasudevan, R. (2019), "Windshield wipers on connected vehicles produce high-accuracy rainfall maps", *Scientific Reports*, Springer US, Vol. 9 No. 1, pp. 1–9, doi: 10.1038/s41598-018-36282-7.

Bartos, M., Wong, B. and Kerkez, B. (2018), "Open storm: A complete framework for sensing and control of urban watersheds", *Environmental Science: Water Research and Technology*, Royal Society of Chemistry, Vol. 4 No. 3, pp. 346–358, doi: 10.1039/c7ew00374a.

Bastos, C.E., Grequi, M. and Galli, R. (2020), “Greenhouses Low-Cost Monitoring and Control System”, *Global Journal of Research In Engineering*, Vol. 20 No. 5.

Becouze-Lareure, C., Dembélé, A., Coquery, M., Cren-Olivé, C., Barillon, B. and Bertrand-Krajewski, J.L. (2016), “Source characterisation and loads of metals and pesticides in urban wet weather discharges”, *Urban Water Journal*, Taylor and Francis Ltd., Vol. 13 No. 6, pp. 600–617, doi: 10.1080/1573062X.2015.1011670.

Benisch, J., Helm, B., Bertrand-Krajewski, J.-L., Bloem, S., Cherqui, F., Eichelmann, U., Kroll, S., *et al.* (2021), “Chapter 7 Operation and maintenance”, *Metrology in Urban Drainage and Stormwater Management: Plug and Pray*, IWA Publishing, pp. 203–262, doi: 10.2166/9781789060119_0203.

Benoit, L., Allard, D. and Mariethoz, G. (2018), “Stochastic Rainfall Modeling at Sub-kilometer Scale”, *Water Resources Research*, Vol. 54 No. 6, pp. 4108–4130, doi: 10.1029/2018WR022817.

Berland, A., Shiflett, S.A., Shuster, W.D., Garmestani, A.S., Goddard, H.C., Herrmann, D.L. and Hopton, M.E. (2017), “The role of trees in urban stormwater management”, *Landscape and Urban Planning*, Elsevier B.V., Vol. 162, pp. 167–177, doi: 10.1016/j.landurbplan.2017.02.017.

Bertrand-Krajewski, J.-L. and Lepot, M. (2022), *UDMT - Urban Drainage Metrology Toolbox - User Manual Version 2022a-2*, Villeurbanne (France).

Bertrand-Krajewski, J.-L., Uhl, M. and Clemens-Meyer, F.H.L.R. (2021), “Chapter 8 Uncertainty assessment”, *Metrology in Urban Drainage and Stormwater Management: Plug and Pray*, IWA Publishing, pp. 263–326, doi: 10.2166/9781789060119_0263.

Bitella, G., Rossi, R., Bochicchio, R., Perniola, M. and Amato, M. (2014), “A novel low-cost open-hardware platform for monitoring soil water content and multiple soil-air-vegetation parameters”, *Sensors (Switzerland)*, Vol. 14 No. 10, pp. 19639–19659, doi: 10.3390/s141019639.

BOSCH. (2018), “BME280-Data sheet”, available at: (accessed 25 January 2023).

Buchanan, W.J. (2004), *RS-422, RS-423 and RS-485*, *The Handbook of Data Communications and Networks*, Springer, Boston, MA, doi: 10.1007/978-1-4020-7870-5_36.

Burgt, A.P. (2020), *Designing a Low-Cost Autonomous Pyranometer*, Bachelor's thesis, University of Twente.

Camargo, L.P. (2017), "Projeto Hydrus: veículo aquático para monitoramento da qualidade da água".

Campbell Scientific. (2020), "Datasheet of Campbell Scientific 03002-L".

Campbell scientific. (2020), "Datasheet of CS300", available at: https://s.campbellsci.com/documents/us/product-brochures/b_cs300.pdf (accessed 15 March 2023).

Campbell Scientific. (2022), "Wind Sentry Series", available at: https://s.campbellsci.com/documents/us/manuals/03002.pdf (accessed 15 March 2023).

Campbell scientific. (2023), "CS215: Capteur de température et d'humidité relative CS215", available at: https://s.campbellsci.com/documents/fr/manuals/cs215%20-%20324.pdf (accessed 25 January 2023).

Campbell seientific. (2023), "03002: Capteur de vitesse et de direction du vent", available at: https://www.campbellsci.fr/03002-wind-sentry (accessed 25 January 2023).

Chan, K., Schillereff, D.N., Baas, A.C.W., Chadwick, M.A., Main, B., Mulligan, M., O'Shea, F.T., *et al.* (2021), "Low-cost electronic sensors for environmental research: Pitfalls and opportunities", *Progress in Physical Geography*, SAGE Publications Ltd, Vol. 45 No. 3, pp. 305–338, doi: 10.1177/0309133320956567.

Cherqui, F., James, R., Poelsma, P., Burns, M.J., Szota, C., Fletcher, T. and Bertrand-Krajewski, J.L. (2020a), "A platform and protocol to standardise the test and selection low-cost sensors for water level monitoring", *H2Open Journal*, IWA Publishing, Vol. 3 No. 1, pp. 437–456, doi: 10.2166/h2oj.2020.050.

Cherqui, F., James, R., Poelsma, P., Burns, M.J., Szota, C., Fletcher, T. and Bertrand-Krajewski, J.-L. (2020b), "A platform and protocol to standardise the test and selection low-cost sensors for water level monitoring", *H2Open Journal*, Vol. 3 No. 1, pp. 437–456, doi: 10.2166/h2oj.2020.050.

Cherqui, F., Szota, C., Poelsma, P.J., James, R., Burns, M.J., Fletcher, T. and Bertrand-Krajewski, J.-L. (2019), "How to manage nature-based solution assets such as stormwater control measures?", *8th Leading-Edge Conference Strategic Asset Management* – LESAM, Vancouver, Canada, 23-27 Sept.

Coloch Tahuico, E.M.J. (2021), *Diseño e Implementación de Tarjeta Electrónica Para Pluviómetros de Balancín Para Comunicación En Red LoRaWAN y Visualización En Tiempo Real*, Doctoral dissertation, Universidad de San Carlos de Guatemala.

CORDIS. (2023), "Innovative stormwater asset management in future cities | Mind4Stormwater Project | Fact Sheet | H2020 | CORDIS | European Commission", available at: https://cordis.europa.eu/project/id/786566 (accessed 4 April 2023).

Cousins, J.J. (2017), "Of floods and droughts: The uneven politics of stormwater in Los Angeles", *Political Geography*, Elsevier Ltd, Vol. 60, pp. 34–46, doi: 10.1016/j.polgeo.2017.04.002.

Cowell, N., Chapman, L., Bloss, W. and Pope, F. (2022), "Field Calibration and Evaluation of an Internet-of-Things-Based Particulate Matter Sensor", *Frontiers in Environmental Science*, Frontiers Media S.A., Vol. 9, doi: 10.3389/fenvs.2021.798485.

Czemiel Berndtsson, J. (2010), "Green roof performance towards management of runoff water quantity and quality: A review", *Ecological Engineering*, Elsevier B.V., Vol. 36 No. 4, pp. 351–360, doi: 10.1016/j.ecoleng.2009.12.014.

Demetillo, A.T., Japitana, M. V. and Taboada, E.B. (2019a), "A system for monitoring water quality in a large aquatic area using wireless sensor network technology", *Sustainable Environment Research*, BioMed Central Ltd, Vol. 1 No. 1, doi: 10.1186/s42834-019-0009-4.

Demetillo, A.T., Japitana, M. v. and Taboada, E.B. (2019b), "A system for monitoring water quality in a large aquatic area using wireless sensor network technology", *Sustainable Environment Research*, Sustainable Environment Research, Vol. 1 No. 1, pp. 10–12, doi: 10.1186/s42834-019-0009-4.

Deplette, M., Paraz, J., Choi, H., Vacherie, S. and Bertrand-Krajewski, J.-L. (2021), *Étalonnage et Mise En Service Des Dispositifs de Mesure En Vue de Quantifier l'évapotranspiration de Toitures Végétalisées Prototypes*, *Unkonw*, Villeurbanne.

Dias, D.C. (2019), *Sistema de Medição de Chuvas Para Pesquisa Aplicada Em Modelos de Terraços Verdes*.

Domínguez-Brito, A.C., Cabrera-Gámez, J., Viera-Pérez, M., Rodríguez-Barrera, E. and Hernández-Calvento, L. (2020), "A DIY low-cost wireless wind data acquisition system used to study an arid coastal foredune", *Sensors (Switzerland)*, Vol. 20 No. 4, pp. 1–31, doi: 10.3390/s20041064.

Dswilan, S., Harmadi and Marzuki. (2021), "Flood monitoring system using ultrasonic sensor SN-SR04T and SIM 900A", *Journal of Physics: Conference Series*, Vol. 1876 No. 1, doi: 10.1088/1742-6596/1876/1/012003.

El-deen, S.K.N., Elborai, H., Sayour, H.E.M. and Yahia, A. (2018), "Wireless Sensor Network Based Solution for Water Quality Real-Time Monitoring", *Egyptian Journal of Solids*, Vol. 41 No. 1, pp. 49–62, doi: 10.21608/ejs.2018.148253.

Endress+Hauser. (2023), "Turbimax W CUS41 | Endress+Hauser", available at: https://www.ca.endress.com/fr/instrumentation-terrain-sur-mesure/CUS41?t.tabId=product-overview (accessed 2 April 2023).

Espinosa-Gavira, M.J., Agüera-Pérez, A., de la Rosa, J.J.G., Palomares-Salas, J.C. and Sierra-Fernández, J.M. (2018), "An on-line low-cost irradiance monitoring network with sub-second sampling adapted to small-scale PV systems", *Sensors (Switzerland)*, Vol. 18 No. 10, pp. 1–12, doi: 10.3390/s18103405.

Faisal, M., Harmadi and Puryanti, D. (2016), "Perancangan system monitoring tingkat kekeruhan air secara realtime menggunakan sensor Tsd-10", *Jurnal Ilmu Fisika*, Vol. 8 No. 1, pp. 9–16.

Farhat, M., Abdul-Niby, M., Abdullah, M. and Nazzal, A. (2017), "A Low Cost Automated Weather Station for Real Time Local Measurements", *Engineering, Technology & Applied Science Research*, Vol. 7 No. 3, pp. 1615–1618, doi: 10.48084/etasr.1187.

Faustine, A. and Mvuma, A.N. (2014), "Ubiquitous Mobile Sensing for Water Quality Monitoring and Reporting within Lake Victoria Basin", *Wireless Sensor Network*, Vol. 06 No. 12, pp. 257–264, doi: 10.4236/wsn.2014.612025.

Faustine, A., Mvuma, A.N., Mongi, H.J., Gabriel, M.C., Tenge, A.J. and Kucel, S.B. (2014), "Wireless Sensor Networks for Water Quality Monitoring and Control within Lake Victoria Basin: Prototype Development", *Wireless Sensor Network*, Vol. 06 No. 12, pp. 281–290, doi: 10.4236/wsn.2014.612027.

Fletcher, T.D., Shuster, W., Hunt, W.F., Ashley, R., Butler, D., Arthur, S., Trowsdale, S., *et al.* (2015), "SUDS, LID, BMPs, WSUD and more – The evolution and application of terminology surrounding urban drainage", *Urban Water Journal*, Taylor and Francis Ltd., Vol. 12 No. 7, pp. 525–542, doi: 10.1080/1573062X.2014.916314.

Flores, E.I.C.Y. (2020), *Estación Meteorológica LoRaWAN*.

Fortes, S., Hidalgo-Triana, N., Sánchez-La-chica, J.M., García-Ceballos, M.L., Cantizani-Estepa, J., Pérez-Latorre, A.V., Baena, E., *et al.* (2021), "Smart tree: An architectural, greening and ict multidisciplinary approach to smart campus environments", *Sensors*, Vol. 21 No. 21, pp. 1–27, doi: 10.3390/s21217202.

Fu, X., Goddard, H., Wang, X. and Hopton, M.E. (2019), "Development of a scenario-based stormwater management planning support system for reducing combined sewer overflows (CSOs)", *Journal of Environmental Management*, Elsevier, Vol. 236 No. August 2018, pp. 571–580, doi: 10.1016/j.jenvman.2018.12.089.

Fulton, J.W., Anderson, I.E., Chiu, C.L., Sommer, W., Adams, J.D., Moramarco, T., Bjerklie, D.M., *et al.* (2020), "QCam: SUAS-based doppler radar for measuring river discharge", *Remote Sensing*, Vol. 12 No. 20, pp. 1–23, doi: 10.3390/rs12203317.

Gasperi, J., Sebastian, C., Ruban, V., Delamain, M., Percot, S., Wiest, L., Mirande, C., *et al.* (2014), "Micropollutants in urban stormwater: Occurrence, concentrations, and atmospheric contributions for a wide range of contaminants in three French catchments", *Environmental Science and Pollution Research*, Springer Verlag, Vol. 21 No. 8, pp. 5267–5281, doi: 10.1007/s11356-013-2396-0.

Gasperi, M. and Hurbain, P. (2010), *Chapter 13: I2C Bus Communication*, *Extreme NXT: Extending the LEGO MINDSTORMS NXT to the Next Level*.

Gastón C. Hillar. (2017), *MQTT Essentials - A Lightweight IoT Protocol - Gastón C. Hillar - Google Books*.

Geetha, S. and Gouthami, S. (2016), "Internet of things enabled real time water quality monitoring system", *Smart Water*, Smart Water, Vol. 2 No. 1, pp. 1–19, doi: 10.1186/s40713-017-0005-y.

Giordan, D., Notti, D., Zucca, F., Pepe, A., Villa, A., Calò, F., Pepe, A., *et al.* (2018), "Low cost, multiscale and multi-sensor application for flooded area mapping", *Natural Hazards and Earth System Sciences*, Vol. 18, pp. 1493–1516.

Goldoni, E., Savazzi, P., Favalli, L. and Vizziello, A. (2022), "Correlation between weather and signal strength in LoRaWAN networks: An extensive dataset", *Computer Networks*, Elsevier, 15 January, Vol. 202, p. 108627, doi: 10.1016/J.COMNET.2021.108627.

Gusri, A.J. and Harmadi. (2021), "Rancang Bangun Alat Penguras Air pada Wadah Penampungan Berbasis Turbidity Sensor SEN0189", *Jurnal Fisika Unand*, Vol. 10 No. 3, pp. 330–336.

Hagino, T. (2021), *Practical Node-RED Programming : Learn Powerful Visual Programming Techniques and Best Practices for the Web and IoT*.

al Haji, A. and al Odwani, A. (2015), "Integrated wireless monitoring and control system in reverse osmosis membrane desalination plants", *MATEC Web of Conferences*, Vol. 35, pp. 1–5, doi: 10.1051/matecconf/20153503001.

Hakim, W.L., Hasanah, L., Mulyanti, B. and Aminudin, A. (2019), "Characterization of turbidity water sensor SEN0189 on the changes of total suspended solids in the water", *Journal of Physics: Conference Series*, Vol. 1280 No. 2, doi: 10.1088/1742-6596/1280/2/022064.

Hendri, H., Enggari, S., Mardison, Putra, M.R. and Rani, L.N. (2019), "Automatic System to Fish Feeder and Water Turbidity Detector Using Arduino Mega", *Journal of Physics: Conference Series*, Vol. 1339, doi: 10.1088/1742-6596/1339/1/012013.

Hernández, R. del C.C., Amondaray, L.R., Martínez, M.H., Ofelia and Montero4, P. (2020), "Implementation of a Low-Cost Weather Station With Raspberry Pi", *Telemática*, Vol. 19 No. 1, pp. 11–21.

Hinrich Kaplan, N., Sohrt, E., Blume, T. and Weiler, M. (2019), "Monitoring ephemeral, intermittent and perennial streamflow: a dataset from 182 sites in the Attert catchment, Luxembourg", *Earth System Science Data*, Vol. 11 No. 3, pp. 1363–1374, doi: 10.5194/essd-11-1363-2019.

Humphrey, M.D., Istok, J.D., Lee, J.Y., Hevesi, J.A. and Flint, A.L. (1997), "A new method for automated dynamic calibration of tipping-bucket rain gauges", *Journal of Atmospheric and Oceanic Technology*, Vol. 14 No. 6, pp. 1513–1519, doi: 10.1175/1520-0426(1997)014<1513:ANMFAD>2.0.CO;2.

Hussein, Z.K., Hadi, H.J., Abdul-Mutaleb, M.R. and Mezaal, Y.S. (2020), "Low cost smart weather station using Arduino and ZigBee", *Telkomnika (Telecommunication Computing Electronics and Control)*, Vol. 18 No. 1, pp. 282–288, doi: 10.12928/TELKOMNIKA.v18i1.12784.

Hydreon corporation. (2023), "Rain Gauge Model RG-15", available at: https://rainsensors.com/products/rg-15/ (accessed 1 February 2023).

Intharasombat, O. and Khoenkaw, P. (2015), "A low-cost flash flood monitoring system", *Proceedings - 2015 7th International Conference on Information Technology and Electrical Engineering: Envisioning the Trend of Computer, Information and Engineering, ICITEE 2015*, pp. 476–479, doi: 10.1109/ICITEED.2015.7408993.

Iskandar, H.R., Saputra, D.I. and Yuliana, H. (2019), "Eksperimental Uji Kekeruhan Air Berbasis Internet of Things Menggunakan Sensor DFRobot SEN0189 dan MQTT Cloud Server", *Jurnal Umj*, No. Sigdel 2017, pp. 1–9.

Islam, Sk.F., Hasan, Md.I., Akter, M. and Uddin, M.S. (2021), "Implementation and Analysis of an IoT-Based Home Automation Framework", *Journal of Computer and Communications*, Vol. 09 No. 03, pp. 143–157, doi: 10.4236/jcc.2021.93011.

Jafari, N.H., Li, X., Chen, Q., Le, C.Y., Betzer, L.P. and Liang, Y. (2021), "Real-time water level monitoring using live cameras and computer vision techniques", *Computers & Geosciences*, Pergamon, 1 February, Vol. 147, p. 104642, doi: 10.1016/J.CAGEO.2020.104642.

JCGM. (2012), "International vocabulary of metrology – Basic and general concepts and associated terms (VIM）", available at: https://www.bipm.org/en/ publications/guides/vim.html.

Jegadeesan, S. and Dhamodaran, M. (2018), "Wireless Sensor Network based Flood and Water Quality Monitoring System using IoT", *Taga Journal of Graphic Technology*.

Johnsen, K.K., Asbjørn, S.T., Nielsen, H. and Bertrand-Krajewski, J.-L. (2023), *The Monitoring of Hydraulic Properties of Green Rooftop Systems by the Use of Pilot Stations*.

Jones, C.S., Li, T., Sukalski, A., Thompson, D.A. and Cwiertny, D.M. (2020), "Use of real-time sensors for compliance monitoring of nitrate in finished drinking water", *Water Science and Technology*, Vol. 82 No. 12, pp. 2725–2736, doi: 10.2166/wst.2020.365.

Kaewwongsri, K. and Silanon, K. (2020), "Design and Implement of a Weather Monitoring Station using CoAP on NB-IoT Network", *17th International Conference on Electrical Engineering/Electronics, Computer, Telecommunications and Information Technology, ECTI-CON 2020*, pp. 230–233, doi: 10.1109/ECTI-CON49241.2020.9158290.

Karki, S., Ziar, H., Korevaar, M., Bergmans, T., Mes, J. and Isabella, O. (2021), "Performance Evaluation of Silicon-Based Irradiance Sensors Versus Thermopile Pyranometer", *IEEE Journal of Photovoltaics*, Vol. 11 No. 1, pp. 144–149, doi: 10.1109/JPHOTOV.2020.3038342.

Kelechi, A.H., Alsharif, M.H., Anya, A.C.E., Bonet, M.U., Uyi, S.A., Uthansakul, P., Nebhen, J., *et al.* (2021), "Design and Implementation of a Low-Cost Portable Water Quality Monitoring System", *Computers, Materials and Continua*, Vol. 69 No. 2, pp. 2405–2424, doi: 10.32604/cmc.2021.018686.

Khattab, A., Abdelgawad, A. and Yelmarthi, K. (2016), "Design and implementation of a cloud-based IoT scheme for precision agriculture", *Proceedings of the International Conference on Microelectronics, ICM*, Vol. 0, pp. 201–204, doi: 10.1109/ICM.2016.7847850.

Kombo, O.H., Kumaran, S. and Bovim, A. (2021), "Design and Application of a Low-Cost, Low- Power, LoRa-GSM, IoT Enabled System for Monitoring of Groundwater Resources with Energy Harvesting Integration", *IEEE Access*, Institute of Electrical and Electronics Engineers Inc., Vol. 9, pp. 128417–128433, doi: 10.1109/ACCESS.2021.3112519.

Koshoeva, B.B., Mikheeva, N.I., Mikheev, D.I. and Bakalova, A.T. (2021), "Arduino-based automated system for determining water flow consumption in open flow", *Journal of Physics: Conference Series*, Vol. 2142 No. 1, p. 012009, doi: 10.1088/1742-6596/2142/1/012009.

Kotamäki, N., Thessler, S., Koskiaho, J., Hannukkala, A., Huitu, H., Huttula, T., Havento, J., *et al.* (2009), "Wireless in-situ Sensor Network for Agriculture and Water Monitoring on a River Basin Scale in Southern Finland: Evaluation from a Data User's Perspective", *Sensors*, Vol. 9 No. 4, pp. 2862–2883, doi: 10.3390/s90402862.

Koutalakis, P., Tzoraki, O. and Zaimes, G. (2019), "Uavs for hydrologic scopes: Application of a low-cost UAV to estimate surface water velocity by using three different image-based methods", *Drones*, Vol. 3 No. 1, pp. 1–15, doi: 10.3390/drones3010014.

Kumar, P., Morawska, L., Martani, C., Biskos, G., Neophytou, M., Di Sabatino, S., Bell, M., *et al.* (2015), "The rise of low-cost sensing for managing air pollution in cities", *Environment International*, Elsevier Ltd, Vol. 75, pp. 199–205, doi: 10.1016/j.envint.2014.11.019.

Lambrou, T.P., Anastasiou, C.C., Panayiotou, C.G. and Polycarpou, M.M. (2014), "A low-cost sensor network for real-time monitoring and contamination detection in drinking water distribution systems", *IEEE Sensors Journal*, Vol. 14 No. 8, pp. 2765–2772, doi: 10.1109/JSEN.2014.2316414.

Lanza, L., Leroy, M., Alexandropoulos, C., Stagi, L. and Wauben, W. (2006), "WMO LABORATORY INTERCOMPARISON OF RAINFALL INTENSITY GAUGES", *Td-N° 1304*, No. 84, pp. 1–139.

Lanza, L.G. and Vuerich, E. (2009), "The WMO Field Intercomparison of Rain Intensity Gauges", *Atmospheric Research*, Elsevier B.V., Vol. 94 No. 4, pp. 534–543, doi: 10.1016/j.atmosres.2009.06.012.

Lee, H., Kang, J., Kim, S., Im, Y., Yoo, S. and Lee, D. (2020), "Long-term evaluation and calibration of low-cost particulate matter (PM) sensor", *Sensors (Switzerland)*, MDPI AG, Vol. 20 No. 13, pp. 1–25, doi: 10.3390/s20133617.

Lemaire-Potteau, E., Perrin, M. and Genies, S. (2009), "BATTERIES | Charging Methods", *Encyclopedia of Electrochemical Power Sources*, Elsevier, 1 January, pp. 413–423, doi: 10.1016/B978-044452745-5.00885-6.

Leonowicz, Z., Institute of Electrical and Electronics Engineers, IEEE Electromagnetic Compatibility Society, IEEE Power & Energy Society, IEEE Industry Applications Society and Industrial and Commercial Power

Systems Europe (4th : 2020 : Online). (2020), “Conference proceedings : 2020 IEEE International Conference Environment and Electrical Engineering and 2020 IEEE Industrial and Commercial Power Systems Europe (EEEIC / I & CPS Europe) : 9-12 June, 2020, Madrid, Spain”.

Liu, F., Olesen, K.B., Borregaard, A.R. and Vollertsen, J. (2019), “Microplastics in urban and highway stormwater retention ponds”, *Science of the Total Environment*, Elsevier B.V., Vol. 671, pp. 992–1000, doi: 10.1016/j.scitotenv.2019.03.416.

Lockridge, G., Dzwonkowski, B., Nelson, R. and Powers, S. (2016), “Development of a low-cost arduino-based sonde for coastal applications”, *Sensors (Switzerland)*, Vol. 16 No. 4, pp. 1–16, doi: 10.3390/s16040528.

Loizou, K. and Koutroulis, E. (2016), “Water level sensing: State of the art review and performance evaluation of a low-cost measurement system”, *Measurement: Journal of the International Measurement Confederation*, Elsevier B.V., Vol. 89, pp. 204–214, doi: 10.1016/j.measurement.2016.04.019.

López, E., Vionnet, C., Ferrer-Cid, P., Barcelo-Ordinas, J.M., Garcia-Vidal, J., Contini, G., Prodolliet, J., *et al.* (2022), “A Low-Power IoT Device for Measuring Water Table Levels and Soil Moisture to Ease Increased Crop Yields”, *Sensors (Basel, Switzerland)*, NLM (Medline), Vol. 22 No. 18, doi: 10.3390/s22186840.

López Lorente, J., Liu, X. and Morrow, D.J. (2020), “Worldwide evaluation and correction of irradiance measurements from personal weather stations under all-sky conditions”, *Solar Energy*, Elsevier, Vol. 207 No. January, pp. 925–936, doi: 10.1016/j.solener.2020.06.073.

LoRa Alliance. (2023), “Homepage - LoRa Alliance®”, available at: https://lora-alliance.org/ (accessed 16 March 2023).

Mahardika, S.A., Umi Fadililah, S.T. and Eng, M. (2021), *Sistem Monitoring Dan Kontrol Otomatis Kadar PH Air Serta Kandungan Nutrisi Pada Budidaya Tanaman Hidroponik Menggunakan Blynk Android*, Doctoral dissertation, Universitas Muhammadiyah Surakarta.

Martín-Martín, A., Thelwall, M., Orduna-Malea, E. and Delgado López-Cózar, E. (2021), “Google Scholar, Microsoft Academic, Scopus, Dimensions, Web of Science, and OpenCitations’ COCI: a multidisciplinary

comparison of coverage via citations", *Scientometrics*, Vol. 126 No. 1, pp. 871–906, doi: 10.1007/s11192-020-03690-4.

Math, R.K. and Dharwadkar, N. V. (2017), "A wireless sensor network based low cost and energy efficient frame work for precision agriculture", *2017 International Conference on Nascent Technologies in Engineering, ICNTE 2017 - Proceedings*, doi: 10.1109/ICNTE.2017.7947883.

Mdemu, M., Kissoly, L., Bjornlund, H., Kimaro, E., Christen, E.W., van Rooyen, A., Stirzaker, R., *et al.* (2020), "The role of soil water monitoring tools and agricultural innovation platforms in improving food security and income of farmers in smallholder irrigation schemes in Tanzania", *International Journal of Water Resources Development*, Routledge, Vol. 36 No. 1, pp. 1–23, doi: 10.1080/07900627.2020.1765746.

Menon, G.S., Ramesh, M.V. and Divya, P. (2017), "A low cost wireless sensor network for water quality monitoring in natural water bodies", *GHTC 2017 - IEEE Global Humanitarian Technology Conference, Proceedings*, Vol. 2017-Janua, pp. 1–8, doi: 10.1109/GHTC.2017.8239341.

Michelon, A., Benoit, L., Beria, H., Ceperley, N. and Schaefli, B. (2020), "On the value of high density rain gauge observations for small Alpine headwater catchments", *Hydrology and Earth System Sciences Discussions*, No. January, pp. 1–31, doi: 10.5194/hess-2019-683.

Mind4stormwater. (2022), "GitHub - fcherqui/Mind4stormwater: Water-related projects", available at: https://github.com/fcherqui/Mind4stormwater (accessed 2 September 2022).

Mittelbach, H., Casini, F., Lehner, I., Teuling, A.J. and Seneviratne, S.I. (2011), "Soil moisture monitoring for climate research: Evaluation of a low-cost sensor in the framework of the Swiss soil moisture experiment (SwissSMEX) campaign", *Journal of Geophysical Research Atmospheres*, Vol. 116 No. 5, pp. 1–11, doi: 10.1029/2010JD014907.

Montserrat, A., Gutierrez, O., Poch, M. and Corominas, L. (2013), "Field validation of a new low-cost method for determining occurrence and duration of combined sewer overflows", *Science of the Total Environment*, Elsevier B.V., Vol. 463–464, pp. 904–912, doi: 10.1016/j.scitotenv.2013.06.010.

Moody, J.A. and Martin, R.G. (2015), “Measurements of the initiation of post-wildfire runoff during rainstorms using in situ overland flow detectors”, *Earth Surface Processes and Landforms*, Vol. 40 No. 8, pp. 1043–1056, doi: 10.1002/esp.3704.

Moore, J.A., Gendre, B., Coward, D.M., Crisp, H. and Klotz, A. (2020), “The Zadko Observatory”, *Robotic Observatories Workshop*, No. April 2009, pp. 1–5.

Morales-Morales, C., Najera-Medina, P.R., Castro-Bello, M., Morales-Morales, J. and Hernandez-Romano, J. (2020), “Wireless Real-Time Monitoring System Applied in a Tomato Greenhouse”, *2020 IEEE International Autumn Meeting on Power, Electronics and Computing, ROPEC 2020*, Institute of Electrical and Electronics Engineers Inc., doi: 10.1109/ROPEC50909.2020.9258762.

Morawska, L., Thai, P.K., Liu, X., Asumadu-Sakyi, A., Ayoko, G., Bartonova, A., Bedini, A., *et al.* (2018), “Applications of low-cost sensing technologies for air quality monitoring and exposure assessment: How far have they gone?”, *Environment International*, Vol. 116 No. February, pp. 286–299, doi: 10.1016/j.envint.2018.04.018.

Moreno-Rangel, A., Sharpe, T., Musau, F. and McGill, G. (2018), “Field evaluation of a low-cost indoor air quality monitor to quantify exposure to pollutants in residential environments”, *Journal of Sensors and Sensor Systems*, Vol. 7 No. 1, pp. 373–388, doi: 10.5194/jsss-7-373-2018.

Morón, C., Diaz, J.P., Ferrández, D. and Saiz, P. (2018), “Design, development and implementation of a weather station prototype for renewable energy systems”, *Energies*, MDPI AG, Vol. 11 No. 9, doi: 10.3390/en11092234.

Morris, A.S. and Langari, R. (2016), *Measurement and Instrumentation*, *Measurement and Instrumentation*, Elsevier, doi: 10.1016/C2013-0-15387-1.

Moyón Rivera, C.W. and Ordóñez Berrones, D.K. (2019), *Construcción de Un Prototipo de Red de Nodos Inteligentes Para Supervisar La Calidad y Niveles Del Agua Potable En Los Tanques de Reserva de EP-EMAPAR*, Bachelor’s thesis, Escuela Superior Politécnica de Chimborazo.

Müller, A., Österlund, H., Marsalek, J. and Viklander, M. (2020), "The pollution conveyed by urban runoff: A review of sources", *Science of the Total Environment*, Vol. 709, doi: 10.1016/j.scitotenv.2019.136125.

Mwemezi, K.W. (2020), *Innovative Secured Water Quality Monitoring System Using Remote Sensors : Case of Pangani Water Basin*, Doctoral dissertation, NM-AIST.

Nagahage, E.A.A.D., Nagahage, I.S.P. and Fujino, T. (2019), "Calibration and validation of a low-cost capacitive moisture sensor to integrate the automated soil moisture monitoring system", *Agriculture (Switzerland)*, Vol. 9 No. 7, doi: 10.3390/agriculture9070141.

Nasution, T.H., Dika, S., Sinulingga, E.P., Tanjung, K. and Harahap, L.A. (2020), "Analysis of the use of SEN0161 pH sensor for water in goldfish ponds", *IOP Conference Series: Materials Science and Engineering*, Vol. 851 No. 1, doi: 10.1088/1757-899X/851/1/012053.

Nasution, T.H., Siagian, E.C., Tanjung, K. and Soeharwinto. (2018), "Design of river height and speed monitoring system by using Arduino", *IOP Conference Series: Materials Science and Engineering*, Vol. 308 No. 1, pp. 1–8, doi: 10.1088/1757-899X/308/1/012031.

Nazer, M., Hajibeigy, M.T., Yong, S., Noum, E. and Ghadimi, A. (2018), "A Self Continuous Lake Water Quality Monitoring System for Early Pollution Detection", Vol. 10.

Ndulue, E. and Ranjan, R.S. (2021), "Performance of the FAO Penman-Monteith equation under limiting conditions and fourteen reference evapotranspiration models in southern Manitoba", *Theoretical and Applied Climatology*, Theoretical and Applied Climatology, Vol. 143 No. 3–4, pp. 1285–1298, doi: 10.1007/s00704-020-03505-9.

NF EN 17075. (2018), *NF EN 17075*.

Nguyen, B.T. and Rittmann, B.E. (2018), "Low-cost optical sensor to automatically monitor and control biomass concentration in microalgal cultivation", *Algal Research*, Elsevier, Vol. 32 No. August 2017, pp. 101–106, doi: 10.1016/j.algal.2018.03.013.

Nickel, J.P., Sacher, F. and Fuchs, S. (2021), "Up-to-date monitoring data of wastewater and stormwater quality in Germany", *Water Research*, Elsevier Ltd, Vol. 202 No. March, p. 117452, doi: 10.1016/j.watres.2021.117452.

Nouman, A.S., Chokhachian, A., Santucci, D. and Auer, T. (2019), "Prototyping of environmental kit for georeferenced transient outdoor comfort assessment", *ISPRS International Journal of Geo-Information*, Vol. 8 No. 2, doi: 10.3390/ijgi8020076.

Offset Electronics. (2023), "SEN-15901 data sheet", available at: https://cdn.sparkfun.com/assets/d/1/e/0/6/DS-15901-Weather_Meter.pdf (accessed 25 January 2023).

Othaman, N.N.C., Isa, M.N.M., Hussin, R., Ismail, R.C., Naziri, S.Z.M., Murad, S.A.Z., Harun, A., *et al.* (2021), "Development of Soil Electrical Conductivity (EC) Sensing System in Paddy Field", *Journal of Physics: Conference Series*, Vol. 1755 No. 1, doi: 10.1088/1742-6596/1755/1/012005.

OTT HydroMet. (2023a), "OTT Pluvio^2 L 400 RH Weighing Rain Gauge, 400 cm^2/750 mm, Heated Rim | OTT HydroMet", available at: https://www.otthydromet.com/en/p-ott-pluvio-weighing-rain-gauge/70.040.021.9.0 (accessed 25 January 2023).

OTT HydroMet. (2023b), "OTT PLS - Pressure Level Sensor - OTT Hydromet", available at: https://www.ott.com/products/water-level-1/ott-pls-pressure-level-sensor-959/ (accessed 8 February 2023).

Panjabi, K., Rudra, R., Gregori, S., Goel, P., Daggupati, P., Shukla, R. and Mekonnen, B. (2018), "Development and Field Evaluation of a Low-Cost Wireless Sensor Network System for Hydrological Monitoring of a Small Agricultural Watershed", *Open Journal of Civil Engineering*, Vol. 08 No. 02, pp. 166–182, doi: 10.4236/ojce.2018.82014.

Patalano, A., García, C.M. and Rodríguez, A. (2017), "Rectification of Image Velocity Results (RIVeR): A simple and user-friendly toolbox for large scale water surface Particle Image Velocimetry (PIV) and Particle Tracking Velocimetry (PTV)", *Computers and Geosciences*, Vol. 109 No. December, pp. 323–330, doi: 10.1016/j.cageo.2017.07.009.

Patrignani, A., Knapp, M., Redmond, C. and Santos, E. (2020), "Technical overview of the kansas mesonet", *Journal of Atmospheric and Oceanic Technology*, Vol. 37 No. 12, pp. 2167–2183, doi: 10.1175/JTECH-D-19-0214.1.

Payero, J.O., Qiao, X., Khalilian, A., Mirzakhani-Nafchi, A. and Davis, R. (2017), "Evaluating the Effect of Soil Texture on the Response of Three Types of Sensors Used to Monitor Soil Water Status", *Journal of Water Resource and Protection*, Vol. 09 No. 06, pp. 566–577, doi: 10.4236/jwarp.2017.96037.

Pellerin, B.A., Stauffer, B.A., Young, D.A., Sullivan, D.J., Bricker, S.B., Walbridge, M.R., Clyde, G.A., *et al.* (2016), "Emerging Tools for Continuous Nutrient Monitoring Networks: Sensors Advancing Science and Water Resources Protection", *Journal of the American Water Resources Association*, Vol. 52 No. 4, pp. 993–1008, doi: 10.1111/1752-1688.12386.

Pereira, W.F., Fonseca, L. da S., Putti, F.F., Góes, B.C. and Naves, L. de P. (2020), "Environmental monitoring in a poultry farm using an instrument developed with the internet of things concept", *Computers and Electronics in Agriculture*, Elsevier B.V., Vol. 170, doi: 10.1016/j.compag.2020.105257.

Placidi, P., Gasperini, L., Grassi, A., Cecconi, M. and Scorzoni, A. (2020), "Characterization of low-cost capacitive soil moisture sensors for IoT networks", *Sensors (Switzerland)*, MDPI AG, Vol. 20 No. 12, pp. 1–14, doi: 10.3390/s20123585.

Placidi, P., Morbidelli, R., Fortunati, D., Papini, N., Gobbi, F. and Scorzoni, A. (2021), "Monitoring soil and ambient parameters in the iot precision agriculture scenario: An original modeling approach dedicated to low-cost soil water content sensors", *Sensors*, MDPI AG, Vol. 21 No. 15, doi: 10.3390/s21155110.

Polotu. (2022), "Pololu 12V Step-Up Voltage Regulator U3V12F12", available at: https://www.pololu.com/product/2117 (accessed 4 September 2022).

Prabhakaran, P. and Ravindran, R.M. (2019), "A Survey of Wireless Sensor Network in Precision Agriculture with different Cloud based IoT Schemes", *Integrated Intelligent Research (IIR)*, No. 60, pp. 60–63.

Precis mecanique. (2023), “Pluviomètres automatiques”, available at: https://www.precis-mecanique.com/specialites/precipitations-cumul-detection/pluviometres-automatiques.html (accessed 25 January 2023).

Prudencio, L. and Null, S.E. (2018), “Stormwater management and ecosystem services: A review”, *Environmental Research Letters*, Vol. 13 No. 3, doi: 10.1088/1748-9326/aaa81a.

Pule, M., Yahya, A. and Chuma, J. (2017), “Wireless sensor networks: A survey on monitoring water quality”, *Journal of Applied Research and Technology*, Universidad Nacional Autónoma de México, Centro de Ciencias Aplicadas y Desarrollo Tecnológico. This is an open access article under the CC BY-NC-ND license (http://creativecommons.org/licenses/by-nc-nd/4.0/)., Vol. 15 No. 6, pp. 562–570, doi: 10.1016/j.jart.2017.07.004.

pycom. (2022), “LoPy4 - Pycom - Quadruple Bearer MicroPython enabled Dev Board”, available at: https://pycom.io/product/lopy4/ (accessed 4 September 2022).

Qiao, X.J., Kristoffersson, A. and Randrup, T.B. (2018), “Challenges to implementing urban sustainable stormwater management from a governance perspective: A literature review”, *Journal of Cleaner Production*, Elsevier Ltd, Vol. 196, pp. 943–952, doi: 10.1016/j.jclepro.2018.06.049.

Qin, Y., Alam, A.U., Pan, S., Howlader, M.M.R., Ghosh, R., Hu, N.X., Jin, H., *et al.* (2018), “Integrated water quality monitoring system with pH, free chlorine, and temperature sensors”, *Sensors and Actuators, B: Chemical*, Elsevier B.V., Vol. 255, pp. 781–790, doi: 10.1016/j.snb.2017.07.188.

Qingchuan ZHU. (2023), “QingChuan-ZHU/Low-cost-weather-station-Arduino-Nano-Code”, available at: https://github.com/QingChuan-ZHU/Low-cost-weather-station-Arduino-Nano-Code (accessed 25 January 2023).

Radogna, A.V., Latino, M.E., Menegoli, M., Prontera, C.T., Morgante, G., Mongelli, D., Giampetruzzi, L., *et al.* (2022), “A Monitoring Framework with Integrated Sensing Technologies for Enhanced Food Safety and Traceability”, *Sensors*, MDPI, Vol. 22 No. 17, doi: 10.3390/s22176509.

Rai, A.C., Kumar, P., Pilla, F., Skouloudis, A.N., Di Sabatino, S., Ratti, C., Yasar, A., *et al.* (2017), "End-user perspective of low-cost sensors for outdoor air pollution monitoring", *Science of the Total Environment*, Elsevier B.V., Vol. 607–608, pp. 691–705, doi: 10.1016/j.scitotenv.2017.06.266.

Ramadhan, A.J. (2020), "Smart water-quality monitoring system based on enabled real-time internet of things", *Journal of Engineering Science and Technology*, Vol. 15 No. 6, pp. 3514–3527.

Rao, A.S., Marshall, S., Gubbi, J., Palaniswami, M., Sinnott, R. and Pettigrovet, V. (2013), "Design of low-cost autonomous water quality monitoring system", *Proceedings of the 2013 International Conference on Advances in Computing, Communications and Informatics, ICACCI 2013*, pp. 14–19, doi: 10.1109/ICACCI.2013.6637139.

Rivas-Sánchez, Y.A., Moreno-Pérez, M.F. and Roldán-Cañas, J. (2019), "Environment control with low-cost microcontrollers and microprocessors: Application for green walls", *Sustainability (Switzerland)*, Vol. 11 No. 3, doi: 10.3390/su11030782.

Robinson, D.A., Campbell, C.S., Hopmans, J.W., Hornbuckle, B.K., Jones, S.B., Knight, R., Ogden, F., *et al.* (2008), "Soil Moisture Measurement for Ecological and Hydrological Watershed-Scale Observatories: A Review", *Vadose Zone Journal*, Vol. 7 No. 1, pp. 358–389, doi: 10.2136/vzj2007.0143.

Roger Meier. (2023), "Roger Meier's Freeware", available at: https://freeware.the-meiers.org/ (accessed 15 March 2023).

Rossi, F., Motta, O., Matrella, S., Proto, A. and Vigliotta, G. (2015), "Nitrate removal from wastewater through biological denitrification with OGA 24 in a batch reactor", *Water (Switzerland)*, Vol. 7 No. 1, pp. 51–62, doi: 10.3390/w7010051.

Rozaq, I.A., Setyaningsih, N.Y.D. and Gunawan, B. (2020), "Pengkondisian Sinyal Sensor Salinitas DFR0300 Menggunakan Arduino Due", *Proceeding SENDIU*.

RS. (2022), "UPF50B250RV | Résistance Film métallique 250Ω ±0.1%, 0.5W | RS", available at: https://fr.rs-online.com/web/p/resistances-traversantes/8073753 (accessed 2 September 2022).

Rusydi, A.F. (2018), “Correlation between conductivity and total dissolved solid in various type of water: A review”, *IOP Conference Series: Earth and Environmental Science*, Vol. 118 No. 1, doi: 10.1088/1755-1315/118/1/012019.

Saha, S., Rajib, R.H. and Kabir, S. (2018), “IoT Based Automated Fish Farm Aquaculture Monitoring System”, *2018 International Conference on Innovations in Science, Engineering and Technology, ICISET 2018*, IEEE, No. October, pp. 201–206, doi: 10.1109/ICISET.2018.8745543.

Saleh, M., Elhajj, I.H., Asmar, D., Bashour, I. and Kidess, S. (2016), “Experimental evaluation of low-cost resistive soil moisture sensors”, *2016 IEEE International Multidisciplinary Conference on Engineering Technology, IMCET 2016*, pp. 179–184, doi: 10.1109/IMCET.2016.7777448.

Salehi, M., Aghilinasrollahabadi, K. and Esfandarani, M.S. (2020), “An investigation of stormwater quality variation within an industry sector using the self-reported data collected under the stormwater monitoring program”, *Water (Switzerland)*, Vol. 12 No. 11, pp. 1–16, doi: 10.3390/w12113185.

Salgado, J.A., Feio, M.C., Silva, L.M., Monteiro, V., Afonso, J.L. and Afonso, J.A. (2020), “Development of a Compact and Low-Cost Weather Station for Renewable Energy Applications”, *Lecture Notes of the Institute for Computer Sciences, Social-Informatics and Telecommunications Engineering, LNICST*, Vol. 315 LNICST, pp. 127–139, doi: 10.1007/978-3-030-45694-8_10.

Salman, A.K., Aldulaimy, S.E., Mohammed, H.J. and Abed, Y.M. (2021), “Performance of soil moisture sensors in gypsiferous and salt-affected soils”, *Biosystems Engineering*, Elsevier Ltd, Vol. 209, pp. 200–209, doi: 10.1016/j.biosystemseng.2021.07.006.

Sanyal, J., Carbonneau, P. and Densmore, A.L. (2014), “Low-cost inundation modelling at the reach scale with sparse data in the Lower Damodar River basin, India”, *Hydrological Sciences Journal*, Taylor & Francis, Vol. 59 No. 12, pp. 2086–2102, doi: 10.1080/02626667.2014.884718.

Saputra, R.E., Irawan, B. and Nugraha, Y.E. (2017), “System design and implementation automation system of expert system on hydroponics nutrients control using forward chaining method”, *2017 IEEE Asia Pacific*

Conference on Wireless and Mobile (APWiMob), Vol. 2017-Novem, IEEE, pp. 41–46, doi: 10.1109/APWiMob.2017.8284002.

Sarkar, I., Pal, B., Datta, A. and Roy, S. (2020), "Wi-Fi-Based Portable Weather Station for Monitoring Temperature, Relative Humidity, Pressure, Precipitation, Wind Speed, and Direction", *Advances in Intelligent Systems and Computing*, Vol. 933 No. August, pp. 399–404, doi: 10.1007/978-981-13-7166-0_39.

Schellart, A., Blumensaat, F., Clemens-Meyer, F., van der Werf, J., Mohtar, W.H.M.W., Ramly, S., Muhammad, N., *et al.* (2021), "Chapter 11 Data collection in urban drainage and stormwater management systems – case studies", *Metrology in Urban Drainage and Stormwater Management: Plug and Pray*, IWA Publishing, pp. 415–469, doi: 10.2166/9781789060119_0415.

Schenk, H., Hirsch, T., Wittmann, M., Wilbert, S., Keller, L. and Prahl, C. (2015), "Design and Operation of an Irradiance Measurement Network", *Energy Procedia*, Elsevier B.V., Vol. 69, pp. 2019–2030, doi: 10.1016/j.egypro.2015.03.212.

SDI-12 Support Group. (2009), *SDI-12 A Serial-Digital Interface Standard for Microprocessor-Based Sensors*.

Semenov, E.S., Ivanchenko, G.S., Kharchenko, A. V. and Kolobanov, R. V. (2019), "Mobile weather station based on ATmega2560 microprocessor", *IOP Conference Series: Materials Science and Engineering*, Vol. 537 No. 3, doi: 10.1088/1757-899X/537/3/032086.

Shamsi, S.M., Abdullah, H.B. and Bakar, L. (2020), "Development of Integrated EC and pH Sensor for Low-Cost Fertigation System", *IOP Conference Series: Earth and Environmental Science*, Vol. 515 No. 1, doi: 10.1088/1755-1315/515/1/012016.

Shi, B., Catsamas, S., Kolotelo, P., Wang, M., Lintern, A., Jovanovic, D., Bach, P.M., *et al.* (2021), "A low-cost water depth and electrical conductivity sensor for detecting inputs into urban stormwater networks", *Sensors*, Vol. 21 No. 9, doi: 10.3390/s21093056.

Shrenika, R.M., Chikmath, S.S., Ravi Kumar, A. V., Divyashree, Y. V. and Swamy, R.K. (2017), "Non-contact Water Level Monitoring System Implemented Using LabVIEW and Arduino", *Proceedings - 2017*

International Conference on Recent Advances in Electronics and Communication Technology, ICRAECT 2017, Institute of Electrical and Electronics Engineers Inc., pp. 306–309, doi: 10.1109/ICRAECT.2017.51.

Siyang, S. and Kerdcharoen, T. (2016), "Development of unmanned surface vehicle for smart water quality inspector", *2016 13th International Conference on Electrical Engineering/Electronics, Computer, Telecommunications and Information Technology, ECTI-CON 2016*, pp. 3–7, doi: 10.1109/ECTICon.2016.7561370.

SM, S.N., Reddy Yasa, P., MV, N., Khadirnaikar, S. and Pooja Rani. (2019), "Mobile monitoring of air pollution using low cost sensors to visualize spatio-temporal variation of pollutants at urban hotspots", *Sustainable Cities and Society*, Elsevier, Vol. 44 No. October 2018, pp. 520–535, doi: 10.1016/j.scs.2018.10.006.

Smith, R.J. (2017), "Compare DHT22, DHT11 and Sensirion SHT71", available at: https://www.kandrsmith.org/RJS/Misc/Hygrometers/calib_dht22_dht11_sht71.html (accessed 23 February 2021).

Smith, R.J. (2018), "Compare DHT22, AM2302, AM2320, AM2321, SHT71, HTU21D, Si7021, BME280", available at: https://www.kandrsmith.org/RJS/Misc/Hygrometers/calib_many.html (accessed 23 February 2021).

SparkFun. (2022), "SparkFun Nano Power Timer - TPL5110 - PRT-15353 - SparkFun Electronics", available at: https://www.sparkfun.com/products/15353 (accessed 4 September 2022).

Steele, D.D., Scherer, T.F., Akyuz, F.A., Wamono, A., Desutter, T.M. and Tuscherer, S.R. (2014), "Evaluation of a Low-Cost Optical Rain Sensor", *ASABE/CSBE North Central Intersectional Meeting*, Vol. 7004, pp. 1–12, doi: 10.13031/sd14063.

Sulzer, M., Christen, A. and Matzarakis, A. (2022), "A Low-Cost Sensor Network for Real-Time Thermal Stress Monitoring and Communication in Occupational Contexts", *Sensors*, MDPI, Vol. 22 No. 5, doi: 10.3390/s22051828.

Sumitra, I.D., Hou, R. and Supatmi, S. (2017), "Design and deployment of wireless sensor networks for flood detection in Indonesia", *Lecture Notes in Computer Science (Including Subseries Lecture Notes in Artificial*

Intelligence and Lecture Notes in Bioinformatics), Vol. 10602 LNCS No. October 2018, pp. 313–325, doi: 10.1007/978-3-319-68505-2_27.

Sun, B., Ahmed, F., Sun, F., Qian, Q. and Xiao, Y. (2016), "Water quality monitoring using STORM 3 Data Loggers and a wireless sensor network", *International Journal of Sensor Networks*, Vol. 20 No. 1, pp. 26–36, doi: 10.1504/IJSNET.2016.074270.

Tagle, M., Rojas, F., Reyes, F., Vásquez, Y., Hallgren, F., Lindén, J., Kolev, D., *et al.* (2020), "Field performance of a low-cost sensor in the monitoring of particulate matter in Santiago, Chile", *Environmental Monitoring and Assessment*, Environmental Monitoring and Assessment, Vol. 192 No. 3, doi: 10.1007/s10661-020-8118-4.

Tai, A.Y.C., Chen, L.W.A., Wang, X., Chow, J.C. and Watson, J.G. (2017), "Atmospheric deposition of particles at a sensitive alpine lake: Size-segregated daily and annual fluxes from passive sampling techniques", *Science of the Total Environment*, Elsevier B.V., Vol. 579, pp. 1736–1744, doi: 10.1016/j.scitotenv.2016.11.117.

Tebbs, E., Wilson, M., Mulligan, H., Chan, K., Gupta, M., Maurya, V. and Srivastava, P. (2019), "Satellite Soil Moisture Observations : Applications in the UK and India Report of Pump Priming Project", No. December.

Texas Instruments. (2018), "ADS111x Ultra-Small, Low-Power, I 2C-Compatible, 860-SPS, 16-Bit ADCs With Internal Reference, Oscillator, and Programmable Comparator", available at: https://www.ti.com/lit/ds/symlink/ads1115.pdf?ts=1680318144803&ref_url=https%253A%252F%252Fwww.ti.com%252Fproduct%252FADS1115%253Futm_source%253Dgoogle%2526utm_medium%253Dcpc%2526utm_campaign%253Dasc-dc-null-prodfolderdynamic-cpc-pf-google-wwe_int%2526utm_content%253Dprodfolddynamic%2526ds_k%253DDYNAMIC%2BSEARCH%2BADS%2526DCM%253Dyes%2526gclid%253DCj0KCQjwiZqhBhCJARIsACHHEH9A4jHjF4xGYgQU4oStG9GLdrvLurbX-V4aVovvuOVeSese44jdgFAaAoZYEALw_wcB%2526gclsrc%253Daw.ds (accessed 1 April 2023).

The Things Network. (2023), "The Things Network", available at: https://www.thethingsnetwork.org/ (accessed 16 March 2023).

Thebault, E., Sage, J., Ferrier, V., H, B.K., Berthier, E., Thebault, E., Sage, J., *et al.* (2020), *La Gestion Patrimoniale Des Ouvrages et Aménagements Dédiés à La Gestion Des Eaux Pluviales Urbaines. Retour d'expérience Auprès d'une Sélection de 21 Collectivités*, doi: https://hal.archives-ouvertes.fr/hal-03010195.

Theisen, A., Ungar, M., Sheridan, B. and Illston, B.G. (2020), "More science with less: Evaluation of a 3D-printed weather station", *Atmospheric Measurement Techniques*, Vol. 13 No. 9, pp. 4699–4713, doi: 10.5194/amt-13-4699-2020.

Thomas, A.O., Bos, D., Morison, P. and Tim, D. (2016), "Operation and Maintenance of Stormwater Control Measures L ' entretien des techniques alternatives pou r la gestion des eaux pluviales", pp. 1–4.

Tohsing, K., Phaisathit, D., Pattarapanitchai, S., Masiri, I., Buntoung, S., Aumporn, O. and Wattan, R. (2019), "A development of a low-cost pyranometer for measuring broadband solar radiation", *Journal of Physics: Conference Series*, Vol. 1380 No. 1, doi: 10.1088/1742-6596/1380/1/012045.

Trevathan, J., Read, W. and Schmidtke, S. (2020), "Towards the development of an affordable and practical light attenuation turbidity sensor for remote near real-time aquatic monitoring", *Sensors (Switzerland)*, Vol. 20 No. 7, doi: 10.3390/s20071993.

Ula, D.A. (2020), *Rancang Bangun Sistem Monitoring Kualitas Air Layak Konsumsi Berbasis Internet of Things Dengan Metode Fuzzy Tsukamoto Sebagai Sistem Pendukung Keputusan*, Doctoral dissertation, Universitas Islam Negeri Maulana Malik Ibrahim.

Valente, A., Silva, S., Duarte, D., Pinto, F.C. and Soares, S. (2020), "Low-cost lorawan node for agro-intelligence iot", *Electronics (Switzerland)*, Vol. 9 No. 6, pp. 1–17, doi: 10.3390/electronics9060987.

Valenzuela, C., Sosa, C., del Refugio Castañeda, M., Palomeque, J. and Amaro, I.A. (2018), "Turbidity measurement system for aquaculture effluents using an open-source software and hardware", *Nature Environment and Pollution Technology*, Vol. 17 No. 3, pp. 957–961.

Vos, L.W., Raupach, T.H., Leijnse, H., Overeem, A., Berne, A. and Uijlenhoet, R. (2018), "High-Resolution Simulation Study Exploring the Potential of Radars, Crowdsourced Personal Weather Stations, and

Commercial Microwave Links to Monitor Small-Scale Urban Rainfall", *Water Resources Research*, Blackwell Publishing Ltd, Vol. 54 No. 12, pp. 10,293-10,312, doi: 10.1029/2018WR023393.

Wade, A.J., Palmer-Felgate, E.J., Halliday, S.J., Skeffington, R.A., Loewenthal, M., Jarvie, H.P., Bowes, M.J., *et al.* (2012), "Hydrochemical processes in lowland rivers: Insights from in situ, high-resolution monitoring", *Hydrology and Earth System Sciences*, Vol. 16 No. 11, pp. 4323–4342, doi: 10.5194/hess-16-4323-2012.

Wang, J., Yu, C.W. and Cao, S. (2021), "Urban development in the context of extreme flooding events", *Indoor and Built Environment*, Vol. 0 No. August, pp. 1–4, doi: 10.1177/1420326X211048577.

WeihaiJingxun Electronic. (2020), "Selection Manual", available at: https://www.mitrakatigasejahtera.com/images/produk/alat-ukur-udara/jxct-china/Selection-Manual-IoT-Sensors-Solution-2020.pdf (accessed 25 January 2023).

Wisudawan, H.N.P. (2021), "Design and Implementation of Real-Time Flood Early Warning System (FEWS) Based on IoT Blynk Application", *Elkha*, Vol. 13 No. 2, p. 113, doi: 10.26418/elkha.v13i2.49003.

WMO. (2008), *Guide to Hydrological Practice Volume I Hydrology-From Measurement to Hydrological Information*.

Wollheim, W.M., Mulukutla, G.K., Cook, C. and Carey, R.O. (2017), "Aquatic Nitrate Retention at River Network Scales Across Flow Conditions Determined Using Nested In Situ Sensors", *Water Resources Research*, Vol. 53 No. 11, pp. 9740–9756, doi: 10.1002/2017WR020644.

Wong, B.P. and Kerkez, B. (2016), "Real-time environmental sensor data: An application to water quality using web services", *Environmental Modelling and Software*, Elsevier Ltd, Vol. 84, pp. 505–517, doi: 10.1016/j.envsoft.2016.07.020.

Wootton, C. (2016), "Serial Peripheral Interface (SPI)", *Samsung ARTIK Reference*, Apress, Berkeley, CA, pp. 335–349, doi: 10.1007/978-1-4842-2322-2_21.

Yang, P. and Ng, T.L. (2017), “Gauging Through the Crowd: A Crowd-Sourcing Approach to Urban Rainfall Measurement and Storm Water Modeling Implications”, *Water Resources Research*, John Wiley & Sons, Ltd, Vol. 53 No. 11, pp. 9462–9478, doi: 10.1002/2017WR020682.

Yu, L., Rozemeijer, J.C., Peter Broers, H., van Breukelen, B.M., Middelburg, J.J., Ouboter, M. and van der Velde, Y. (2021), “Drivers of nitrogen and phosphorus dynamics in a groundwater-fed urban catchment revealed by high-frequency monitoring”, *Hydrology and Earth System Sciences*, Vol. 25 No. 1, pp. 69–87, doi: 10.5194/hess-25-69-2021.

Yuan, F., Huang, Y., Chen, X. and Cheng, E. (2018), “A Biological Sensor System Using Computer Vision for Water Quality Monitoring”, *IEEE Access*, Vol. 6, pp. 61535–61546, doi: 10.1109/ACCESS.2018.2876336.

Yuniarti, N., Hariyanto, D., Yatmono, S. and Abdillah, M. (2021), “Design and Development of IoT Based Water Flow Monitoring for Pico Hydro Power Plant”, *International Journal of Interactive Mobile Technologies*, Vol. 15 No. 7, pp. 69–80, doi: 10.3991/ijim.v15i07.18425.

Yuzhakov, M.S., Kazanin, V.A., Berzin, A.K., Kuleshov, G.E., Badin, A. v. and Filchenko, D.I. (2021), “IoT based system for real-time monitoring the hydrogen-ion activity in water bodies”, *Journal of Physics: Conference Series*, Vol. 1989 No. 1, doi: 10.1088/1742-6596/1989/1/012021.

Zakaria, Y. and Michael, K. (2017), “An Integrated Cloud-Based Wireless Sensor Network for Monitoring Industrial Wastewater Discharged into Water Sources”, *Wireless Sensor Network*, Vol. 09 No. 08, pp. 290–301, doi: 10.4236/wsn.2017.98016.

Zhang, D., Heery, B., O’Neil, M., Little, S., O’Connor, N.E. and Regan, F. (2019), “A low-cost smart sensor network for catchment monitoring”, *Sensors (Switzerland)*, Vol. 19 No. 10, pp. 1–22, doi: 10.3390/s19102278.

Zhou, B., Bian, C., Tong, J. and Xia, S. (2017), “Fabrication of a miniature multi-parameter sensor chip for water quality assessment”, *Sensors (Switzerland)*, Vol. 17 No. 1, pp. 1–14, doi: 10.3390/s17010157.

Zhu, Q. (2023a), “QingChuan-ZHU/Low-cost-rainfall-monitoring-station-Arduino-MKR-WAN-1310-code”, available at: https://github.com/QingChuan-ZHU/Low-cost-rainfall-monitoring-station-Arduino-MKR-WAN-1310-code (accessed 1 February 2023).

Zhu, Q. (2023b), “QingChuan-ZHU/Low-cost-rainfall-monitoring-staion-The-Things-Network-payload-formatters-code”, available at: https://github.com/QingChuan-ZHU/Low-cost-rainfall-monitoring-staion-The-Things-Network-payload-formatters-code/tree/main (accessed 1 February 2023).

Zhu, Q. (2023c), “QingChuan-ZHU/Node-RED-design-for-low-cost-rain-fall-monitoring-staion”, available at: https://github.com/QingChuan-ZHU/Node-RED-design-for-low-cost-rain-fall-monitoring-staion (accessed 1 February 2023).

Zhu, Q. (2023d), “QingChuan-ZHU/low-cost-TBRG-calibration-data-logger”, available at: https://github.com/QingChuan-ZHU/low-cost-TBRG-calibration-data-logger (accessed 6 February 2023).

Zhu, Q. (2023e), “GitHub - QingChuan-ZHU/Low-cost-water-turbidity-monitoring-station”, available at: https://github.com/QingChuan-ZHU/Low-cost-water-turbidity-monitoring-station (accessed 2 April 2023).

Zhu, Q. (2023f), “GitHub - QingChuan-ZHU/Low-cost-water-turbidity-system-reference-data-logger”, available at: https://github.com/QingChuan-ZHU/Low-cost-water-turbidity-system-reference-data-logger (accessed 2 April 2023).

Zhu, Q., Cherqui, F. and Bertrand-Krajewski, J.-L. (2023), “End-user perspective of low-cost sensors for urban stormwater monitoring: a review”, *Water Science & Technology*.

Zhu, X. and Lipeme Kouyi, G. (2019), “An Analysis of LSPIV-Based Surface Velocity Measurement Techniques for Stormwater Detention Basin Management”, *Water Resources Research*, doi: 10.1029/2018WR023813.

Appendices

APPENDIX A: EXPLORATION AND LESSONS IN USING LOW-COST TURBIDIMETER TO MONITOR WASTEWATER

This section presents the work about using the low-cost turbidimeter SEN-0189 to measure wastewater turbidity. Material and methods including tested low-cost sensor, used reference sensor, low-cost and reference data loggers, installation, and calibration are described firstly. Preliminary results and discussion are given afterward.

1. Material and methods

1.1 Low-cost sensor: SEN-0189

After literature review and market investigation, it seems that the turbidimeter module used in washing machine is the only off-the-shelf low-cost choice. This kind of module provided by DFRobot is named SEN-0189 (~ 10 €). The sensor appearance and schematic are shown below Figure 1. Characteristics of this module given by supplier is doubtful.

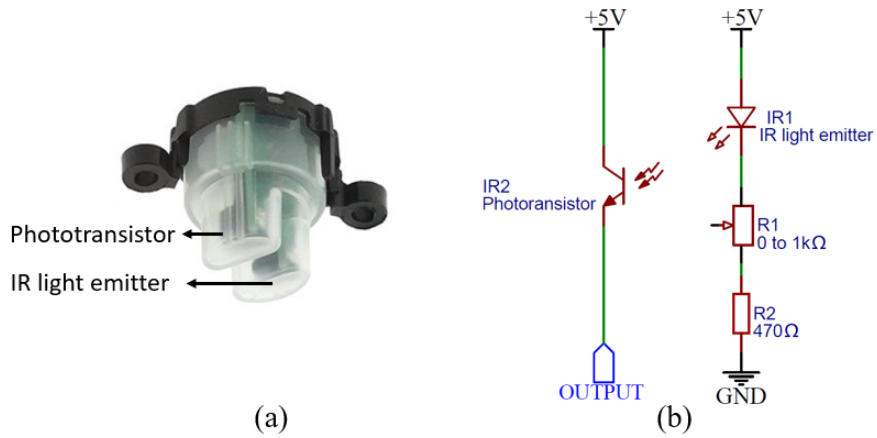

Figure 1. (a) Appearance of SEN-0189 sensor, size 44×30×34 mm, (b) Schematic of the sensor.

According to our investigation, as shown in Figure 1, the sensor of SEN-0189 contains an infrared (IR) light emitter and a phototransistor and resistors. The emitter and phototransistor are placed face to face. The increase in turbidity of the water will reduce the IR light received by the photoresistor. This is the principle of this kind of low-cost turbidimeter. As shown in the middle of (b) right part, there is a variable resistor (marked R1). The original setup value of this variable resistor is variance sensor to sensor but is the optimum value that could make the sensor has highest resolution. It is no need for end-uses to change this variable resistor by themselves.

DFRobot provides and interface board. According to our investigation, this board has two modes: when choosing (Aqualabo, 2023)digital mode, the operational amplifier inside it is set as a comparator to identify water turbidity is higher than a set value or not. When choosing analog mode, the operational amplifier inside it is set as a voltage follower. In our usage, this circuit is used and set in analog mode.

1.2 Reference sensor: Turbimax W CUS41 and Aqualabo sensor

In the field test, a traditional reference sensor Turbimax W CUS41 with transmitter Liquisys CUM M 223/253 provided by the same manufacturer is installed beside the low-cost turbidimeter system. Manufacturer (Endress+Hauser, 2023) indicates that its enlarged uncertainty is 5% of the measured value.

In the field test, a turbidity measurement kit from Aqualabo (Aqualabo, 2023) is also installed beside the low-cost turbidimeter system. The kit includes a sensor and a station to send data online through LoRa wireless network. According to the data sheet, manufacturer indicates that its enlarged uncertainty is 5% of NTU reading.

1.3 Full scale deployment

Low-cost data logger

The hardware design of low-cost data logger is shown in Figure 2.

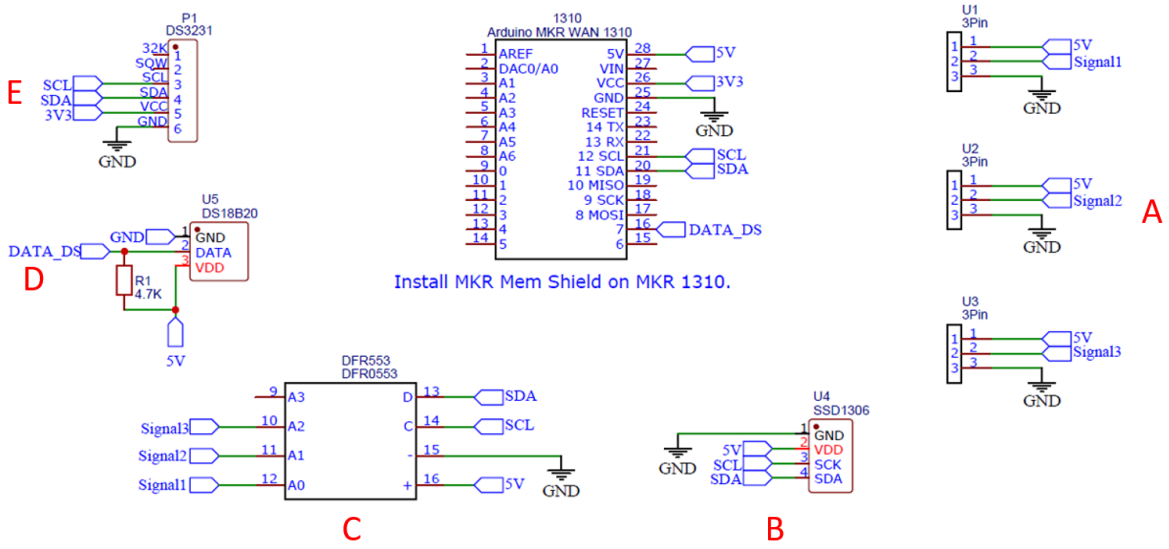

Figure 2. Hardware components of low-cost data logger

The core of low-cost data logger is Arduino MKR WAN 1310, from right to left in clockwise direction:

(A) Three interfaces to power and read the output of three SEN-0189.

(B) Little OLED Screen SSD1306 interface.

(C) Additional analog to digital converter module DFR0553 which has a chip ADS1115 to read output voltage of SEN-0189.

(D) Water temperature sensor DS18B20 interface.

(E) Real time clock module DS3231.

The system is powered by outer power supply by the USB port of Arduino. Real board is shown in Figure 3.

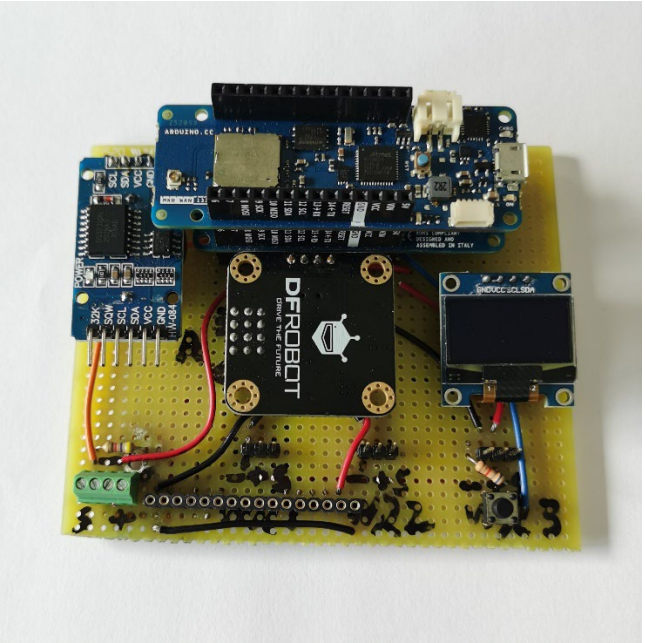

Figure 3. Real low-cost data logger board.

Arduino code structure is same to the rainfall monitoring station and shared in GitHub (Zhu, 2023e).

Reference data logger

Reference sensor Turbimax W CUS41 and its transmitter Liquisys CUM M 223/253 need a data logger to record their output. A data logger is built by open-source hardware. Duo to that the output of CUM M 223/253 is 4 to 20 mA signal, the reference data logger has same design as the data logger in Chapter 6 for low-cost pressure water level sensor. Hardware schematic and real board are shown in Figure 4 and Figure 5 separately.

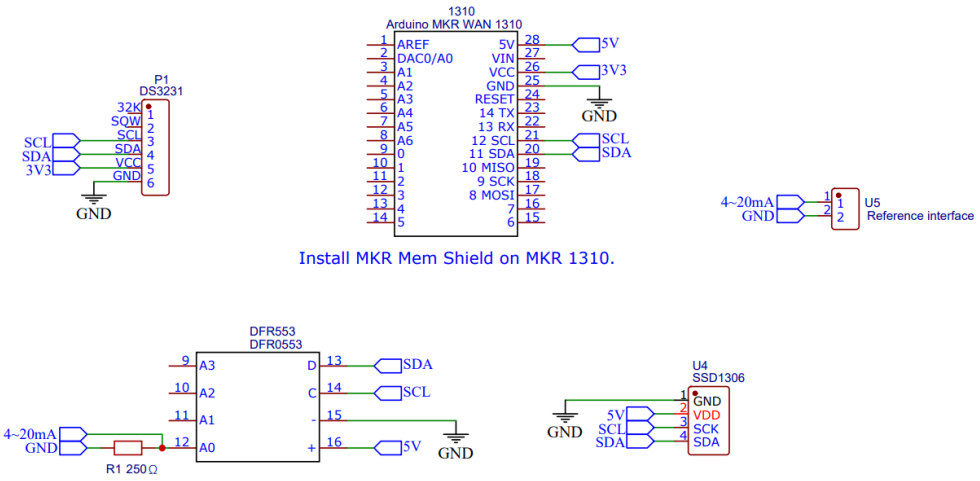

Figure 4. Hardware schematic of reference data logger. Reference interface in the right.

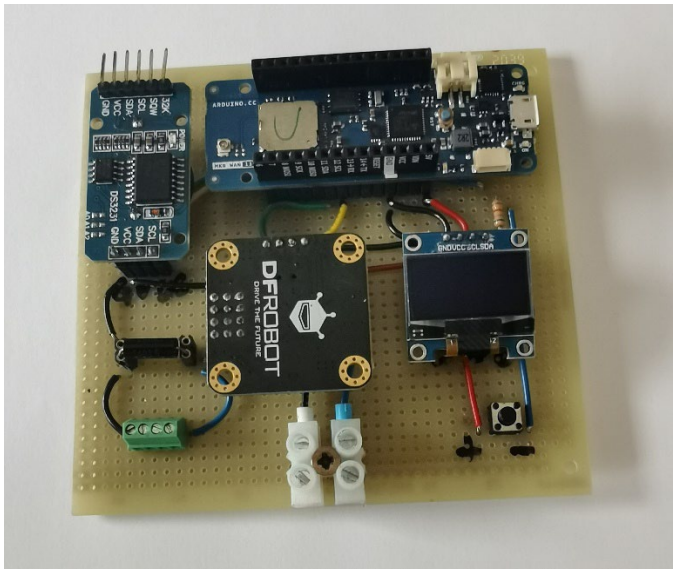

Figure 5. Real reference data logger board.

Arduino code structure is same to the code for rainfall monitoring station and shared in GitHub (Zhu, 2023f).

1.4 Installation

DIY low-cost turbidimeter probe

A DIY housing is made for SEN-0189 sensor to test it in the benchmark, the main body of the housing is a Polyvinyl Chloride (PVC) tube that has an outer diameter 32 mm and an inner diameter 25 mm. The cover of SEN-0189 sensor is removed (black part on the top of (a)) and the wall of tube is polished thin to plug part of the sensor into the tube. At beginning, elastic SMX hybrid polymer-based mastic-glue is used to combine the tube and sensor. The initial trial connection of the system is shown in Figure 6.

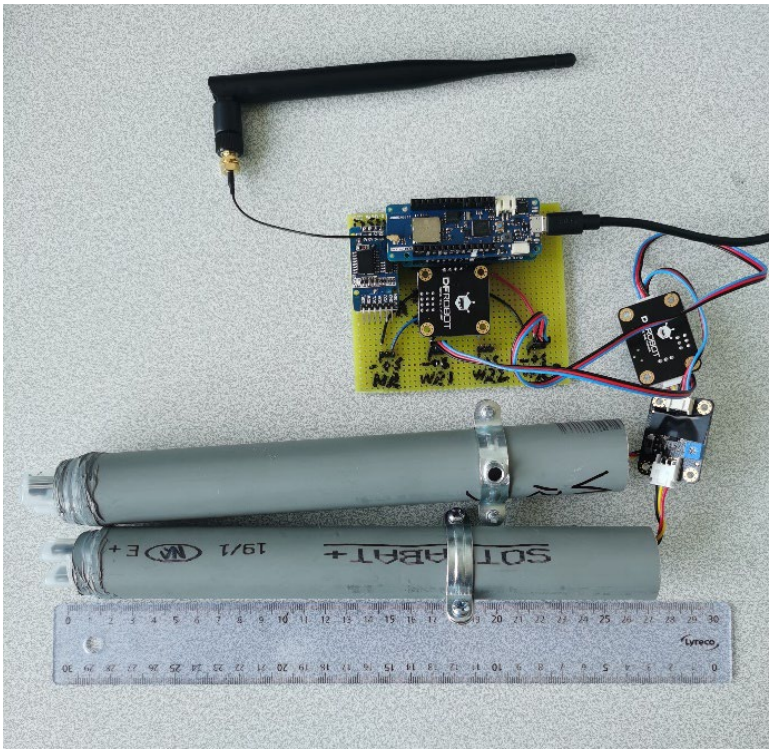

Figure 6. Low-cost water turbidity monitoring station initial setup (no screen at first): antenna on the top, main board in the middle, DFRobot interface circuit on the right, DIY sensor probe on the bottom.

After about two months in wastewater test, water enters one DIY turbidimeter probe as shown in Figure 7.

Figure 7. Water enters one DIY turbidimeter probe (the left one).

Construction silicone sealant is used to build the new probe as shown in Figure 8.

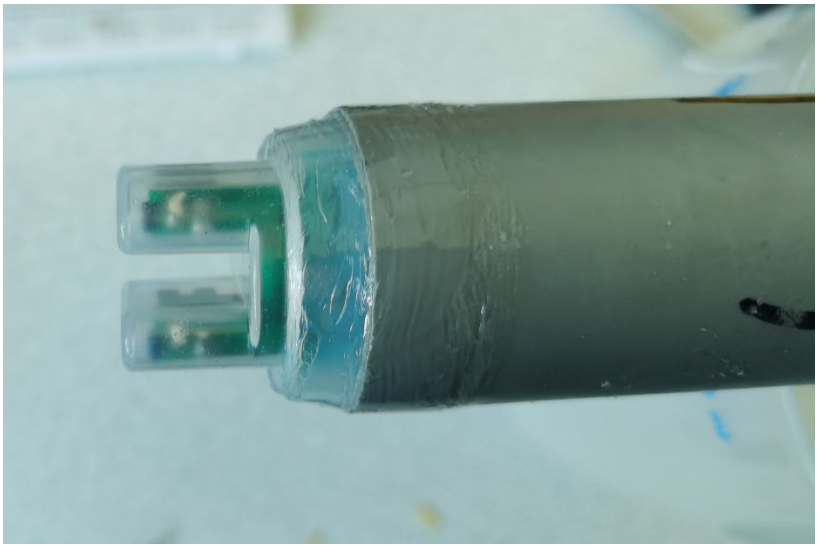

Figure 8. Using construction silicone sealant to connect tube and sensor.

After three months in wastewater test, no water is inside the new probe as shown in Figure 9.

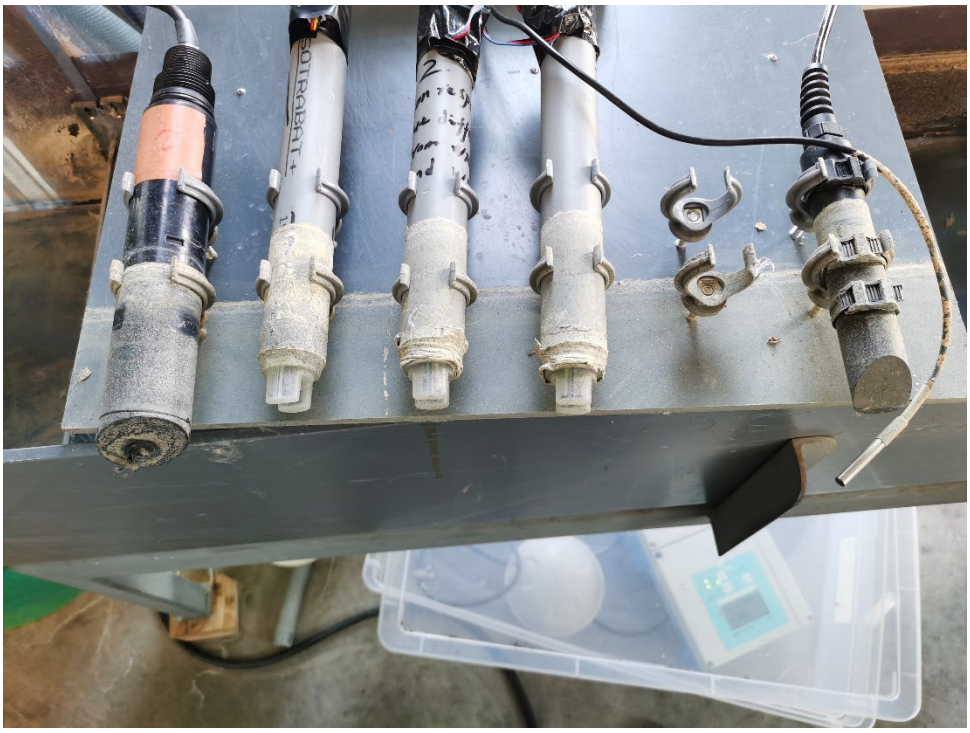

Figure 9. Sensors on 2022-00-02, from left to right: reference sensor Turbimax W CUS41 probe, one DIY low-cost turbidimeter probe using construction silicone sealant, two DIY low-cost turbidimeter tube using elastic SMX hybrid polymer-based mastic-glue, reference Aqualabo probe and water temperature sensor DS18B20.

In field installation

Low-cost and reference turbidimeters are installed in an artificial canal testbench in Feyssine, Lyon, France as shown in Figure 10 and Figure 11. Wastewater is flowing in the canal.

Figure 10. Turbidimeters first test setups on 2022-05-12. Low-cost data logger is in the box on the top. Turbidimeters are on the bottom: from left to right, reference sensor Turbimax W CUS41, low-cost sensor No. 1 to 3 and reference Aqualabo sensor.

Figure 11. Installation of low-cost and reference turbidimeters on 2022-07-22, add a reference DIY data logger and screens on data loggers. A shade to reduce the effects of sunlight.

There are three water turbidity monitoring station in the testbench: (i) half low-cost station contains traditional sensor Turbimax W CUS41 with its transmitter Liquisys CUM M 223/253 and DIY data logger (ii) low-cost station contains low-cost sensor SEN-0189 with DIY data logger (iii) off-shelf-commercial wireless station kit coming from Aqualabo.

1.5 Calibration

As shown in Figure 12, in filed calibration, all the turbidimeter probes are calibrated by technician one by one using AMCO Clear® Primary Turbidity Standard.

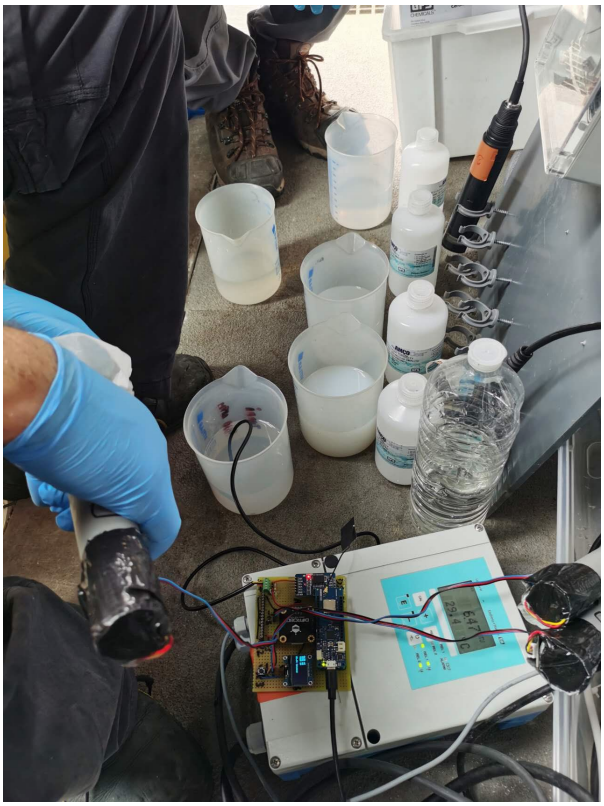

Figure 12. Turbidimeter in field calibration.

2. Results and discussion

2.1 Operation

Operation details are given in Table 1.

Table 1. Low-cost turbidimeter test operation details.

Time	Operation	Note
2022-05-12	Check in laboratory	Calibration all sensors.
2022-05-13	Installation in field	Without reference sensor DIY data logger.
2022-05-31	Improvement in field	Improve the code of low-cost data logger.
2022-06-23		Calibrate all sensors.
		Install reference sensor DIY data logger and add screens.
2022-07-01		Clean sensors, water enters DIY low-cost turbidimeter probe No.1.
2022-07-11		Install new DIY low-cost turbidimeter probe.
2022-07-22		Add a shade to remove the effect of sunlight.
2022-11-02	End in field test	Reference sensor DIY data logger cannot save data in SD card.

The test was begun at 2022-05-13 and end at 2022-11-02 due to the stop usage of the man-made canal. Due to many improvements during this period, the reliable data are from 2022-07-22 to 2022-11-02. However, all the sensors were not cleaned during this period. And the man-made canal is not aways full of water and cannot exactly know when there is water inside it and the water quality. So, there is no long-term comparison between low-cost and reference sensors as Chapter 4 and Chapter 5. Some points will be discussed by data in this Chapter.

2.2 Low-cost turbidimeter assessment

Calibration

On 2022-06-23, after more than one month in wastewater usage, three DIY turbidimeter probes No.1, No.2 and No.3 are calibrated in field. All the sensors have been cleaned as much as possible before calibration, results are given in Figure 13.

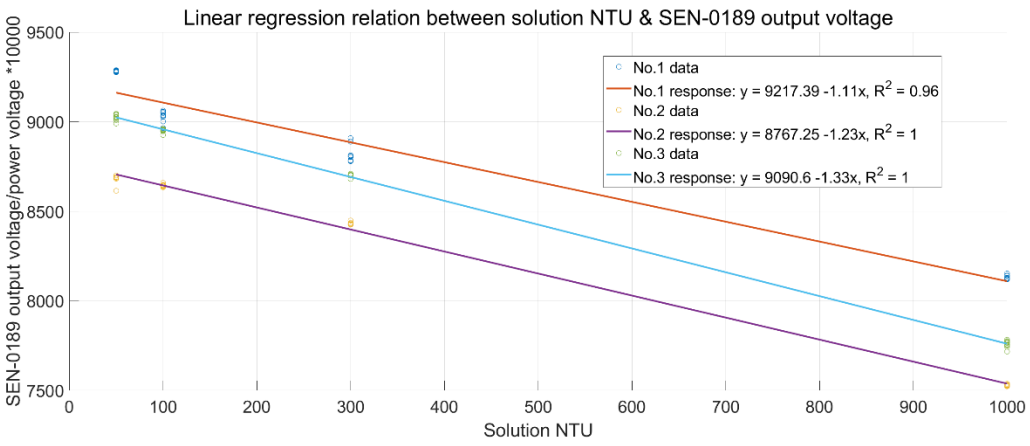

Figure 13. Linear regression relation between solution NTU and SEN-0189 response.

In Figure 13, y axis is chosen to be SEN-0189 output voltage in millivolt divided by power voltage in millivolt and then multiplied by 10000 due to that low-cost turbidimeter SEN-0189 is a voltage divider essentially, power voltage will influence the output voltage.

On 2022-07-01, water is detected to enter probe No.1. Probe No.1 may have broken during second calibration. This could explain the response nonlinearity of DIY low-cost probe No.1 during calibration. Therefore, the further discussion only focusses on low-cost probe No.2 and No.3.

Calibration functions are shown in Figure 14 and Figure 15.

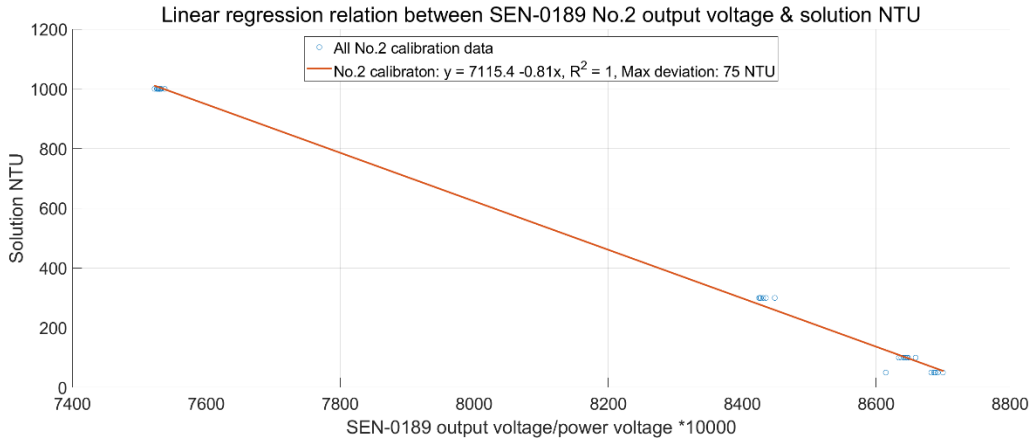

Figure 14. Low-cost turbidimeter No.2 calibration and maximum deviation when using the calibration function to explain sensor output.

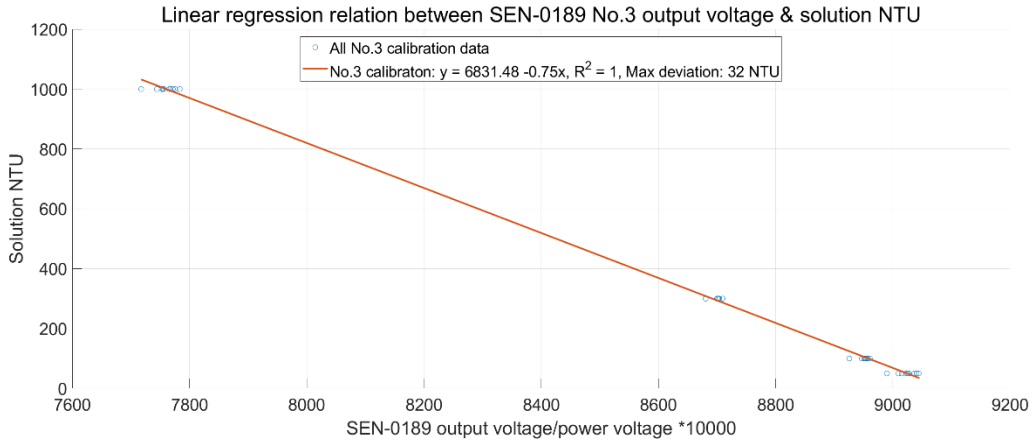

Figure 15. Low-cost turbidimeter No.3 calibration and maximum deviation when using the calibration function to explain sensor output.

According to above two figures, one could determine that low-cost turbidimeter probe No.2 has a calibration function:

$$NTU = 7115.4 - 0.81v \qquad \text{Equation 1}$$

low-cost turbidimeter No.3 has a calibration function:

$$NTU = 6831.48 - 0.75v \qquad \text{Equation 2}$$

Where v is SEN-0189 output voltage in millivolt divided by power voltage in millivolt and then multiplied by 10000.

According to the maximum deviation when using the above calibration function to explain turbidimeter raw output voltage and the resolution itself also has uncertainty, one could conservatively estimate that low-cost turbidimeter has an enlarged uncertainty 100 NTU.

2.3 Sunlight influence

As shown in Figure 16, it is obvious that every day around 07:20 in the morning, low-cost turbidimeter output voltages will have a peak. This is due to that at this time, intense direct sunlight hits the low-cost sensors. A shade as shown in Figure 11 could eliminate this effect effectively.

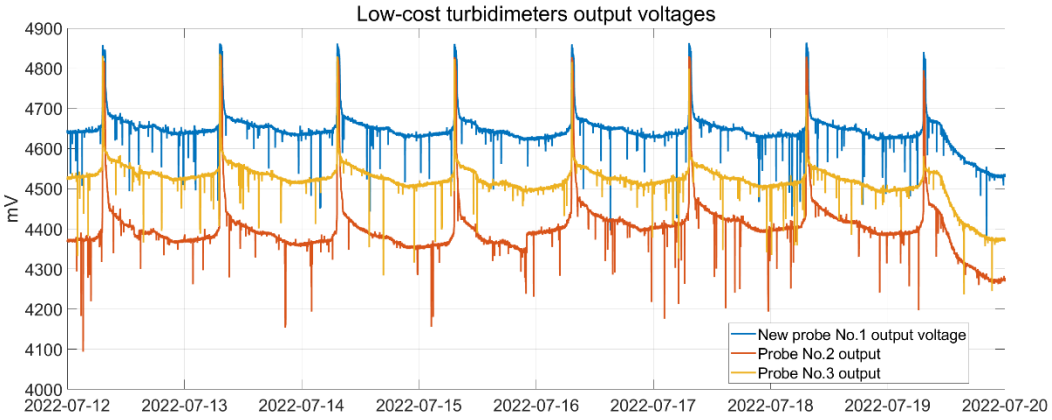

Figure 16. Three low-cost turbidimeters output voltages

2.4 Short term comparison

As shown in Figure 9, sensors are very dirty and not cleaned from 2022-07-22 to 2-22-11-02. So, it is meaningless to compare their performance for a long time. Their outputs during the first few days after 2022-07-22 are shown in Figure 17.

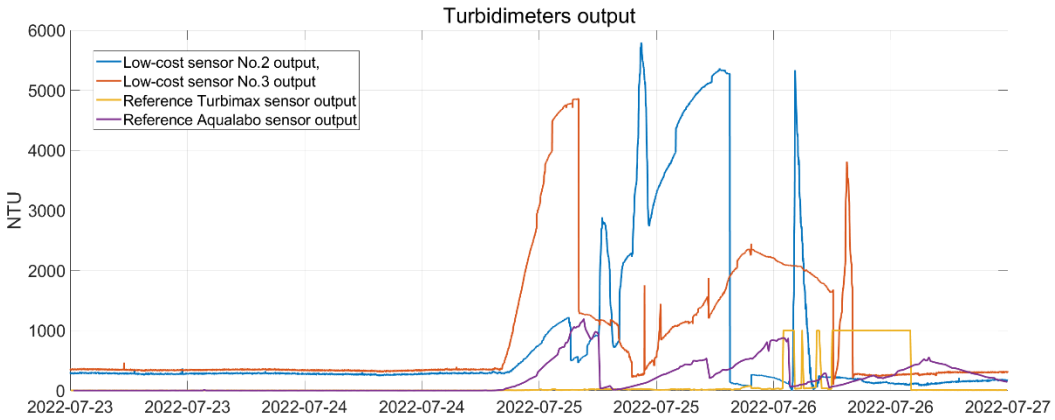

Figure 17. Turbidimeters output at the beginning of the final installation setup

From above figure, it is obvious that all turbidimeters outputs are very different. For low-cost turbidimeters, it is obvious that when reference sensors output 0 NTU, their output is about 350 NUT. This may be due to that their calibration function is established by standard solution at a temperature of around 25 degrees, but the wastewater is at a temperature of around 33 degrees. In addition, the very high NTU output of low-cost turbidimeters may be due to that some dirt is attached to the sensor. However, two reference sensors output are also very different, this illustrated the difficulty of in *situ* water quality monitoring. According to the laboratory technician, it is normal that the turbidimeter outputs are saturated.

3. Summary

This section describes our work using about using low-cost turbidimeter SEN-0189 *in situ*. Turbidimeters require a lot of maintenance to guarantee results reliable. Even if the hardware is not expensive, the cost of maintenance work prevents it from being a low-cost sensor.

APPENDIX B: LOW-COST RAIN GAUGES RESULTS

This section is a supplement to Chapter 5.

1. ORG No.2

Comparison between low-cost ORG No.2 and reference TBRG are shown from Figure 18 to Figure 20.

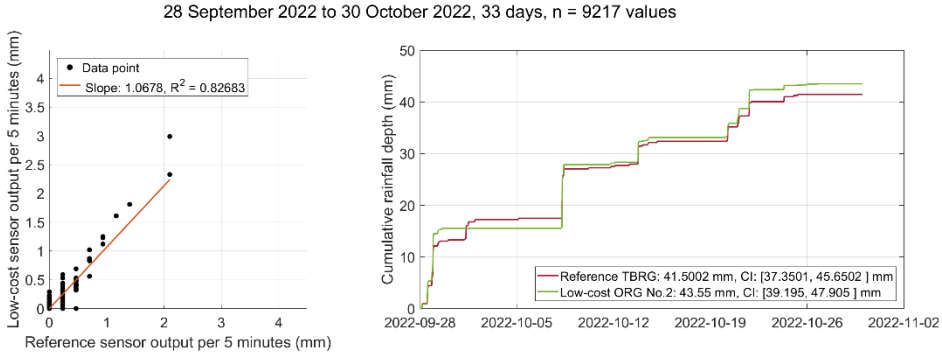

Figure 18. Comparison of low-cost ORG No.2 with reference TBRG from 28 September 2022 to 30 October 2022.

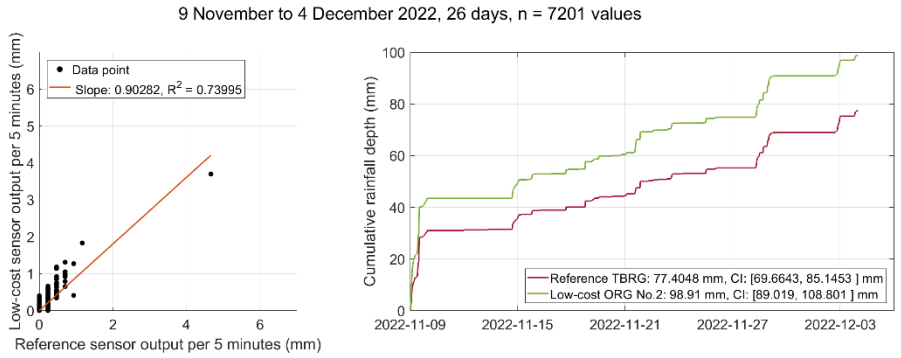

Figure 19. Comparison of low-cost ORG No.2 with reference TBRG from 9 November to 4 December 2022.

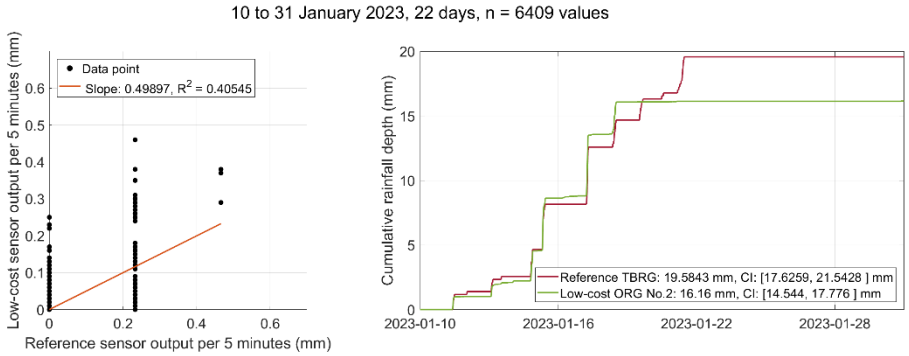

Figure 20. Comparison low-cost ORG No.2 with reference TBRG between 10 to 31 January 2023.

The data for all periods are displayed in Figure 21. The regression results are given in Table 2.

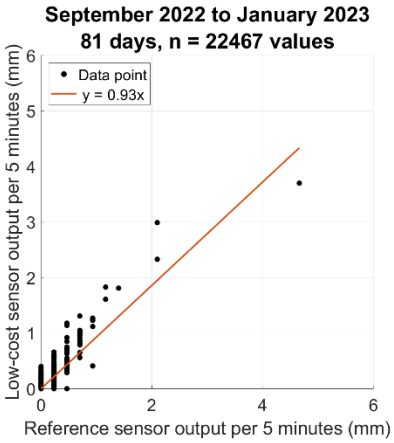

Figure 21. Ordinary least square regression results of ORG No.2 from September 2022 to January 2023.

Table 2. Regression results for the low-cost ORG No.2.

Parameter	With 0 intercept	With free intercept
b11	0	0.0013
b12	0.9315	0.9291
u(b11)	0	0.0002
u(b12)	0.0036	0.0036
cov(b11, b12)	0	0
ResVar1	0.0010	0.0010
IC95 b11	0	[0.0009, 0.0017]
IC95 b12	[0.9245, 0.9385]	[0.9221, 0.9362]
Standard error	0.0313	0.0313

According to the above table, the selected correlation function, with two significant figures, is:

$$y = 0.93x \qquad \text{Equation 3}$$

with a standard error ε = 0.0313.

Daily outputs of rain gauges are compared in Figure 22 and regression results in Table 3.

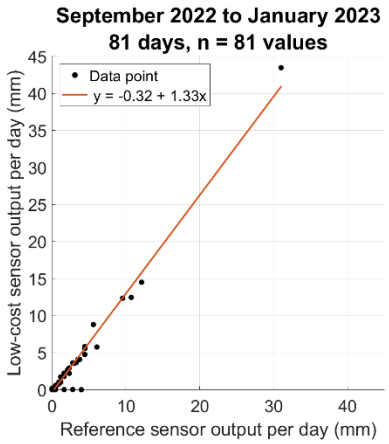

Figure 22. Low-cost ORG No.2 and reference TBRG daily output comparison.

Table 3. Regression results of ORG No.2 daily output.

Parameter	With 0 intercept	With free intercept
b11	0	-0.3234
b12	1.3058	1.3345
u(b11)	0	0.1075
u(b12)	0.0237	0.0245
cov(b11, b12)	0	-0.0010
ResVar1	0.8744	0.7945
IC95 b11	0	[-0.5342, -0.1126]
IC95 b12	[1.2594, 1.3522]	[1.2865, 1.3825]
Standard error	0.9351	0.8914

According to above table, the selected correlation function is:

$$y = -0.32 + 1.33x \qquad \text{Equation 4}$$

When using the inverse function of Equation 4 to correct the low-cost ORG No.2 daily output, relative enlarged uncertainty of the resolution corresponding to 70%, 80%, 90% correctness rates are given in Table 4.

Table 4. Relative Enlarged Uncertainty (EU) of the low-cost ORG No.2 daily output.

Correctness rate	Relative enlarged uncertainty
70%	12%
80%	18%
90%	44%

2. TBRG final installation with initial funnel

2.1 TBRG No.2

Low-cost TBRG No.2 and reference TBRG cumulative output tips are shown in Figure 23.

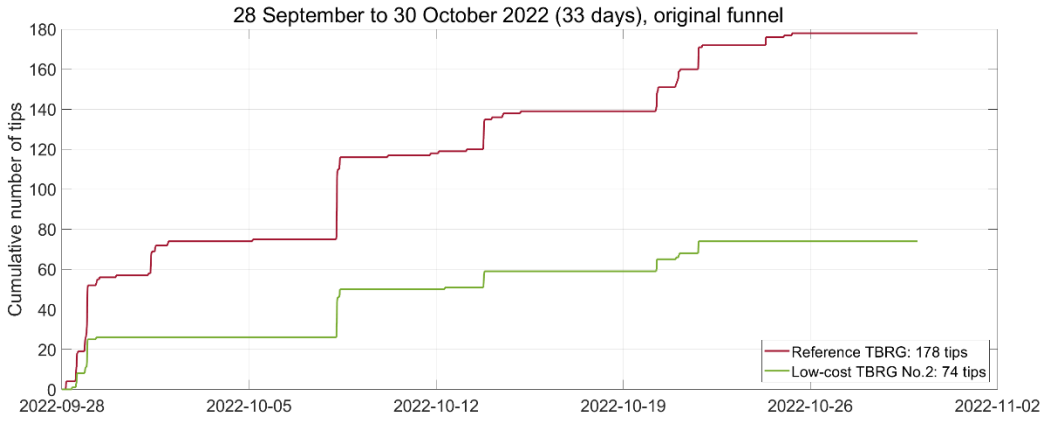

Figure 23. Low-cost TBRG No.2 performance from 28 September to 30 October 2022.

Figure 24 shows data from 28 September to 30 October 2022. The regression results are given in Table 4-11.

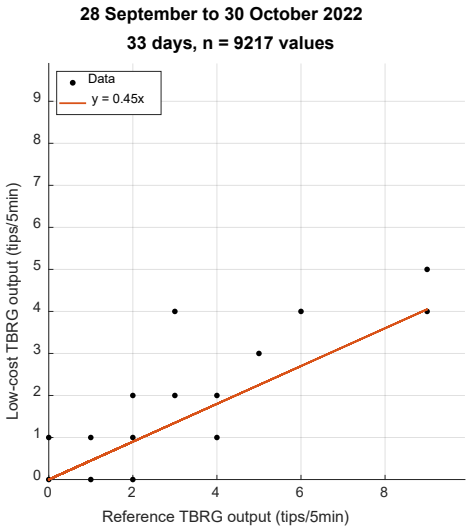

Figure 24. Low-cost TBRG No.2 and reference TBRG output comparison from 28 September to 30 October 2022.

The correlation function has been selected from the regression results given in Table 4-11.

Table 5. Regression results for the low-cost TBRG No.2.

Parameter	With 0 intercept	With free intercept
b11	0	-0.0008
b12	0.4549	0.4552
u(b11)	0	0.0008
u(b12)	0.0035	0.0035
cov(b11, b12)	0	0
ResVar1	0.0058	0.0058
IC95 b11	0	[-0.0023, 0.0008]
IC95 b12	[0.4480, 0.4619]	[0.4483, 0.4622]
Standard error	0.0762	0.0762

According to Table 4-11, the selected correlation function is:

$$y = 0.45x \qquad \text{Equation 5}$$

Get that the low-cost TBRG No. has a resolution 0.233/0.45 = 0.52 mm/tip, one can redraw Figure 23. Results are shown in Figure 25.

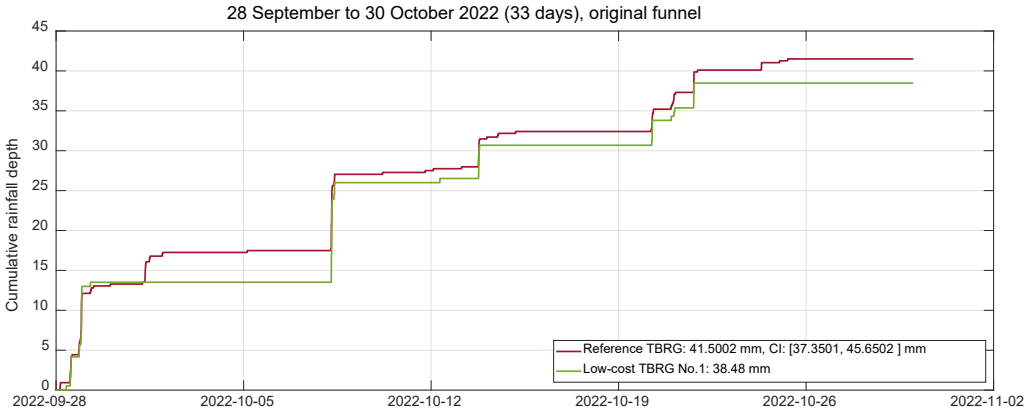

Figure 25. Revised low-cost TBRG No.2 performance from 28 September to 30 October 2022.

2.2 TBRG No.3

Low-cost TBRG No.3 and reference TBRG cumulative output tips are shown in Figure 26.

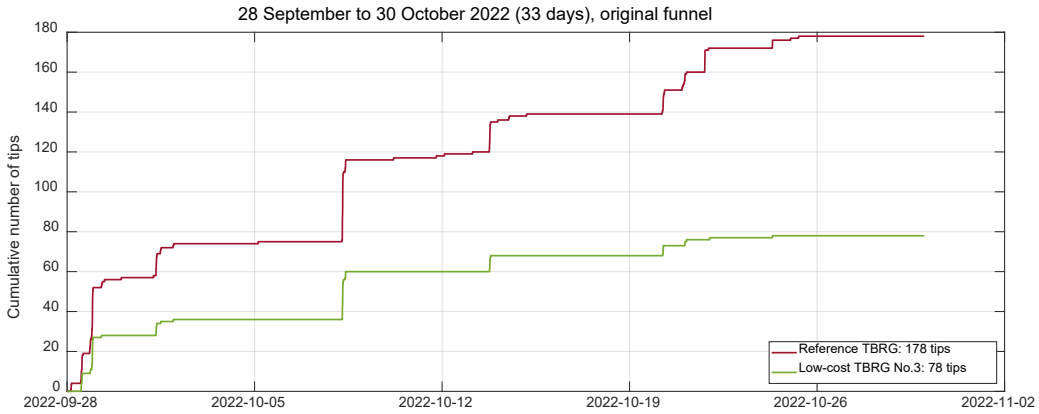

Figure 26. Low-cost TBRG No.3 performance from 28 September to 30 October 2022.

Figure 27 shows data from 28 September to 30 October 2022. The regression results are given in Table 6.

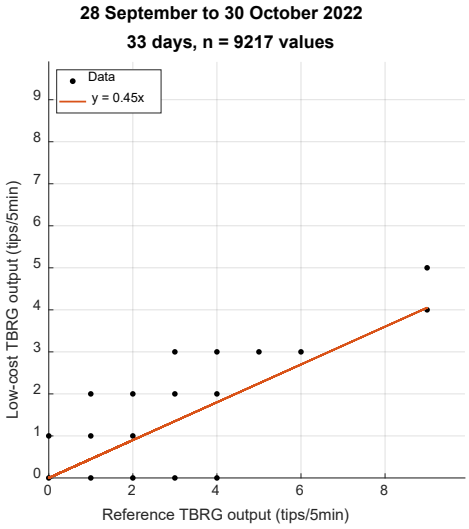

Figure 27 Low-cost TBRG No.3 and reference TBRG outputs comparison.

Table 6. Regression results for the low-cost TBRG No.3.

Parameter	With 0 intercept	With free intercept
b11	0	-0.0003
b12	0.4549	0.4551
u(b11)	0	0.0009
u(b12)	0.0038	0.0038
cov(b11, b12)	0	0.0000
ResVar1	0.0067	0.0067
IC95 b11	0	[-0.0020, 0.0013]
IC95 b12	[0.4475, 0.4624]	[00.4476, 0.4625]
Standard error	0.0817	0.0817

According to Table 6, the selected correlation function is:

$$y = 0.45x \qquad \text{Equation 6}$$

Get that the low-cost TBRG No. has a resolution 0.233/0.45 = 0.52 mm/tip, one can redraw Figure 26. Results are shown in Figure 28.

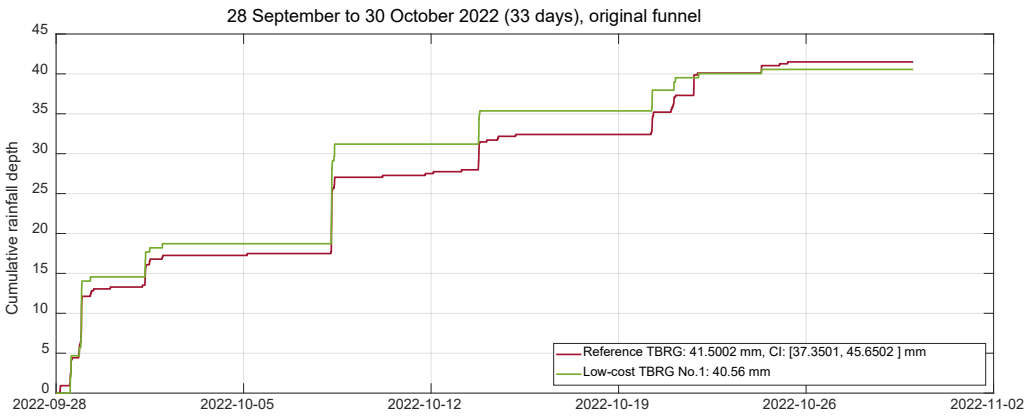

Figure 28. Revised low-cost TBRG No.3 performance from 28 September to 30 October 2022.

3. TBRG final installation, with enlarged additional funnel

3.1 TBRG No.2

Low-cost TBRG No.2 and reference TBRG cumulative output tips are shown in Figure 29 and Figure 30.

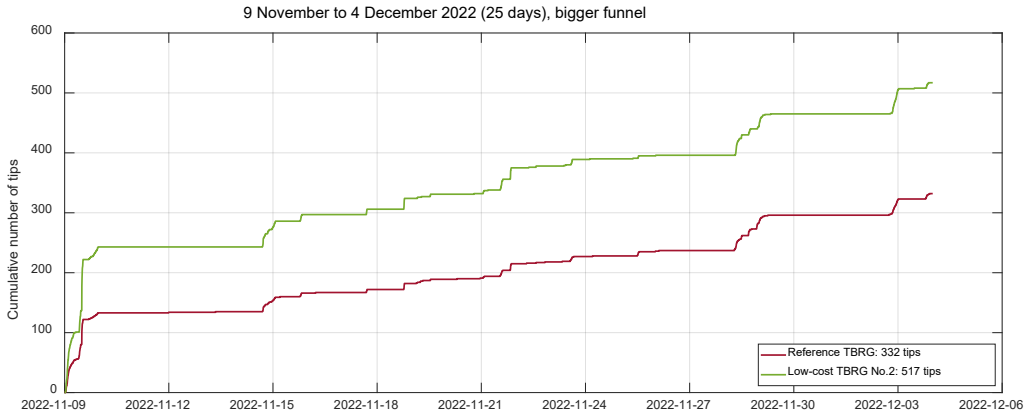

Figure 29. Low-cost TBRG No.2 performance from 9 November 2022 to 4 December 2022.

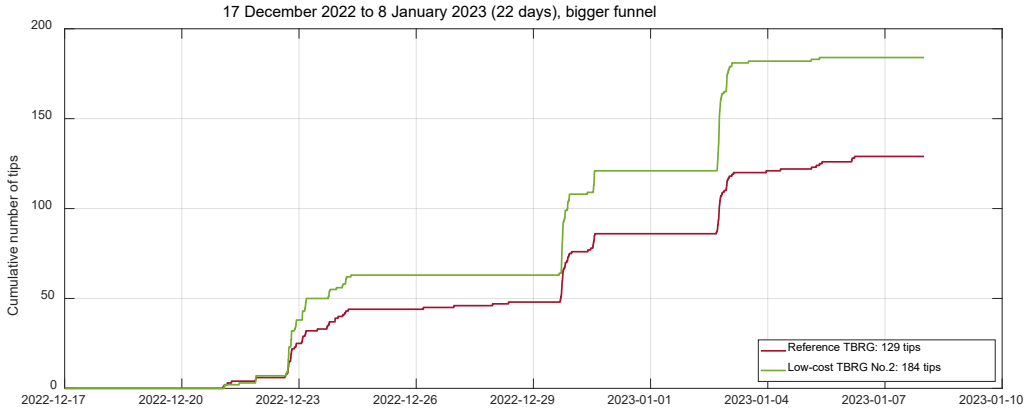

Figure 30. Low-cost TBRG No.2 performance from 17 December 2022 to 8 January 2023.

Regression results and details are given in Figure 31 and Table 7.

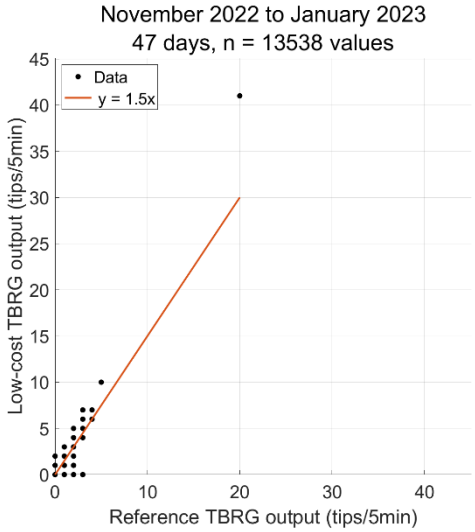

Figure 31. Low-cost TBRG No.2 and reference TBRG outputs comparison.

Table 7. Regression results for the low-cost TBRG No.2.

Parameter	With 0 intercept	With free intercept
b11	0	0.0003
b12	1.5105	1.5104
u(b11)	0	0.0022
u(b12)	0.0081	0.0081
cov(b11, b12)	0	0.0000
ResVar1	0.0649	0.0649
IC95 b11	0	[-0.0040, 0.0047]
IC95 b12	[1.4947, 1.5263]	[1.4944, 1.5263]
Standard error	0.2547	0.2547

According to Table 7, the selected correlation function is:

$$y = 1.5x \qquad \text{Equation 7}$$

Get that the low-cost TBRG No. has a resolution 0.233/1.5 = 0.15 mm/tip, relative enlarged uncertainty of the resolution corresponding to 43%, 70%, 80%, 90%, 94% correctness rates are given in Table 8.

Table 8. Relative Enlarged Uncertainty (EU) of the low-cost ORG No.2 output.

Correctness rate	Relative enlarged uncertainty
43%	0.059 mm/tip
70%	0.06 mm/tip
80%	0.06 mm/tip
90%	0.06 mm/tip
94%	0.06mm/tip

3.2 TBRG No.3

Low-cost TBRG No.3 and reference TBRG cumulative output tips are shown in Figure 32.

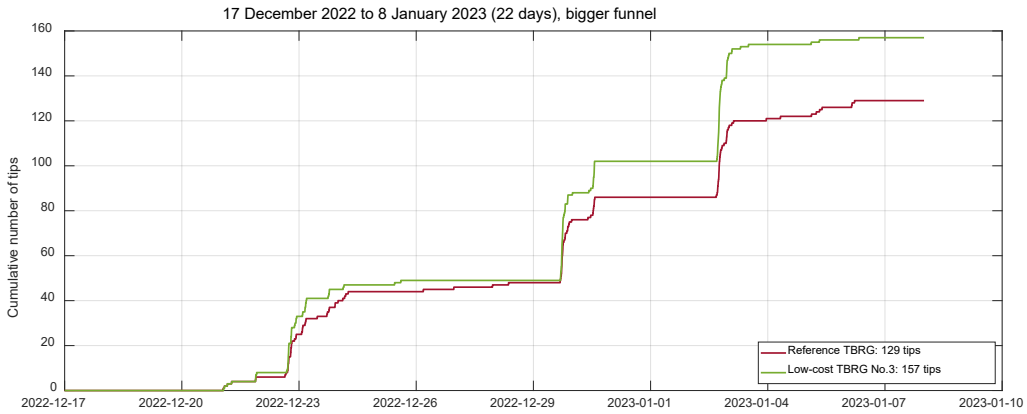

Figure 32 Low-cost TBRG No.3 performance from 17 December 2022 to 8 January 2022.

Due to the inadequate points distribution of the data with a time step five minutes. Daily data are used to regression, results and details are given in Figure 33 and Table 9.

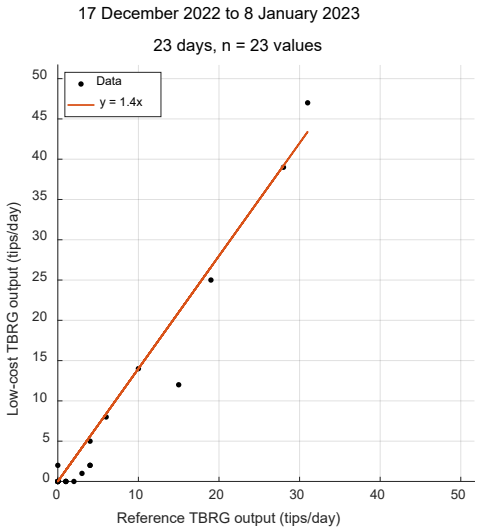

Figure 33. Low-cost TBRG No.3 and reference TBRG outputs comparison.

Table 9. Regression results for the low-cost TBRG No.3.

Parameter	With 0 intercept	With free intercept
b11	0	-1.0880
b12	1.3556	1.4110
u(b11)	0	0.6057
u(b12)	0.0512	0.0577
cov(b11, b12)	0	-0.0187
ResVar1	6.6349	6.0249
IC95 b11	0	[-2.2751, 0.0990]
IC95 b12	[1.2552, 1.4559]	[1.2979, 1.5242]
Standard error	2.5758	2.4546

According to Table 9, the selected correlation function is:

$$y = 1.4x \qquad \text{Equation 8}$$

Get that the low-cost TBRG No.3 has a resolution 0.233/1.4 = 0.17 mm/tip, relative enlarged uncertainty of the resolution corresponding to 70%, 80%, 90% correctness rates are given in Table 10.

Table 10. Relative Enlarged Uncertainty (EU) of the low-cost ORG No.3 daily output.

Correctness rate	Relative enlarged uncertainty
70%	0.039 mm/tip
80%	0.043 mm/tip
90%	0.043 mm/tip

3.3 TBRG No.4

Low-cost TBRG No.4 and reference TBRG cumulative output tips are shown in Figure 34.

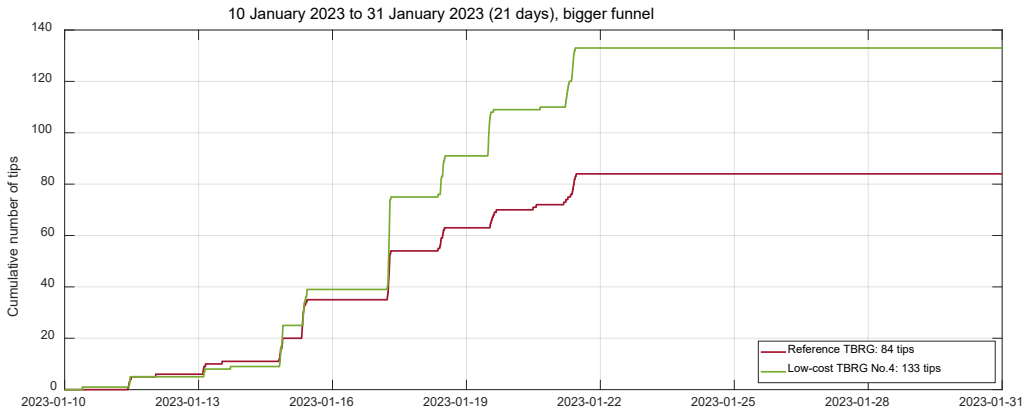

Figure 34. Low-cost TBRG No.4 performance from 10 to 31 January 2023.

Due to the inadequate points distribution of the data with a time step five minutes. Daily data are used to regression, results and details are given in Figure 35 and Table 11.

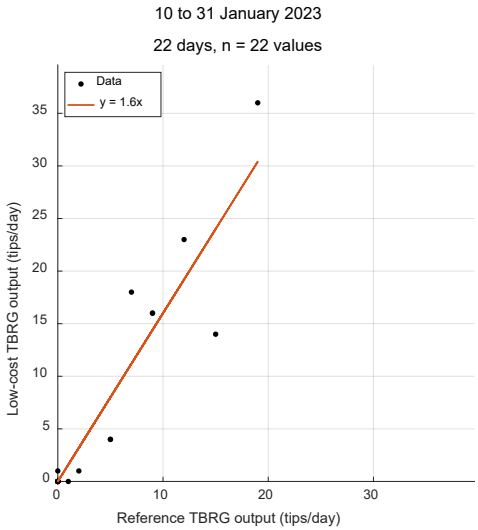

Figure 35. Low-cost TBRG No.4 and reference TBRG outputs comparison.

Table 11. Regression results for the low-cost TBRG No.4.

Parameter	With 0 intercept	With free intercept
b11	0	-0.2771
b12	1.6325	1.6559
u(b11)	0	0.8882
u(b12)	0.1063	0.1320
cov(b11, b12)	0	-0.0665
ResVar1	11.2622	11.7681
IC95 b11	0	[-2.0180, 1.4639]
IC95 b12	[1.4241, 1.8409]	[1.3972, 1.9146]
Standard error	3.3559	3.4305

According to Table 11, the selected correlation function is:

$$y = 1.6x \qquad \text{Equation 9}$$

Get that the low-cost TBRG No. has a resolution 0.233/ = mm/tip, relative enlarged uncertainty of the resolution corresponding to 70%, 80%, 90% correctness rates are given in Table 12.

Table 12. Relative Enlarged Uncertainty (EU) of the low-cost ORG No.4 daily output.

Correctness rate	Relative enlarged uncertainty
27%	0.058 mm/tip
70%	0.059 mm/tip
80%	0.059 mm/tip
90%	0.059 mm/tip
93%	0.059 mm/tip

3.4 TBRG No.5

Low-cost TBRG No.5 and reference TBRG cumulative output tips are shown in Figure 36.

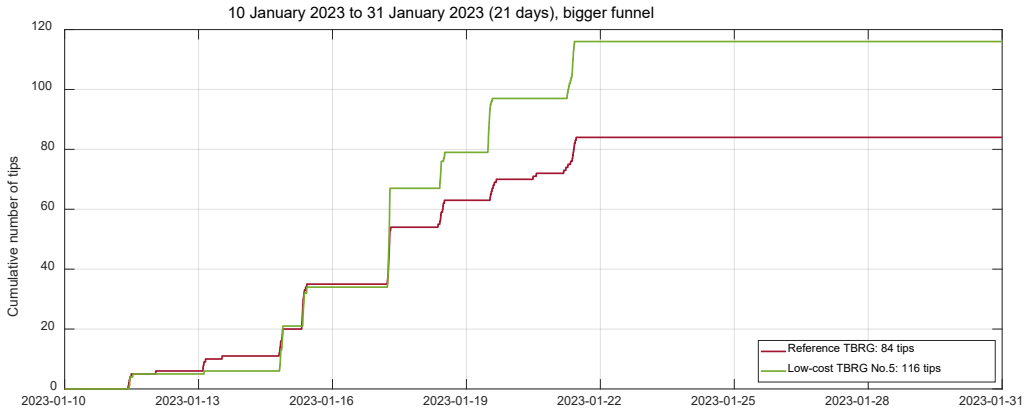

Figure 36. Low-cost TBRG No.5 performance from 10 to 31 January 2023.

Due to the inadequate points distribution of the data with a time step five minutes. Daily data are used to regression, results and details are given in Figure 37 and Table 13.

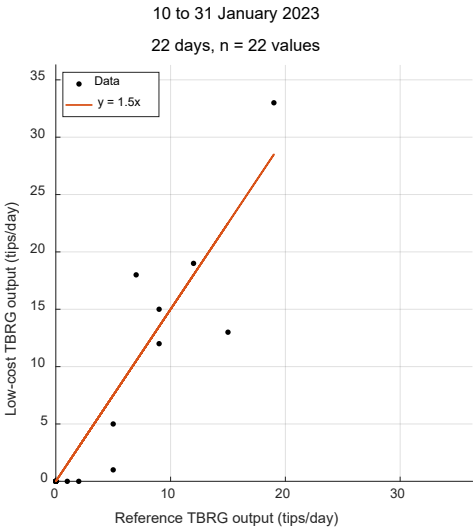

Figure 37. Low-cost TBRG No.5 and reference TBRG outputs comparison.

Table 13. Regression results for the low-cost TBRG No.5.

Parameter	With 0 intercept	With free intercept
b11	0	-0.4160
b12	1.4548	1.4899
u(b11)	0	0.8731
u(b12)	0.1049	0.1298
cov(b11, b12)	0	-0.0643
ResVar1	10.9508	11.3693
IC95 b11	0	[-2.1272, 1.2952]
IC95 b12	[1.2493, 1.6603]	[1.2356, 1.7447]
Standard error	3.3092	3.3718

According to Table 13, the selected correlation function is:

$$y = 1.5x \qquad \text{Equation 10}$$

Get that the low-cost TBRG No. has a resolution 0.233/1.5 = 0.16 mm/tip, relative enlarged uncertainty of the resolution corresponding to 70%, 80%, 90% correctness rates are given in Table 14.

Table 14. Relative Enlarged Uncertainty (EU) of the low-cost ORG No.5 daily output.

Correctness rate	Relative enlarged uncertainty
31%	0.048 mm/tip
70%	0.049 mm/tip
80%	0.049 mm/tip
90%	0.049 mm/tip
32%	0.049 mm/tip

3.5 TBRG No.6

Low-cost TBRG No.3 and reference TBRG cumulative output tips are shown in Figure 38.

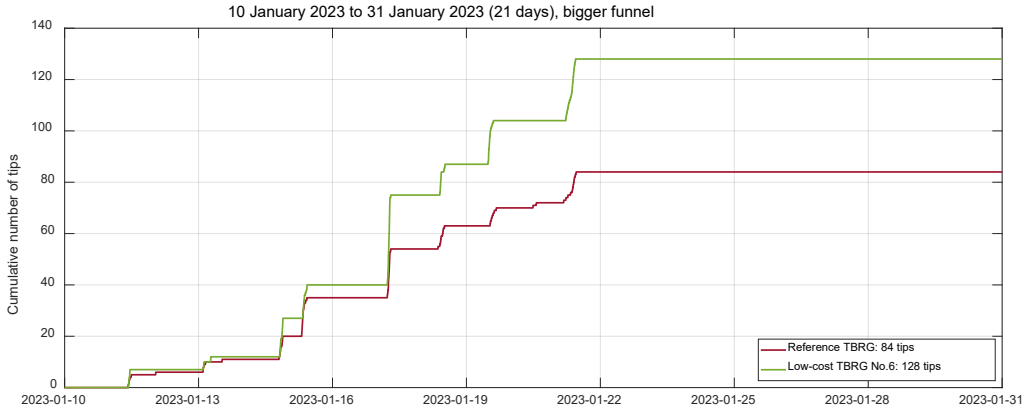

Figure 38. Low-cost TBRG No.6 performance from 10 to 31 January 2023.

Due to the inadequate points distribution of the data with a time step five minutes. Daily data are used to regression, results and details are given in Figure 39 and Table 15.

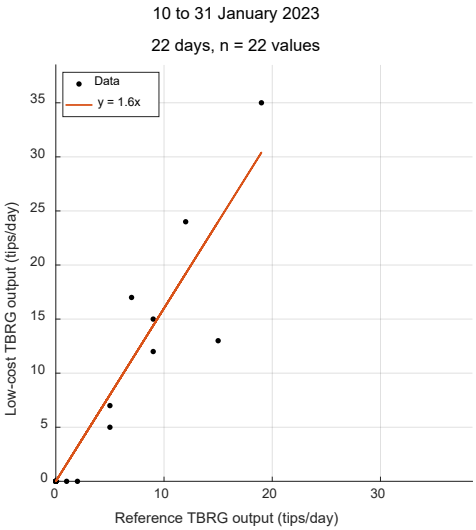

Figure 39. Low-cost TBRG No.6 and reference TBRG outputs comparison.

Table 15. Regression results for the low-cost TBRG No.6.

Parameter	With 0 intercept	With free intercept
b11	0	-0.2956
b12	1.5763	1.6012
u(b11)	0	0.8702
u(b12)	0.1042	0.1293
cov(b11, b12)	0	-0.0639
ResVar1	10.8191	11.2949
IC95 b11	0	[-2.0012, 1.4100]
IC95 b12	[1.3720, 1.7806]	[1.3478, 1.8507]
Standard error	3.2892	3.3608

According to above table, the selected correlation function is:

$$y = 1.6x \qquad \text{Equation 11}$$

Get that the low-cost TBRG No. has a resolution 0.233/1.6 = 0.15 mm/tip, relative enlarged uncertainty of the resolution corresponding to 70%, 80%, 90% correctness rates are given in Table 4.

Table 16. Relative Enlarged Uncertainty (EU) of the low-cost ORG No.6 daily output.

Correctness rate	Relative enlarged uncertainty
33%	0.059 mm/tip
70%	0.06 mm/tip
80%	0.06 mm/tip
90%	0.06 mm/tip
98%	0.06 mm/tip

4. Calibration

4.1 TBRB No.2

Table 17. Raw data of low-cost TBRG No.2 calibration.

Pump speed (mL/min)	Duration time (s)	Number of tips	Water displacement (g)
7	2139.929	185	290.35
7	1096.652	93	149
7	1091.692	93	148.2
15	1161.114	203	338.53
15	581.556	101	169.47
15	671.943	116	195.97
30	347.121	110	204.75
30	433.658	137	255.97
30	504.486	159	298.07
45	306.999	146	273.56
45	318.032	150	284.3
45	370.708	171	331.51
60	249.169	149	299.13
60	292.456	175	351.15
60	592.101	352	710.59
75	256.864	185	389.55
75	260.85	187	395.56
75	262.602	190	398.3

4.2 TBRG No.3

Table 18. Raw data of low-cost TBRG No.3 calibration.

Pump speed (mL/min)	Duration time (s)	Number of tips	Water displacement (g)
7	335.04	25	45.83
7	356.56	25	48.24
7	361.45	25	49.1
15	156.51	25	45.68
15	160.61	25	46.79
15	164.73	25	48.02
30	88.96	25	53.31
30	91.38	25	54.05
30	99.07	27	58.68
45	63.2	25	56.49
45	62.44	25	55.86
45	64.47	25	57.73
60	48.21	25	57.86
60	49.43	25	59.26
60	48.54	25	58.07
75	42.32	26	63.93
75	43.58	26	66
75	49.29	28	74.42

4.3 TBRG No.4

Table 19. Raw data of low-cost TBRG No.4 calibration.

Pump speed (mL/min)	Duration time (s)	Number of tips	Water displacement (g)
3	1316.114	50	74.48
3	1358.55	51	77.27
3	1331.131	50	75.7
7	618.314	53	81.95
7	600.639	51	79.84
7	618.882	52	81.91
10	435.973	51	82.86
10	441.045	52	83.81
10	430.504	51	81.58
15	284.929	50	81.22
15	323.413	56	92.37
15	311.827	55	89.03
20	212.079	50	80.96
20	210.647	50	80.22
20	214.707	51	81.88
25	185.333	51	88.7
25	175.206	51	83.59
25	183.211	51	87.56
30	143.618	51	83
30	146.024	52	83.89
30	144.361	51	83.1
35	125.047	51	84.11
35	123.716	51	83.36
35	124.479	50	83.74
40	109.875	51	84.5
40	109.203	51	84.16
40	108.234	51	83.51
45	105.434	55	91.8
45	99.753	52	87.07
45	99.581	52	86.44
50	92.839	53	89.77
50	92.504	53	89.39
50	90.976	53	89.08
55	84.554	53	90.26
55	85.054	53	90.63
55	84.515	53	89.9
60	78.649	53	91.24
60	79.06	54	92.79
60	78.795	53	91.67

4.4 TBRG No.5

Table 20. Raw data of low-cost TBRG No.5 calibration.

Pump speed (mL/min)	Duration time (s)	Number of tips	Water displacement (g)
3	1346.225	51	76.61
3	1399.134	52	79.8
3	1398.996	52	79.84
7	696.566	59	92.72
7	642.052	55	85.73
7	686.023	59	91.66
10	472.065	57	89.86
10	496.035	61	94.6
10	425.837	52	81.04
15	306.578	55	87.63
15	267.562	51	76.51
15	283.958	55	81.1
20	219.295	55	83.49
20	236.87	57	90.47
20	231.894	55	88.77
25	183.934	57	88.28
25	180.381	54	86.69
25	203.011	60	97.34
30	152.483	54	88.21
30	147.535	50	85.08
30	177.442	58	102.57
35	154.511	56	103.91
35	132.918	53	89.72
35	126.778	53	85.57
40	132.314	58	102.24
40	128.915	52	99.7
40	106.714	51	82.76
45	136.306	70	119.17
45	124.297	59	108.94
45	113.805	59	99.38
50	94.348	55	91.3
50	101.021	56	97.97
50	103.056	56	100.07
55	109.037	59	116.32
55	107.104	59	114.3
55	99.318	57	106.01
60	79.238	53	92.32
60	83.558	55	97.35
60	86.618	58	100.67

4.5 TBRG No.6

Table 21. Raw data of low-cost TBRG No.6 calibration.

Pump speed (mL/min)	Duration time (s)	Number of tips	Water displacement (g)
3	1440.696	53	82.65
3	1366.413	50	78.48
3	1460.033	54	83.72
7	695.678	59	93.07
7	617.606	54	82.51
7	618.688	54	82.56
10	568.094	70	108.51
10	463.658	57	88.53
10	461.836	58	88.21
15	343.674	65	98.37
15	290.207	55	83.24
15	298.687	55	85.4
20	215.724	53	82.39
20	225.819	55	86.21
20	217.957	51	83.21
25	175.996	52	84.21
25	186.561	55	89.4
25	177.207	51	84.96
30	170.719	56	98.43
30	156.641	53	90.47
30	159.632	52	92.05
35	138.074	53	93.03
35	131.898	53	89.18
35	138.415	53	93.35
40	140.6	63	108.97
40	120.25	53	92.87
40	114.171	51	88.56
45	110.096	54	95.89
45	109.016	53	95.16
45	106.314	52	92.84
50	103.754	58	100.52
50	99.982	55	97.03
50	101.798	55	98.71
55	90.399	54	96.42
55	92.022	54	98.02
55	93.561	55	99.8
60	86.741	55	100.76
60	89.393	57	103.86
60	93.766	58	109.01

APPENDIX C: RESUME SUBSTANTIEL EN LANGUE FRANÇAISE

Le déploiement à grande échelle de capteurs à faible coût pourrait révolutionner le domaine de la métrologie en hydrologie urbaine, en particulier pour les systèmes décentralisés de gestion des eaux pluviales, en élargissant le champ de la recherche et en améliorant le suivi des solutions de gestion de l'eau en milieu urbain. Dans cette thèse, un capteur est considéré comme étant de faible coût selon deux critères possibles : (i) son prix est au moins 10 fois inférieur à celui des capteurs traditionnels équivalents, ou (ii) des publications indiquent qu'il fonctionne avec du matériel open-source pour construire une station de mesure à faible coût. Cependant, ce domaine en est encore à ses débuts et nécessite un cadre d'évaluation plus systématique pour garantir la fiabilité des données et faciliter sa mise en œuvre par les chercheurs et les praticiens. Par conséquent, cette thèse vise à i) tester des capteurs à faible coût sélectionnés pour le suivi de dispositifs de gestion des eaux pluviales à la source avec une pratique métrologique appropriée, ii) améliorer ou adapter des capteurs à faible coût pour qu'ils puissent être utilisés en hydrologie urbaine et iii) proposer une méthodologie d'évaluation de leurs performances, dont leurs incertitudes.

Compte tenu des objectifs ci-dessus, les principales étapes du travail ont été les suivantes :

i. Une revue bibliographique des capteurs à faible coût utilisés par d'autres chercheurs pour mesurer des grandeurs météorologiques, la quantité et la qualité de l'eau.
ii. Une sélection de capteurs à faible coût ayant un potentiel d'application en hydrologie urbaine d'après la revue bibliographique de la littérature et les communications dans la communauté des logiciels libres.
iii. Le développement, l'installation, l'entretien et l'amélioration de stations de mesure à faible coût sur les sites expérimentaux sélectionnés.
iv. La collecte de données *in situ* pendant plusieurs semaines ou mois et, si possible, pendant une année entière.
v. L'évaluation finale des performances des capteurs à faible coût.

Dans la pratique, les trois dernières étapes ont été exécutées de manière itérative, avec des stations de mesure à faible coût progressivement améliorées à partir des observations d'interruption ou de défaillance des mesurages ou d'enregistrement des données. Conformément aux objectifs et aux étapes ci-dessus, la thèse comprend sept chapitres, décrits dans le tableau 1.

Tableau 1. Structure de la thèse.

Chapitre 1	• Contexte de la métrologie des eaux pluviales à faible coût ; • Objectifs et structure de la thèse.
Chapitre 2	• Revue bibliographique des capteurs météorologiques à faible coût ; • Revue bibliographique des capteurs de quantité d'eau à faible coût ; • Revue bibliographique des capteurs de qualité de l'eau à faible coût.
Chapitre 3	• Description des méthodes d'évaluation des performances des capteurs ; • Description des sites expérimentaux.
Chapitre 4	• Description des dispositifs d'essai des capteurs météorologiques à faible coût ; • Présentation des résultats des essais de capteurs météorologiques à faible coût.
Chapitre 5	• Description de la conception et des dispositifs d'essai de stations de mesure des précipitations à faible coût ; • Présentation des résultats de l'évaluation des performances *in situ* des pluviomètres à faible coût, des résultats de l'étalonnage et des résultats de l'évaluation des performances de stations de mesure des précipitations à faible coût.
Chapitre 6	• Description de la conception de stations de mesure de niveau d'eau à faible coût et des installations d'essai ; • Présentation des résultats de l'étalonnage des capteurs de niveau d'eau à faible coût et des résultats de l'évaluation des performances de la station de mesure de niveau d'eau à faible coût.
Chapitre 7	• Conclusions et perspectives.

Le chapitre 1 présente le contexte du travail, le lien avec le projet Cheap'eau[3], les objectifs et la structure de la thèse (tableau 1). Même si les capteurs à bas coût ont émergé il y a déjà quelques décennies, l'électronique polyvalente et à faible coût comme Arduino pourrait aujourd'hui donner aux chercheurs en hydrologie urbaine une nouvelle opportunité de construire leurs propres systèmes de mesure pour développer leurs travaux, et les déployer à grande échelle à des coûts très abordables. Cependant, la plupart des capteurs à faible coût disponibles dans le commerce ont été initialement conçus à des fins d'enseignement, ou comme composants pour d'autres produits (industrie), ou encore pour une utilisation DIY (Do It Yourself) par des passionnés d'électronique. Leur fiabilité pour la recherche et les applications opérationnelles dans le domaine de l'hydrologie urbaine est donc à évaluer. Cette thèse est liée au projet collaboratif Cheap'eau qui vise à évaluer si et comment des capteurs à faible coût peuvent être utilisés par les chercheurs et les praticiens pour la métrologie des eaux pluviales. En plus de cette thèse, divers capteurs à faible coût sont également testés par les partenaires du projet Cheap'eau pour le suivi d'installations de gestion des eaux pluviales comme les toitures végétalisées, les bassins de rétention ou les

[3] Le projet collaboratif Cheap'Eau a pour objectif de concevoir et/ou évaluer des systèmes innovants et économes pour la surveillance / gestion de la quantité et de la qualité des eaux pluviales en différents points d'un système d'assainissement. Il regroupe l'Université Lyon 2, l'INSA Lyon, l'INRAE, l'ISA-CNRS, Aegir, le GRAIE et la Métropole de Lyon. Il est financé par l'Agence de l'Eau Rhône-Méditerranée-Corse. Voir http://graie.org/othu/progr_cheapeau.htm

tranchées drainantes. Les résultats et les conclusions du projet Cheap'eau en cours seront publiés séparément à la fin de l'année 2023.

Dans le chapitre 2, une revue bibliographique a été réalisée sur les connaissances et les pratiques actuelles concernant l'utilisation de capteurs à faible coût pour mesurer (i) les grandeurs météorologiques, (ii) la quantité d'eau et (iii) la qualité de l'eau. L'étude porte sur les capteurs météorologiques pour le mesurage de l'humidité de l'air, de la vitesse du vent, du rayonnement solaire et des précipitations ; sur les capteurs de quantité d'eau pour le mesurage du niveau et du débit de l'eau, et de l'humidité du sol ; et sur les capteurs de qualité de l'eau pour le mesurage du pH, de la conductivité, de la turbidité, de l'azote et du phosphore.

Dans cette revue bibliographique, nous avons inclus des capteurs à faible coût prêts à l'emploi référencés par les communautés des logiciels libres et la littérature scientifique de la manière la plus systématique possible. Des tests de divers capteurs à faible coût, utilisant différents dispositifs et méthodes dans des environnements variés, ont été rapportés. Il n'existe à ce jour aucune revue bibliographique consacrée à la métrologie des eaux pluviales à faible coût avec un cadre métrologique unifié prenant en compte de nombreux paramètres et fournissant des retours d'expérience à partir de capteurs disponibles dans le commerce. Dans notre étude, les performances des capteurs à faible coût disponibles sur le marché sont résumées à l'aide de six indicateurs : (i) exactitude, (ii) répétabilité, (iii) reproductibilité, (iv) résolution, (v) temps de réponse, et (vi) sensibilité à l'environnement, besoins en maintenance et longévité.

Bien entendu, d'après l'expérience des auteurs de la présente étude, de nombreux autres aspects doivent être pris en compte lors de la construction d'une station d'un réseau de mesure. Par exemple, l'horloge en temps réel intégrée de certains Arduino peut facilement dériver avec le temps. La plupart des microcontrôleurs à bas coût ne sont pas protégés, ce qui signifie qu'ils peuvent être facilement perturbés par des interférences externes. L'efficacité énergétique est également essentielle pour garantir l'autonomie des systèmes en extérieur. Toutefois, les performances globales d'une station de mesure sont principalement régies par le capteur qu'elle met en œuvre.

La revue bibliographique est très instructive puisqu'elle montre qu'il existe déjà plusieurs capteurs et solutions à faible coût disponibles. Des capteurs à faible coût ont été identifiés pour mesurer en continu et *in situ* plusieurs grandeurs intéressantes pour l'hydrologie urbaine (recherche) et la gestion des eaux pluviales (exploitation), notamment la météorologie et la quantité d'eau. Il existe de nombreux capteurs à faible coût pour mesurer

l'humidité de l'air, la vitesse du vent, le rayonnement solaire, les précipitations, le niveau de l'eau et l'humidité du sol. Mais leurs performances et leurs incertitudes doivent encore être mieux quantifiées au moyen d'essais et d'évaluations supplémentaires. Le mesurage du débit nécessite des modules de capteurs et une conception de système plus créative, mais ils ne sont pas loin de donner des résultats relativement fiables.

Le mesurage de la qualité de l'eau au moyen d'appareils à faible coût exige par contre aujourd'hui davantage de connaissances, et les utilisateurs ont clairement besoin de compétences spécifiques, avec une adaptation à la matrice d'eau concernée (eaux pluviales dans le présent document, mais il pourrait s'agir d'eau potable, d'eau de rivière, etc.). Les articles examinés ne présentent pas suffisamment d'exemples reproductibles avec des références à la littérature et aux méthodes métrologiques. Par exemple, la comparaison entre capteurs, même avec un capteur traditionnel plus coûteux utilisé comme référence, n'équivaut pas à un véritable étalonnage.

Dans une plus large mesure que pour les capteurs traditionnels, la qualité des données générées par les capteurs à faible coût ne dépend pas seulement des capteurs eux-mêmes, mais aussi de l'utilisateur et de ses connaissances, compétences et pratiques métrologiques.

C'est pourquoi les utilisateurs de capteurs et de systèmes de mesure à faible coût ne doivent pas seulement avoir des compétences en électronique et en informatique. Ils doivent être formés à la métrologie, y compris aux principes de mesure, à l'étalonnage et à la vérification périodiques indispensables des capteurs et des systèmes de mesure, à l'évaluation de l'incertitude, etc.

En ce qui concerne l'exactitude des capteurs à faible coût, il existe plusieurs discussions sur son évaluation : (i) de nombreux articles ne tiennent pas compte de l'exactitude des capteurs de référence lorsqu'ils testent des capteurs à faible coût et présentent leurs résultats ; (ii) de nombreux articles ne distinguent pas les ensembles de données d'étalonnage et de validation lorsqu'ils testent des capteurs à faible coût ; (iii) très différente des capteurs traditionnels, la sortie des capteurs à faible coût est souvent très primitive, il n'y a quasiment pas d'étalonnage par le fabricant pour adapter le signal de sortie, ce qui donne aux utilisateurs plus de liberté mais implique également plus de travail préparatoire dans l'utilisation des capteurs ; (iv) l'exactitude des capteurs à faible coût dépend très fortement de la construction d'une équation d'étalonnage spécifique par les utilisateurs. Par exemple, la sortie des capteurs de niveau d'eau à ultrasons est le temps de retour de l'impulsion ultrasonore. Les utilisateurs peuvent améliorer l'exactitude en tenant compte des grandeurs d'influence que sont la température et l'humidité ;

(v) certains utilisateurs utilisent des méthodes inadaptées pour étalonner les capteurs à faible coût : par exemple, verser trop d'eau dans le pluviomètre revient à simuler un épisode de forte pluie irréaliste.

En ce qui concerne la répétabilité et la reproductibilité des capteurs à faible coût, certains documents utilisent l'écart-type relatif regroupé et l'analyse de la variance pour les estimer. Mais de nombreux articles ignorent ces deux critères importants. Presque aucun document ne vérifie intentionnellement la reproductibilité des capteurs à faible coût. En fait, cela devrait être au fabricant de s'assurer que chaque capteur est étalonné en usine. Mais les capteurs à faible coût ne comportent souvent aucune garantie de répétabilité et de reproductibilité, et c'est à l'acheteur qu'il incombe de la vérifier. Des tests spécifiques pour chaque capteur à faible coût sont donc obligatoires avant utilisation (comme cela devrait être le cas pour n'importe quel capteur), mais cela pose un autre problème : lorsqu'on prévoit d'utiliser des centaines de capteurs à faible coût, il est très coûteux de les tester tous un par un. Le développement de systèmes de test automatisés peut faciliter cette tâche, mais reste coûteux.

Dans de nombreux cas, les utilisateurs ne peuvent pas évaluer la résolution des capteurs à faible coût parce qu'ils ne disposent pas de l'équipement nécessaire. Il existe un risque d'utilisation non éclairée des capteurs à faible coût si les utilisateurs se fient uniquement aux informations fournies par les fabricants. En effet, certaines fiches techniques de capteurs à faible coût sont de mauvaise qualité (la fiabilité et l'assurance qualité sont coûteuses). Par exemple, la fiche technique du kit de station météorologique SEN-15901 donne des valeurs de résolution différentes dans différentes langues, comme indiqué dans les sous-sections relatives aux capteurs de vitesse du vent et de précipitations. Un autre problème se pose, car de nombreux capteurs à faible coût ne fournissent qu'une tension : l'utilisation d'un convertisseur analogique numérique avec plus de bits peut augmenter en théorie la résolution, mais nécessite une adaptation au cas par cas. Cependant, plus important encore, la performance originale de certains capteurs à faible coût est limitée par leur principe, comme c'est le cas par exemple pour les turbidimètres à faible coût. En outre, certains capteurs à faible coût ont une résolution plus élevée que les capteurs de référence utilisés pour les tester. Par exemple, le pluviomètre optique RG-15 a une résolution théorique de 0.02 mm.

En ce qui concerne le temps de réponse, il semble que les capteurs à faible coût examinés puissent effectuer des mesurages toutes les minutes. Dans certains cas, il peut être préférable de lire le signal de sortie à un pas de temps

de quelques secondes puis de calculer la moyenne ou la médiane pour bénéficier de la répétabilité sur l'estimation de la valeur moyenne ou médiane.

Très peu d'informations sont données sur la sensibilité à l'environnement, les besoins en maintenance et la longévité des capteurs à faible coût. Certains articles utilisent l'analyse de variance (ANOVA) pour évaluer la sensibilité à l'environnement. En effet, la plupart des capteurs à faible coût doivent être modifiés pour être adaptés à une application *in situ* : boîtier, revêtement, etc. Cette sensibilité n'est donc pas uniquement liée au capteur à faible coût lui-même. Par exemple, les capteurs d'humidité de l'air et de niveau d'eau dotés d'un boîtier étanche devraient avoir une plus grande longévité. Nous supposons que tous les capteurs de qualité de l'eau à faible coût dont il est question dans cette étude seront encrassés lorsqu'ils seront immergés dans des eaux pluviales et/ou des eaux usées pendant des mois, ce qui (i) nécessitera des nettoyages fréquents et (ii) réduira leur longévité. Il serait intéressant de mettre au point un dispositif capable de prélever automatiquement des échantillons d'eau et de nettoyer les capteurs de qualité de l'eau.

Le chapitre 3 propose un cadre métrologique dans lequel l'évaluation des capteurs à faible coût repose sur des indicateurs clés, en particulier l'incertitude élargie et le taux d'exactitude. En supposant que les capteurs de référence fournissent des "valeurs de référence" des grandeurs d'intérêt, le taux d'exactitude est défini comme le pourcentage de valeurs fournies par un capteur à faible coût qui concordent avec les valeurs fournies par le capteur de référence correspondant utilisé dans les mêmes conditions *in situ*, en tenant compte de leurs incertitudes élargies respectives. Pour être représentatif, le taux d'exactitude doit être calculé à partir de grandes séries de données, car les petites séries ne permettent pas d'obtenir des résultats fiables. Une fonction de corrélation est également proposée pour estimer les valeurs réelles les plus probables (c'est-à-dire les valeurs de référence) des grandeurs d'intérêt à partir des valeurs fournies par les capteurs à faible coût, en tenant compte des corrections de décalage du zéro et de pente. Deux sites d'essai de capteurs à faible coût sont également présentés au chapitre 3.

Au chapitre 4, un test comparatif d'une durée de 15 mois entre les capteurs météorologiques à faible coût et les capteurs de référence a été réalisé. Le tableau 2 indique les capteurs à faible coût et les capteurs de référence utilisés pour chaque grandeur mesurée, ainsi que leurs prix respectifs. Les principaux résultats des comparaisons sont résumés dans les tableaux 3 et 4.

Tableau 2. Capteurs à faible coût et de référence testés, avec leur nom commercial et leur fourchette de prix.

Grandeur mesurée	Capteur à faible coût	Gamme de prix	Capteur de référence	Gamme de prix
Intensité des précipitations	WH-SP-RG	~ 15 €	OTTPluvio²L	~ 4250 €
			Précis Mécanique 3029	~ 750 €
Vitesse du vent	WH-SP-WS01	~ 20 €	Campbell Scientific 03002-L	~ 750 €
Direction du vent	WH-SP-WD	~ 20 €		
Température et humidité de l'air	BME280	~ 5 €	Campbell Scientific CS215-L	~ 280 €
	DHT22	~ 5 €		
Rayonnement solaire	JXBS-3001-ZFS	~ 100 €	Campbell Scientific CS300	~ 300 €
	Si1145	~ 10 €		

Tableau 3. Résumé de la comparaison entre les capteurs météorologiques à faible coût et de référence.

Nom du capteur	Grandeur mesurée	Equation de correlation [a]	Incertitude élargie [b]
WH-SP-WS01	Vitesse du vent	$y = 10 + 81\,x$	0.24 m/s
WH-SP-WD	Direction du vent	NC [c]	NC
BME280	Température de l'air	$y = -0.7 + 1.1x$	2.0 °C
	Humidité de l'air	NC [d]	NC
DHT22	Température de l'air	$y = 0.6 + x$	2.3 °C
	Humidité de l'air	$y = -1.5 + x$	5.7 %RH
JXBS-3001-ZFS	Rayonnement solaire total	$y = 161 + 1.16\,x$	227 Wh/m^2
Si1145	Rayonnement solaire total	$y = 7013 + 1.666\,x$	303.7 Wh/m^2

[a] y correspond aux valeurs des capteurs à faible coût, x aux valeurs des capteurs de référence.

[b] Dans le calcul du taux d'exactitude des capteurs à faible coût, les valeurs des capteurs à faible coût sont corrigées par la fonction inverse de l'équation de corrélation. L'incertitude élargie dans cette colonne correspond à un taux d'exactitude de 95 %.

[c] NC: non calculé, le capteur WH-SP-WD ne peut pas fournir d'angles de direction du vent contrairement au capteur de référence, ce qui rend difficile l'obtention d'un résultat quantitatif.

[d] Le module BME280 testé a une faible longévité pour le mesurage de l'humidité de l'air, ce qui rend le résultat non significatif.

Tableau 4. Utilisation des capteurs météorologiques à faible coût testés en hydrologie urbaine.

Nom du capteur	Application en hydrologie urbaine?	Commentaires
WH-SP-WS01	possible	Lors d'un test de 15 mois, les performances de ce capteur sont stables et quantifiables.
WH-SP-WD	Réservée	Bien que les performances de ce capteur soient stables, il ne peut pas donner les angles de la direction du vent mais uniquement des secteurs (i.e. très faible résolution).
BME280	Non recommandée	La longévité du capteur testé est très faible : après trois mois, les valeurs mesurées sont incohérentes.
DHT22	Possible	En 15 mois de test, les performances de ce capteur sont stables et quantifiables.
JXBS-3001-ZFS	Réservée	Ce capteur coûte plus de 100 euros, mais son fabricant ne donne aucune information sur son exactitude, ce qui indique un fabricant moins spécialisé.
Si1145	Réservée	Ce capteur ne coûte que quelques euros et peut être utilisé pour estimer le rayonnement total journalier comme un pyranomètre traditionnel qui coûte plusieurs centaines d'euros. Mais l'utilisateur final doit concevoir un boîtier d'installation pour ce capteur.

En résumé, les performances de l'anémomètre à faible coût WH-SP-WS01 sont stables et quantifiables. Les performances de l'anémoscope à faible coût WH-SP-WD sont stables, mais le capteur ne peut pas donner la direction du vent en angles, seulement en secteurs, ce qui peut toutefois être suffisant pour les besoins en hydrologie urbaine. Le capteur d'humidité de l'air à faible coût BME280 n'a eu qu'une longévité de trois mois et des performances médiocres. Le capteur d'humidité de l'air à faible coût DHT22 a des performances stables et quantifiables. Le pyranomètre à faible coût JXBS-3001-ZFS a systématiquement fourni des valeurs plus élevées que le capteur de référence. Enfin, le capteur de lumière à faible coût Si1145 permet d'estimer le rayonnement journalier total, à condition d'adapter le capteur.

Dans le chapitre 5, une station de mesure des précipitations à faible coût a été conçue, construite, installée et testée. Cette station dispose (i) de deux modes d'alimentation électrique : alimentation externe et/ou énergie solaire, (ii) de deux types de pluviomètres à faible coût : le pluviomètre optique RG-15 et le pluviomètre à auget basculant WH-SP-RG, et (iii) de deux méthodes d'enregistrement des données : carte SD *in situ* et/ou transmission des données en ligne via le réseau LoRa vers la plateforme The Things Network et un serveur Node-RED personnalisé, avant transfert final vers la plateforme publique http://opendataeau.org. La plupart des données sont collectées avec un pas de temps d'une minute, y compris l'horodatage, la sortie des pluviomètres, les sorties du panneau solaire et de la batterie, et la température de l'air. Après avoir été testé, le système conçu peut fonctionner de manière indépendante et autonome. La carte et le code Arduino ont été développés progressivement, depuis les versions de base dotées de fonctionnalités élémentaires jusqu'aux versions plus élaborées prenant en compte et résolvant tous les problèmes découverts au cours des périodes de test, y compris l'optimisation de l'horodatage, la minuterie de veille, la protection contre le blocage du code, et le format de données en ligne. Au total, cinq versions du matériel de la station ont été développées et 16 versions des codes ont été écrites. Un enregistreur de données d'étalonnage du pluviomètre à auget à faible coût a été conçu et construit avec un écran pour afficher le nombre de basculements.

Comme l'essai de la station de mesure des précipitations à faible coût a duré plus longtemps que prévu (et que la pluie a été plus rare que prévu pendant la période d'essai), seules des données fiables sur quatre mois pendant la saison hivernale sont disponibles pour évaluer les performances du pluviomètre optique à faible coût RG-15 et du pluviomètre à auget basculeur à faible coût WH-SP-RG. Trois RG-15 et six WH-SP-RG ont été testés au cours de

Tableau 5. Utilisation des capteurs pluviométriques à faible coût testés en hydrologie urbaine.

Capteur / système	**Application en hydrologie urbaine ?**	**Commentaires / conditions d'utilisation**
Pluviomètre optique à faible coût RG-15	Réservée	Le capteur n'est pas un dispositif prêt à l'emploi, un câble doit être ajouté par les utilisateurs, ce qui présente un risque d'endommagement. Le capteur doit être placé dans un endroit où il n'y a pas de perturbations dues à l'ombre créée par d'autres appareils, en particulier l'anémomètre et l'anémoscope. Un nettoyage doux et fréquent de la surface sphérique est nécessaire pour s'assurer qu'il n'y a pas d'interférences. **Plusieurs mois d'utilisation ont montré un fonctionnement stable et sans dérive.** **L'expérience montre clairement une variance importante d'un capteur à l'autre.** **Une comparaison systématique avec un capteur de référence est nécessaire** pour établir une fonction de corrélation afin d'estimer les éventuels biais et les sous-estimations ou surestimations. Avec cette fonction de corrélation, il est alors possible de convertir les données brutes du RG-15 en hauteur de pluie corrigée à chaque pas de temps. Une difficulté majeure réside dans le fait que cette comparaison doit être effectuée *in situ* et qu'aucune méthode d'étalonnage simple ne peut être appliquée.
Pluviomètre à auget basculant à faible coût WH-SP-RG	Réservée ou possible en fonction des adaptations	Le pluviographe à auget à faible coût WH-SP-RG est perturbé par une vitesse de vent élevée et doit donc être solidement fixé pour éviter les vibrations qui peuvent entraîner des faux basculements. **La reproductibilité de ce capteur est acceptable d'après l'étalonnage.** **Plusieurs mois d'utilisation ont montré un fonctionnement stable et sans dérive.** Le capteur est doté d'un auget stable d'un volume d'environ 1.5 mL, mais son cône de réception à section rectangulaire est trop plat est mal conçu par rapport aux pluviomètres à auget basculant de référence. Le cône de réception en plastique non conique peu profond donne une résolution initiale d'environ 0.6 mm/basculement, ce qui est insuffisant pour les applications de recherche. **Les utilisateurs ne devraient pas utiliser ce capteur sans modifier d'abord son cône de réception**, en particulier en l'agrandissant (par exemple, avec un entonnoir imprimé en 3D) pour améliorer la résolution jusqu'à 0,1 mm/basculement. **Les utilisateurs doivent également vaporiser du téflon sur le cône adapté pour s'assurer que les gouttes de pluie peuvent glisser jusqu'à l'auget**. **Un étalonnage systématique en laboratoire est nécessaire** (comme pour un pluviomètre de référence) pour vérifier le fonctionnement et déterminer la résolution réelle (mm/basculement).

Station de mesure artisanale à faible coût	Réservée ou possible en fonction de l'objectif et des connaissances de l'utilisateur	La station de mesure artisanale à faible coût est une occasion de mener une activité de suivi des eaux pluviales avec un budget limité. **Cette possibilité offre une flexibilité sans précédent aux chercheurs, qui peuvent ainsi développer leurs propres instruments**. Même avec l'aide d'une communauté grandissante, le temps consacré à la sélection des composants, au matériel et au développement du logiciel représente une grande partie du coût total qui doit être estimé. **Les chercheurs ayant un objectif de mesure clair et une certaine connaissance du matériel, des logiciels et de la métrologie sont plus à même de réaliser ce type de travail.**

Tableau 6. Utilisation du capteur de niveau d'eau et du système de mesure à faible coût en hydrologie urbaine.

Capteur / système	**Application en hydrologie urbaine ?**	**Commentaires / conditions d'utilisation**
YB-2J-F	Possible	Le capteur de niveau d'eau à pression à faible coût YB-2J-F est un **capteur robuste doté d'un boîtier en acier inoxydable qui n'a envoyé aucune valeur aberrante** lors de mesurages *in situ* continus pendant un an et demi. Le capteur émet un signal 4-20 mA. **Un circuit de traitement du signal doit être développé** par les utilisateurs, comprenant une résistance de précision et un module DFR0553 basé sur une puce ADS1115. Ce circuit s'est avéré efficace. L'étalonnage est obligatoire lors de l'utilisation de ce capteur, comme pour tous les capteurs.
Station de mesure artisanal à faible coût	Réservée ou possible en fonction de l'objectif de l'utilisateur	Le système de mesure de niveau d'eau artisanal à faible coût développé dans cette thèse est conçu pour fonctionner sans entretien ou avec un entretien limité. Le système est alimenté par trois piles AA rechargeables et un panneau solaire de 0.5 W. Cela lui a permis de fonctionner en continu pendant plus d'un an, mais les piles ont récemment montré des signes de détérioration (en hiver lorsque l'ensoleillement est réduit). Le système testé n'avait pas de stockage local des données pour éviter les visites de collecte de données et pour économiser de l'énergie. Cependant, la continuité des données transmises en ligne n'a pas été aussi fiable que prévu, et des données ont été perdues. Le système a été réglé pour fonctionner selon un cycle : 40 minutes de sommeil et moins d'une minute de mesurage, contrôlé par une minuterie. Cependant, le temps de sommeil moyen observé a été de 42 minutes. La régularité de l'horodatage n'est pas satisfaisante car le système ne peut pas passer en mode sommeil à temps, le module de minuterie n'étant pas assez précis et la puissance du signal de communication étant limitée. Nous avons depuis proposé un nouveau système de mise en sommeil qui semble plus fiable. Des travaux supplémentaires ont été effectués pour assembler une chaîne de mesure pratique. Outre le matériel et le logiciel de la station de mesure, une plate-forme de stockage et d'affichage des données et de maintenance a été développée. Le fabricant de la carte de contrôle utilisée dans notre système (Pycom) a fait faillite. Cela révèle une partie des risques auxquels est confrontée une station de mesure artisanale bon à faible coût.

cette période. Sur la base de nos tests et de notre expérience, les principales conclusions et recommandations concernant ces deux pluviomètres et la station de mesure sont résumées dans le tableau 5.

Dans le chapitre 6, le capteur de pression de niveau d'eau à faible coût YB-2J-F a d'abord été étalonné en laboratoire, puis utilisé *in situ* pendant un an et demi. Les principaux travaux et résultats de ce chapitre sont résumés dans le tableau 6.

En résumé, même avec l'aide d'une communauté grandissante, le temps à consacrer à la sélection des composants, à la conception et à l'assemblage du matériel, au développement du logiciel, à l'étalonnage et à la comparaison systématiques des capteurs, représente la plus grande partie du coût total qui doit être estimé lors de l'utilisation de capteurs à faible coût. On considère généralement que les capteurs et les systèmes de mesure à faible coût sont moins précis que les équipements de mesure courants. Mais en quantifiant l'incertitude des systèmes de mesure à faible coût, les hydrologues pourraient s'appuyer sur ces systèmes pour obtenir des données avec une incertitude connue.

Après les essais réalisés durant cette thèse, quatre capteurs sont susceptibles de contribuer au suivi de dispositifs de gestion des eaux pluviales à la source : (i) le capteur de vitesse du vent WH-SP-WS01 avec une incertitude élargie de 0.24 m/s, (ii) le capteur de température et d'humidité de l'air DHT22 avec une incertitude élargie de 2.3 ℃ et de 5.7 %RH, (iii) le pluviomètre WH-SP-RG dont la surface du cône de réception doit être agrandie (la résolution originale n'est que d'environ 0.60 mm/basculement), et (iv) le capteur piézorésistif de niveau d'eau YB-2J-F qui nécessite un circuit de traitement des signaux additionnel pour convertir son courant de sortie en quantité mesurable. Après de nombreuses mises à jour logicielles et matérielles, une conception éprouvée et fiable d'une station de mesure à faible coût a été proposée. Dans cette conception, une carte MKR WAN 1310 est utilisé comme carte de contrôle principale, le module DS3231 comme horloge en temps réel et la carte Lipo Rider Pro comme carte de gestion de l'énergie. Les données sont enregistrées localement sur une carte SD par un Arduino MKR MEM et transmises en ligne via le réseau LoRaWAN. Tous les détails de cette conception sont fournis sous forme de documents open-source.

Cette thèse fournit les bases pour un suivi à grande échelle et à faible coût des dispositifs de gestion des eaux pluviales urbaines à la source. En se référant aux recommandations fournies ci-dessus, les hydrologues pourraient développer leur propre système de mesure à faible coût.

Il reste encore plusieurs questions dans ce domaine et les travaux futurs pourraient inclure les aspects suivants :

- Continuer à collecter davantage de données pour mieux évaluer le comportement et les performances à long terme de ces dispositifs à faible coût. Les stations de mesure des précipitations et des niveaux d'eau à faible coût développées au cours de la thèse sont toujours en service et il sera intéressant de surveiller leur vieillissement et leur longévité.

- Faire en sorte que notre travail puisse être facilement répété / reproduit par d'autres. Par exemple, dessiner des circuits imprimés et partager cette conception, insérer le code dans une bibliothèque Arduino, partager des fichiers de conception d'impression 3D, etc.

- Développer une boîte à outils logicielle pour calculer de manière autonome les taux d'exactitude avec différentes incertitudes élargies. Le taux d'exactitude apparaît comme un outil approprié pour comparer les sorties du capteur testé et du capteur de référence en tenant compte de leurs incertitudes élargies respectives.

- Vérifier davantage la sensibilité des capteurs à faible coût à l'environnement. Par exemple, la sensibilité à la température de l'eau du capteur de niveau d'eau YB-2J-F est actuellement vérifiée par une équipe collaborative.

- Explorer l'utilisation de capteurs de qualité de l'eau à faible coût (par exemple, pH, conductivité, turbidité) pour surveiller les eaux pluviales *in situ* en temps réel. Un travail préliminaire sur les turbidimètres est présenté dans une annexe de la thèse.

- Mettre en place un réseau spatialement réparti de capteurs et de stations de mesure à faible coût à l'échelle du bassin versant pour fournir des données et des connaissances sur les différents dispositifs de gestion à la source des eaux pluviales urbaines.

- Comme les réseaux de capteurs à faible coût prennent de l'ampleur, il serait intéressant d'étudier comment étalonner automatiquement un grand nombre de capteurs.

FOLIO ADMINISTRATIF

THESE DE L'INSA LYON, MEMBRE DE L'UNIVERSITE DE LYON

NOM : ZHU DATE de SOUTENANCE : 26/04/1993

Prénoms : Qingchuan

TITRE : Low-cost sensors for monitoring stormwater source control measures

NATURE : Doctorat Numéro d'ordre : 2023ISAL0035

Ecole doctorale : MEGA de Lyon (Mécanique, énergétique, génie civil, acoustique) – ED162

Spécialité : Génie Civil

RESUME :

The large-scale deployment of low-cost sensors has the potential to revolutionize the field of urban hydrology monitoring, for decentralized stormwater management systems, bringing expanded research scope and improved urban water management. However, this area is still in its infancy stage and needs a more systematic assessment framework to ensure data reliability and facilitate its implementation by researchers and practitioners. To contribute to fill this gap, this thesis explores low-cost monitoring systems dedicated to stormwater source control measures (SCM). Several open-source low-cost sensors and systems have been calibrated and validated in a DIY (Do It Yourself) approach, aiming to assess the medium and long-term performance and identify maintenance problems. This thesis provides: (i) A review of low-cost meteorological, water quantity and quality sensors that are used in the literature published in recent years, in a unified metrological framework considering numerous indicators. (ii) A low-cost meteorological sensors testbench on the INSA GROOF platform, with a comparison between low-cost and conventional sensors. Low-cost anemometer WH-SP-WS01 and air humidity sensor DHT22 are found to have performance comparable to those of conventional sensors. (iii) The development of a low-cost stand-alone rain gauge station, with a method to calibrate low-cost tipping bucket rain gauges, and a comparison between low-cost and conventional rain gauges in winter period. The rainfall catchment funnel of low-cost tipping bucket rain gauge WH-SP-RG needs to be enlarged to improve the resolution. The optical rain gauge RG-15 has significant sensor-to-sensor variability. (iv) The development of a low-cost stand-alone water level monitoring station, with a method to calibrate low-cost pressure water level transmitters, and a one and a half year long operation assessment. The system developed works continuously but the time step of its data is not regular. All low-cost sensors need specific calibration and a correlation function to compare their results with reference sensors.

MOTS-CLÉS : low-cost sensor, meteorological sensor, rainfall monitoring, real time monitoring, stormwater source control measures, water level monitoring

Laboratoire (s) de recherche : Laboratoire DEEP (Déchets Eaux Environnement Pollutions)

Directeur de thèse : Jean-Luc BERTRAND-KRAJEWSKI

Président de jury :

Composition du jury :

VIKLANDER, Maria	LULEA UNIVERSITY OF TECHNOLOGY	Rapporteure
ZHU, David	UNIVERSITY OF ALBERTA	Rapporteur
BRANGER, Flora	INRAE LYON-GRENOBLE	Examinatrice
VERSINI Pierre-Antoine	ENPC	Examinateur
LIPEME KOUYI Gislain	INSA LYON	Examinateur
BERTRAND-KRAJEWSKI, Jean-Luc	INSA LYON	Directeur de thèse
CHERQUI, Frédéric	UNIVERSITE LYON 1	Co-directeur de thèse